COST Action FP1004

Focus Solid Timber Solutions - European Conference on Cross Laminated Timber (CLT)

21- 22nd May 2013
Graz

2nd Edition – April 2014

Edited by:

Richard Harris
Andreas Ringhofer
Gerhard Schickhofer

COST Action FP1004 with TU Graz

Focus Solid Timber Solutions

European Conference on Cross Laminated Timber (CLT)

The State-of-the-Art in CLT Research

Graz University of Technology

May 21-22, 2013

Graz University of Technology, Austria

2nd Edition – April 2014

Edited by

Richard Harris

Andreas Ringhofer

Gerhard Schickhofer

ECOST-MEETING-FP1004-210513-028873

ISBN Number: 1 85790 181 9

Published by The University of Bath

2nd Edition. April 2014

Preface

The hosting and the organisation of scientific conferences is an important field of activity for internationally operating institutes. Furthermore, this is an inherent role for Universities and should be seen as self-evident. It is also the mission of COST Actions to organise meetings, which enable the international research community to hold a scientific discourse on current interdisciplinary topics. This opportunity has to be emphasised, especially in times of increasing application-oriented research activities. With regard to that, it can be said: Individual freedom of research starts where externally demanded convenience ends.

By playing an active role in the frame of COST actions in the past, Graz University of Technology in general, and the Institute of Timber Engineering and Wood Technology in particular, show their regard for international scientific networking. The organisation of a workshop in the frame of COST action E55 “Modelling of the Performance of Timber Structures” at Graz University of Technology in the year of 2007 and, especially, the contribution “Solid timber construction – A construction system for residential houses, office and industrial buildings” in the frame of the final workshop of COST action E5 “Timber frame building systems” in Venice, in the year of 2000, are worth mentioning in this context. The latter topic, seen as an exotic side issue in the year of 2000, is now – one decade later – easily filling up daily conference programs and large auditoriums. Furthermore, it has grown to an economically significant area of R&D in wood sciences. This is also the link to the very successful on-going COST action FP1004, under the leadership of my colleague Richard Harris. The aim of this CLT COST conference at Graz University of Technology is the summarised demonstration of the European state-of-the-art on this topic, combined with the wish to hold an open discourse, which will lead to further progress in research and development.

I’m also happy to note that we will welcome a worldwide enthusiastic CLT community here in Graz, which is a result of this co-organised event. The conference should thus be seen as a contribution to a high-quality and open scientific dialogue with this community. Bernard of Chartres used to say:

‘…we are like dwarfs on the shoulders of giants, so that we can see more than they, and things at a greater distance, not by virtue of any sharpness of sight on our part, or any physical distinction, but because we are carried high and raised up by their giant size.”

With regard to this, the current state-of-the-art of the topic CLT, in connection with our own and further scientific activities in this research field, should be seen as the foundation for following generations and provides those basics which are necessary for further innovation.

Gerhard Schickhofer

May 2013

The orthotropic properties of timber are well known – strong and stable along the grain, weak and susceptible to movement across the grain. By placing laminations across the grain, Cross Laminated Timber uses this anisotropy to advantage, enhancing the mechanical properties of wood, by using wood.

This elegant solution has led to Cross Laminated Timber being the most significant recent innovation in timber engineering. It has opened the potential for new construction types, including tall timber buildings. Through their work at TU Graz, Professor Gerhard Schickhofer and his team continue to lead the world in research in the field.

COST Action FP1004, "*Enhance mechanical properties of timber, engineered wood products and timber structures*" provides a network for learning and development in a range of connected topics, which includes Cross Laminated Timber. This conference, with its proceedings, will record the State-of-the-Art of Cross Laminated Timber and its use. In working with TU Graz to host this Conference, the COST Action is able to bring researchers together, from around the world to learn about Cross Laminated Timber and its applications, as well as to take part in discussions about future research and development.

The structure of this conference is based around the material and its use. The topics move from manufacture, through design to application. What are the threats faced by CLT? What are the opportunities? The culture of COST Action FP1004 is to encourage involvement of delegates and the Day 1 programme includes time for debate and discussion between delegates and the expert speakers.

The conference starts, where all engineering studies should start, with an analysis of the material. What is the State-of-the-Art in manufacturing this material? How can manufacture be applied to more species, to low-cost production from wood available local to its use? How are the engineering properties of the manufactured product predicted and assured?

The conference will move on to design and construction. Presentations on the implementation of Ultimate Limit State, and Serviceability Limit State, methods for reinforcing against local high stresses with screws and the design of connections will provide the latest knowledge.

In seismic design, the use of Cross Laminated Timber produces enormous benefits. Obviously, use of a sustainable material is of great advantage but, in addition, Cross Laminated Timber lays out new opportunities for building systems, which remain serviceable, whilst dissipating energy. Three presentations on seismic behaviour set down cutting-edge understanding for this topic.

TU Graz has led the world in the application of CLT to building systems. Their work in developing an understanding of environmental performance of building fabric, incorporating CLT, has been fundamental to success of the material. The use of Cross Laminated Timber to create the tallest modern timber structures in the world opens opportunities that could not have been imagined ten years ago. The latest of these structures, under construction in Australia, could not have been contemplated five years ago. In the final session, learning about this project from its designer, together with learning about lower rise, more local but equally impressive buildings, will bring Day 1 and the formal part of the conference to a fitting conclusion.

Day 2 will provide the opportunity to visit one of the Austrian Cross Laminated Timber manufacturing plants as well as seeing the use of CLT in construction.

The purpose of the COST programme is to strengthen Europe in scientific and technological research, for peaceful purposes, through the support of cooperation and interaction between European researchers. It is based on an inter-governmental agreement, which has proved to be a highly successful way to spread awareness and build networks between Europe’s researchers. It helps researchers to share not only the results of their work but also their aims and methods. It is open to global cooperation in the mutual interest and builds bridges between research communities.

This conference adheres to these principles. It will be an extraordinary opportunity to hear presentations from highly specialist, invited speakers and to participate in debate. To ensure the opportunity for discussion, numbers are strictly limited and early application for a place is essential. For those unable to attend in person, the proceedings will record the State-of-the-Art.

Richard Harris
Chair COST Action FP1004
May 2013

About COST Action FP1004

Timber and wood-based engineered products are becoming very important as structural materials, especially in the drive towards sustainable technologies and construction. For structural wooden products, it is very important to improve their properties to be more competitive and reliable as a sustainable low-carbon material and a major contributor to affordable buildings. This applies particularly to larger, more complicated structures where timber is becoming a realistic alternative.

This Action aims to boost the performance of structural timber products/construction, thereby improving use of timber in construction in existing and new applications. This includes the enhanced predictability and reliability of timber structures. Improving the mechanical performance of connections and reinforcing timber in weak zones are large-scale research domains in Europe, which will require coordination and scientific/engineering approaches. This COST Action will deliver increased knowledge of improving strengthening, stiffening and toughening techniques, modelling enhanced performance and experience in real projects to create new opportunities for timber construction. Exchanging information will highlight gaps in knowledge and inform future work and potential collaboration between research groups, supporting timber construction and its wider uptake in the European construction industry. This Action may also create opportunities for patenting possible new technologies and products for reinforcing timber mechanical properties.

The scientific programme is divided into three main scientific areas, expressed as Work Groups (WG) with the same aims but different perspectives:

WG 1: Enhance performance of connections and structural timber in weak zones

WG 2: Enhance the mechanical properties of heavy timber structures with a particular emphasis to timber bridges

WG 3: Modelling the mechanical performance of enhanced wood-based systems

COST Action FP1004 website: http://costfp1004.holz.wzw.tum.de/

COST Action FP1004 Core Group

Richard Harris	Chair	R.Harris@Bath.ac.uk
Robert Kliger	Vice-Chair	Robert.Kliger@chalmers.se
Jan-Willem Van de Kuilen	WG 1	VandeKuilen@wzw.tum.de
Roberto Crocetti	WG 2	Roberto.Crocetti@kstr.lth.se
Daniel Ridley-Ellis	WG 3	D.Ridley-Ellis@napier.ac.uk
Kay-Uwe Schober	STSM	Kay-Uwe.Schober@fh-mainz.de
Gerhard Schickhofer	Conference Host	Gerhard.Schickhofer@tugraz.at

Acknowledgements

I would like to express my gratitude to all who voluntarily and with no or limited funding have contributed to this conference and the proceedings.

There is an enormous amount of work that goes into hosting a conference of this size. In addition to the formal presentation of papers, there will be factory and site visits. Many thanks to the administration team at TU Graz, led by Hildegard Weißnar, who have managed the conference registration and organisation.

A special thank you goes to Andreas Ringhofer, who has been vital to the success of the Conference. He has helped manage the submission and editing of papers, has been the link between the COST Action FP1004 and TU Graz and has been part of the organisation team. Thank you to Massimo Fragiacomo, who helped with the Theme 3 papers on seismic behaviour, and to Reinhard Brandner who helped edit the papers from TU Graz. Thank you also to Professor Gerhard Schickhofer, who suggested, at our first meeting in 2011, that COST Action FP1004 hold a conference on Cross Laminated Timber and readily agreed to host this conference at TU Graz, the home of CLT.

Richard Harris
May 2013

Note to Second Edition

The Graz Conference was very successful, attracting nearly 200 delegates from all over the world. The edition of the proceedings published for the conference did not contain the paper presented by Heinz Ferk on the building physics of CLT. In this second edition, this excellent paper is now included and some minor typographical errors are amended. This publication remains just as important as the State-of-the-Art document on CLT Research as it was at the time of the Conference.

Richard Harris

March 2014

Biographies of the Editors

Univ.-Prof. Dipl.-Ing. Dr.techn.

Gerhard Schickhofer

Institute of Timber Engineering and Wood Technology

Graz University of Technology

Austria

Email: gerhard.schickhofer@tugraz.at

Gerhard Schickhofer studied civil engineering at Graz University of Technology and graduated with distinction in 1990 (diploma) and 1994 (doctorate). For his research work he has received different awards (e.g. Josef-Umdasch-Award for his doctoral thesis on “Cross-Laminated Timber” in 1995, the Research Funding Association Award in the area “added value” also for “Cross-Laminated-Timber“ in 1998 and the European Innovation Award for the project “Tanno meets Gemini” in 2004), in his field of activity he has published more than 230 publications and given numerous speeches. In 1999 he habilitated and became an associate professor, between 2002 and 2012 he was manager and scientific director of the Competence Centre “holz.bau forschungs gmbh”. In 2004 he was appointed to a professorship and became the head of the Institute of Timber Engineering and Wood Technology at Graz University of Technology. During his career Prof. Schickhofer was involved in transfer activities in form of more than 20 conferences, workshops and seminars, and has supervised more than 120 diploma theses and numerous doctoral theses.

Prof.

Richard Harris BSc CEng FICE FIStructE

BRE Centre for Innovative Construction Materials

The University of Bath

UK

Email: r.harris@bath.ac.uk

Richard Harris after graduating from the university of Bristol in 1972, worked for 12 years in civil engineering construction, in UK and overseas. In 1984, he joined Buro Happold in Bath as a Structural Engineer. Twenty-five years later, in 2009, he moved to the position of Professor of Timber Engineering at the University of Bath. With Buro Happold, as well as working on the design of building structures in other materials, he was responsible for a number of timber engineering projects, including the Globe Theatre, the Downland Gridshell, the Savill Building gridshell, the Pods Scunthorpe and the WISE development at the Centre for Alternative Technology. As Professor of Timber Engineering at the University of Bath, he is responsible for teaching and research. His research includes tall timber Structures, pre-fabrication of timber structures, metal-free connections in timber structures, timber gridshells, folded-plate timber structures, timber-concrete composites, dynamic response of timber structures and the use of local timber, including Douglas fir. As Chair of COST Action FP1004, he is working in helping to integrate international research in the field of reinforcement of timber structures.

DI

Andreas Ringhofer

Institute of Timber Engineering and Wood Technology

Graz University of Technology

Austria

Email: andreas.ringhofer@tugraz.at

Andreas Ringhofer studied Civil Engineering Sciences with Environment and Construction Management (bachelor programme) and Civil Engineering Sciences and Structural Engineering (master programme) at Graz University of technology. He earned a diploma degree in 2010. From 2011 to 2012 he worked as Project-Assistant and since 2012 he has been Univ.-Assistant at the Institute of Timber Engineering and Wood Technology at Graz University of Technology. His research topics are timber engineering and wood technology, especially connection techniques with self-tapping screws. This is also the topic for his PhD, which he is working on.

Table of Contents

Theme IV | Building Physics and Examples

Theme I

Product and Testing

DI(FH) Dr.techn.

Reinhard Brandner

Institute of Timber Engineering and Wood Technology

Graz University of Technology

Austria

Email: reinhard.brandner@tugraz.at

Reinhard Brandner studied Forest Products Technology and Management at University of Applied Sciences in Salzburg / Kuchl. He earned a diploma degree in 2006. Since 2005 he has been a researcher at the Competence Centre holz.bau forschungs gmbh and since 2009 a Univ.-Assistant at the Institute of Timber Engineering and Wood Technology at Graz University of Technology. He obtained his PhD degree in Civil Engineering Sciences at Graz University of Technology in 2012. His research topics are timber engineering, wood technology and stochastic modelling of materials and structures. He has published more than 20 (peer-reviewed) papers in international journals and conference proceedings.

David Crawford MSc

Centre for Offsite Construction and Innovative Structures,

Edinburgh Napier University

UK

Email: D.Crawford@napier.ac.uk

David Crawford is an Associate Consultant within the Centre for Offsite Construction & Innovative Structures (COCIS), a university/commercial research and outreach centre. David's areas of interest/expertise lie within solid timber construction, and the structural performance of modified timber. Currently David is working extensively on the development of Cross-Laminated Timber (CLT) using UK home-grown resource - the main objective of the project is to add value to the Scottish timber resource by carrying out all research, development & testing work necessary to establish commercial manufacture of CLT panels in the UK.

DI

Helene Unterweiser

Institute of Timber Engineering and Wood Technology

Graz University of Technology

Austria

Email: helene.unterwieser@tugraz.at

Helene Unterwieser studied Civil Engineering at Graz University of Technology. She earned a diploma degree in 2004. From 2004 to 2011 she worked at the Centre of Competence holz.bau-forschungs gmbh in Graz. Her research topics were grading in green and dry condition and wood products (for example resawn glulam). Since 2011 she has been quality manager and deputy of the technical management of the Lignum Test Centre, the testing laboratory of the institute of timber engineering and wood technology.

Production and Technology of Cross Laminated Timber (CLT): State-of-the-Art Report

Reinhard Brandner

Univ.-Assistant, Deputy Director of the Institute [1)] | Area Manager [2)]

Institute of Timber Engineering and Wood Technology, Graz University of Technology [1)]

Competence Centre holz.bau forschungs gmbh [2)]

Graz, Austria

Summary

Cross laminated timber (CLT) has been developed to a worldwide well-known and versatile useable building material. Currently increasing rates in production volume and distribution can be observed. In fact CLT, thanks to its laminar structure making it well suited for use in construction, provides new horizons in timber engineering, in areas which had until now been the realm of mineral building materials like concrete and masonry.

After a short introduction, this paper aims to demonstrate current production processes used for rigid CLT. In section 2 the process steps are described and essential requirements, as well as pros and cons of various production techniques, are discussed. Latest results of R & D and of development and innovation in production technology are presented. In section 3 test and monitoring procedures in the area of the internal quality assurance, known as factory production control (FPC), are presented. Diverse regulations, in the form of technical approvals for CLT as well as in the CLT product standard prEN 16351 [1], are discussed. Additionally, some technological aspects of the product, CLT, together with a comparison of geometrical and production relevant parameters of current technical approvals in Europe are provided in section 4.

In the final and main part of the paper, production and technology is presented in a condensed way. The outlook for current and future developments, as well as the ongoing establishment of the solid construction technique with CLT, is given. The product, CLT, comprises an enormous potential for timber engineering as well as for society as a whole. Standardisation and further innovation in production, prefabrication, joining technique, building physics and building construction make it possible for timber engineering to achieve worldwide success.

1. Introduction

Cross laminated timber (CLT) constitutes a plate-like engineered timber product, which is optimised for bearing loads in and out-of-plane. CLT is composed of an uneven number of layers (in general three, five, seven or even more), each of side-by-side placed boards (or beams), which are arranged crosswise to each other at an angle of 90° and quasi-rigidly connected by adhesive bonding. Because of continuous bonding and, consequently, quasi-rigid composite action between the single layers, a very compact and versatile useable product arises. Product dimensions allow its application as large-sized wall and floor elements as well as for other large-sized load-bearing plane-like but also linear structural components. In this way, modular dimensions, as known from light-weight wooden constructions (e.g. frame system), can be neglected, and window and door openings can be freely placed. The product has opened new dimensions in timber engineering and allows architects and engineers to design and realise monolithic buildings. This is now possible in a manner and dimension that had previously been restricted to reinforced concrete, brick or other mineral based building materials. In this way the product opens up a new building technique, the so-called “solid timber construction technique with cross laminated timber”, which makes it possible to design and construct with timber to previously unknown dimensions and scales.

The first ideas and developments date back roughly two decades, motivated by a missing market for the side-boards from sawmilling at that time. Opposite to the sawmill industry’s perception, in wood technology this material is known to show higher physical (mechanical) properties. In fact of that side-boards were used to make a solid material, locked in-plane to reduce swelling and shrinkage. This locking effect, caused by the crosswise arrangement of the single layers, can be seen in analogy to the single wood fibre (tracheid) or a composite of cells. Every wooden cell constitutes a composite of several cell layers, winding around the cell lumen in varying crosswise fibre angles. Their role and function, shows a specific orientation of the cellulose fibres, forming the primary constituent (total share of 50-60 %) in (clear) wood and (structural) timber. The advantages of this specific orientation between the layers have been well described (e.g. [2]; [3]; [4]; [5]), not only for the load-displacement and failure behaviour of the wooden cell composite but also, in analogy, for artificial fibre composites. In the broader sense CLT can also be seen as a synergetic product or as further development of historical timber construction techniques of logs or staves, with their origins in Central and Northern Europe. The combination of both principles, to a composite with rigidly bonded crosswise layers, constitutes the substantial innovative part of the new solid timber construction technique in CLT (see [6]).

The advantages of CLT, as large-sized and panel-like solid timber construction elements for the building sector, are in particularly obvious in its outstanding capability for pre-fabrication, a dry and clean construction technique, and for the short erection times on site (e.g. roughly one to two days per family house). The high dimensional stability underlines accuracy, with the lowest tolerances well-known for timber construction in general. Further decisive criteria which argue for this product are the ability to transfer loads two-dimensionally and the low mass, which make CLT ideal for reconstruction and upgrading of existing buildings (e.g. from Wilhelminian time) and also for resisting exceptional loadings (e.g. earthquakes). In contrast to light-weight timber structures (e.g. framing, post and beam system) the advantages of a clear separation of load-bearing from insulation & installation layers, the low air permeability, the distinctive specific storage capacity for humidity and temperature, the independence of modular dimensions in arranging window and door openings, as well as advantages in fastening of services and furniture also have to mentioned. The low mass, the stiffness and the bearing capacity against in-plane and out-of-plane stresses makes it ideal in multi-storey residential and office buildings, for schools, single family houses, halls and the conversion and upgrading of existing buildings and constructions, and for wide-span structures such as bridges. In particular, for wide-span structures, rib floors or box beams, as composites of CLT with linear timber products such as (finger jointed) construction timber, duo or trio beams or glued laminated timber (GLT, glulam), or constructed as folded-plate panels are really advantageous. Not at least because of its versatile applicability, the development and establishment of production capacities has grown rapidly, at 15-20% per year (see Fig. 1). These developments have been realised primarily in Austria and Germany, with a current production volume of roughly 500,000 m^3/a (2012), and a share of two-thirds of the total worldwide production volume solely in Austria. Worldwide activities in R&D, as well as processes for erection of small & medium buildings, are ongoing and observable.

Although, on first view, CLT seems to be becoming a mass market product, in reality sales are different from products like GLT and a production of “standard” stock CLT elements is unimaginable. In fact, in terms of incorporation or integration of an engineering department which itself acquires projects and provides customers (e.g. architects, civil engineers, carpenters and builders) with technical support, production and selling of CLT is very different. Thus the processes of cutting and joining have to be directly embedded in the overall production process.

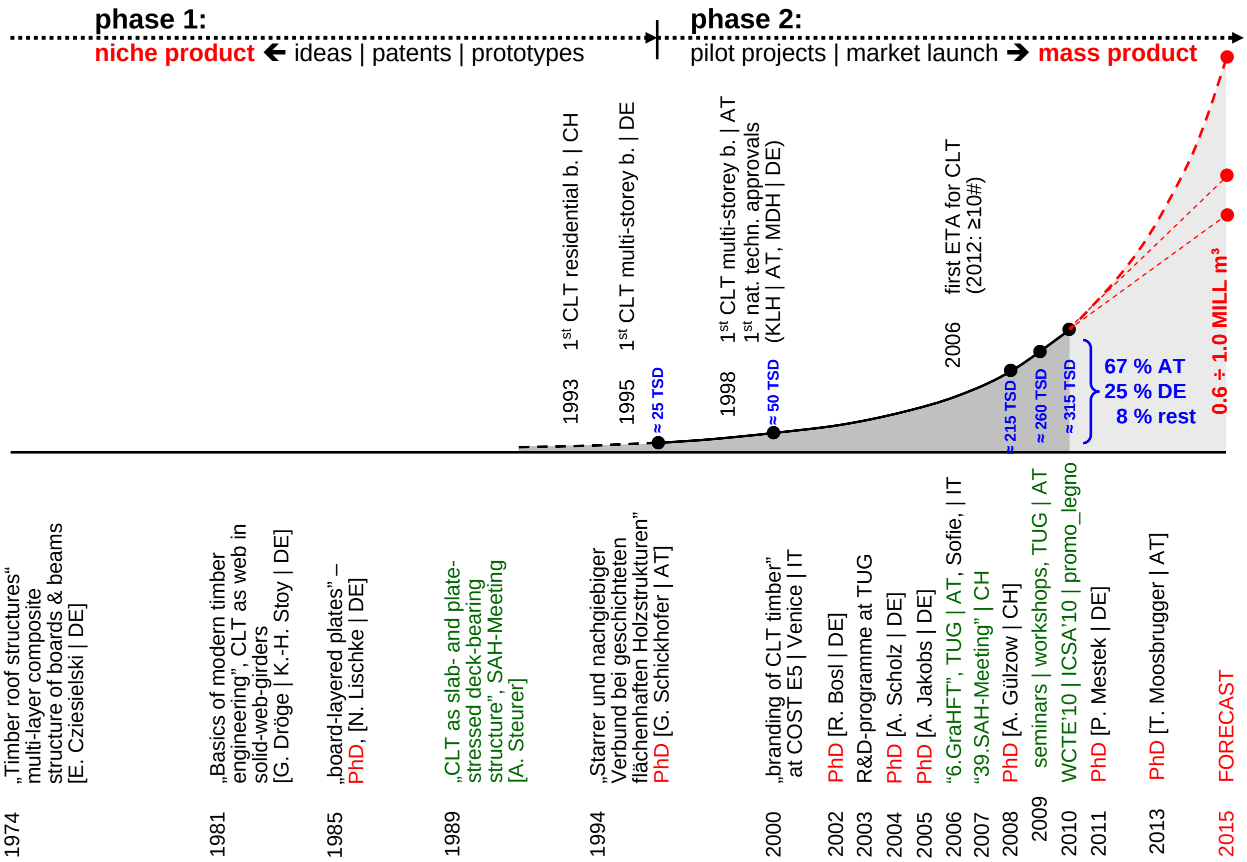

Fig. 1 Development of CLT – timeline ([7]; adapted)

For a maximum and reliable exploitation of CLT's potential and its worldwide distribution it is necessary to standardise its production, the design process and handling / joining technology, to the greatest possible extent. In that sense international regulations in the form of standards, which comprise all five areas "production & quality assurance", "testing and evaluation", "design & verification", "construction & assembling" and "joining technique", are essential; the value comes in reliable distribution and handling of the product, its technology and, hereby, an established solid timber construction technique. Of course, current regulations are primarily subject to the individual producers and given in technical approvals, in Europe, enforced by the DIBt (Deutsches Institut für Bautechnik, Berlin, Germany), the OIB (Österreichisches Institut für Bautechnik, Vienna, Austria) or European Technical Approvals (ETAs), with reference to national or European standards. The developments in standardisation within the past few years, not only in Europe, but also in Canada, United States and China, allow expectations with regard to the imminent launch of required documents.

This paper provides information on the topics "production & quality assurance" with accompanying data on the main technological characteristics of CLT. It is intended to give an overview of current production, with a focus on the industrial scale, as currently established in Europe.

2. Production and Processing of CLT: Overview and step-by-step

The production process of CLT is, in most steps, largely comparable with that of glulam. The relevant steps for production of CLT are shown in Fig. 2.

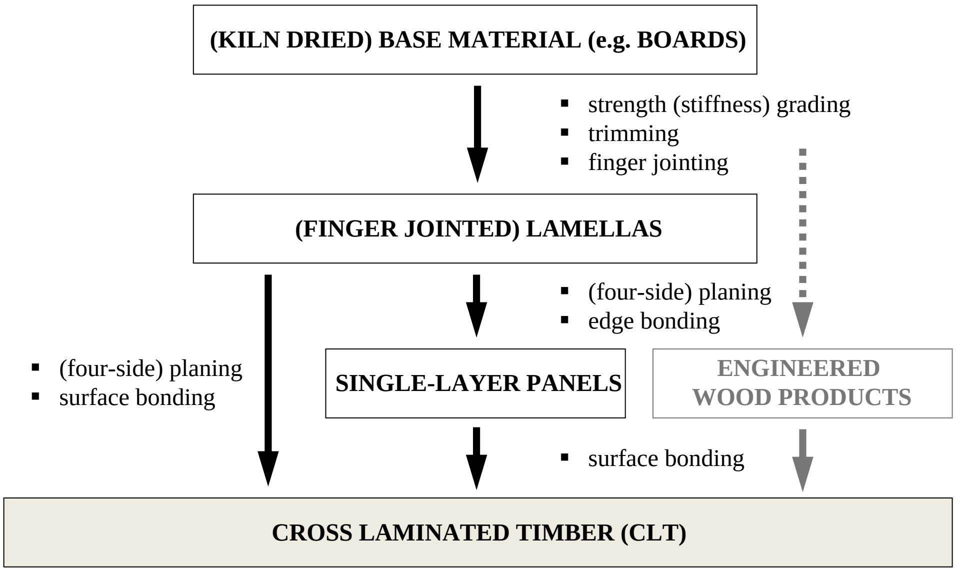

Fig. 2 CLT production process: overview

Basically, the production of CLT can be divided into following steps: (1) strength or stiffness grading of already (kiln) dried boards, (2) cutting out of local growth characteristics which do not meet the requirements of the strength class and finger jointing of the residual board segments to endless lamellas, (3) division and cutting of lamellas for later use in longitudinal and transverse layers of CLT, (4; optionally) adhesive bonding of lamellas to single-layer panels, (5) assembling and adhesive bonding of lamellas or single-layer panels to CLT, and (6) cutting and joining to structural elements (customising). The following sections show all relevant steps and process parameters are discussed.

2.1 Characteristics of Raw Material and Grading Process

Normally, CLT is composed of boards with thickness t_B = (12 to 45) mm (see also prEN 16351 [1]); following current technical approvals, a range of as high as (4 to 80) mm, which comprises veneer and beams, is allowed (see Table 5). In view of standardisation, and with a focus on construction tenders, in Austria the widely accepted standard for CLT layer thicknesses is t_B = (20, 30, 40) mm. Further standardisation, in particular in regard to layups of CLT elements optimised for stresses out-of-plane (e.g. for floors and roofs) and in-plane (e.g. for walls), is highly recommended. There is no upper limit for the board width but, due to rolling shear stresses between the CLT-layers, a minimum width of $w_B \geq 4t_B$ is recommended and thus anchored in current technical approvals. If this requirement is not kept, or the distance between relieves d_R is too short ($d_R < 4t_B$), then a reduced resistance in rolling shear has to be considered. Following prEN 16351 [1] the board width is regulated to (40 to 300) mm. The reference board width is proposed in accordance with structural timber and thus is $w_{B,ref}$ = 150 mm, as given in EN 338 [8] and EN 384 [9]. In general, only boards of prismatic cross section are used for CLT. In some cases profiling of the longitudinal edge may be meaningful, e.g. by tongue-and-groove or special types of clearance profiles (e.g. [10]). In this way, the emersion of adhesive is widely prevented and there is the possibility of including shadow gaps, to allow for effect of swelling and shrinkage. Furthermore, higher stability is provided, during pressing, in top layers composed of profiled single boards. Special emphasis has to be put on the assurance that all laminations of the same layer in CLT are of equal thickness. This is to secure that, during surface pressing, all zones in the CLT are exposed to the same transverse pressure and thereby fulfil the requirements on maximum gap widths between the boards of different layers; this depends on the adhesive system used, e.g. for one-component polyurethane adhesive, the bond line thickness has to be within (0.1 to 0.3) mm.

Currently for CLT, softwood species are mainly used. The main species is Norway spruce (*Picea abies*), in assortment with a small amount of White fir (*Abies alba*). Furthermore, softwood species such as Scots pine (*Pinus sylvestris*), European larch (*Larix decidua*), Douglas fir (*Pseudotsuga menziesii*) and Swiss stone pine (*Pinus cembra*) are used; the last mentioned species is primary for CLT of high appearance quality and thus for the top layers. Worldwide CLT, and the solid timber construction technique, uses other species, including Maritime pine (*Pinus pinaster*) in Sardinia / Italy. The use of hardwoods is, of course, also possible and has been already made, within the project “massive_living” (three-storey building) in Brucknerstrasse, Graz / Austria, where one of the 22 flats was realised completely with wall elements of CLT composed of silver birch (*Betula pendula*). Further possible species are poplar (*Populus spp.*), ash (*Fraxinus excelsior*), which are economical of interest, available in adequate sawmilling qualities, and providing a minimum in mechanical properties as required for structural load-bearing CLT. Hardwood species for appearance grade and use in the system may optimise the mechanical potential of CLT. The potential for an increase in bending stiffness, by means of more rigid transverse layers in shear or top layers of higher bending stiffness (e.g. birch, ash, black locust), or the improvement of the rolling shear resistance of CLT, by means of species like birch or poplar for the transverse layers, without increase or even reduction of overall thickness, is obvious.

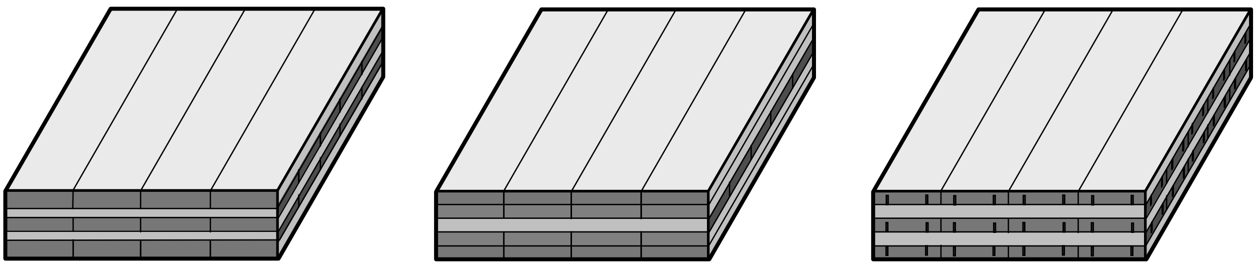

Fig. 3 Five-layered CLT element (schematically): homogeneous, symmetrical layup (left); (multiple) double outer layers (middle); base material with relieves (right)

As required by, and perhaps driven by, other functions of CLT (e.g. air tightness, higher resistance against rolling shear, acoustic appearance or tactile requirements), it is possible to substitute single layers by laminar engineered timber products, e.g. laminated veneer lumber (LVL), oriented strand board (OSB), plywood or single- or multi-layer solid wood panels. The suitability of the substitute has to be verified, particularly if such a layer is explicitly taken into account in load transfer.

The base material for CLT is in general technical (kiln) dried and conditioned to a moisture content of $u = (12 \pm 2)$ %. Following current technical approvals a range as wide as (8 to 12) % ± 2 % can be found. In the next stage the material is visually or mechanically strength (stiffness) graded, e.g. according to EN 14081-1 [11] or DIN 4074-1 [12]. Within a single layer, all boards have to be of the same grade, otherwise the grade of the single layer has to be assigned according to the lowest grade of the boards used. Currently, in Europe, the strength class system of EN 338 [8] applies, although this system has been developed for structural timber, which is mainly stressed edgewise in bending. Common strength classes are C24, for a homogeneous layup, and, if combined, with C16 / C18 for the transverse layers. In fact, as for glulam, the bearing capacity of CLT stressed out-of-plane in bending is primary governed by the resistance of the top layers in tension parallel to grain and a demand-oriented grading of boards, according to requirements in tension parallel to grain, is recommended.

According to the glulam standard, prEN 14080 [13], the grading in T-classes, based on the characteristic 5 %-quantile of strength and characteristic mean of E-modulus in tension parallel to grain, is suggested. Following the current technical approvals in Europe, the product CLT is primary composed of C24 according to EN 338 [8]. Of course many technical approvals allow a specified amount of boards (i.e. 10 % or 30 % per board layer) dedicated to the next lower strength class, without consideration in the mechanical properties of CLT. It is assumed that this regulation can be traced back to a rough interpretation of DIN 4074-1 [12] (section 6.3.2), which gives tolerances for visual grading where a deviation of ≤ 10 % from grading criteria within ≤ 10 % of the material volume is allowed. This disagrees with the statement in the previous paragraph of this paper that it is in generally not permissible to mix boards of different grades within one layer ([6]). Although not common today, in some cases (e.g. in case of a CLT floor plate which is primary stressed in bending) stiffness rather than strength grading of the board material, in conjunction with compliance of minimum requirements on strength, can be more constructive. In fact, in this way, CLT elements have to be designed for serviceability (according to the deflection or in cases of longer spans according the vibrations) more than for ultimate limit state. This is because the transverse layers make CLT more flexible in shear. Consequently, the optimisation of stiffness is an important target to achieve economy and value. Based on several research works, which address the homogenisation effect as a consequence of the common action of boards in a (quasi) rigid composite (e.g. in glulam), it is well known that the dispersion in strength properties of system products like GLT or CLT, in comparison to that of their base material, is significantly reduced. The homogenisation is even more pronounced and increases with increasing dispersion in strength properties of the base material (board; elements) (see e.g. [14]; [15]; [16]; [5]). In general, and in comparison to mechanical grading, lower selectivity in visual grading normally leads to a higher dispersion in strength properties of boards. If boards (elements) are used in a CLT (system), then higher homogenisation effects can be expected (e.g. in resistance to bending out-of-plane and against tension and compression stresses in-plane). Consequently, stiffness grading, combined with a method assuring the compliance with minimum requirements on strength (e.g. by exclusion of specific growth characteristics or by stressing of each board with a predefined proof load), can be a very constructive and economic grading concept.

The layup of CLT is in general symmetrical. In cases where additional layers are applied and rigidly connected (e.g. acoustic panels), in some circumstances it can be advisable to apply a counteracting layer to maintain dimensional stability, which is, in regard to swelling and shrinkage, equivalent to the additional layer(s). Normally CLT is composed homogeneously of layers of equal strength properties. A combined but symmetric composition of layers with different strength classes is possible but requires special consideration in calculating the mechanical properties, e.g. by taking into account the rigid composite theory. Some compositions of CLT, which are optimised for example for stresses out-of-plane, feature two or more parallel layers as combined top-layers, applied to optimise the performance of the CLT’s bending stiffness by increasing the moment of inertia (see Fig. 3, middle).

2.2 Production of finger jointed Lamellas

Based on longitudinal incremental results as output from strength grading, local (discrete) growth characteristics which do not meet the requirements of the strength class are cut out and the remain board segments joined again by means of finger joints (FJs). Thus finger joints provide an economical approach for joining board segments longitudinally; discrete sections, with a possible negative impact on the target strength distribution of the board sample, are removed selectively, with the aim that the main part of the original board remains.

The finger joint itself constitutes a self-centring profile representing a folded scarf joint. By maximising the bond surface and minimising longitudinal losses of board material, optimised profile finger joints enable simple, fast and form-fit connection between elements. For CLT lamellas, profiles that have been already optimised and approved for the production of glulam are used with finger length l_{FJ} = (15 or 20) mm. For an overview of these profiles and of main geometric parameters see Table 1. Of course it is also possible to joint whole CLT elements by means of large finger joints (LFJs) with finger lengths of $l_{FJ} \geq 45$ mm; this is discussed in more detail in section 2.6.

Tab. 1 Finger joint profiles, geometric measures and loss in cross section

l_{FJ} [mm]	p [mm]	b_t [mm]	b_n [mm]	l_t [mm]	α [°]	$v(b_n)$ [%]
15	3.8	0.42	0.52	0.5	5.6	13.6%
20	5.0	0.50	0.60	0.5	5.7	12.0%
20	6.2	1.00	1.11	0.5	6.0	17.8%
50 [1)]	12.0	2.00	2.48	3.0	4.6	20.7%

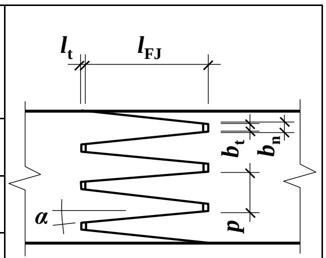

l_{FJ} … finger length; p … pitch; b_t … tip width; b_n … base width; l_t … tip gap; α … flank angle; $v(b_n)$ … loss in cross section

1) recommended profile for large finger joints (see EN 387 [17])

The position of finger joints can be edgewise (fingers visible on the side face; as common in glulam) or flatwise (fingers visible on the narrow face) (see Fig. 4). The advantage of flatwise finger joints is primarily in regard to a higher visual quality, as no fingers are visible on the surface of CLT. Additional advantages are in regard to building physics (e.g. airtightness).

The glued finger joint constitutes a quasi-brittle longitudinal joint between board segments, which are made into endless lamellas. In cases where these lamellas are stressed in tension parallel to grain, within the joint and between the edges, these stresses have to be primarily transferred by shear. These shear stresses are optimal for bonded joints in general. Due to the loss in cross section and the specific stress situation, finger joints have to be positioned within the clear wood zone of boards, e.g. in a zone free of knots and apparent local or global grain deviation. In doing so, finger joints which are stronger than the board segments they join are possible, although the cross section at the finger tips is reduced up to (12 to 18) % (see Table 1). The shear stresses at the edges occur in interaction with stresses perpendicular to grain. These stresses perpendicular to grain are minimised by reducing the angle α. According to [18] the optimum angle would be $\alpha = 4°$; at $\alpha > 5.7°$ a significant reduction in strength was observed. Furthermore, due to stress concentrations at the finger gap, a ratio of $l_t / b_t > 1.00$ or at least of > 1.50 is proposed. More details and further discussion as well as a literature survey can be found e.g. in [18], [19], [20], [21], [22] and [5].

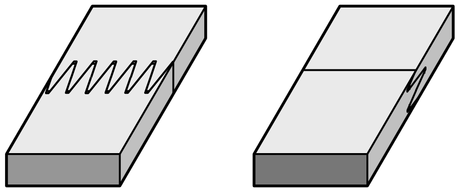

Fig. 4 Edgewise finger joint (left); flatwise finger joint (right)

The production requirements for finger joints are regulated in EN 385 [23] and prEN 15497 [24]. Some technical approvals for CLT also give regulations in reference to DIN 1052 [25]. The main requirements are: (1) finger joints have to be placed within the clear wood zone of structural timber elements, i.e. free of local (e.g. knots) and global grain deviations and reaction wood; (2) the suitability of the adhesive system used has to be assured (e.g. by technical approvals, EN 301 [26] (type I) or EN 15425 [27]); (3) the technical requirements for using an adhesive system (moisture content, temperature, applied quantity, possibilities of application, bonding pressure, hold time, etc.), as regulated by the relevant standards, as well as by the adhesive producer, have to be met. In particular the bonding pressure and the applied quantity of adhesive have to be adjusted to the timber species. Whereas a too low pressure may lead to an insufficient wetting of adhesive on all flange surfaces and to too low adhesion between the adherends during the transport of the lamellas, in contrast, a too high pressure may provoke undue splitting of the adherends at the finger base or even of the whole jointed board segments. Thus the longitudinal bonding pressure has to be adapted according to the parameters (i) finger joint profile, (ii) timber species, (iii) moisture content of the adherends, and (iv) cross-section dimension of the adherends. Overall the same regulations as already given for finger joint connections in solid timber or glulam occur.

To assure an optimum performance of the finger joints, i.e. the suitability of the adhesive system used to produce strong, stiff and durable joints, it is necessary to adjust the adhesive system to the requirements on the structure and to the timber species. To minimise stress concentrations within finger joints, the application of adhesives that show comparable elastic and shear properties as the adherends is recommended. In general, and as mentioned before, only adhesive systems that are permitted for use in load-bearing timber structures (e.g. according to EN 301 [26], EN 15425 [27] or according to technical approvals) are allowed. Currently, mainly melamine-urea-formaldehyde (MUF) and one-component polyurethane adhesives (1K-PUR) are used. Both adhesives have a nearly uncoloured bond line. 1K-PUR is generally more flexible but also more vulnerable to higher temperatures ($T < 60°$) if not modified adequately. Both adhesives are also resistant to exposure to sunlight and humidity and also to hydrolysis. The advantages of MUF are its higher resistance against high temperatures (e.g. in case of fire) and its gap-filling and penetrating properties. Furthermore the curing process can be accelerated by increasing the temperature or by means of high-frequency technology. The disadvantages are the emission of formaldehyde, its limited storage stability (1K-systems) and the strict mixing ratio of resin and hardener (2K-systems). In contrast, 1K-PUR can be easily adapted to the individual production requirements, in particular in regard to its reactivity and curing time. Polyurethanes are also free of formaldehyde and provide some amount of internal pressure during bonding. Due to the increasing formation of gas cavities with increasing bond line thickness, the tolerances in thickness of boards within the same CLT layer have to be strictly kept.

With the focus now on the strength, in general the performance of finger joints, stressed in tension parallel to grain, depends primary on the performance of the joined timber elements, the adhesive and the quality of production. Thus the resistance of finger joints is governed by that of the weakest element. In timber engineering, the resistance of adhesive bonding has to be at least as strong as of the joined timber elements. Consequently, a single finger joint connection can be reduced to a serial system of $N = 2$ joined timber elements, constrained in strength by the weaker of the two. Of course, although the quality of joined timber elements is essential, the complexity of production parameters influencing the joint performance individually is subject to each producer and production line (e.g. bonding pressure, adhesive, moisture content, temperature, vibrations immediately after pressing, curing time). This makes it impossible to objectively model and rule explicit requirements for the finger joint performance. Consequently, and in line with current regulations on finger joint tensile strength for glulam in EN 1194 [28], it is recommended that minimum requirements are regulated in relation to the joined timber elements and thus dependent on the strength class of each CLT layer (e.g. [29]; [5]).

To define minimum requirements of the tension strength parallel to grain of finger joints, the median strength and thus the failure probability of a series of n finger joints and that of a series of $m = (n + 1)$ board segments, which together comprise a lamella at reference length, are kept equal, with $f_{t,0,B,50,m} = f_{t,0,FJ,50,n}$. In compliance with EN 1194 [28], a reference length $l_{L,ref} = 2{,}000$ mm of the lamella is applied. Examinations on Central European glulam lamellas showed an expected distance between finger joints of $E[d_{FJ}] = [2.0 \text{ to } 2.5]$ m ([30]), which is in good agreement with $l_{L,ref}$. Thus on average, and "to be on the safe side", at least one finger joint per reference lamella ($n \geq 1 = m - 1$) has to be considered. The minimum requirement on the 5 %-quantile of finger joint tension strength, $f_{t,0,FJ,05}$, dependent on board tension strength, $f_{t,0,B,05}$ at $l_{B,ref} = l_{L,ref} = 2{,}000$ mm, can be formulated as:

$$f_{t,0,FJ,05} \geq \zeta_{05} \cdot f_{t,0,B,05}. \tag{1}$$

Based on extensive test experiences, a coefficient of variation $CV[f_{t,0,B}] = (30 \pm 10)$ % for board tension strength parallel to grain can be expected. This range can be further divided into a sub-range of $CV[f_{t,0,B}] = (35 \pm 5)$ % in case of visual graded boards or mechanically graded boards in only two (three) classes (including the class of reject), and $CV[f_{t,0,B}] = (25 \pm 5)$ % if the boards are mechanically graded in more than two (three) classes (see [31]; [29]; [5]). In regard to the tension strength of finger joints, a range of $CV[f_{t,0,FJ}] = (15 \pm 5)$ % is expected (see [29]; [5]). Based on an extensive data analysis, and in agreement with EN 385 [23] and prEN 15497 [24], the two-parametric lognormal distribution 2pLND is taken as representative distribution for $f_{t,0,B}$ and $f_{t,0,FJ}$. For simplicity both properties are modelled as being independent of each other. Thus a very simple model approach can be formulated. Table 2 provides the minimum requirements on the finger joint tension strength based on the expected ranges of $CV[f_{t,0,B}]$, $CV[f_{t,0,FJ}] = 15$ % and $n \leq 2$ (see also [5]). Thus a very simple approach, of high practical relevance, is given.

Tab. 2 Minimum requirements on finger joint tension strength parallel to grain

$f_{t,0,FJ,05} \geq \zeta_{05} \cdot f_{t,0,B,05}$	$\boldsymbol{\zeta_{05} \geq 1.40}$	for $CV[f_{t,0,B}] = (35 \pm 5)$ %
	$\boldsymbol{\zeta_{05} \geq 1.20}$	for $CV[f_{t,0,B}] = (25 \pm 5)$ %

Regulations for continuous internal as well as semi-annual external quality assurance can be found in the technical approvals as well as in prEN 16351 [1], the European standard for CLT. Further details on quality assurance procedures are discussed later in section 3.

2.3 Production of Single Layers (optional)

In general, the producers of CLT aim to reduce the width of gaps. This is done in respect of building physic aspects (in particular in regard to fire design, airborne sound and airtightness) but also in regard to joining techniques, in particular considering pin-shaped fasteners such as nails, screws or dowels. A further reason is due to aesthetics, if the surface of CLT is left visible in final use.

As consequence, some CLT production lines produce, as an intermediate step, single-layer panels that are further cross-wise surface bonded to CLT. These solid panels are applied for the whole CLT or only for specific layers (e.g. for the top). In doing so, gaps can be completely eliminated or at least reduced to gaps between the panels. A further advantage occurs in final surface pressing of the CLT. As the surface of these panels is already smooth, equalised and, of course, more precise in thickness than CLT composed of single boards, a lower surface bonding pressure is required. Depending on the thickness of the single-layer panels and the timber species (both are relevant parameters for the expected plate stiffness and thus for the resistance against pressing) a pressure achievable in vacuum presses or by bracket, nail or screw pressing can be sufficient for an adequate bond quality. The suitability of each pressing procedure, in particular in connection with the adopted adhesive system and the allowed tolerances in glue-line thickness, has to be clarified and assured; for further details see section 2.5. In contrast to an incomplete and undefined edge bonding that sporadically occurs during edge and surface pressing of single boards to CLT, a further advantage of single-layer panels is the defined edge bonding between the lamellas. In particular, in case of large-sized CLT elements, edge pressing is normally limited to layers with orientation in direction of production. Therefore these layers are overlapping the transverse layers.

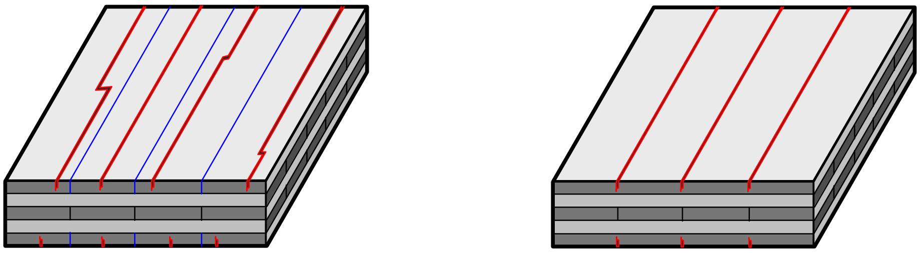

Fig. 5 Checks due to swelling and shrinkage in CLT with edge bonded top layers (left) and without edge bonding (right)

As already mentioned, defined edge bonding has advantages in building physics (e.g. in regard to fire, airborne sound and airtightness). In fact numerous technical approvals for CLT allow a ratio of w_B / t_B smaller than four, if the boards or laminations are edge bonded. Nevertheless, the generally expected climatic variations cause internal stresses due to swelling and shrinkage creating and create unavoidable checks on the surface of CLT and within CLT layers. Thus the advantages of edge bonding on building physics and the mechanical potential of CLT are limited. As consequence of the quasi-rigid connection between the boards, an irregular pattern of checks can be expected; longitudinal checks seldom occur in the bond line. In contrast, in CLT composed of layers of boards without or only undefined edge bonding, the swelling and shrinkage takes place between the boards and results in a more regular pattern of gaps (see Fig. 5).

During the production of single-layer panels, the suitability of the adhesive system used for edge bonding has to be assured in the framework of an internal and external quality control procedure. Examples of frequently used and suitable adhesive systems are aminoplast adhesives according to EN 301 [26] (type I; melamine-formaldehyde, MF and melamine-urea-formaldehyde, MUF) and one-component polyurethane adhesives (1K-PUR) according to EN 15425 [27]. For more information on adhesives and quality control see section 3.

In producing single-layer wood panels as an intermediate product in CLT production, in principle three approaches can be used:

2.3.1 Approach 1: Single-Layer Panels made by Edge Bonding of Boards or Lamellas

The board material has to be strength (or stiffness) graded, e.g. according to EN 14081-1 [11] or DIN 4074-1 [12]. Thus the same requirements as given in section 2.1 and 2.2 apply. The four-sided planed boards of specific length, with or without finger joints, are continuously joined to endless plates by edge bonding. These single-layer panels are subsequently equalised and formatted according the dimensions required for longitudinal and transverse layers of CLT. As these layers are subsequently made into CLT, there are normally no specific mechanical requirements on the edge bonding providing the requirement that $w_P \geq 4\ t_B$ is fulfilled, with w_P as the width of the panel, or the expected distance between checks due to swelling and shrinkage, or the distance between relieves. This limit has been introduced to prevent early failures in rolling shear and has been anchored in numerous technical approvals for CLT.

2.3.2 Approach 2: Single-Layer Panels according to EN 13986 [32]

The requirements according to EN 13986 [32] or of appropriate technical approvals apply. Subsequently it has to be assured that the physical / mechanical properties, as required for composing single layers to CLT of a specific strength class, are met. It has to be mentioned that the mechanical properties of single-layer panels, according to EN 13986 [32], are based on plate-strips. The strength grading as mentioned before in section 2.3.1 does not apply. Thus the suitability and quality of the panels for the production of CLT has to be assured by the implementation of an adequate internal and external quality assurance. EN 13986 [32] gives also specific requirements on the shear strength of the edge bonding, which are regulated depending on service class in use.

2.3.3 Approach 3: Single-Layer Panels gained by axial splitting of Glulam

In this approach single-layer panels are made by axial splitting glulam, which is normally done by band resaws. In general only homogeneously composed glulam is used. The strength grading for finger jointed lamellas of the glulam beam (e.g. according to EN 14081-1 [11] or DIN 4074-1 [12]) is of course not transferable to the panels. As for the second approach in section 2.3.2, again, an adequate internal and external quality assurance procedure has to be set up to approve the adequacy of the panels for CLT production.

In a further step, independent of the approach and before pressing the single-layer CLT, panels are in general planed or sanded. To guarantee that the whole surface area of CLT is under equal and uniformly distributed pressure, smoothness and the prevention of a minor tolerance in average thickness (e.g. according to [33] of ± 0.15 mm) has to be maintained.

2.4 Application of Adhesive for Surface Bonding

In general the guidelines and requirements of the adhesive manufactures have to be followed. It has to be remarked that some parameters, like bonding pressure, quantity of applied adhesive, moisture content of adherends and others have been based on experience with glulam. In the meantime, some adhesive producers have adapted their regulations for CLT. In particular the parameters bonding pressure and applied quantity are of relevance (see e.g. section 2.5.1). In comparison with GLT, the possibility that the applied adhesive is pressed out from the bond lines of the plate-like product CLT is significantly reduced. This aspect requires consideration in regulating the pressing conditions. This is also confirmed in section 2.5.1 referencing [34]. In this work very good and sufficient bond qualities were reached by applying the minimum of quantity of adhesive per square meter, as recommended by adhesive producers.

The application of the adhesive for surface bonding is normally carried out mechanically and contactless (i) on single lamellas in a continuous through-feed device or (ii) in a positioning or press bed on pre-positioned CLT layers. A line-wise discrete application of adhesive is preferred.

2.5 Composing and Pressing of Boards or Single Layers to CLT

2.5.1 Some general Comments and Recommendations for Bonding Pressure

In general CLT can be composed of flexible connected boards, lamellas or layers, e.g. by joining them crosswise by means of ring-shank nails (e.g. [35]), hardwood dowels (e.g. [36]) or hardwood screws (e.g. [37]). Of course, more generally CLT is composed of quasi-rigidly connected lamellas or layers, i.e. by surface bonding. This contribution focuses on quasi-rigidly composed CLT elements.

Dependent on the pressure device, the following differentiation can be made:

(1) surface bonding by means of hydraulic press equipment;

(2) surface bonding by means of vacuum press equipment;

(3) surface bonding utilising the pressure of screws, brackets or nails.

Depending on the device, bonding pressures of (0.10 to 1.00) N/mm² and even higher can be provided by (1) a hydraulic equipment, whereas vacuum presses (2) and pressing with screws, brackets or nails (3) attain bonding pressures in the range of (0.05 to 0.10) N/mm² and (0.01 to 0.20) N/mm², respectively (see e.g. [38]).

Of course regulations of an ideal surface bonding pressure for CLT are still missing. Thus a more general discussion for further clarification is provided. In general, in cases of suitable surface condition of flatness and of only negligible deviations in thickness of the adherends within and between the single layers for CLT production, theoretically no bonding pressure is required. In practice there will be always some roughness on the surface, warp and twist of the adherends and deviations in the thickness of the adherends. Thus a minimum bonding pressure is required and has to be regulated to the best level to suit the main parameters. The demand on a minimum bonding pressure can be also due to the adhesive application system (e.g. in case of line-wise application, a specific minimum pressure securing a complete wetting of the surface is required). Thus the main parameters defining the requirements on a minimum bonding pressure are (i) to secure a complete wetting, and (ii) to secure a defined permitted bond line thickness. In regard to (ii) types of adhesive can be differentiated first into close-contact adhesives and gap-filling adhesives and secondly into swelling adhesives (e.g. polyurethane adhesives) and shrinking adhesives (e.g. aminoplast- and phenoplast-adhesives). For securing a defined bond line thickness, the two parameters of applied quantity and bonding pressure have to be borne in mind. According to [38], and due to swelling and shrinking, the minimum bonding pressure in case of phenol or melamine based adhesives is in general in the range of (1.40 to 2.00) N/mm² (!) whereas for polyurethanes (0.01 to 0.10) N/mm² should be sufficient. Following the regulations for the production of glulam in EN 386 [39] and prEN 14080 [13], a surface pressure of 0.60 N/mm² for $t_B \leq 35$ mm and (0.80 to 1.00) N/mm² for 35 mm < $t_B \leq 45$ mm thick lamellas without relieves is given. The regulations, depending on the lamella thickness, take account of the resistance of lamellas against deformation, i.e. against longitudinal and transverse bending deformation and torsion.

Beside the minimum also the maximum allowable bonding pressure requires regulation. It is known that a too high pressure causes damage of the adherends' surfaces ([40]), e.g. by crushing the cell structure. Consequently a reduced adhesive penetration and shear resistance ([41]) can be observed in combination with an increasing possibility of excessive squeezing-out of adhesive from the bond line, which causes insufficient bonding. Thus the bonding pressure has also to be regulated in relation to the timber species. This, on the one hand due to the expected resistance against torsional and bending deformations and, on the other hand due to the differences in the stress-strain curves in compression perpendicular to grain, which affects the relationship to the proportional limit of the linear-elastic course. On the basis of compression perpendicular to grain, tests accomplished on Norway spruce (*Picea abies*) according to EN 408 [42], the following statistics can be found: $f_{c,90,mean}$ = (3.0 to 3.4) N/mm², $f_{c,90,05}$ = (2.2 to 2.5) N/mm² and a coefficient of variation CV[$f_{c,90}$] = (22 to 28) % ([43]). The proportional limit can be estimated to be at 30 % of $f_{c,90}$ (according to [44] roughly at 50 %). Thus, to widely (≥ 95 %) prevent plastic deformations on the surfaces of adherends, the upper limit of bonding pressure can be estimated at 1.10 N/mm². In [44] it was found that the cell structure in Norway spruce starts to be damaged at 0.60 N/mm² and 1.00 N/mm², respectively, in cases of horizontal and vertical annual growth rings; a decrease in shear strength was already noticed at a pressure of ≥ 0.40 N/mm² and ≥ 1.0 N/mm². Following [45], in Norway spruce the internal pressure has to be limited to ≤ 1.0 N/mm². Thus the externally applied pressure needs to be adapted to the adhesive system, if it swells or shrinks, and the swelling pressure of the timber itself as consequence of surface wetting. Of course, as the annual ring pattern for products like glulam or CLT is not restricted in case of Norway spruce or comparable timber species, the surface bonding pressure has to be limited to ≤ (0.4 to 0.6) N/mm².

To summarise briefly, the required surface bonding pressure can be defined as function of (i) the adhesive system, (ii) the timber species, (iii) the geometry of the adherends in regard to roughness and flatness of the surface and allowed tolerances in thickness, (iv) the adhesive application system, and (v) the applied quantity of adhesive. The applied quantity itself depends on the roughness of the adherend's surface and consequently on the timber species (for example: ring-porous vs. diffuse-porous hardwoods).

For clarifying the consequences of the interacting parameters, bonding pressure and applied quantity on the CLT production, a comprehensive research project was conducted (see [34]). In this project, two types of 1K-PUR adhesives, three bonding pressures of (0.1, 0.3, 0.6) N/mm² and various applied quantities, which were defined to secure a complete wetting in unidirectional surface bonding in relation to bonding pressure, were investigated. Furthermore, the effect of cyclic climatic variations (20 °C / 90 % rel. humidity and 30 °C / 40 % rel. humidity; quantities of cycles: 0, 10, 21, 25) on the properties of bonding was also analysed. This was done in specific laboratory conditions and produced three-layered CLT elements of Norway spruce of strength class C16 and C24 according to EN 338 [8]. The surface bonding properties were investigated by means of rolling shear tests on whole CLT elements in bending according to EN 408 [42], block (rolling) shear tests on the single glue line according to EN 392 [46] and delamination tests according to EN 391 [47], approach B. To summarise, although the applied adhesive quantities were overall on the lower limit of producer's recommendations, the investigated bonding pressures were found to be sufficient to realise adequate bond qualities, providing that the dispersion in thickness between boards of the same CLT layer was kept low. The relevance of this demand can be easily demonstrated by a simple calculation example: With Hooke's law for linear elastic material and with the parameters for C18 according to EN 338 [8] with $E_{c,90,mean}$ = 380 N/mm², it can be shown that, to compress a 40 mm thick board by 0.10 mm, an average surface pressure of 0.95 N/mm² is required. In contrast, parameters like warp or twist of the board material showed nearly no or at least a negligible effect on surface bonding. This is because of the relatively low E-modules longitudinal and transverse in bending and the G-modulus of timber in torsion. Of course, a positive relationship between bonding pressure and shear strength was observed in cases where the applied adhesive quantity was beneath the recommended quantity and thus too low or the deviations in thickness too high.

Thus it can also be stated that, for CLT composed of single boards, a low pressure can be sufficient, providing that a very strict and small tolerance in the thickness of lamellas within one CLT layer is secured. Therefore, the board thickness should be controlled in framework of the internal quality assurance procedures. Following the calculation example above, and in regard to the thickness range of CLT lamellas, a tolerance of $\leq (\pm\ 0.10)$ mm is advised; although this demand is stricter than that already partly anchored in technical approvals for CLT (see e.g. [33], [48], [49]). This strict tolerance is also argued by the requirements on the allowed bond line thickness of e.g. (0.1 to 0.3) mm in case of 1K-PUR.

2.5.2 CLT Production by means of Hydraulic Press Equipment

Using hydraulic press equipment, it is possible to provide nearly every desired surface pressure. Of course current systems provide an upper limit of 0.8 (1.5) N/mm², which makes them flexible enough to extend the productions for thicker and thus stiffer single-layer elements, and also for hardwoods. In contrast to vacuum facilities or nail, bracket or screw pressing, it is possible to provide specific edge pressure, e.g. solely on the top, transverse or on individual layers for assuring homogeneously closed gaps. Of course hydraulic press systems are normally restricted to produce standard CLT elements without curvature or of other shapes. As consequence of parallel pressing surfaces, it is not possible to balance local unevenness or deviations in thickness as it is, for example, in a vacuum press.

Fig. 6 Placing and aligning of the single layers (left); positioning of layers and application of adhesive (right) (© Minda-Industrieanlagen GmbH / DE)

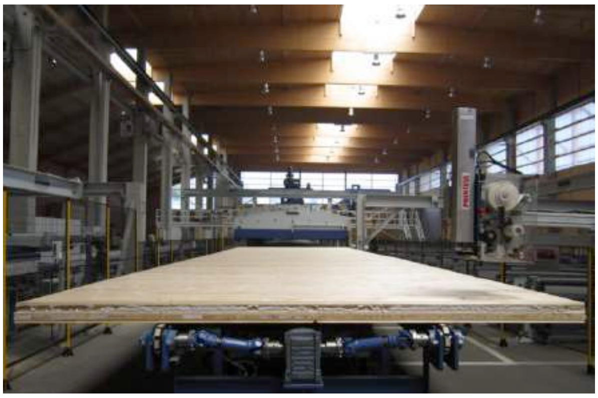

Fig. 7 Hydraulic surface and edge pressing device (left); unloading of ready produced CLT (right) (© Minda-Industrieanlagen GmbH / DE)

A great advantage of hydraulic facilities is their flexibility in regard to automation of process steps before, during and after pressing. This comprises the positioning and alignment of single boards or layers, the application of adhesive, the conveying into and out of the press, the application of specific edge pressure and the pressing itself, where differentiation has to be made also in regard to the adhesive system and the curing process (cold, hot or with high frequency). Depending on the production volume and market orientation, modular processing units with different degrees in automation are provided by some press producers. For example Minda-Industrieanlagen GmbH / DE offers a press system (see Fig. 6 and Fig. 7) with stages of expansion semi-mechanically equipped with three press cycles per shift up to twelve press cycles per shift in a fully mechanical processing. Thus it is possible to move step-by-step into the CLT market.

Depending on the CLT production, further differentiation can be made in press facilities for small CLT elements, which are further connected by large finger joints, and large-sized CLT elements with a dimension of up to l / w / t = ≤ 18.0 m / ≤ 3.5 m / ≤ 400 mm. Dependent on the required production volume and the adhesive properties, single or multiple CLT elements can be produced in one press cycle. Also dependent on the production volume and the degree of automation, it can be meaningful to adapt the adhesive system to allow for example one press cycle every 40 minutes.

Further differentiation can be made in the production of CLT elements with or without edge bonding and with or without door and window openings. In the last case the adhesive application system has to be adapted to omit these openings. In regard to the press system itself, further differentiation is possible in fixed press facilities and moving CLT elements (e.g. Minda-Industrieanlagen GmbH / DE, Springer Maschinenfabrik AG / AT, Kallfass GmbH / DE) and horizontally displaceable press facilities as e.g. constructed by Fr. Leiße & Söhne GmbH & Co. KG / DE. The productivity of current press systems allows a CLT production volume of 25,000 m³ per year and shift.

A comparable press facility is provided by Ledinek Engineering d.o.o. / SI. Here a pneumatic press system is combined with tie bars.

2.5.3 CLT Production by means of Vacuum Press Equipment

Another possibility, for production of CLT as rigid composite by adhesive bonding, is to press single boards or layers by vacuum (see Fig. 8). In doing so a pressure of (0.05 to 0.10) N/mm² can be reached. Thus specific and strict requirements on the surface quality, in particular on evenness and minor tolerances in thickness have to be met to assure an adequate bond line quality.

Also, limits in warp and twist have to be considered. For reduction of the stiffness against bending and torsion deformations, relieves are made longitudinal to the grain and, according to prEN 16351 [1], not deeper than 90 % of the lamella thickness and in width not wider than 4 mm. As already mentioned, unless the compliance of the ratio d_R / $t_B \geq 4$ is kept, reduced rolling shear strength of CLT must be considered. Because of the limited bonding pressure, a limit in processable layer thickness or timber species can occur. In regard to the requirements on adherends' surface, evenness and thickness tolerances usage of single-layer panels can be advantageous.

Fig. 8 Vacuum press in combination with an adhesive application system (© woodtec Fankhauser GmbH / CH)

Overall vacuum press facilities allow an economical surface bonding and are well suited for small and medium-sized CLT productions with a production capacity of (2,000 to 5,000) m³ per year per shift. The processing itself is in general semi-mechanical. The boards or layers are placed manually, whereas adhesive application is operated semi-mechanical. It is also possible to compress the top layers by means of lateral pressing bars before the air in the airtight synthetic rubber foil is evacuated and the CLT is compressed homogeneously. This homogeneously distributed pressure in principle enables production of curved or general shaped CLT elements and offers also the production of composite elements like box-beams or rib floors. Also local thickness deviations can be balanced to some extent and sufficient bond qualities achieved.

2.5.4 CLT Production by means of Bracket, Nail or Screw Pressing

Another alternative approach for producing CLT as rigid composite is to provide the bonding pressure discretely by nails, screws or brackets. The commonly achieved pressure is within (0.01 to 0.20) N/mm² and thus comparable with vacuum press facilities. Consequently, the same requirements on the base material used for making CLT apply, see section 2.5.3. The advantage of this approach is given by the minimum effort and investments necessary to produce CLT. Of course, in comparison to a flexibly manufactured CLT, e.g. where the layers are solely connected by nails, screws or brackets, knowledge and experience about adhesive bonding is required to assure a proper production.

To prevent damage of tools that are used later in cutting and joining processes, it is advised to use aluminium instead of steel fasteners. Following [50] aluminium brackets can be found as being appropriate. To achieve a sufficient and widely homogeneously distributed bonding pressure it is required to regulate the spacings between the discretely placed fasteners. Therefore the rules for screw pressings in DIN 1052 [25] can be used as basis. According to this standard only self-tapping full-threaded wood screws with a nominal diameter $d \geq 4$ mm are allowed. The maximum area allocable per screw is $A \leq 15{,}000$ mm² and the maximum spacing 150 mm. The thickness of structural timber used for each layer is restricted to $t \leq 35$ mm whereas the use of engineered timber products according to DIN 1052 [25], section 14.1 (4) up to $t \leq 50$ mm are allowed.

2.6 Large Finger Joints between CLT Elements

As consequence of an alternative production process of CLT, where at first small CLT elements are produced in single or multi-layer cycle presses and afterwards joined to larger CLT elements, but also to join already large-sized CLT elements or cut-outs from door or window openings, large finger joints as connections can be used. These large finger joints comprise the whole cross section of joined elements. The advantage of producing small elements, e.g. as done in [48], is given by the small-scaled press and the much smaller forces as well as in the handling of the elements before and after pressing.

A common and standardised profile for large finger joints is with l_{FJ} = 50 mm as given in Tab.1. The production requirements are based on the experiences gained with glulam and are given in reference to EN 387 [17] and section 3.5. As consequence of the joint, the bending strength of CLT elements at that position has to be reduced based on a 25 % reduction of the characteristic 5 %-quantile bending strength of the base material (see e.g. [48]). Of course, in cases of adequate planning processes this does not or only negligibly restricts the design process.

2.7 Finish of Standard CLT Elements

After pressing, standard CLT elements are trimmed on their edges. The surface of the elements after pressing is treated differently, without further processing by planing or sanding. Depending on later use, also, the application of additional non load-bearing layers like OSB, acoustic panels, gypsum plaster boards or three-layered solid wood panels is possible (see also section 2.1). These additional layers are primarily connected by surface bonding.

2.8 Cutting and Joining: Customising

Cutting and joining of CLT elements immediately after production and finishing constitute essential and logical process steps in an order-related, small (single) batch production. It is the aim to continue the precision in production into cutting and joining. Approved devices are portal machines which operate as multiple processing centres (e.g. of Hans Hundegger Maschinenbau GmbH / DE) which, after the CLT element has been aligned accurately, accomplish all relevant processes for dimensioning and further joining, like trimming, cutting, milling (e.g. for connection technique, stepped rabbet or profiling of edges for later joining of e.g. ceiling elements, for installation channels, etc.), drilling (on both surfaces and all edges up to 2 m in depth from one side) on both surfaces (top and bottom) and all four edges (see Fig. 9), including marking and labelling. The tools (moulding cutters, saws, chain saws, etc.) provided in tool magazines are readily available. Thus large-sized CLT elements in thickness up to 350 mm, in length up to 16 m and in width up to 4.3 m can be ready processed to wall, floor and ceiling elements. Another advantage of these processing centres is the possibility to encase the device for minimising emissions of noise, dust and chips whereby dust and chips as by-products can be collected concentrated.

Depending on the CLT production volume and the market orientation, for securing a continuously running production, it can be meaningful to operate more than one processing centre in parallel. Therefore process centres in various dimensions and configuration are available and systems provided which allow step-by-step adaptation on production volume and market demands. Depending on the required flexibility, three- to five-axis machining centres are available. Of course not only the processing centres but also the combination with software packages, together with a well-operating process planning office for optimising the layout and thus the degree of utilisation of CLT elements, creates an economical and powerful customising centre and added value on the product CLT. Meanwhile, also, customising centres without their own CLT production have been established in combination or cooperation with carpentry or assembly companies.

  

Fig. 9 Machining centre: moulder (left), chain saw (middle), saw (right) (© Hans Hundegger Maschinenbau GmbH / DE)

In regard to the assembling on site, it is essential to optimise the logistics and to load the elements on trucks, after cutting and joining, inverse to the later required order.

3. Factory Production Control (FPC) – Internal Quality Assurance

The aim of this section is to present the main internal test and monitoring procedures as required and regulated within technical approvals for CLT as well as within prEN 16351 [1] so far as the factory production control (FPC) is concerned. The following sections give (minimum) requirements individually for each quality criteria whereby the requirements of prEN 16351 [1] are treated first. Consequently, additional processes for quality assurance and monitoring, as partly given in technical approvals of Germany and the European Technical Approvals, are briefly presented.

Complementary to FPC, an external quality control by an independent accredited institution is required, normally semi-annually. Thereby the conformity of production and monitoring processes, according to the underlying guidelines, approvals and standards is assessed. These institutions are also responsible for initial type testing and the determination of some process parameters (e.g. declared strength values for (large) finger joints, etc.). These external test and evaluation procedures are not part of this section.

Within the frame of FPC, it is also required to establish an internal guidance procedure for quality control. This procedure should provide regulations and responsibilities for testing and monitoring of production processes and in particular of actions in cases where test results are conspicuous or do not meet the requirements.

3.1 Control of climatic Conditions during Production

To secure bonding, the requirements given by the adhesive manufacturer, i.e. in regard to temperature of adherends and surrounding, the relative humidity and moisture content of the adherends, the applied adhesive quantity, the time schedule, the bond pressure, etc. have to be met. The prEN 16351 [1] recommends to some of these parameters general minimum conditions for the production of CLT, e.g.

- during bonding: $T \geq 15°C$ and rel. humidity (40 to 75) %;
- during curing: $T \geq 18°C$ and rel. humidity ≥ 30 %;
- moisture content of adherends $u = (6 \text{ to } 15)$ % (≤ 18 % in case of preservative treatment);
- maximum difference in moisture content between two parallel layers $\Delta u \leq 5$ %.

3.2 Delivery Control of Adhesives

According to prEN 16351 [1], control of every dispatch of adhesive is required in regard to quality and suitability for the production of CLT or for a specific process step (e.g. finger joints, edge and surface bonding). Additionally, the adhesive system used for large finger joints has to be controlled in every shift to which it applies. The adhesive systems, which are principally allowed for use in CLT production according to prEN 16351 [1] are:

- phenoplast- and aminoplast-adhesives according to EN 301 [26], type I or according to technical approvals which certify the appropriateness of the adhesive system for load bearing timber structures and in particular for CLT for use in service class one or two; these adhesives (primary MUF) are, in principal, applied for bonding of (large) finger joints as well as for edge and surface bonding; if used for (large) finger joints the minimum holding time for longitudinal pressure and the mixing ratio of synthetic resin and hardening agent have to be monitored in addition; for large finger joints the applicability is additionally limited to adhesive systems which are certified for bond line thicknesses up to 1 mm;
- one-component polyurethane adhesives (1K-PUR) according to EN 15425 [27] or according to technical approvals which certify the appropriateness of the adhesive system for load bearing timber structures and in particular for CLT for use in service class one or two; this type of adhesive is in principal suitable for bonding of (large) finger joints as well as edge and surface bonding;
- emulsion-polymer-isocyanate adhesive (EPI) so far the requirements as given in EN 15425 [27] or of a technical approval which certifies the appropriateness of the adhesive system for load bearing timber structures and in particular for CLT in service class one or two are met; this type of adhesive is in principle allowed for bonding of finger joints as well as for edge and surface bonding but according to prEN 16351 [1] not for large finger joints.

3.3 Delivery Control of the Base Material used for load-bearing Purposes (Solid Timber / single-layer Wood Panels)

According to prEN 16351 [1], CLT can be produced of structural timber graded according to EN 14081-1 [11] and / or of engineered timber products (e.g. single-layer panels) that meet the requirements of EN 13986 [32] or EN 14374 [51]. For structural timber so far only softwood species are considered. In regard to the single layers it is allowed that ≥ 90 % of the board material is of the declared strength class, e.g. according to EN 338 [8], whereas up to ≤ 10 % of the boards can be of a strength class with a maximum deviation from the declared strength values of 35 %.

3.4 Minimum FPC Requirements on Finger Joints

The requirements on production of finger joints in prEN 16351 [1] follow in principle that of EN 385 [23] or prEN 15497 [24]. In the framework of FPC, the fulfilment of minimum requirements on finger joint strength can be tested in tension parallel to grain or bending. Following prEN 16351 [1] similar regulations as in the glulam product standard EN 1194 [28] can be found, see

$$f_{\mathrm{t,0,FJ,k}} \geq 5 + f_{\mathrm{t,0,B,k}}; \qquad (2)$$

$$f_{\mathrm{m,FJ,k}} \geq 8 + 1.4 \cdot f_{\mathrm{t,0,B,k}}. \qquad (3)$$

Testing comprises at least three specimens per shift and production line of the highest produced strength class or strength profile and per adhesive. The test can be performed flatwise in four-point bending or in tension parallel to grain, both in reference to EN 408 [42]. Deviating from this standard the maximum (failure) load has to be reached within (60 ± 15) s. Furthermore, in case of bending tests the test span can be reduced to $l_{span} \geq 15 \cdot t_L$ and in tension to a free test length of $l_{free} \geq 3 \cdot w_L$, respectively, with t_L and w_L as thickness and width of the laminations. It has to be secured that at least five of the last 100 test values are below the declared characteristic 5 %-quantile of the finger joint strength $f_{FJ,dc,k}$ and that within the last 15 tests none of the tests was below $f_{FJ,15}$, with $f_{FJ,15} = k_{15} \cdot f_{FJ,dc,k}$ and k_{15} as parameter which considers the dispersion in strength (restricted to $CV[f_{FJ}] \geq 10$ %) and the sample size assuming a lognormal distributed strength.

Tab. 3 Minimum requirements on $f_{m,FJ,k}$

strength class acc. to EN 338 [8]	**$f_{m,FJ,k}$ [N/mm²] acc. to DIN 1052 [25]**	**grading class acc. to DIN 4074-1 [12]**	**$f_{m,FJ,k}$ [N/mm²] acc. to DIN 68140-1 [52]**
C16	≥ 25	**S7 / MS7**	-
C24	≥ 30	**S10 / MS10**	≥ 30
C30	≥ 35	**S13**	≥ 35
C35	≥ 40	**MS13**	≥ 40
C40	≥ 45	**MS17**	≥ 45

Following the German technical approvals for CLT, in general testing of at least two specimens per shift is required. FPC in regard to finger joint strength can be also done by bending and tension tests, the last one with a minimum test length of $l_{free} \geq 200$ mm. The requirements on the bending strength $f_{m,FJ,k}$ are regulated in reference to DIN 1052 [25], annex H, Table H.1 or DIN 68140-1 [52] (seeTable 3).

The minimum requirement on tension strength is for example in [53] regulated by 70 % of $f_{m,FJ,k}$ according to DIN 1052 [25], see

$$f_{t,0,FJ,k} \geq 0.7 \cdot f_{m,FJ,k}. \tag{4}$$

Of course, in regard to the arguments in section 2.2, it is recommended to regulate the minimum requirements on the finger joint strength based on tension tests parallel to grain and according to the formulations in section 2.2, Table 2, and thus in dependency on the stochastics of the material.

3.5 Minimum FPC Requirements on Large Finger Joints

According to FPC in prEN 16351 [1], the production requirements on bond line thickness and tip gap of the finger joint have to be controlled on at least one specimen per shift. The maximum allowed bond line thickness is 0.5 mm for phenoplast- and aminoplast-adhesives and 0.3 mm for 1K-PUR. The relative tip gap has to be within $e = (0.02 \text{ to } 0.10)$, with $e = l_t / l_{FJ}$. The characteristic 5 %-quantile of the bending strength of large finger joints $f_{m,LFJ,k}$, determined by means of four-point bending tests on by large finger joints connected full-size CLT-elements according to EN 408 [42], has to be at least as high as the declared value $f_{m,LFJ,dc,k}$.

FPC requirements concerning large finger joints in German technical approvals for CLT is frequently referred to EN 387 [17]. This standard again gives requirements on the geometry, the bond line thickness (in general ≤ 0.5 mm) and the tip gap l_t = (1 to 6) mm. The compliance has to be controlled on at least one cylindrical specimen (diameter 25 mm) per shift or at least on one per ten produced joints taken from the centre of the joint. If all test results, over a period of at least three months, reach the requirements, then the sampling may be reduced to one per 30 produced joints but at least one per shift. The bending strength of large finger joints has to be determined on full-size jointed CLT elements according to EN 408 [42] and EN 386 [39]. For example in [48] the minimum required strength is defined as share of the bending strength of the board material, see e.g.

$$f_{\mathrm{m,LFJ,k}} \geq 0.75 \cdot f_{\mathrm{m,B,k}} \,. \tag{5}$$

3.6 Minimum FPC Requirements on Edge Bonding

According to prEN 16351 [1], the resistance of edge bonding has to be controlled by means of block shear tests. Per shift, at least one specimen comprising the whole width of a single-layer panel has to be taken and at least two bond-lines tested according to EN 392 [46]. Before testing the compliance of the bond line thickness with allowed values has to be checked. The minimum requirements on shear strength are regulated in relationship with the share of fibre and wood on the fractured surface, see Table 4.

The shear strength f_v has to be calculated as

$$f_\mathrm{v} = k \cdot \frac{F_u}{A}, \text{ with } A = b \cdot t \text{ and } k = 0.78 + 0.0044 \cdot t \,, \tag{6}$$

with F_u as the ultimate failure load, A as shear area and k as thickness correction factor.

Tab. 4 Requirements on edge bonds according to prEN 16351 [1]

	average value			single value		
f_v [N/mm²]	6.0	8.0	≥ 11.0	4.0 to 6.0	6.0	≥ 10.0
FF [%] 1)	≥ 90 %	≥ 72 %	≥ 45 %	100 %	≥ 74 %	≥ 20 %
1) share of fractured surface covered by fibres (share of wood failure)						

3.7 Minimum FPC Requirements on Surface Bonding

3.7.1 Delamination according to prEN 16351 [1]

For controlling of adhesion, or of the resistance against fractures in the bond line, specimens of defined geometry have to be exposed to a specific series of climatic conditions and afterwards the delamination of their bond lines determined. Therefore at least one specimen per 20 m³ produced CLT (or in case of positive results over a time period of at least three months; at least one per 40 m³) comprising the whole depth of CLT, in width ≥ (75 ± 5) mm and in length large enough for a surface of A ≥ 10,000 mm² or a cylindrical specimen with a diameter of ≥ (95 ± 5) mm has to be taken. After determination of mass and measurement of the length of all bond lines visible on the end-grains the specimen has to be exposed to the following conditions:

- completely submerged and surrounded by water of T = (10 to 20) °C;
    - exposition to a vacuum of (70 to 85) kPa (absolute pressure (15 to 30) kPa) for 30 min;

  - exposition to a pressure of (500 to 600) kPa (absolute pressure (600 to 700) kPa) for 120 min;
- drying in a chamber at $T = (65 \text{ to } 75)$ °C, (8 to 10)% rel. humidity and air velocity of (2 to 3) m/s till (100 to 110)% of the mass before testing is reached; this should be possible within (10 to 15) h;

Afterwards, the proportion of delamination has to be determined on all bond lines. The maximum proportion of delamination per single bond line and per specimen has to be calculated as

$$\mathrm{Delam}_{\max} = 100 \cdot \frac{l_{\text{max,delam}}}{l_{\text{glue line}}} \; [\%], \tag{7}$$

and the overall share per each specimen as

$$\mathrm{Delam}_{\text{tot}} = 100 \cdot \frac{l_{\text{tot,delam}}}{l_{\text{tot,glue line}}} \; [\%]. \tag{8}$$

The allowed proportions of delamination are $\mathrm{Delam}_{\max} \leq 40$ % and $\mathrm{Delam}_{\text{tot}} \leq 10$ %. In the case that one or both criteria are exceeded, each bond surface has to be split and the proportion determined for the surface of fractured wood or covered by fibres. Per each bond surface, a minimum proportion of wood and fibre failure of 50 % and, on average of all bond surfaces per specimen, a minimum of 70 % (maximum average delamination of 30 %) has to be achieved, otherwise the test has failed.

3.7.2 Delamination according to DIN 53255 [54] / DIN 68705-4 [55] and alternative test methods

FPC requirements on delamination in German technical approvals for CLT are in general referenced to DIN 53255 [54]. Therein is provided a method for testing the quality and resistance of surface bonding in cross laminated wood and timber products. It examines the local dissociation of each individual bond line by means of a special designed dissociation tool. As in prEN 16351 [1], a minimum average proportion of wood and fibre failure on all bond surfaces per specimen of 70 % is required. Before testing, each specimen has to be exposed to a cycle of specific climatic conditions according to DIN 68705-4 [55], specification for BST 100. In doing so it is differed between a cold water test (24 h completely submerged at $T = (20 \pm 2)$ °C) and a hot water test (4 h completely submerged in boiling water, followed by (16 to 20) h storage in a climate chamber at $T = (60 \pm 2)$ °C, 4 h completely submerged in boiling water and (2 to 3) h cooling down completely submerged in water at $T = (20 \pm 5)$ °C).

Alternatively some approvals allow block shear tests according to DIN 52187 [56] on at least 10 specimens per working day. The average shear strength of the last ten tests shall met $f_{v,\text{mean}} \geq 1.5$ N/mm² and the characteristic 5 %-quantile of the last 100 tests $f_{v,k} \geq 1.25$ N/mm² but no value below 1.00 N/mm².

A further alternative is to perform shear tests according to EN 789 [57], annex C on at least one specimen per working day and thickness range of produced CLT.

Some approvals allow also delamination tests according to EN 391 [47], approach B instead of the delamination test according to DIN 53255 [54]. The climatic conditions as well as the limits are equal to prEN 16351 [1] (see section 3.7.1). Tests which exceed the limit $\mathrm{Delam}_{\text{tot}} \leq 10$ % have to be exposed to a second cycle of equal climatic conditions and with a new limit of $\mathrm{Delam}_{\text{tot}} \leq 15$ %. If this limit is also exceeded the specimen has to be tested according to

DIN 53255 [54]. The required minimum average share of wood and fibre failure on all bond surfaces per specimen is 70 %.

3.7.3 Discussion: Experiences made with Delamination

In reference to section 2.5.1 and the research project reported in [34], some results and experiences made in regard to delamination are presented. Fig. 10 gives an overview of the results gained by testing CLT specimens in rolling shear according to EN 408 [42] ($l_{span} = 12 \cdot t$) and in delamination according to EN 391 [47], approach B. The results of delamination comprise the maximum delamination per bond line ($Delam_{max}$) and the maximum delaminated bond surface per specimen $A_{delam,max}$. The presented results embrace nine sub-series per each test; three variations in surface pressure (SP; (0.1, 0.3, 0.6) N/mm²) and three variations in number of climatic cycles (CC; 0, 10, 25) the specimens were exposed before testing. The climate was varied weekly between 20 °C / 90 % rel. humidity and 30 °C / 40 % rel. humidity. Thus one climate cycle took two weeks and caused a variation in moisture content of (12 to 17) %. Per each sub-series at least five specimens were tested in rolling shear and ten in delamination.

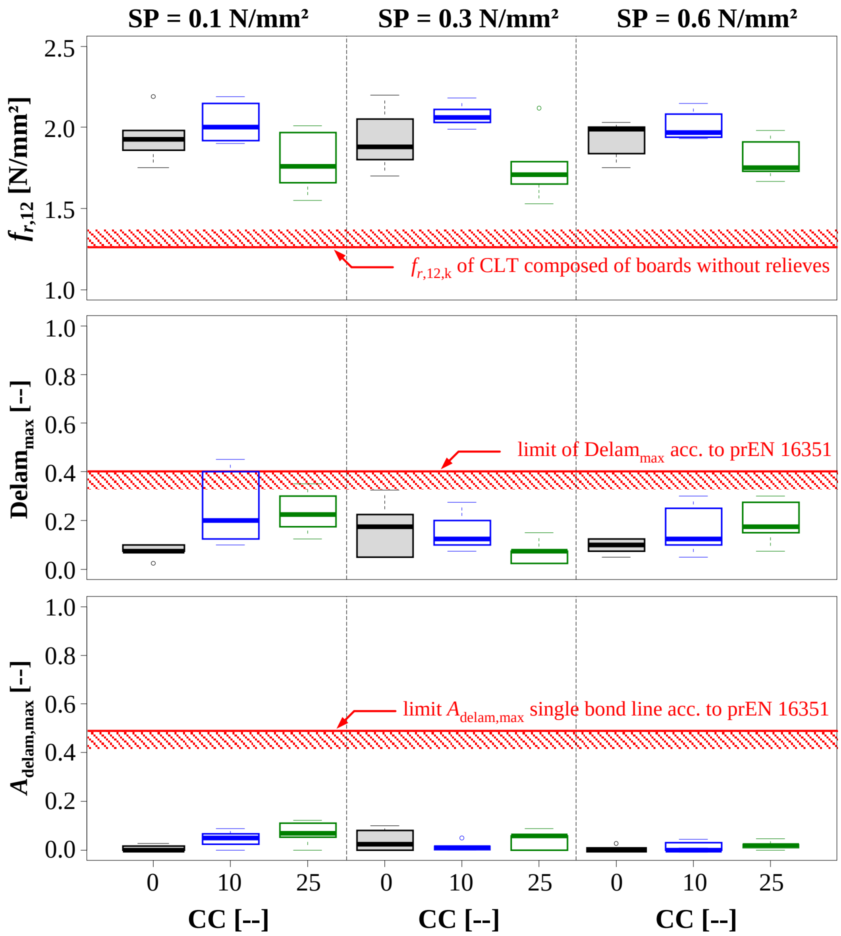

Fig. 10 Results (excerpt) of CLT tested in rolling shear ($f_{r,12}$; above) and delamination ($Delam_{max}$; middle and $A_{delam,max}$; below) in dependency on surface pressure (SP) and number of climatic cycles (CC) together with FPC limits according to prEN 16351 [1] ([34])

To summarise the results briefly: All specimens tested in rolling shear delivered strength results on the safe side. The limits, according to prEN 16351 [1] for the two criteria examined in regard to delamination, $Delam_{max}$ and $A_{delam,max}$, were also met, apart from one sub-series where the limit of $Delam_{max}$ was exceeded. Of course, these specimens also passed the test afterwards in examining $A_{delam,max}$. Although, and after a slight increase from CC = 0 to CC = 10, a reduction in $f_{r,12}$ at CC = 25 can be observed; in delamination no relationship between CC and $Delam_{max}$ nor to $A_{delam,max}$ was found. In some sub-series a coherent course of $Delam_{max}$ and $A_{delam,max}$ is given; a relationship between $f_{r,12}$ and properties of delamination cannot be confirmed.

Focusing on delamination the variation in $A_{delam,max}$ is much smaller than in $Delam_{max,}$ which indicates a higher stability in the results of $A_{delam,max}$. Although it is not possible to relate the delamination results to real examples of structures and to define limits for $Delam_{max}$ and $A_{delam,max}$ based on these tests, based on the experiences made during testing, the combined judgement of delaminated bond lines and bond surfaces was in principle found to truly indicate the bond line quality.

3.7.4 Delamination: Conclusions

To summarise, the approach presented in section 3.7.1, which examines the delamination of surface bonding in combination with splitting of the surfaces by a metal wedge, is preferred. This is because it is judged to provide a higher degree in comparability and reproducibility than the alternative methods in section 3.7.2. Of course a fundamental and quantifiable relationship between exposure to extreme climatic test conditions and the practical relevance, in particular in respect to the established service class system, is up until now, not available. As is the case for glulam, the limits in delamination for CLT are of empirical basis, developed and exhibited by experiences made so far. Due to the cross-laminated structure of CLT and the higher internal stresses due to swelling and shrinkage, adaptation of the limits, established so far for glulam, was necessary.

3.8 FPC Requirements on rolling shear strength of CLT

Following the FPC regulations in German technical approvals for CLT, the testing of one specimen per working day in rolling shear, by means of a four-point bending test according to EN 408 [42] but with reduced span of $l_{span} \geq 15t$, is required.

3.9 FPC Requirements on maximum Bond-Line Thickness according to prEN 16351 [1]

Following prEN 16351 [1], the maximum allowed bond line thickness for aminoplast- and phenoplast-adhesives is $t_a \leq 0.6$ mm and $t_a \leq 0.3$ mm, respectively, for common and separate application of resin and hardener. In case of 1K-PUR the limit is $t_a \leq 0.3$ mm.

3.10 Additional FPC Requirements

“Additional requirements”, according to FPC, comprise regulations of (i) the used timber species, (ii) the durability of the base material(s), (iii) criteria for preservative treated base material(s), (iv) criteria for classifying the resistance of CLT if exposed to fire, (v) the dimensions, geometry and assembly, and (vi) the compliance with release limits on formaldehyde and other harmful agents. Further information can be found in the technical approvals as well as in prEN 16351 [1].

4. Main geometrical and technological Parameters of CLT

Within this section, the main geometrical and for production of CLT relevant parameters are presented. An overview of the regulation of these parameters, according to current technical approvals for CLT in Europe, is provided in Table 5. To summarise, producers aim to reduce the regular gap width between boards or single-layer panels within one CLT layer. Following the regulations, gaps of ≤ 2 mm and ≤ 4 mm between boards in top and core layers respectively are common. The approvals are widely restricted to softwoods, whereby Norway spruce (*Picea* *abies*) is definitely preferred. The strength classes of the base material are dominated by C16 and C24 according to EN 338 [8]. In this regard, the regulations on the base material quality, within each CLT layer, can be said to be somehow relaxed. Common dimensions of CLT are in length up to 18 m (or even 30 m), in width up to 4 (4.8) m and in thickness seldom above (300 to 400) mm. Although hydraulic press facilities dominate the production of CLT in volume, no tendency can be observed concerning the production parameters "single-layer panels" and "edge bonding". Also the requirements on FPC can be said to be diverse.

Tab. 5 Overview of some geometrical and technical characteristics of European CLT producers

technical approval	dimension CLT **l** [m] / **w** [m] / **t** [mm] further information	dimension BM (SP) 1) **w** [mm] / **t** [mm] further information	timber species 2) strength class	max gap width [mm]	single-layer panels (Y/N/possible)	edge bonding (Y/N/possible)	adhesive system 3)	surface pressing	FPC test procedures for CLT 4)
[50]	≤18/≤4/60÷400 ≥3 layers	250÷1200/15÷45	SW ≥C16	2(4)	Y	N	EN301 1K-PUR	bonding pressure by brackets	RS; BS; FJ
[58]	≤30/≤4.8/≤300 ≥3 layers	80÷220/10÷33 TL *w*/*t*≥4	SW ≥C16	6	N	-	EN301	-	RS; FJ; DL (D)
[59]	≤30/≤4.8/30÷300 ≥3 layers	80÷220/10÷33 TL *w*/*t*≥4	SW ≥C16	6	N	N	EN301 EN15425	-	-
[60] 5)	-/-/19÷42 3 layers	T*l* 60÷150/5.75 C*l* 19÷150/7.5÷30.5	SW	-	Y	-	-	-	D; B(t)
[61] 5)	-/-/16÷57 3 layers	T*l* 80÷140/5.5÷13.2 C*l* 80÷140/5÷31.6	SW ≥C16	-	Y	-	EN301 MF	-	D; B(t)
[62] 6)	≤3(18)/≤1.25/ 60÷300	60÷240/12÷40 TL *w*/*t*≥2.4	≥C24 ≥GL24	>>	-	-	1K-PUR	-	-
[63] 6)	≤3(18)/≤1.25/ 60÷300	60÷240/12÷40 TL *w*/*t*≥2.4	SW ≥C24 ≥GL24	>>			EN301	-	D; FJ; LFJ; BS
[64]	≤18/≤3/36÷280 3÷13 layers	70÷280/12÷40 TL *w*/*t*≥4	SW C16-C35	2(4)	N	N	EN301 EN15425 MUF	-	-
[65]	≤18/≤3/36÷280 3÷7 layers	70÷220/12÷40 TL *w*/*t*≥4	SW ≥C16	4	-	-	EN301 MUF	-	RS or Sh; D; FJ
[66]	≤5/≤1.25(24)/ 60÷350 ≥3 layers	80÷250/18÷45 TL *w*/*t*≥4	SW C16/C24	TL 2 LL 0	Y	LL Y	EN301 SP: MUF 1K-PUR	-	-

technical approval	dimension CLT *l* [m] / *w* [m] / *t* [mm] further information	dimension BM (SP) [1] *w* [mm] / *t* [mm] further information	timber species [2] strength class	max gap width [mm]	single-layer panels (Y/N/possible)	edge bonding (Y/N/possible)	adhesive system [3]	surface pressing	FPC test procedures for CLT [4]
[48]	large elements ≤22/≤3.5/51÷215 system format ≤5/≤1.25(24)/ 54÷350	large elements 100÷200/17÷43 system format 80÷250/18÷45 TL *w*/*t*≥4	SW C16/ C24	4	Y	Y/N	EN301 SP: MUF 1K- PUR	large elements vacuum 80÷90 kPa system format hydraulic	RS or Sh; D; FJ; LFJ
[67]	≤18/≤3.5/60÷400 3÷11 layers	LL 80÷260/15÷45 TL 80÷260/15÷40 TL *w*/*t*≥4 solid wood panels -/15÷45	S,P,F, L	LL 3 TL 6	Y/N	N	EN301 MUF	pneumatic 0.5÷0.8 MPa	-
[68]	≤16.5/≤3/42÷350 3÷20 layers	40÷300/14÷45 TL *w*/*t*≥4 solid wood panels (TL) 250÷1,600/-	S,P,F ≥C16	2(4)	pos.	pos. TL Y	EN301 EN154 25 SP: EPI 1K- PUR	-	-
[53]	≤16.5/≤3/42÷500 3÷27 layers	40÷300/14÷45 TL *w*/*t*≥4 solid wood panels (TL) 250÷1,600/-	SW ≥C16	2(4)	pos.	pos. TL Y	EN301 SP: EPI 1K- PUR	-	RS; DL, D or BS; FJ
[69]	≤16.5/≤2.95/ 57÷250 3÷9 layers	80÷240/10÷40 TL *w*/*t*≥4	S ≥C16	3(6)	-	-	EN301 1K- PUR	hydraulic ≥0.6 MPa	-
[70]	≤16.5/≤3/57÷500 3÷27 layers	80÷240/10÷40 TL *w*/*t*≥4	S ≥C16	3(6)	-	-	EN301 1K- PUR	-	RS; D; FJ
[10]	≤16/≤3.2/50÷300 ≥3 layers	80÷200/18÷40 TL *w*/*t*≥4	S,P,D T*l* C24 C*l* C16	6	-	-	EN301 1K- PUR	-	RS or Sh; D; FJ
[35]	≤6/≤3.25/≤345 ≥3 layers	140÷260/23	SW ≥C16	-	-	-	EN301	ring shank nails	FJ

technical approval	dimension CLT *l* [m] / *w* [m] / *t* [mm] further information	dimension BM (SP) 1) *w* [mm] / *t* [mm] further information	timber species 2) strength class	max gap width [mm]	single-layer (Y/N/possible)	edge bonding (Y/N/possible)	adhesive system 3)	surface pressing	FPC test proced for CLT 4)
[71]	≤18/≤3/60÷300 3÷9 layers	LL 80÷240/20÷80 TL 80÷240/20÷40 TL *w*/*t*≥4	S,P,F, L,D ≥C16	LL 3 TL 6	-	-	EN301 EN154 25	hydraulic 0.6 MPa	-
[72][5)]	3L -/-/13÷49 5L -/-/27÷42 3 or 5 layers	3L: T*l* 91÷190/4.5÷12 C*l* 44÷150/4÷25 5L: T*l* 117÷190/4.5÷8.5 C*l* 44÷150/5÷9	≥C16	-	-	TL Y	approv al	-	D; B(t)
[49]	≤20/≤4/45÷280 3÷7 layers	40÷300/15÷40 TL *w*/*t*≥4	SW ≥C16	2(4)	pos.	pos.	EN301	vacuum 80÷90 kPa	RS or Sh; D; FJ
[33]	≤20/≤2.5/60÷200 ≥3 layers	80÷160/20÷40	SW T*l* ≥C24 C*l* ≥C16	-	-	-	EN301 1K-PUR	vacuum 80÷90 kPa	RS; D; FJ
[36]	≤10/≤3/≤400 orientation 90°, 45° or 0°	≥100/24÷60	SW ≥C16	10	-	-	-	hardwood dowels *d*=20 mm	-
[73]	≤15.5/≤3.45/ 27÷210 3÷7 layers	60÷300/9÷30 TL *w*/*t*≥4	S,F C16÷ C30	2(4)	-	LL pos.	EN301	-	D or BS; FJ
[74]	≤20/≤4/57÷280 3 or 5 layers	80÷200/19÷45 TL *w*/*t*≥4	S or sim. ≥C16	3	pos.	LL pos.	EN301 MUF	-	-

1) BM base material; SP single-layer panel; TL transverse layers; LL longitudinal layers; T*l* top layer; C*l* core layers; *w* width; *t* thickness

2) SW softwood species; S Norway spruce; P Scots pine; F White fir; L European larch; D Douglas fir; sim. similar timber species strength class according to EN 338 [8] (or EN 1194 [28], prEN 14080 [13])

3) data of technical approvals complemented by manufacture's data (product leaflet, reports, etc.); adhesives according EN 301 [26] only of type I

4) RS … rolling shear of CLT; BS … block shear CLT; FJ … finger joint; DL … delamination CLT; D … delamination (dispartment at glue line) according to DIN 53255 [54]; B(t) … transverse third-point bending; Sh … (rolling) shear test

5) 3- or 5-layers wood panels for load bearing purposes

6) dissolved cross laminated timber products for load bearing purposes

As differential swelling and shrinkage rates apply, the rates of swelling and shrinkage of CLT of Norway spruce (*Picea abies*), in- and out-of-plane, providing that the moisture content of CLT is kept within (6 to 22) % are:

- for both directions in-plane: 0.02 % per each percent change in moisture content
- for the direction out-of-plane: 0.24 % per each percent change in moisture content

5. Discussion and Conclusion

This paper provides an overview of current production techniques for cross laminated timber (CLT). The focus is on industrial production lines, although also productions for small and median scaled producers are addressed. The work focusses on CLT as rigid composite, composed of cross-wise arranged and surface bonded layers of boards or single-layer panels.

To summarise in brief: currently, and in regard to the production volume of CLT, hydraulic press facilities are dominant. Their further gain in market share, in particular at large productions with automated lines, is expected and supported by the currently available modular press and production systems. Of course, no clear trend regarding the production parameter “edge bonding” has been observed. In fact, as the occurrence of checks, due to swelling and shrinkage under exposure of CLT to cyclic climatic conditions, cannot be avoided, the benefit of edge-bonding relating to building physics and connection techniques (e.g. in case of pin-shaped fasteners) has to be questioned. Thus producers aim to reduce the gap widths between boards or single-layer panels within the CLT layers. Latest developments in press technology allow lateral pressure individually on all CLT layers. This enables production of CLT elements with gap widths of zero but without edge bonding. Furthermore, there is a trend that machine manufacturers offer their facilities, together with CLT production licences (e.g. woodtec Fankhauser GmbH / CH with [33]; Hans Hundegger Maschinenbau GmbH / DE with [35]).

Further distribution of CLT, not only in Europe but worldwide, makes an ongoing standardisation and creation of corresponding harmonised regulations essential. The first important steps in this regard are in process (e.g. the product standard prEN 16351 [1] for CLT and the efforts in harmonising the lamella thickness with t_L = (20, 30, 40) mm. Further steps, in particular concerning the design procedures, the detailing (building physics; leading details; structural engineering) and joining technique are required.

The product, CLT, provides timber engineering but also the whole building sector with new possibilities and horizons. Currently the potential of CLT is seen in multi-storey timber construction for office and residential buildings and thus for the renaissance of timber engineering in our cities. To improve its economics, in particular in competition to mineral building materials like reinforced steel, masonry and steel structures, the development of CLT building systems, and thus the establishment of the solid timber construction techniques with CLT, is seen as the next milestone (see also the four-year research project “focus_sts” at the competence centre holz.bau forschungs gmbh / AT). Therefore it is essential to address the peculiarities of timber as building material, in particular its vulnerability to moisture. As consequence of the establishment of a building system, a vertical extension of CLT production lines by assembling stations is expected. Within these stations whole wall and ceiling elements, including not only windows and door installation but also the finale facade systems with insulation, as known from current production lines for light-weight timber constructions, can be ready processed. Another possibility is also to prefabricate plug-and-play facade modules. Parallel to this the extension of engineering offices directly or in close cooperation with CLT producers is predicted.

Thereby the solid timber construction technique with CLT is not judged as a competitor for the existing timber building sector with focus on linear timber elements. The building technique with CLT has already been shown to open and extend the possibilities to realise structures in timber. In fact CLT is in direct competition with mineral based solid building materials, like reinforced concrete and masonry. Further extension of this position is expected. This is, in particular, enforced by the understanding that, providing the minimum principles shown in this paper are maintained, the product CLT has not yet reached the mechanical potential of the base material. Also local timber species can be utilised sustainably and added value gained regionally, which makes it certain that CLT will be established worldwide. In consequence, further small and medium scale production lines and companies as well as some big worldwide operators, all in the field of CLT, will be created.

Acknowledgement: This work was accomplished and financed by Graz University of Technology, Institute of Timber Engineering and Wood Technology. The support has to be thankfully acknowledged.
In addition, the support provided by companies as producers of press facilities as well as cutting and joining facilities are also thankfully acknowledged.

6. References

[1] prEN 16351:2011-11, “Timber structures – Cross laminated timber – Requirements”

[2] Schickhofer G., “*Starrer und nachgiebiger Verbund bei geschichteten, flächenhaften Holzstrukturen*”, 1994, Dissertation, Institute of Steel, Timber and Shell Structures, Graz University of Technology

[3] Salmén L., “Micromechanical understanding of the cell-wall structure”, 2004, *C. R. Biologies*, 327:873-880

[4] Wathén R., “*Studies on fiber strength and its effect on paper properties*”, 2006, Dissertation, KLC communications, No. 11, University of Technology, Helsinki, Finland, ISSN 1457-6252, p. 97

[5] Brandner R., *Stochastic System Actions and Effects in Engineered Timber Products and Structures*, Dissertation, Institute of Timber Engineering and Wood Technology, Graz University of Technology, 2012, p. 467.

[6] Augustin M., Blaß H.J., Bogensperger T., Ebner H., Ferk H., Fontana M., Frangi A., Hamm P., Jöbstl R.A., Moosbrugger T., Richter A., Schickhofer G., Thiel A.B., Traetta G. and Uibel T., *BSPhandbuch: Holz-Massivbauweise in Brettsperrholz – Nachweise auf Basis des neuen europäischen Normenkonzepts*, Verlag der Technischen Universität Graz, 2010, ISBN 978-3-85125-109-8

[7] Schickhofer G., “Cross Laminated Timber (CLT) in Europe – from Conception to Implementation”, 2010, presentation, University of British Columbia, Department of Wood Science, Vancouver, Canada

[8] EN 338:2009-10, “Structural timber – Strength classes”

[9] EN 384:2010-04, “Structural timber – Determination of characteristic values of mechanical properties and density”

[10] Z-9.1-721 “*ED-BSP (Brettsperrholz) aus Fichte, Kiefer oder Douglasie*”, EUGEN DECKER – Holzindustrie KG, Deutsches Institut für Bautechnik (DIBt), 2008, valid until 25.09.2013

[11] EN 14081-1:2005-11, “Timber structures – Strength graded structural timber with

rectangular cross section - Part 1: General requirements”

[12] DIN 4074-1:2012-06, “Strength grading of wood – Part 1: Coniferous sawn timber”

[13] prEN 14080:2012-02, “Timber structures – Glued laminated timber and glued solid timber – Requirements”

[14] Daniels H. E., “The Statistical Theory of the Strength of Bundles of Threads. I”, 1945, *Proceedings of the Royal Society A*, 183:405-435

[15] Sexsmith R. G., Boyle P. D., Rovner B. and Abbott R. A., “*Load sharing in vertically laminated, post-tensioned bridge decking*”, 1979, Technical Report No. 6, Forintek Canada Corp., Western Forest Products Laboratory, Vancouver, British Columbia, ISSN 0708-6172, p. 18

[16] Bakht B. and Jaeger L. G., “Load sharing in timber bridge design”, 1991, *Canadian Journal of Civil Engineering*, 18:312-319

[17] EN 387:2001-10, “Glued laminated timber – Large finger joints – Performance requirements and minimum production requirements”

[18] Aicher S. and Klöck W., “Spannungsberechnungen zur Optimierung von Keilzinkenprofilen für Brettschichtholz-Lamellen”, *Bauen mit Holz*, 1990, 92(5):356-358, 360-362

[19] Colling F. and Ehlbeck J., “Tragfähigkeit von Keilzinkenverbindungen im Holzleimbau”, *Bauen mit Holz*, 1992, 94(7):586-593

[20] Radovic B. and Rohlfing H., “Über die Festigkeit von Keilzinkenverbindungen mit unterschiedlichem Verschwächungsgrad”, *Bauen mit Holz*, 1993, 3:196-201

[21] Groom L.H. and Leichti R.J., “Effect of adhesive stiffness and thickness on stress distributions in structural finger joints”, *Journal of Adhesion*, 1994, 44:69-83

[22] Smardzewski J., “Distribution of stresses in finger joints”, *Wood Science and Technology*, 1996, 30:477-489

[23] EN 385:2001-10, “Finger jointed structural timber – Performance requirements and minimum production requirements”

[24] prEN 15497:2011-08, “Structural finger jointed solid timber – Performance requirements and minimum production requirements”

[25] DIN 1052:2008-12, “Design of timber structures – General rules and rules for buildings”

[26] EN 301:2006-06, “Adhesives, phenolic and aminoplastic, for load-bearing timber structures – Classification and performance requirements”

[27] EN 15425:2008-02, “Adhesives – One component polyurethane adhesives for load bearing timber structures – Classification and performance requirements”

[28] EN 1194:1999-09, “Timber structures - Glued laminated timber – Strength classes and determination of characteristic values”

[29] Brandner R. and Schickhofer G., “*Glued laminated timber in bending: thoughts, experiments, models and verification*”, 11th World Conference on Timber Engineering (WCTE), Riva del Garda, Italy, 2010, p. 11

[30] Colling F., *Tragfähigkeit von Biegeträgern aus Brettschichtholz in Abhängigkeit von den festigkeitsrelevanten Einflussgrößen*. Dissertation, Universität Fridericiana Karlsruhe, 1990, p. 205

[31] Brandner R. and Schickhofer G., “Glued laminated timber in bending: new aspects

concerning modelling”, *Wood Science and Technology*, 2008, 42(5):401-425

[32] EN 13986:2002-06, “Wood-based panels for use in construction – Characteristics, evaluation of conformity and marking”

[33] Z-9.1-576 “*Woodtec Massivholzplatten*”, Woodtec Fankhauser GmbH, Deutsches Institut für Bautechnik (DIBt), 2010, valid until 31.05.2015

[34] Brandner R. and Schickhofer G., “*SSTC 1.1.2-5 clt_panel_pressdruck: Untersuchungen betreffend der Definition eines für die Produktion von Brettsperrholz optimalen Pressdruckes*”, 2012, Research Report, Institute of Timber Engineering and Wood Technology, Graz University of Technology, Competence Centre holz.bau forschungs gmbh, p. 76

[35] Z-9.1-602 “*MHM-Wandelemente (Massiv-Holz-Mauer-Wandelemente*”, MHM Entwicklungs GmbH, Deutsches Institut für Bautechnik (DIBt), 2009, valid until 30.06.2010

[36] Z-9.1-574 “*THOMA-Holz 100 System*”, Ing. Erwin Thoma Holz GmbH, Deutsches Institut für Bautechnik (DIBt), 2008, valid until 30.06.2013

[37] ETA-11/0338, “*Elements jointed with 'wooden screws"made of beech – Solid wood slab element – element of dowel jointed timber boards to be used as a structural element in buildings*”, Rombach Bauholz+Abbund GmbH, Deutsches Institut für Bautechnik (DIBt), 2011, valid until 17.10.2016

[38] Kairi M., “*Glued / Screwed Joints / Screw Glued Wooden Structures*”, Chapter 4.4, In: Johansson C. J., Pizzi T. and Leemput M. V. eds., COST Action E13 “Wood Adhesion and Glued Products”, Working Group 2: Glued Wood Products: State of the Art Report, 2002, 2nd Edition, ISBN 92-894-4892-X

[39] EN 386:2001-10, “Glued laminated timber – Performance requirements and minimum production requirements”

[40] Hoyle R. and Woeste F., “*Wood Technology in the Design of Structures*”, 1989, Fifth Edition, Iowa State University Press, p. 380

[41] Kiviluoto J. and Muilu J., “*Liimasauman mikroskopia*”, 1988, VTT, Tiedotteita 561

[42] EN 408:2010-07, “Timber structures – Structural timber and glued laminated timber – Determination of some physical and mechanical properties”

[43] Brandner R., Schickhofer G., Ruli A. and Halili Y., “*Non-KInd B_S_H – Leistungspotential von Brettschichtholz – Beanspruchung auf Längsdruck und Querdruck: Zusammenfassende Darstellung*”, 2006, Research Report, Institute of Timber Engineering and Wood Technology, Graz University of Technology, Competence Centre holz.bau forschungs gmbh, p. 106

[44] Wassipaul F., “*Einfluß des Preßdruckes auf die Festigkeit der Leimverbindung bei Brettschichtträgern*”, 1982, Ingenieurholzbau in Forschung und Praxis, Bruderverlag, Karlsruhe

[45] Baumann H. and Marian J. E., “Der Verleimungs-Pressdruck als Funktion physikalischer Faktoren”, 1961, *Holz als Roh- und Werkstoff*, 19(11):441-4xx

[46] EN 392:1995-01, “Glued laminated timber – Shear test of glue lines”

[47] EN 391:2001-10, “Glued laminated timber – Delamination test of glue lines”

[48] Z-9.1-534 “*Binderholz Brettsperrholz BBS*”, Binderholz Bausysteme GmbH, Deutsches

Institut für Bautechnik (DIBt), 2012, valid until 06.12.2014

[49] Z-9.1-793 "*Brettsperrholzelemente STEPHAN – FLEXcross*", Stephan Holzbau GmbH, Deutsches Institut für Bautechnik (DIBt), 2012, valid until 14.06.2016

[50] Z-9.1-680 "*HMS – Element*", Haas FERTIGBAU GmbH & HMS Bausysteme GmbH, Deutsches Institut für Bautechnik (DIBt), 2007, valid until 31.01.2012

[51] EN 14374:2004-11, "Timber structures – Structural laminated veneer lumber Requirements"

[52] DIN 68140-1:1998-02, "Wood finger jointing – Part 1: Finger jointing of softwood for load-bearing structures"

[53] Z-9.1-559 "*CLT – Cross Laminated Timber*", Stora Enso Wood Products Oy Ltd, Deutsches Institut für Bautechnik (DIBt), 2012, valid until 13.01.2017

[54] DIN 53255:1964-06, "Testing of wood adhesives and glued wood joints; shear and delamination tests for determining the failing strength of plywood bonds (plywood and coreboard)"

[55] DIN 68705-4:1981-12, "Plywood; core-plywood for building purposes"

[56] DIN 52187:1979-05, "Testing of wood; determination of ultimate shearing stress parallel to grain"

[57] EN 789:2004-10, "Timber structures – Test methods – Determination of mechanical properties of wood based panels"

[58] Z-9.1-501 "*MERK Dickholz ® (MDH)*", Finnforest Merk GmbH, Deutsches Institut für Bautechnik (DIBt), 2009, valid until 31.01.2014

[59] ETA-10/0241 "*LenoTec – Solid wood slab elements to be used as structural elements in buildings*", Finnforest Merk GmbH, Deutsches Institut für Bautechnik (DIBt), 2010, valid until 12.08.2015

[60] Z-9.1-640 "*Massivholzplatten – Layer-plus-static*", Rettenmeier Holding AG, Deutsches Institut für Bautechnik (DIBt), 2006, valid until 30.09.2011

[61] Z-9.1-209 "*Dreischichtplatten aus Nadelholz der Fa. Schwörer Haus KG*", SchwörerHaus KG, Deutsches Institut für Bautechnik (DIBt), 2011, valid until 01.09.2016

[62] ETA-05/0211 "*Lignotrend block panel elements: Timber units for walls, roofs and ceilings*", LIGNOTREND AG, Deutsches Institut für Bautechnik (DIBt), 2010, valid until 29.11.2015

[63] Z-9.1-555 "*LIGNOTREND-Elemente*", LIGNOTREND AG, Deutsches Institut für Bautechnik (DIBt), 2008, valid until 25.06.2013

[64] ETA-09/0036 "*MM – CLT: Cross Laminated Timber (CLT) – Solid wood slab elements to be used as structural elements in buildings*", Mayr-Melnhof Kaufmann Gaishorn GmbH, Österreichisches Institut für Bautechnik (OIB), 2009, valid until 22.03.2014

[65] Z-9.1-638 "*Brettsperrholz: M1 BSP crossplan*", Mayr-Melnhof Kaufmann Gaishorn GmbH, Deutsches Institut für Bautechnik (DIBt), 2011, valid until 01.01.2016

[66] ETA-06/0009 "*MM – CLT: Binder Brettsperrholz BBS: Multilayered timber elements for walls, ceilings, roofs and special construction components*", Binderholz Bausysteme GmbH, Deutsches Institut für Bautechnik (DIBt), 2011, valid until 20.12.2016

[67] ETA-11/0189 "*Derix Cross Laminated Timber: Solid wood slab element to be used as a*

structural element in buildings”, W. u. J. Derix GmbH & Co., Deutsches Institut für Bautechnik (DIBt), 2011, valid until 10.06.2016

[68] ETA-08/0271 “*CLT – Cross Laminated Timber: Solid wood slab elements to be used as structural element in buildings*”, Stora Enso Wood Products Oy Ltd, Deutsches Institut für Bautechnik (DIBt), 2011, valid until 27.04.2014

[69] ETA-06/0138 “*KLH solid wood slabs: Solid wood slab element to be used as structural elements in buildings*”, KLH Massivholz GmbH, Österreichisches Institut für Bautechnik (OIB), 2006, valid until 26.07.2011

[70] Z-9.1-482 “*KLH-Kreuzlagenholz*”, KLH Massivholz GmbH, Deutsches Institut für Bautechnik (DIBt), 2010, valid until 17.11.2015

[71] ETA-11/0210 “*Merkle BSP: Solid wood slab elements to be used as structural element in buildings*”, Merkle Holz GmbH, Deutsches Institut für Bautechnik (DIBt), 2011, valid until 05.07.2016

[72] Z-9.1-465 “*NORDPAN Drei- und Fünfschichtplatten*”, NORDPAN SPA AG, Deutsches Institut für Bautechnik (DIBt), 2010, valid until 14.03.2015

[73] Z-9.1-809 “*Heißerer Brettsperrholz*”, Gebrüder Heißerer, Deutsches Institut für Bautechnik (DIBt), 2010, valid until 24.05.2015

[74] ETA-12/0281, “*NORITEC X-LAM: Cross Laminated Timber (CL T) – Solid wood slab elements to be used as structural elements in buildings*”, NORITEC Holzindustrie GmbH, Österreichisches Institut für Bautechnik (OIB), 2012, valid until 19.08.2017

Feasibility of Cross-Laminated Timber Production from UK Sitka spruce

David Crawford, Dr. Robert Hairstans & Ryan E. Smith

Centre for Offsite Construction +

Innovative Structures

Edinburgh Napier University

Edinburgh, Scotland. (cocis@napier.ac.uk)

Summary

Cross-Laminated Timber (CLT) is an innovative wood product, which can be used for almost all superstructure elements. It is generally produced from kiln-dried, fast growing timber. Currently the majority of CLT used within the UK construction industry is manufactured in central mainland Europe and imported to the UK. The goal of this study is to establish the conditions required for implementing a CLT production and construction capability using available UK timber stock, thus offering a low carbon alternative to multi-story steel and concrete commercial constructions.

1. Introduction

The search for low carbon building products has led to an increase in timber usage in the UK construction industry however the majority of timber used for building in the UK is imported [1]. Locally grown and sourced timber is more economically and environmentally sustainable long term [2]. This project addresses the potential for wood building products that make greater use of UK grown timber resources. One such product is Cross-Laminated Timber (CLT) panel that can be used to form complete floors, walls and roofs. CLT is generally produced from industrially dried, quick growing softwood boards, stacked at right angles and glued together over their entire surface in generally 3, 5 or 7 layers. In an ever-changing regulatory environment, this prefabricated product is ideally suited to the creation of low-impact buildings. Currently, however, there is no UK manufacturer and as with most timber products, all CLT panels used within the UK are imported from central Europe or Scandinavia.

Given the above this European Regional Development Funded (ERDF) project, supported by Scottish Government, Scottish Enterprise and Forestry Commission Scotland, is to facilitate the commercial manufacture of CLT products in Scotland and add value to the Scottish timber resource. In order to determine the feasibility of manufacturing CLT from UK timber it was deemed necessary to research and develop a CLT production process and evaluate its associated mechanical properties in comparison to imported CLT.

2. Market Demand

First conceived in Switzerland in 1975, CLT manufacturing processes have been under continuous development ever since. Originating in central Europe, there are now a large number of CLT production sites within Austria, Germany, Czech Republic and Switzerland. Fig. 1 provides an overview of the various manufacturers and a percentage breakdown for CLT production by volume (m^3) in 2011. Of the manufacturers listed, BinderHolz, KLH, Mayr-Melnhof Kaufmann, Metsa Wood and Stora Enso are the larger volume producers who mainly supply the UK. Further, three of these five main manufacturers work, own or have alliances with UK formatting operations, which act as a route to market for manufacturers.

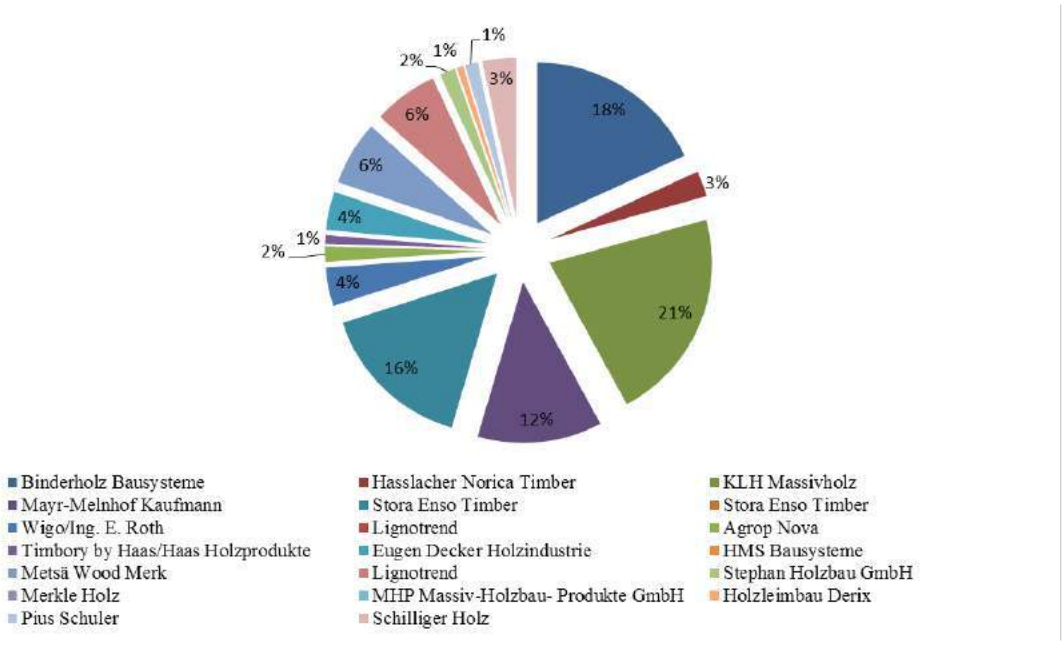

Fig. 1 European CLT Manufacturers (2011)

Although CLT was first introduced to the UK in 2001, it was not until the founding of Eurban in 2003 and KLH (UK) in 2005 that the product was an accessible form of construction and therefore capable of competing with concrete and steel. An assessment of the completed CLT projects in the UK from 2003 to 2011 illustrates that the demand for CLT has increased each year; over 50% more projects were completed in 2011 in comparison to the year prior [3]. Fig. 2 shows the various construction sectors and the related number of completed projects between 2003 and 2011 in the UK. Education has been the most dominant building sector to date due to the introduction of the Government investment schemes such as the ‘Building Schools for the Future’ [4] and the ‘Priority School Building programme’ [5]. Given that CLT is still relatively new to the UK construction industry, its growth and recognition will only help to promote the use and specification of CLT in current and developing sectors.

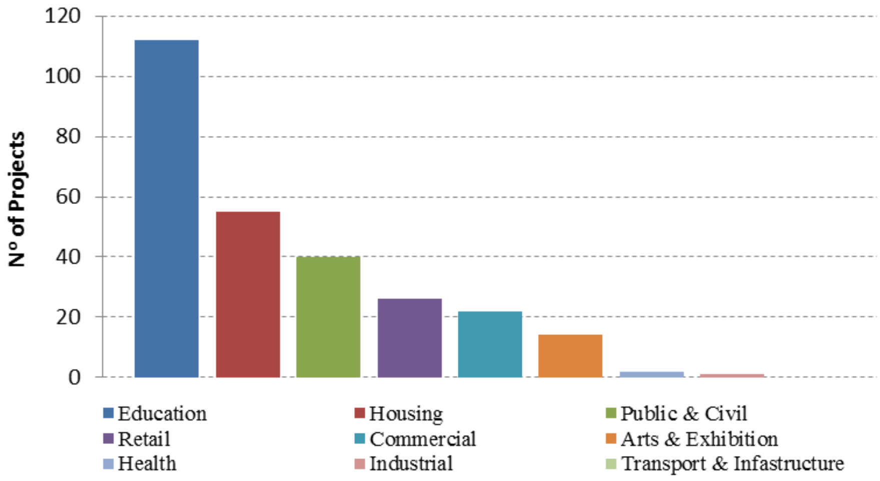

Fig. 2 CLT UK Market data by sector (2003-2011) [3]

The commercial construction industry perceives CLT to be a more expensive product in comparison to traditional steel and concrete construction methods in the UK. However, when considering the various benefits of CLT (i.e. reduced foundation costs, reduced construction time etc.) and the overall life cycle analysis of a typical building, CLT has the ability to be a cost competitive low carbon alternative to traditional building materials [2]. However, for CLT to be truly sustainable, environmentally, socially and economically, it should utilise local resource and serve the local market to reduce transportation requirements, create security of supply and provide employment.

Currently CLT production facilities supplying the UK market are required to travel in excess of 700 miles (supplier and destination dependent). Various locations in Scotland could be considered for CLT production and the distance to London (≈400 miles), the nexus of building in the UK, is significantly less than that from Europe. In addition, transportation costs from central Europe and Scandinavia are variable depending upon the supplier and the final destination; they are between 30% and 50% greater than would be expected from within the UK. Another driver for CLT production in the UK is unpredictability in the fluctuating exchange rate that accompanies imported product. This results in large variations in total project cost that would be eliminated if UK manufacture were established.

3. UK Timber Resource

In order to determine the viability of UK timber and manufacture of CLT, suitability of resource needs to be assessed. Sitka spruce accounts for approximately 50% of the UK softwood resource and over 60% within Scotland. It is therefore anticipated that Sitka spruce would be the primary species considered for CLT production in the UK [6]. The Sitka spruce material selected for this study was typical of what is produced by the main sawmills in Scotland and thus the results give a fair representation of the available resource.

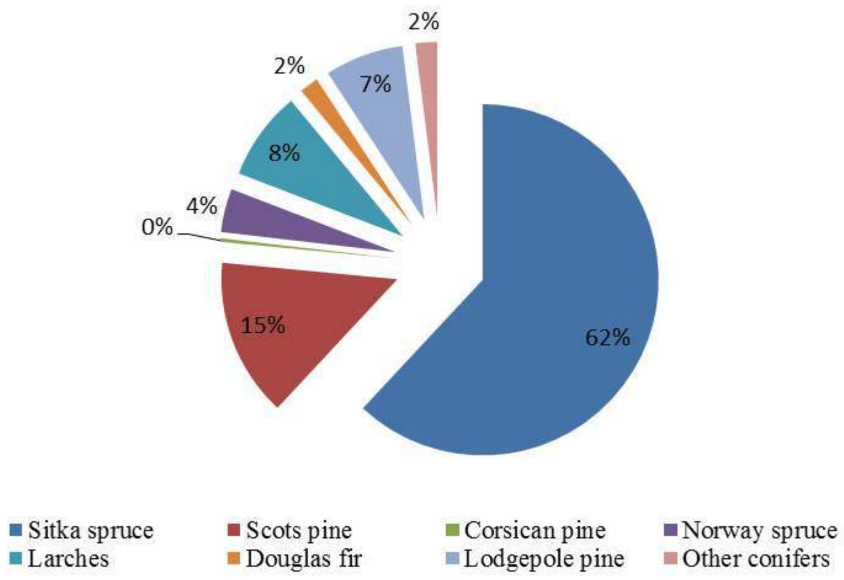

Fig. 3 UK Timber resource (2011) [6]

Recent figures from the Forestry Commission suggest that the standing volume of timber felled in 2011 was in the region of 7.7Mm³ over bark standing (obs) which produced approximately 1.67Mm³ of sawnwood. A breakdown of this material is as follows:

- 62% Fencing (27%), Pallet and packaging (35%)
- 33% Construction
    - Stress graded to C16 (95%)
    - Kiln dried to circa 20% moisture content.

Recent Forestry Commission forecast suggests opportunity for a significant rise in the volume of sawnwood production for at least the next 25 years evidence of this is shown in Fig. 4.

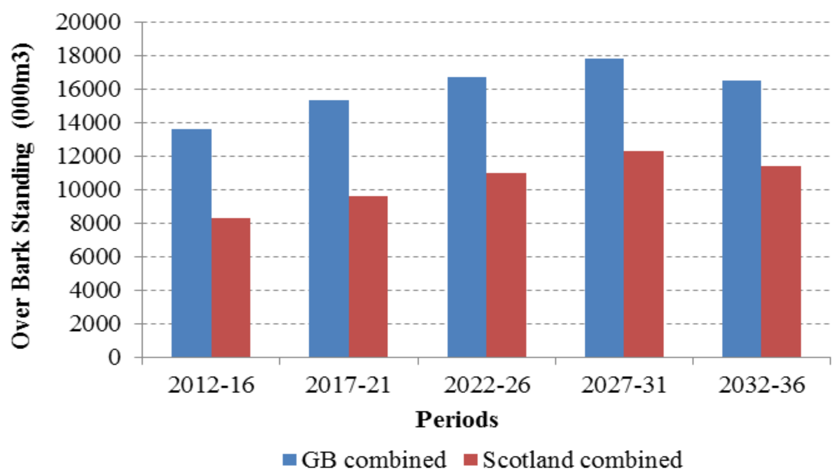

Fig. 4 Forecast of standing timber availability from Scottish forests in comparison to GB[6]

The majority of sawmills in the UK only dry construction timber to circa 20% moisture content and currently there is little demand for timber dried beyond this level. CLT production requires

12±2% moisture content in large volumes; factors such as drying time, cost and material waste are critical, as they will impact upon the overall product price. There are various methods that can be considered for drying timber and previous studies using small-scale humidifier type kilns have proved effective for UK Sitka spruce. However this is likely to be unsuitable for large volume production (i.e. >10,000m^3 per annum) and therefore the commercial viability of drying UK Sitka spruce to 12±2% moisture content is an area that requires additional research.

4. UK CLT - VIABILITY

The current barrier to the use of UK-grown CLT is availability of UK based manufacturing facilities and test data for specification. The viability process described here is intended to determine test data for future specification.

Manufacturers in Europe are currently aiming towards the standardisation of CLT panels by standardising lamella thickness at 20mm, 30mm and 40mm and it is anticipated that these dimensions will be adopted for UK CLT production. However, for this study the panel lay-ups manufactured are required to be consistent with timber dimensions that are available from UK sawmills whilst taking into consideration the various specifications of European CLT manufacturers in order to allow relative comparison to take place.

Panels were fabricated from Scottish grown Sitka spruce and transported to an accredited test facility to undergo a series of structural assessments to determine local and global modulus of elasticity (stiffness in bending) and modulus of rupture (strength in bending) in accordance with BS EN 408. Information from this process has been used to assess the feasibility of application of these components in wall, floor and roof applications.

4.1 Manufacturing process

The manufacturing stage of the project took place at the premises of Nor-Build in Forres, Morayshire. The workshops at Nor-Build are well equipped, having two large woodworking machine shops, metal working equipment and a large floor area for setting up efficient production lines. Critical to this type of project was the existence of a cross cutting line capable of handling timber in lengths of over five metres. A five head planer moulder was also available, and ample covered storage space. Unfortunately it was not possible to control the climate within the production hall and this had implications for the quality assurance of the adhesive between lamination layers. A flow chart detailing the relevant work stages (Fig. 5) was developed prior to any work being carried out in order to streamline the fabrication process.

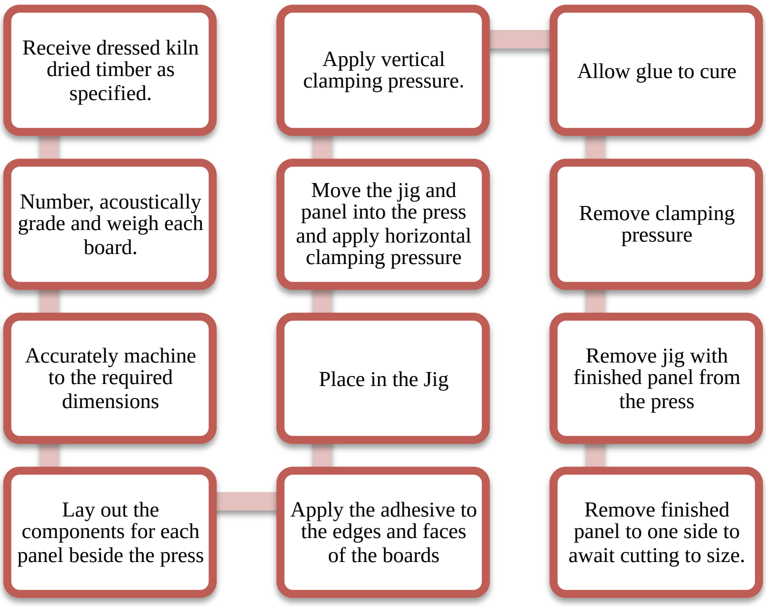

Fig. 5 Process flow chart – CLT fabrication

A precise specification was established for the CLT lamellae - all of the timber was required to have a moisture content of 12±3%. This moisture content level was specified in order to be as close as possible to the anticipated equilibrium moisture content of the panels in service and is also compatible with the polyurethane (PU) adhesives used in the fabrication of the test panels. The lamella dimensions were based upon standard milling profiles produced by BSW Timber Ltd. Three Sitka spruce profiles were considered: a smaller 20 × 95mm cross section cut from the side of the logs, and a larger 40 x 95mm cross section cut from the core of the log and a larger 40 × 140mm profile.

As sawmills in Scotland are generally set up to produce timber with a moisture content of circa 20%, the desired specification of 12±3% moisture content required an alternative kiln cycle to be implemented in order to reduce the percentage of reject material. However this was a one-off, conducted on a relatively small scale, and at this stage requires further optimisation to make it commercially viable for larger volumes of timber.

Fig. 6 Method for moving panels in and out of the press

The *Italepresse SCF/8* (Fig. 6) provided by Edinburgh Napier University was originally manufactured for veneer lamination with maximum platen dimensions of 400mm × 1250mm × 3200mm and a maximum vertical pressure of 160 metric tonnes. Although not designed for CLT production some minor modifications to the press allowed the fabrication of both face and edge bonded panels. A number of screw-type clamps that could be bolted on to the machine were designed to provide horizontal clamping force for edge bonding.

5. TEST PROGRAMME

A key objective of the test work was to determine the relative mechanical properties of UK resource CLT for a range of panel configurations (i.e. timber species, lamella thickness, lamella width and number of layers). Currently CLT is manufactured and tested under the Common Understanding Assessment Procedure (CUAP) and various European Technical Approval (ETA) documents. It is stated within the CUAP that mechanical properties of CLT will be determined in accordance with BS EN 408 [7] and take into consideration the principles of BS EN 789 [8].

To undertake test work sufficient to determine compliance with these requirements a range of different permutations were considered, with two final panel types selected for structural testing. The details of these panel dimensions are shown in Tab. 1 and Fig. 7.

Tab. 1 Panel type, test permutations

Sample Ref	Lamella dimensions		Make Up	Panel Dimensions					
				Edgewise			Flatwise		
	Depth	Width	No	Depth	Width	Length	Depth	Width	Length
	mm	mm		mm	mm	mm	mm	mm	mm
HG-SS1	40	95	3	140	120	2550	120	380	2550
HG-SS2	20	95	5	140	100	2680	100	380	2680
HG-SS3	40	140	3	170	120	3200	120	420	3200

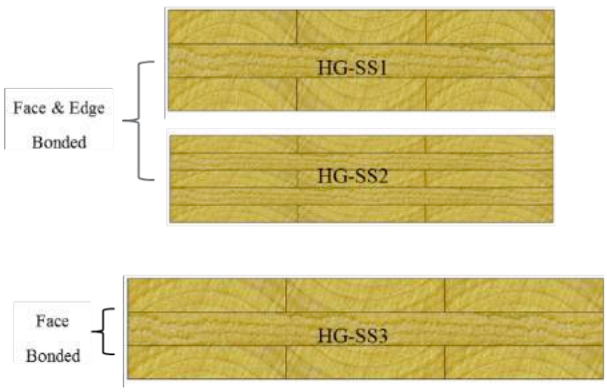

Fig. 7 CLT panel types and dimensions

The samples shown in Fig. 7 are representative of the final tests pieces. UK grown Sitka spruce 1 (HS-SS1) samples were fabricated using 40 x 95mm Sitka spruce graded to C16 specification prior to leaving BSW Timber Ltd sawmill. Home-grown Sitka spruce 2 (HG-SS2) samples were fabricated using 20 × 95mm sawn falling boards that were non graded material. Each of the HG-SS1 and HG-SS2 samples were face and edge bonded during the fabrication process. UK grown Sitka spruce 3 (HG-SS3) panels were formed using material supplied by John Gordon & Son’s sawmill, which was graded as standard C16 material. The HG-SS3 samples were face glued only.

The range of panels investigated varied in height due to lamella thickness and number, and correspondingly also varied in length and width. It should also be noted that due to the dimensional constraints of the CLT press the maximum size of panel to be tested was limited. In order to determine the structural performance of these panel configurations, testing was carried out in accordance with BS EN 408 [7] for strength and stiffness properties for both orientations of a beam (edgewise) and a floor/roof (flatwise) as shown in Fig. 8.

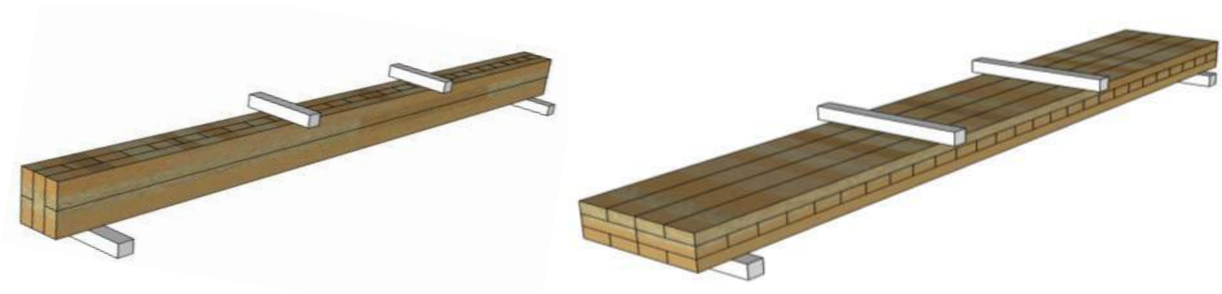

a) Edgewise (beam) *b) Flatwise (floor)*

Fig. 8 BS EN 408 – strength and stiffness in two orientations

5.1 Acoustic Analysis

Prior to fabrication, each of the boards was labelled, weighed and acoustically analysed using a Brookhuis MTG Acoustic Grader to determine dynamic MoE (Fig. 9). This technique forms a vital part of the process since it gives each board an identity to which characteristics can be attributed; in this case MoE was the characteristic of most importance.

Fig. 9 CLT - Lamellae analysis

This information is particularly valuable when assessing the performance of the CLT panels, since individual lamellae can be located within the panel. The mean dynamic MoE values for the lamellas within each panel type are summarised in Fig. 10, the results of which were used to calculate the effective bending stiffness for each of the relative panel types. Further research would allow the contribution of each of the individual lamellas to the overall panel performance to be better understood.

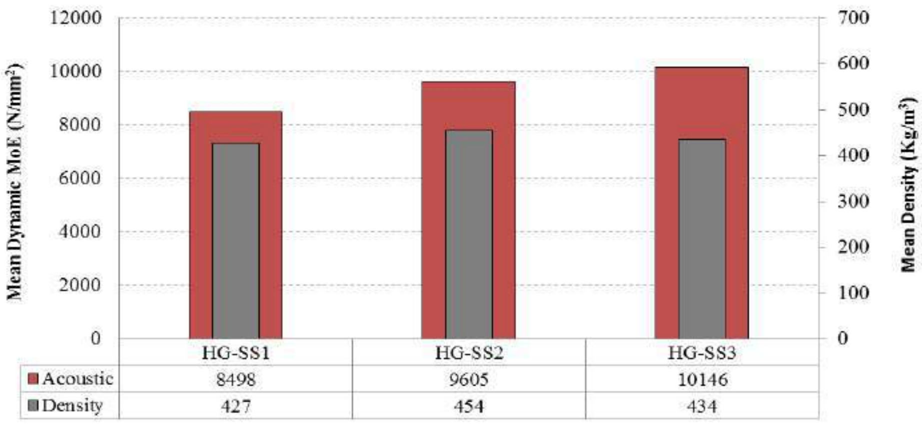

Fig. 10 Mean Dynamic MoE and Density for varying sample group

The dynamic MoE results shown have been corrected for density but have not been corrected for moisture content (timber was supplied at 12±3% moisture content) and for this reason no adjustment factors have been applied. The HG-SS1 sample group has a value of 8498N/mm^2. This is comparable to the mean MoE value for C16 grade material as defined in BE EN 338 (7). This is to be expected, given that the material supplied by BSW Timber Ltd was standard C16 grade. Approximately 400 boards from the HG-SS2 sample group were measured and a mean dynamic MoE of > 9600N/mm^2 was obtained. The HG-SS3 sample group returned a mean dynamic MoE value in excess of 10000N/mm^2. Given that this material was graded as standard C16 by John Gordon & Son's sawmill, the results are higher than might otherwise have been expected. It was noted that the mean density of the Sitka spruce analysed during this study is > 410 kg/m^3. Bending strength, MoE and density are considered the most crucial mechanical properties of wood for this study as they are used to directly assign structural timber to a strength class according to EN338.

A recent study carried out by J. Moore found that the UK Sitka spruce resource is grade limited not by strength or density but by stiffness [9]. Stiffness is a key factor when considering the design of timber structures and has a direct influence on other critical parameters such as vibration. Due to the re-distribution of stresses, within the lamellas, cross lamination results in an enhancement in performance and less stiff timber is anticipated to be suitable for CLT. As current calculation methods for connection performance are directly related to the material density, material properties such as strength and density are also important factors when considering CLT design

5.2 DATA ANALYSIS METHODS

A number of different methods exist for the analysis and design of CLT elements. The main methods have been considered during this study and a relative comparison made in order to determine which method is most suitable when considering CLT formed using UK grown timber. The methods considered during this study include the Simplified Design Method, the Timoshenko Method, the Shear Analogy Method and the Mechanically Jointed Beams Theory (Gamma Method). Each of these methods considers an effective moment of inertia (I_{eff}) where only the boards in the direction perpendicular to the action of the loading are taken into account.

6. Bending Strength and Stiffness

Four tests were carried out for each sample group in the edgewise (e.g. beam) and flatwise (e.g. floor) orientations. Given the limited number of tests undertaken, it would be misrepresentative to present 5th percentile characteristic values, therefore mean values are presented for bending strength. In the case of stiffness a mean modulus of elasticity (MoE) is shown for each sample group in each orientation. Values for density, moisture content, bending strength, and modulus of elasticity (MoE) were calculated and are presented within the subsequent sections of this report.

6.1 Edgewise

When considering the HG-SS1 sample group (Fig. 11), a mean edgewise bending strength of 43N/mm^2 was obtained. A mean edgewise bending strength of 42N/mm^2 was achieved for the HG-SS2 sample group. The HG-SS3 sample group returned a mean edgewise bending strength value of 36N/mm^2.

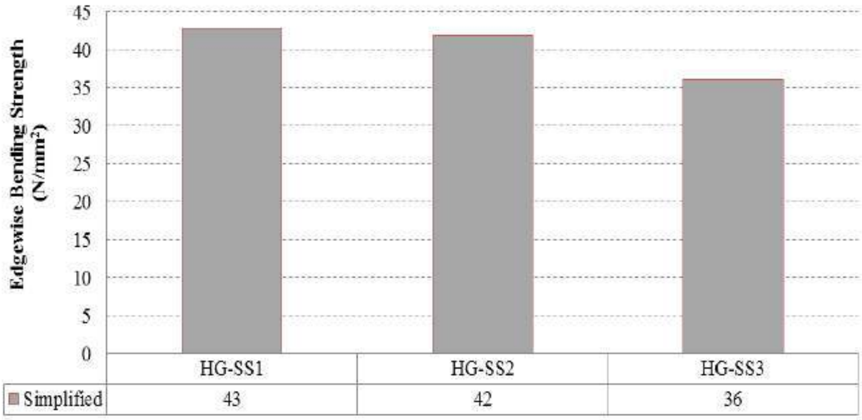

Fig. 11 Edgewise Bending Strength

A mean edgewise MoE was determined for each sample group (Fig. 12), for the HG-SS1 sample group a value of 9364N/mm^2 was achieved. When comparing this value to the mean dynamic MoE for the lamellas (8498N/mm^2) an increase of approximately 10.2% is apparent. When considering the results from the 5-layer system (HG-SS2) a mean value of 10205N/mm^2 was obtained, an increase of approximately 6.2% over the mean dynamic MoE of the lamellas. The mean edgewise MoE achieved from the HG-SS3 sample group was 9385N/mm^2 and the mean dynamic MoE was 10146N/mm^2 a comparison of the two values indicated a decrease of approximately 7.5%.

Fully bonded CLT samples provided additional performance when considering edgewise strength and stiffness. Conversely, it was noted that samples which were only face bonded returned a mean MoE which was less than or relatively similar to the mean dynamic MoE of the material specified. The results of this study would suggest that fully bonded CLT panels (i.e. face and edge bonded) provide an increase in stiffness, compared with the raw material specified for use in the fabrication of CLT. However the study considered a relative small sample set and it is therefore recommended that a future programme of work be carried out in order to fully validate this statement.

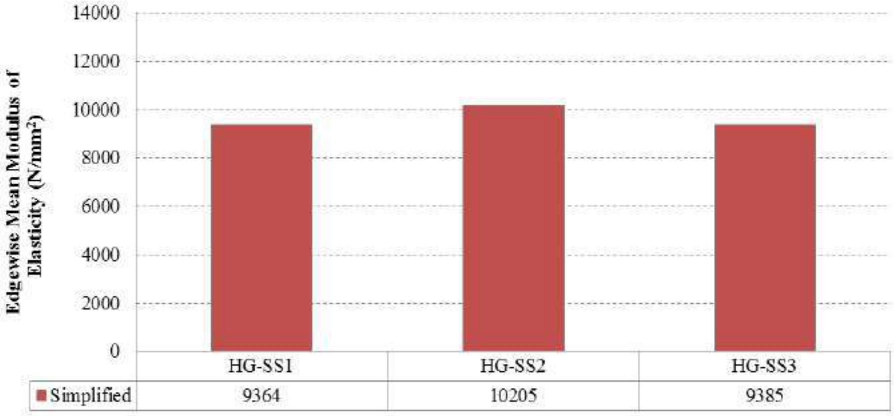

Fig. 12 Edgewise Bending Stiffness

6.2 Flatwise

A direct comparison of the bending strength results using the three different analysis methods described in section 5.2 (Fig. 8) shows that the results obtained using the Timoshenko and Shear Analogy method are directly comparable, however the Gamma method shows a marginal increase (≈4%) in comparison.

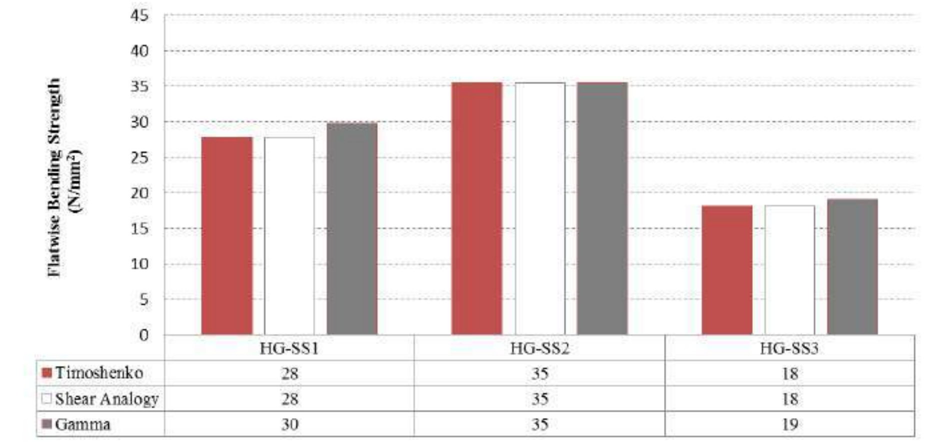

Fig. 13 Flatwise Bending Strength

Compared in Fig. 14 are the MoE results using the different analysis methods (Timoshenko, Shear Analogy and Gamma method). It is clear from the results obtained that there is a notable increase when MoE is calculated using the Gamma method. This is explained by the approach adopted during the calculations: the Gamma method does not take into consideration the influence of shear deformation and hence an over-estimated value is obtained.

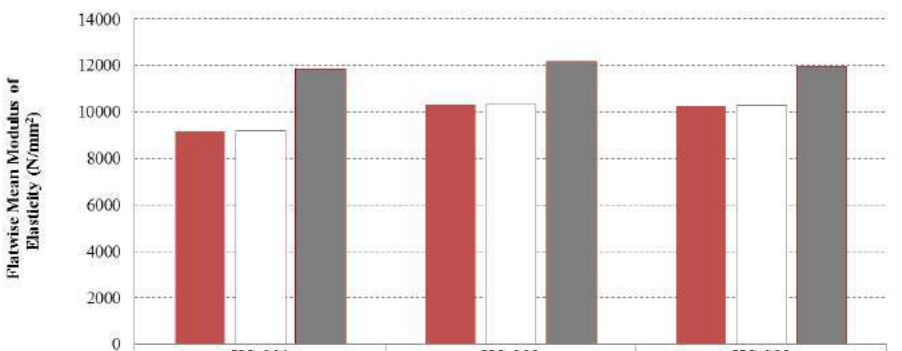

	HG-SS1	HG-SS2	HG-SS3
Timoshenko	9192	10328	10278
Shear Analogy	9192	10328	10278
Gamma	11862	12143	11974

Fig. 14 Flatwise Bending Stiffness

Another consideration is the influence of shear deformation when testing at varying span to depth conditions. It is suggested that the shear deformation of CLT panels loaded uniformly may be neglected for elements having a span to depth ratio higher than 20 [10]. However, other literature and CLT panel producers give as a boundary condition a minimum span to depth ratio of 30 before neglecting the shear deformation of the panel. A previous study carried out by Blass and Fellmoser [11], showed that shear deformation has a significant influence where the span to depth ratio is less than 30 evidence of which is provided in Fig. 15.

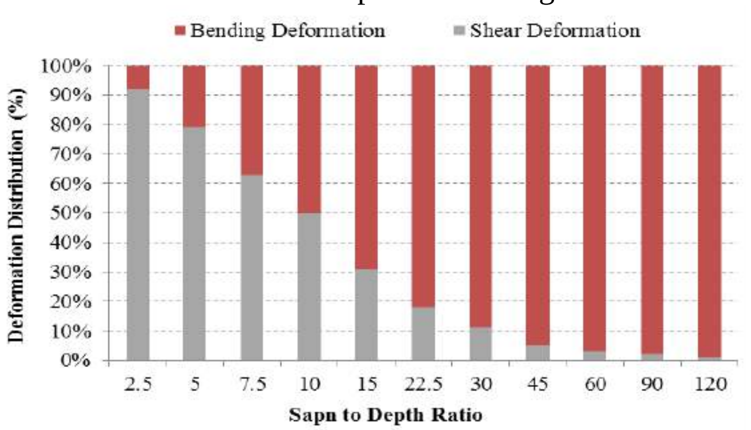

Fig. 15 Influence of shear deformation at varying span to depth ratios (10)

Of the various tests carried out during this study, the span to depth ratio was approximately 19. Literature suggests that at this span to depth ratio the contribution of shear deformation would be in the region of 22%. If we compare the mean local MoE for the HG-SS1 sample group obtained using the Gamma method (11862N/mm^2) with the mean local MoE obtained from the Timoshenko and the Shear Analogy method (9192N/mm^2), a 25% decrease is apparent.

6.3 Effective Bending Stiffness

We know from previous studies that the UK Sitka spruce resource is typically limited by stiffness rather than strength or density [9]. The effective bending stiffness of CLT is a measure of the material stiffness in relation to the cross sectional make-up of the panel.

In order for a UK CLT product to be competitive in the market it will have to compete with imported CLT products. CLT products from Europe are fabricated largely from C24 graded material (90% C24 and 10% C16). In most cases this is simply because the material is widely available rather than as a specification of the designer. However, there are instances where a high degree of performance is required and thus a UK product must be competitive in this regard as well. Fig. 16 shows $EI_{effective}$ values for the HG-SS1, HG-SS2 and HG-SS3 samples, which have been compared directly with imported products of similar dimensions.

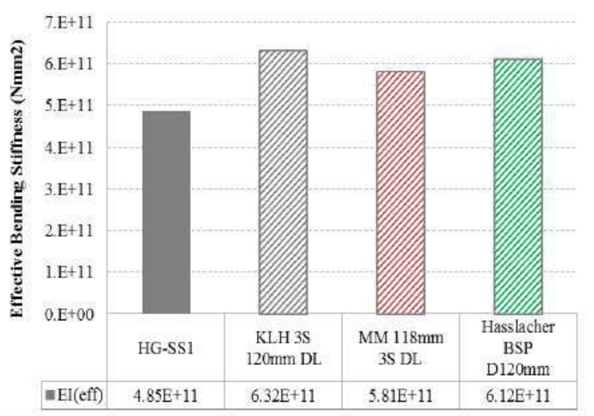

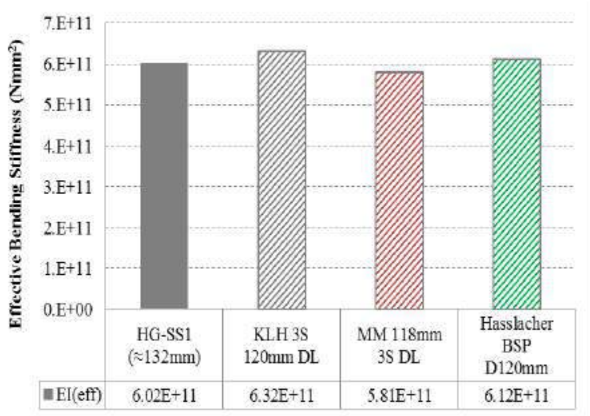

a) Home Grown SS1 *b) Home Grown SS1 – Increased depth of section*

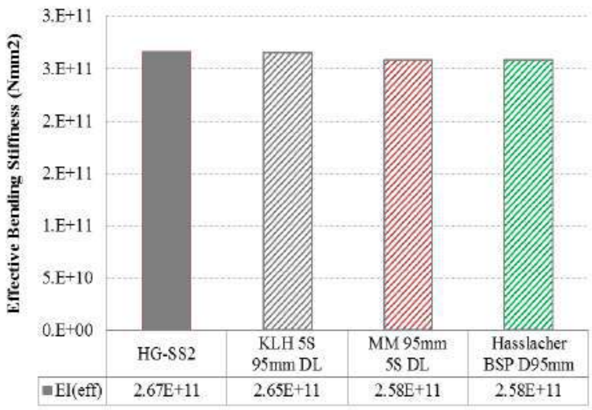

c) Home Grown SS2

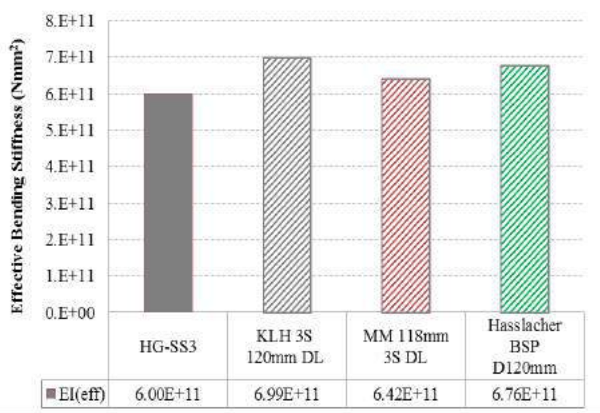

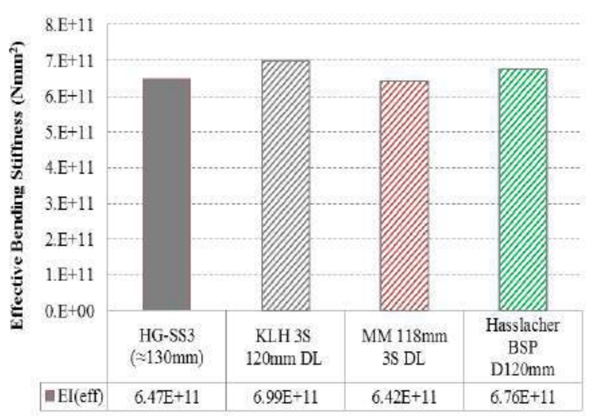

d) Home Grown SS3 *e) Home Grown SS3 – Increased depth of section*

Designation: KLH 3S 120mm DL = KLH 3 layer system (40/40/40mm), 380mm panel width
MM 118mm 3S DL = Mayr Melnholf 3 layer system (39/40/39mm), 380mm panel width
Hasslacher BSP D120mm = Hasslacher 3 layer system (39/40/39mm), 380mm panel width
KLH 5S 95mm DL = KLH 5 layer system (19/19/19/19/19mm), 390mm panel width
MM 95mm 5S DL = Mayr Melnholf 5 layer system (19/19/19/19/19mm), 390mm panel width
Hasslacher BSP D95mm = Hasslacher 5 layer system (19/19/19/19/19mm), 390mm panel width
KLH 3S 120mm DL = KLH 3 layer system (40/40/40mm), 420mm panel width
MM 118mm 3S DL = Mayr Melnholf 3 layer system (39/40/39mm), 420mm panel width
Hasslacher BSP D120mm = Hasslacher 3 layer system (39/40/39mm), 420mm panel width

Fig. 16 EIeffective comparison

Fig. 16 c) shows that the HG-SS2 samples fabricated from un-graded sideboard material (traditionally used for fencing and pallets) achieve a mean effective bending stiffness, which is comparable to imported European products. Another way to increase the performance of these panels would be through the use of acoustic tools to segregate higher grade material for use within the outer layers and lower grade material for the outer layers.

When considering the HG-SS1 and HG-SS3 sample groups, it is clear that the imported European products achieve greater values. However, this would be expected given that the raw material used to fabricate the HG-SS samples were stress graded C16 and the other imported panels are produced using predominately C24 graded material. One simple way of increasing the effective bending stiffness is to increase the thickness of the panels (i.e. increase the thickness of individual lamellas or total the number of layers). By increasing the depth of section of the HG-SS1/HG-SS3 panels by approximately 10% (Fig. 16 b) and e)) it is evident that a UK CLT product equals the level of performance of an imported product.

7. Conclusions and Recommendations

Sitka spruce accounts for approximately 50% of the UK softwood resource and it is anticipated that this would be the primary species considered for CLT production in the UK. Panels produced using UK Sitka spruce material show promising results in terms of both strength and stiffness, with panels fabricated using the saw-falling (sideboard) 20 × 95mm boards obtaining consistently good results.

Currently UK Sitka spruce sideboard material is not graded for structural purposes and is typically specified for use within pallets, fencing and other low value applications. Given the structural properties obtained from the HG-SS2 sample group (panels fabricated using sideboard material) it is particularly encouraging as there is potential to add considerable value to the UK timber resource. However in order to fully optimise the local resource available for application in the manufacture of CLT it will be necessary to carry out a further degree of grading (i.e. structural grading of sideboard material).

If the dynamic stiffness results from the acoustic grading process are considered (Tab. 2), it can be seen that approximately 28% of the HG-SS1 battens are greater than or equal to 9500N/mm^2. It was also noted that circa 50% of the HG-SS2 boards returned a dynamic MoE value which is greater than or equal to 9500N/mm^2.

Tab. 2 Potential Grading Yield

Sample Group	**Dynamic Stiffness**	
	9500 – 11000 N/mm^2	**11000 > N/mm^2**
HG-SS1 (40 x 95mm)	19.76%	8.30%
HG-SS2 (20 x 95mm)	24.00%	25.18%
Note: Acoustic grading results are based on average density and have not been corrected for moisture content.		

Although these figures are only for a small sample range, they do show that the current UK resource has the potential to yield higher-grade material than C16 for CLT production. It is therefore considered that the implementation of an in-line grading device within a CLT production plant would allow material to be pre-selected and specified for optimum use within each panel i.e. higher grade material (sideboards) in the outer laminations and lower grade (centre cut) material in the inner laminations.

The findings from this basic research study show that CLT can be produced using UK Sitka spruce, further the structural performance is not dissimilar to the products, which are currently imported from central Europe. However in order for CLT to be commercially feasible there are a number of aspects, which require additional research.

For investment in UK CLT manufacture to take place a robust business plan is required to ensure investor confidence in the proposed new product and this requires market research, market testing and competitor analysis. One of the main areas that require additional research is the dimensional stability of UK Sitka spruce when drying (at a commercial scale) to levels below 20% moisture content. A programme of work is currently being devised to assess the distortion of varying sample dimensions at different target moisture content values.

Through Scottish Enterprise and European Regional Development Funding the Centre for Offsite Construction + Innovative Structures has developed knowledge transfer linkages from emerging (North America) and established (Austria & Germany) markets for flow of information and long-term strategic partnerships. As such we are currently evaluating the required facility capability and associated cost, time and funding requirements for UK CLT production.

8. Acknowledgements

This work is supported by European Regional Development Funding, Scottish Enterprise and Forestry Commission Scotland. The Centre for Offsite Construction + Innovative Structures would also like to acknowledge and thank BSW Timber Ltd, Norbuild Timber Fabrication & Fine Carpentry Ltd and Purbond for their continued support.

9. References

[1] Federation TT. *Statistical Review*; 2011.

[2] Suttie E. *Five most effective ways of adding value to home grown timber*. Building Research Establishment; 2011.

[3] TimberFirst. *Market Report*; 2012.

[4] Education Df. *Building Schools for the Future*. [cited; Available from: http://www.education.gov.uk/schools/adminandfinance/schoolscapital/funding/bsf

[5] Education Df. *Priority School Building programme*. [cited; Available from: http://www.education.gov.uk/schools/adminandfinance/schoolscapital/priority-school-building-programme

[6] Commision F. *Standing timber volume for coniferous trees in Britain*.: National Forest Inventory. ; 2011.

[7] BSI. BS EN 408:2010+A1:2012. *Timber structures - Structural timber and glued laminated timber - Determination of some physical and mechanical properties*: BSI 2011.

[8] BSI. BS EN789: 2004. *Timber structures - Test methods - Determination of mechanical properties of wood based materials*: BSI 2005.

[9] Moore J. *Wood properties and uses of Sitka spruce in Britain*. Edinburgh: Forestry Commission; 2011.

[10] Mestek P, Kreuzinger H, Winter S. Design of Cross Laminated Timber (CLT). Munich: Timber Structures and Building Construction Technical University Munich.

[11] Fellmoser P, Blass H. Influence of rolling shear modulus on strength and stiffness of structural bonded timber elements. Germany; 2004.

Characteristic Values and Test Configurations of CLT with Focus on Selected Properties

Helene Unterwieser
Quality manager, sub-agent of technical management
Lignum Test Centre, Institute of Timber Engineering and Wood Technology/
Graz University of Technology, Graz, Austria

Gerhard Schickhofer
Head of Laboratory and Institute
Institute of Timber Engineering and Wood Technology/
Graz University of Technology

Summary

The overall aim of this paper is to define characteristic properties for strength, stiffness and density of cross laminated timber (CLT) and list them in a table according to that for glued laminated timber (GLT). As several mechanical properties have already been investigated, in a manifold variety of researches, this paper aims to sharply define characteristic values, or rather bearing models, for determination of strength values for CLT dependent on the basic material (boards). A bearing model is a function that describes the strength property of a structural element; it is based on statistical analysis and is derived from the strength properties of the individual component parts (for CLT, these are the boards), and their various modification factors (e.g. height factor). However, it should be mentioned, in this context, that further research needs to be conducted concerning altered boundary conditions of several material properties. The bearing model for bending can be regarded as an obvious example, which is valid in its present form for a base material made of boards and CLT with the reference dimensions.

Due to the definition of test arrangements and the related determinations of mechanical properties, the test results of CLT can be properly compared with each other. It can be shown that the calculation of the global modulus of elasticity in bending, based on tests, is more sensitive than the local modulus of elasticity, because of the influence of rolling shear modulus and shear correction coefficient. Suggested test setups for bending, shear in-plane and torsional shear should deliver the required shear values, which are defined as characteristic values.

1. Introduction

At present, mechanical material properties of cross laminated timber (CLT), e. g. strength and stiffness, are incompletely regulated in technical approvals. There is a present necessity for a standard of CLT (DRAFT EN 16351:2012 [1]), needs to be developed to satisfy the essential requirements of this product. Added to the requirements in the context of production and, as a consequence, examination as well as determination, mechanical and physical properties of the material can be defined. In order to determine the mechanical properties of CLT there are two different approaches:

- determination on the basis of the mechanical properties of the single layers in combination with bearing models
- determination on the basis of testing of CLT elements.

If the declaration is made via the single layer, in order to be able to define the mechanical properties of CLT through developing an adequate model, it is of outmost importance to be aware of the connection between the lay-up – geometric conditions (number of layers, layer thickness, cross section of the individual board and of CLT) and the type of layer (timber, wood based panels) – or rather its characteristic value in terms of strength and stiffness

In the course of determination on the basis of testing of CLT, it is possible to directly declare the defined characteristic values of strength and stiffness. However, this implies defining and fixing test configurations, which can be used to compare various examinations and enables an extraordinarily robust determination of mechanical properties. In this regard the determination of the modulus of elasticity in bending should be mentioned as an example. The chosen test configurations, concerning the determination of deformation (local, global) and the coupled analysis parameters for shear modulus and rolling shear modulus, partly produce fundamental differences in the results and, hence, make the definition of a “correct” modulus of elasticity much more difficult.

Added to the characteristic properties of strength and stiffness, representative values relevant to calculation and construction, such as the partial safety factor γ_M, and material properties, such as the modification factor concerning load-duration class and moisture content, k_{mod}, deformation factor, k_{def} etc., need to be defined for the product CLT.

Therefore, it can be regarded as the overall aim of this paper to present the first extensive definition of the characteristic material properties of CLT, similar to timber or glued-laminated timber (GLT). Generally, bearing models on the basis of the basic material are used for this. The final determinations made in this paper are based on the results of research and, in this context, partly on assumptions deduced from GLT. Hence, these assumptions need to be qualified concerning some aspects, such as regarding the definition of the valid cross section, or rather the basic reference material. The presentation of the characteristic values of strength and stiffness of CLT, shown in Tab. 11, is intended to begin a discussion about the questions of whether and how the product, CLT, can be regulated by strength classes.

Added to this, it can be regarded as another aim of this paper to define the influences relevant to determining mechanical bending properties of CLT on the basis of the defined test configuration. With regard to determining the shear strength, in the context of load in-plane, the suggested test configurations are presented.

2. Determination of the basis of design and material properties of CLT

2.1 Partial safety factor for material properties γ_M

Because of using boards with similar strength (a result of grading) and similar dimensions, the product CLT has a lower dispersion of material data in comparison with singular boards. The partial safety factor concerning material property and capacities to withstand stress γ_M is defined for CLT – equal to GLT – as

$\gamma_M = 1.25$.

2.2 Modification factor for duration of load and moisture content k_{mod}

The modification factors, k_{mod}, highly depend on the service class and the load-duration class. Therefore, it is possible to adjust the strengths to real conditions regarding load and wood moisture. CLT is similar to the categories for solid timber and glued laminated timber. Tab 1 is an excerpt of table 3.1 of the ÖNORM EN 1995-1-1:2009 [2] with an additional entry for CLT.

Tab. 1 Values of k_{mod}

Material	Standard	Service class	Load-duration class				
			Permanent action	Long term action	Medium action	Short term action	Instantaneous action
Solid timber Glued laminated timber	EN 14081-1 EN 14080	1	0.60	0.70	0.80	0.90	1.10
		2	0.60	0.70	0.80	0.90	1.10
		3	0.50	0.55	0.65	0.70	0.90
Cross laminated timber1)	prEN 16351	1	0.60	0.70	0.80	0.90	1.10
		2	0.60	0.70	0.80	0.90	1.10
1) It is proposed, that the use of CLT in service class 3 is not allowed.							

2.3 Deformation factor k_{def}

The deformation factor k_{def} highly depends on the service class. Hence, the long-term influence on load-bearing lay-ups and structural members needs to be taken into consideration, due to the effect of creep. [3] shows the verification that CLT should be assigned to the material plywood, due to its crossed lay-up, or rather due to the stress towards rolling shear. Added to this, it should be mentioned that, according to the number of layers, there needs to be a difference. In concrete terms, this means that for CLT with seven or less layers the k_{def}-values need to be increased by approx. 10 %. Tab. 2 presents an excerpt of table 3.2 of the ÖNORM EN 1995-1-1:2009 [2] with an additional entry for CLT.

Tab. 2 Values for k_{def}

Material	Standard		Service class		
			1	2	3
Solid timber Glued laminated timber	EN 14081-1 EN 14080		0.60	0.80	2.00
Plywood	EN 636	Typ EN 636-1	0.80	-	-
		Typ EN 636-2	0.80	1.00	-
		Typ EN 636-3	0.80	1.00	2.50
Cross laminated timber1)	prEN 16351	> 7s	0.80	1.00	-
		≤ 7s	0.85	1.10	-
1) It is proposed, that the use of CLT in service class 3 is not allowed.					

2.4 Shrinkage and swelling coefficient

The differential shrinkage and swelling coefficient of European softwood is defined as 0.24 % in terms of mean of tangential and radial shrinkage (swelling). In the context of CLT an additional shrinkage- and swelling coefficient in terms in-plane of CLT needs to be taken into consideration, see Tab. 3.

Tab. 3 Values for shrinkage and swelling coefficients parallel to grain and in-plane of CLT

Material		**Shrinkage and swelling coefficient in % per % change in the moisture content below fibre saturation**
Cross laminated timber	In-plane	0.02-0.04
	Out-of-plane	0.24

2.5 Reference cross section for CLT

The following characteristic strength values are partly based on bearing models for glulam. For this reason it is necessary to define a reference cross section for CLT. Tab. 4 and Fig. 1 show the defined reference dimensions for GLT, CLT and the basic material (board).

Tab. 4 Reference cross sections for GLT, CLT and basic material (boards)

	Height-Depth/Thickness	Width
GLT Basic material – board	$h_{GLT,ref}$ = 600 mm $t_{l,GLT,ref}$ = 40 mm	$b_{GLT,ref}$ = 150 mm $b_{l,GLT,ref}$ = 150 mm
CLT Basic material – board	$h_{CLT,ref}$ = 150 mm $t_{l,CLT,ref}$ = 30 mm	$b_{CLT,ref}$ = 600 mm $b_{l,CLT,ref}$ = 150 mm

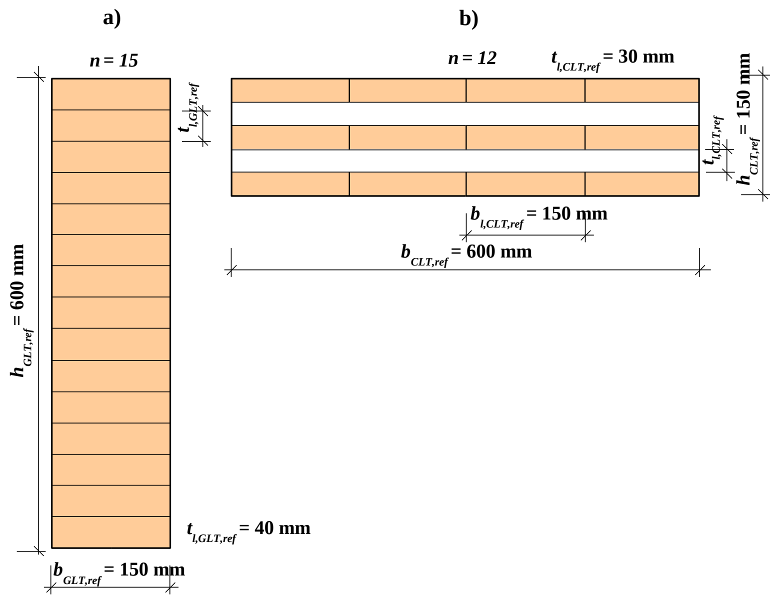

Fig. 1 Reference cross sections for GLT (a) and CLT (b)

2.6 Bending strength (load out-of-plane)

In the course of determining the characteristic bending strength of CLT, a bearing model for bending, on the basis of the tensile strength values of the basic material (boards), needs to be defined according to eq. (1).

$$f_{m,CLT,k} = k_{m,CLT} \cdot f_{t,0,l,k}^{\ 0,8} \tag{1}$$

This bearing model, based on the model of GLT [4], was developed by [5] and is valid in the context of the following basic conditions:

- basic material: timber boards,
- homogeneous lay-up,
- 5 layers, $h_{\mathrm{CLT,ref}}$ = 150 mm,
- same layer thickness $t_{l,\mathrm{CLT,ref}}$,
- number of boards within the top layer $n_{\text{top layer}} \geq 4$

The parameter $k_{m,CLT}$ considers various effects, which are presented in eq. (2).

$$k_{m,CLT} = k_{sys,CLT} \cdot k_{CLT/GLT} \cdot k_{h,CLT} \cdot k_{CV\_t} \tag{2}$$

The system strength factor $k_{sys,CLT}$ considers the system effect of parallel arranged lamellas in longitudinal direction and is defined with $k_{sys,CLT}$ = 1.1 for a number of boards within the top layer $n_{\text{top layer}} \geq 4$. The system strength factor $k_{sys,CLT}$ decreases with decreasing number of boards in the longitudinal direction.

The factor $k_{CLT/GLT}$ considers the influence of the layers perpendicular to span on the homogenisation of CLT in comparison to GLT.

$k_{h,CLT}$ is a height factor and based on GLT. By application, the reference height of CLT $h_{CLT,ref}$ = 150 mm regards to the reference height of GLT $h_{GLT,ref}$ = 600 mm.

The factor k_{cv_t} considers the dispersion of the basic material (boards).

Added to the bearing model of bending, a verification of the finger joint of the lamella with respect to the tensile strength is needed according to eq. (3).

$$f_{t,j,k} \geq k_{t,j} \cdot f_{t,0,l,k} \tag{3}$$

The parameters $k_{m,CLT}$ and $k_{t,j}$ depend on the coefficient of variation $CV[f_{t,0,l}]$ of the tensile strength of the basic material and are presented in Tab. 5 (cf. [5] and [6]).

Tab. 5 Parameters of the bearing model of bending of CLT and the verification of the finger joint of the lamella

	$CV[f_{t,0,l}]$	
	25 % ± 5 %	**35 % ± 5 %**
$k_{m,CLT}$	3.00	3.50
$k_{t,j}$	1.20	1.40

The following example in Tab. 6 presents an application of the previously mentioned bearing model.

Tab. 6 Example of determination of the characteristic bending strength of CLT and the characteristic tensile strength of the finger joints according to the models

5-layer CLT, $b_{CLT,ref}$ = 600 mm, $h_{CLT,ref}$ = 150 mm		
strength class of lamella: T14 according to [7]		
$f_{t,0,l,k}$ [N/mm²]	lamella $CV[f_{t,0,l}]$	
	25 % ± 5 %	35 % ± 5 %
14,0	**bearing model – bending CLT**	
	$f_{m,CLT,k} = 3.0 \cdot 14.0^{0,8} = 24.8\,\text{N/mm}^2$	$f_{m,CLT,k} = 3.5 \cdot 14.0^{0,8} = 28.9\,\text{N/mm}^2$
	model – finger joint	
	$f_{t,j,k} \geq 1.2 \cdot 14.0 = 16.8\ \text{N/mm}^2$	$f_{t,j,k} \geq 1.4 \cdot 14.0 = 19.6\ \text{N/mm}^2$

From the example in Tab. 6, it becomes evident that a characteristic bending strength of CLT of $f_{m,CLT,k}$ = 28.9 N/mm² could be the result of the strength class of the lamellas T14 in combination with a dispersion of $CV[ft,0,l]$ = 35 % ± 5 %.

Note: According to the table 8 of FprEN 14080:2012 [7] the dispersion of the basic material is irrelevant achieving the homogenous GLT strength class GL 24h, in combination with the strength class of the lamellas T14.

The strength classes of CLT could be implemented in a similar way as the ones of GLT (cf. Tab. 7).

Tab. 7 Examples of possible strength classes of CLT

strength class			
lamella	**GLT according to [7]**	**CLT**	
		lamella $CV[f_{t,0,l}]$	
		25 % ± 5 %	35 % ± 5 %
T14	GL 24h	CL 24h	CL 28h
T18	GL 28h	CL 30h	CL 34h

In this context it should be mentioned that the existent bearing model, which is based on the bearing model of GLT, is valid for homogenous CLT elements with 5 layers of the same thickness, at least four lamellas running parallel in the top layers ($k_{sys,CLT}$) and a reference thickness of 150 mm ($k_{h,CLT}$).

With regard to the size effect a comparable procedure, as for the size factor for GLT, is proposed for CLT. The size factor for GLT is defined with eq. (4).

$$k_{h,GLT} = (600/h)^{0,1} \tag{4}$$

For heights different from reference height $h_{CLT,ref}$ = 150 mm, a size (height) factor $k_{h,CLT}$ should be applied. Because to date no systematic investigations have been conducted regarding the thickness effect or rather the number of layers $n \neq 5$ for CLT, the size factor for CLT (eq. (5)) is based on the size factor for GLT (eq. (4)).

$$k_{h,CLT} = (150/h)^{0,1} \tag{5}$$

The use of the size factor, $k_{h,CLT,}$ ranges between 60 mm and 280 mm in the context of heights of CLT. Consequently, the size factor $k_{h,CLT}$ of these heights ranges between 1.1 and 0.94.

Tab. 8 Example of using the size factor $k_{h,CLT}$

CLT	$f_{m,CLT,k}$ [N/mm²]	height [mm]	$k_{h,CLT}$ [-]	$f_{m,CLT,k,h=200}$ [N/mm²]
CL 28h	28.0	200	0.97	**27.2**

2.7 Tensile strength parallel to grain (load in-plane)

The characteristic tensile strength of CLT parallel to grain considers the system effect of the parallel arranged lamellas and is determined by a function depending on the tensile strength of the single lamella, see eq. (6). This model is valid for homogenous CLT with the same thickness of layers and the reference dimensions $b_{CLT,ref}/h_{CLT,ref}$ = 600/150 mm ($n_{\text{top layer}} \geq 4$) as well as with consideration of the net section property A_{net} of the layers parallel to grain.

$$f_{t,0,CLT,net,k} = k_{sys,t,0} \cdot f_{t,0,l,k} \tag{6}$$

This calculation is based on an investigation of the system effect of parallel lamellas on the determination of tensile strength of GLT regarding the reference cross section $b_{GLT,ref}/h_{GLT,ref}$ = 150/600 mm, see [8]. The application of these assumptions of GLT to CLT seems reasonable and plausible.

According to [8] the system strength factor $k_{sys,t,0}$ highly depends on the dispersion and the number of lamellas n (for $n \leq 15$) and can be determined according to the eq. (7) and eq. (8).

$$k_{sys,t,0} = \min\begin{Bmatrix} 0.075 \cdot \ln(n)+1 \\ 1.20 \end{Bmatrix} \quad \text{for } CV[f_{t,0,l}] = 25\% \pm 5\% \tag{7}$$

$$k_{sys,t,0} = \min\begin{Bmatrix} 0.130 \cdot \ln(n)+1 \\ 1.35 \end{Bmatrix} \quad \text{for } CV[f_{t,0,l}] = 35\% \pm 5\% \tag{8}$$

The eq. (7) and eq. (8) can also be applied for the product CLT in order to identify the system effect of parallel lamellas in one direction.

Tab. 9 provides an example of determining, not only the characteristic tensile strength of CLT, but also the ratio between characteristic tensile and bending strength.

Tab. 9 Example of determining the characteristic tensile strength of CLT

5-layer CLT, $b_{CLT,ref}$ = 600 mm , $h_{CLT,ref}$ = 150 mm, n = 12				
strength class of lamella: T14 according to [7]				
lamella $CV[f_{t,0,l}]$	**$k_{sys,t,0}$ [-]**	**$f_{t,0,CLT,net,k}$ [N/mm²]**	**$f_{m,CLT,k}$ [N/mm²]**	**$f_{t,0,CLT,net,k} / f_{m,CLT,k}$ [-]**
25 % ± 5 %	1.186	$f_{t,0,CLT,net,k} = 1.186 \cdot 14.0 = 16.6$	24.0	$16.6/24.0 = 0.69$
35 % ± 5 %	1.323	$f_{t,0,CLT,net,k} = 1.323 \cdot 14.0 = 18.5$	28.0	$18.5/28.0 = 0.66$

It should be mentioned that, in the context of the FprEN 14080:2012 [7], the characteristic tensile strength of GLT has been determined with 80 % of the characteristic bending strength.

2.8 Tensile strength perpendicular to grain (load out-of-plane)

Similar to the characteristic strength value of tension perpendicular to grain of GLT according to FprEN 14080:2012 [7], the characteristic tensile strength perpendicular to grain for CLT is defined as

$f_{t,90,CLT,k} = 0.50$ N/mm².

2.9 Compression strength parallel to grain (load in-plane)

With regard to the net section properties A_{net}, the characteristic value of compression strength parallel to grain of CLT is determined to be similar to the model of GLT (cf. [8]) by considering the density of the basic material and the number of boards in reference cross section (for $n \leq 15$).

$$f_{c,0,CLT,net,k} = (0.1 \cdot \rho_{l,k} / (1 - 0.1/\sqrt{n}) - 8) \cdot (1 - 0.3/\sqrt{n}) \tag{9}$$

The consideration of the reference cross section of $b_{CLT,ref}/h_{CLT,ref}$ = 600/150 mm leads to the board number of $n = 12$.

Tab. 10 presents an example of determining the compression strength of CLT parallel to grain.

Tab. 10 Example of determining the compression strength of CLT parallel to grain

5-layer CLT, $b_{CLT,ref}$ = 600 mm , $h_{CLT,ref}$ = 150 mm, n = 12	
strength class of lamella: T14 according to [7]	
$\rho_{l,k}$ [kg/m³]	**$f_{c,0,CLT,net,k}$ [N/mm²]**
350	$f_{c,0,CLT,k} = (0.1 \cdot 350 / (1 - 0.1/\sqrt{12}) - 8) \cdot (1 - 0.3/\sqrt{12}) = 28.7$

Another possibility consists of determining the compression strength parallel to grain with consideration of the bending strength of CLT.

$f_{c,0,CLT,net,k} = f_{m,CLT,k}$

This approach results in comparison with eq. (9) in conservative characteristic values for the compression strength. This definition is recommended because there are to date no systematic investigations regarding the compression strength of CLT. Another point is that the derivation of the buckling curves of second order is based on the ratio $f_m/f_c = 1.0$. From this perspective, the established definition of the compression strength parallel to grain by the bending strength is understandable and effective.

2.10 Compression strength perpendicular to grain (load out-of-plane)

Based on [9] the characteristic compression strength perpendicular to grain is determined as

$f_{c,90,CLT,k} = 2.85$ [N/mm²].

In this context it needs to be mentioned that the coefficient $k_{c,90,CLT}$ ranges between 1.0 and 1.8 [9], depending on the load introduction.

2.11 Shear strength (load in-plane)

Due to production, CLT has joints between the lamellas of each layer or rather shows seasoning cracks within the edge bonding. Hence, with regard to the design, it is highly advisable to consider CLT not as perfect plane. Based on the shear force transfer in CLT, two mechanisms are activated which are described in [10] in detail.

- mechanism I – shear
- mechanism II – torsional shear

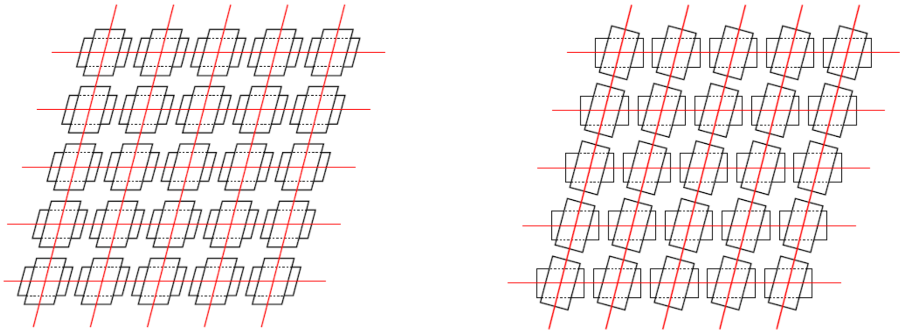

Fig. 2 Mechanism I – shear (left side) and mechanism II – torsional shear (right side) [10]

Several researchers on the topic of shear ([11], [12], [13]) have indicated shear strengths ranging from 6 N/mm² to 11 N/mm², in the context of investigating shear strength of single boards, or rather of FE-calculations (cf. section 3.3.1). The strength value of torsional shear, granted by the latest approvals amounts to $f_{T,node,k}$ = 2.5 N/mm². This value is verified by research conducted at the TU Graz ([14]). The based test configuration is described in section 3.3.2.

Both shear values depend on the cross section of the boards and in case of the shear value of mechanism I on following factors:

- thickness of board: substantial reduction of shear strength in connection with great thickness of boards
- position in log and of the annual growth rings: significant reduction of shear strength concerning boards with vertical annual rings
- gap width: substantial reduction of the shear strength in the context of great gap width

The characteristic values of shear $f_{v,CLT,IP,k}$ and torsion $f_{T,node,k}$ also depend on the system (concerning the lay-up) of CLT. The present determinations are based on the testing of cross sections of single boards; further research work is needed.

The characteristic shear strength $f_{v,CLT,IP,k}$ (shear, mechanism I – IP = **I**n-**P**lane) is determined as a conservative value of:

$$f_{v,CLT,IP,k} = 5.0\,[\text{N/mm}^2].$$

The characteristic torsional shear strength $f_{T,node,k}$ (mechanism II) is determined as:

$$f_{T,node,k} = 2.5\,[\text{N/mm}^2].$$

2.12 Shear strength (load out of plane)

2.12.1 Shear strength in longitudinal and plate thickness direction

The characteristic shear strength $f_{v,CLT,OP,k}$ (OP – **Out-of-Plane**) in longitudinal and plate thickness direction is determined without further experimental results with:

$$f_{v,CLT,OP,k} = 3.0\,[\text{N/mm}^2].$$

Further research work is given also in relation to the existing size effect. The crack factor, k_{cr}, should be set at 1.0.

2.12.2 Shear strength in transverse direction (rolling shear)

The rolling shear strength $f_{r,CLT,k}$ is substantially influenced by the dimension of the single lamella, the lay-up and the production. Due to the system effect of the parallel boards within a layer, an increase of the rolling shear strength of the basic material ($f_{r,k}$ = 1.0 N/mm² according to [15]) can be expected. Based on the existing approvals, the rolling shear strength $f_{r,CLT,k}$ ranges from 0.7 N/mm² to 1.5 N/mm². One reason for this band can be seen in the production process of CLT. Relieves in the single lamellas are applied for production of CLT in the vacuum pressing jig. The resulting tensile stresses perpendicular to grain, which results as a consequence of the reduction of the lamella width by the grooves, may lead to a slight rolling of the layers.

In compliance with the ratio $b/t \geq 4$ and for edge bonded CLT the rolling shear strength is determined as:

$$f_{r,CLT,k} = 1.25 \text{ [N/mm²]}.$$

If the ratio $b/t \geq 4$ is ignored in the context of CLT without edge bonding (e.g. due to the use of relieves), it is highly advisable to determine the rolling shear strength as:

$$f_{r,CLT,k} = 0.70 \text{ [N/mm²]}.$$

2.13 Modulus of elasticity parallel to grain

The characteristic modulus of elasticity parallel to grain $E_{0,CLT,mean}$ of CLT is determined in terms of the tensile modulus of elasticity of the basic material:

$$E_{0,CLT,mean} = E_{t,0,l,mean} \text{ [N/mm²]}.$$

The 5%-value of the characteristic modulus of elasticity $E_{0,CLT,05}$ is determined, analogous with GLT, according to FprEN 14080:2012 [7] as:

$$E_{0,CLT,05} = 5/6 \cdot E_{0,CLT,mean}.$$

2.14 Modulus of elasticity perpendicular to grain

The mean value of the characteristic modulus of elasticity perpendicular to grain $E_{90,CLT,mean}$ of CLT is defined analogical to GLT according to FprEN 14080:2012 [7] as:

$$E_{90,CLT,mean} = 300 \text{ [N/mm²]}.$$

For design proposes the modulus of elasticity perpendicular to grain is assumed as $E_{90,CLT,mean} = 0$.

Analogous with GLT, the 5%-value of the characteristic modulus of elasticity perpendicular to grain $E_{90,CLT,05}$ is determined according to FprEN 14080:2012 [7] as:

$$E_{90,CLT,05} = 5/6 \cdot E_{90,CLT,mean} = 250 \text{ [N/mm²]}.$$

2.15 Compression modulus of elasticity perpendicular to grain

The mean value of the characteristic compression modulus of elasticity perpendicular to grain $E_{c,90,CLT,mean}$ of CLT was investigated in [9] and is defined as:

$$E_{c,90,CLT,mean} = 450\,[\text{N/mm}^2].$$

The 5%-value of the characteristic compression modulus of elasticity perpendicular to grain $E_{c,90,CLT,05}$ is determined as:

$$E_{c,90,CLT,05} = 5/6 \cdot E_{c,90,CLT,mean} = 375\,[\text{N/mm}^2].$$

2.16 Shear modulus

The mean value of the characteristic shear modulus $G_{CLT,mean}$ of CLT is defined analogical to GLT according to FprEN 14080:2012 [7] as:

$$G_{CLT,mean} = 650\,[\text{N/mm}^2].$$

With regard to the approvals given by the manufacturing firms of CLT the shear modulus is frequently defined in combination with the strength class of the basic material, or with the strength class of GLT. As a consequence, the shear modulus ranges between 650 and 690 N/mm² (for C24 according to the ÖNORM EN 338:2009 [16], or rather GL 24h according to the ÖNORM EN 1194:1999 [17]).

Analogous with GLT, the 5%-value of the characteristic shear modulus $G_{CLT,05}$ is determined according to FprEN 14080:2012 [7] as:

$$G_{CLT,05} = 5/6 \cdot G_{CLT,mean} = 540\,[\text{N/mm}^2].$$

2.17 Rolling shear modulus

Depending on the shear modulus in longitudinal-transverse direction, the characteristic rolling shear modulus $G_{r,CLT,mean}$ is defined as:

$$G_{r,CLT,mean} = 1/10 \cdot G_{CLT,mean} = 65 \text{ N/mm}^2.$$

In the context of the prevailing approvals, the rolling shear modulus is defined as 50 N/mm². Consequently, this results in a ratio of 1/13, if the shear modulus $G_{CLT,mean}$ = 650 N/mm² is taken into consideration. Research ([13], [18]) has shown the dependence of the rolling shear modulus of a board on the position within the log. Hence, boards with sloped annual rings and heartwood boards show high values concerning the rolling shear modulus (cf. 3.2.2.).

Analogous with GLT, the 5%-value of the characteristic rolling shear modulus $G_{r,CLT,05}$ is determined according to FprEN 14080:2012 [7] as:

$$G_{r,CLT,05} = 5/6 \cdot G_{r,CLT,mean} = 54\,[\text{N/mm}^2].$$

2.18 Mean and characteristic density

In order to be able to determine the mean density $\rho_{CLT,mean}$ of CLT the mean density of the basic material is used.

$$\rho_{CLT,mean} = \rho_{l,mean} \text{ [kg/m}^3\text{]}$$

The characteristic density $\rho_{CLT,k}$ is determined on the basis of the characteristic density of the basic material.

$$\rho_{CLT,k} = 1.10 \cdot \rho_{l,k} \text{ [kg/m}^3\text{]}$$

Analogous with GLT, the lay-up of CLT causes a homogenisation. Hence, an increase of the characteristic value in combination with a decrease of the dispersion is to be expected (cf. [19]).

Note: If fasteners are set in the side faces or rather in the narrow faces of CLT, the homogenisation effect does not occur in the same way. If only one layer of CLT contains the fastener, the density of the basic material should be used.

2.19 Characteristic strength and stiffness values and density of homogeneous CLT – summary

Tab. 11 provides an insight into the characteristic values of strength, stiffness and density using the example of CLT strength class CL 24h and CL 28h with the T14 as basic material. Some mechanical properties were defined by assumptions and conclusions regarding GLT, as seen in section 2.6 to 2.18. There is certainly need for further research.

Tab. 11 Characteristic strength and stiffness properties in N/mm² and densities in kg/m³ for homogeneous cross laminated timber

	base material	**T14**	
	$CV[f_{t,0,l}]$	25 % ± 5 %	35 % ± 5 %
		CLT strength class	
property[a)]	**symbol**	**CL 24h**	**CL 28h**
Bending strength	$f_{m,CLT,k}$	24	28
Tensile strength	$f_{t,0,CLT,net,k}$	16	18
	$f_{t,90,CLT,k}$	0.5	
Compression strength	$f_{c,0,CLT,net,k}$	24	28
	$f_{c,90,CLT,k}$	2.85	
Shear strength (shear and torsion) – in-plane	$f_{v,CLT,IP,k}$	5.0	
	$f_{T,node,k}$	2.5	
Shear strength – out-of-plane	$f_{v,CLT,OP,k}$	3.0	
	$f_{r,CLT,k}$ – $b/t \geq 4{:}1$	1.25	
	$f_{r,CLT,k}$ – $b/t < 4{:}1$	0.70	
Modulus of elasticity	$E_{0,CLT,mean}$	11,000	
	$E_{0,CLT,05}$	9,167	
	$E_{90,CLT,mean}$	300	
	$E_{90,CLT,05}$	250	
	$E_{c,90,CLT,mean}$	450	
	$E_{c,90,CLT,05}$	375	
Shear modulus	$G_{CLT,mean}$	650	
	$G_{CLT,05}$	540	
Rolling shear modulus	$G_{r,CLT,mean}$	65	
	$G_{r,CLT,05}$	54	
Density	$\rho_{CLT,k}$	385	
	$\rho_{CLT,mean}$	420	

a) Properties are calculated on the basis of the reference cross section given in table 4 and according to section 2.6 to 2.18 respectively.

3. Test configurations of CLT for determination of chosen material properties

3.1 Cross section of CLT for testing

The characteristic values for strength and stiffness, shown in section 2.6 to 2.17, are based on reference cross sections of CLT and the basic material. These reference cross sections are also used in testing and for determination of the mechanical properties (cf. Tab. 12).

Tab. 12 Reference cross sections of CLT and basic material (boards)

	Basic material – board	CLT
width	$b_{l,CLT,ref}$ = 150 mm	$b_{CLT,ref}$ = 600 mm
depth/thickness	$t_{l,CLT,ref}$ = 30 mm	$h_{CLT,ref}$ = 150 mm

3.2 Bending strength and stiffness for load out-of-plane

Generally, the bending properties – bending strength and modulus of elasticity in bending – of CLT are determined according to the four-point-bending test setup suggested by ÖNORM EN 408:2012 [20]. This standard defines the span as $l = 18 \cdot h \pm 3 \cdot h$ with a distance of $6 \cdot h$ between the load points.

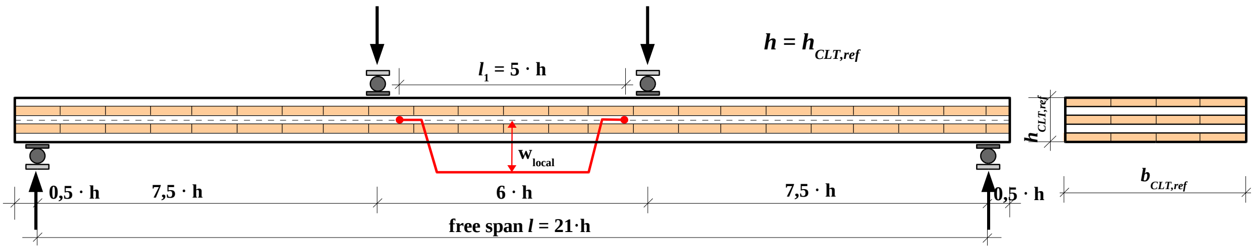

Fig. 3 Test arrangement for determination of bending strength and stiffness for load out-of-plane

Laboratory tests concerning bending strength and stiffness of CLT (basic material C24 and higher) have verified the claim that, in the context of defining the span as $18 \cdot h$ no bending failure, but a rolling shear failure is frequently caused. As a consequence, a definite statement regarding the bending strength cannot be made. This fact was observed in CLT plates with boards of grade class C24 and higher as well as plates with and without grooves. Hence, in contrast to ÖNORM EN 408:2012 [20], or rather the draft of EN 16351:2012 [1], a uniform testing setup concerning bending strength and stiffness of CLT with a span of $l = 21h$ is suggested.

The ÖNORM EN 408:2012 [20] suggests two approaches – local and global – in order to determine the modulus of elasticity in bending. It is highly advisable to determine the modulus of elasticity in bending of CLT on the basis of a local deformation measurement, since the local modulus of elasticity in bending remains in stable condition compared with the global modulus of elasticity in bending (cf. section 3.2.1 and 3.2.2). The determination of the mechanical bending properties is based on following points:

- beam theory, rigid bond
- effective cross sections
- $E_{90,CLT,mean} = 0$ (gaps and shrinkage cracks in the cross layers)
- $G_{CLT,mean} = 650$ N/mm², $G_{r,CLT,mean} = 65$ N/mm².

3.2.1 Local modulus of elasticity in bending

Within the area of no shear force, the local modulus of elasticity in bending is determined between the load points with a reference length of $l_1 = 5 \cdot h$. It can be assumed that the influence of the load application area (stress peaks) on the bending moment has already declined within a length of $0.5 \cdot h$. Hence, a uniform bending moment is used in the context of calculation. FE-analyses with consideration of a tolerance of 1 % showed that the degradation of the stress peaks (with consideration of the width of the load plates) takes place over a length of about $1.5 \cdot h$ and thus a non-shear-force-area of approximately $l_{1,FE} = 3 \cdot h$ exists, see Fig. 4 and Tab. 13.

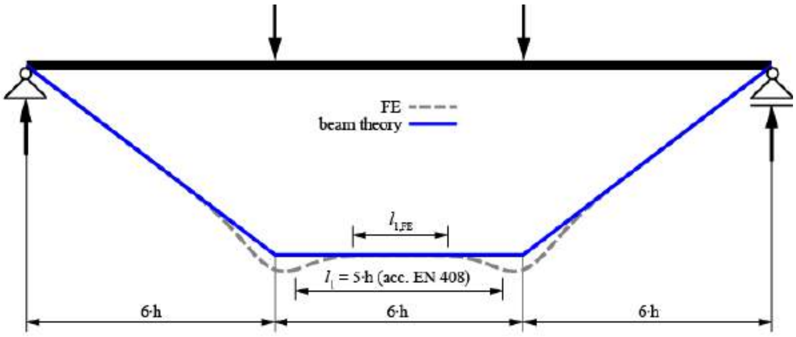

Fig. 4 Comparison of the qualitative bending stresses based on the beam theory and by FE-analysis with modelling the real support and load points

Tab. 13 Determined reference length l1,FE for calculating the modulus of elasticity in bending and ratio of l1,FE/h – examples for different CLT lay-ups

CLT - no. layer - CLT height -layer thickness	**$l_{1,FE}/h$**	**l_1/h acc. EN 408**
CLT-5s-115-23	2.5	5.0
CLT-5s-200-40	2.8	
CLT-5s-160-32	2.9	
CLT-5s-146-32/27/28/27/32	2.7	

Taking this effect into account, the local modulus of elasticity has an influence of approximately 2.5% and can be neglected. The adoption of a reference length of $l_1 = 5 \cdot h$ is applicable and the determination of the local modulus of elasticity, compared to determine the global modulus of elasticity, is stable.

3.2.2 Global modulus of elasticity in bending

The determination of the global modulus of elasticity in bending is based on the deformation measured within the centre of the beam. As a consequence, the influence of the shear deformation needs to be taken into consideration.

The shear correction coefficient κ, which needs to be considered in this case, highly depends on the cross-sectional lay-up and the stiffness of the single layers. Hence, with regard to homogenously structured rectangular sections (e.g. GLT), this factor is defined as 1.2. However, due to the fact that CLT has shear-flexible transverse layers, their influence on shear stiffness via the shear correction coefficient needs to be taken into consideration. Added to the rolling shear modulus, the lay-up of the transverse layer (edge bonding, side-by-side, gaps) can be regarded as a substantial influence on the shear correction coefficient.

Note: The shear correction coefficient, κ, for rectangular cross sections is mostly taken as 0.83, which corresponds to the reciprocal value of 1.2. Differences in data result from the definition of the shear stiffness.

Generally, the shear correction coefficient is determined by integrating over the cross section and ignoring the widths of boards in the transversal layer. However, based on FE-calculations, Feichter [13] was able to verify the claim that the shear correction coefficient regarding widths of boards of 120 mm to 150 mm is about 10 % to 15 % higher in comparison with the conventional determination of the shear correction coefficient with integrating via the cross section. In order to apply the shear correction coefficient for use in practice, equations and diagrams are defined in [13], which depend on the ratio between shear modulus and rolling shear modulus.

Another parameter, which needs to be taken into consideration in the context of determining the global modulus of elasticity in bending, or rather the shear correction factor, can be seen in the rolling shear modulus $G_{r,CLT,mean}$ or rather $G_{r,mean}$ of the basic material. In present approvals, the rolling shear modulus, $G_{r,CLT,mean,}$ is mostly defined as a value of either 50 N/mm² or 60 N/mm². In this regard it should be mentioned that the rolling shear modulus is given as $1/10 \cdot G_{CLT}$ in DIN 1052:2008 [15]. In the course of FE-calculation Feichter [13] analysed the influencing factors of the rolling shear modulus of boards and varied not only the width and thickness, but also the position within the stem (from heart boards, side boards, boards with sloped and vertical growth rings). The outcome of the analysis concerning the thickness of boards of 32 mm verified the claim that heart wood boards and boards with sloped annual rings showed a rolling shear modulus up to 150 N/mm² and thus significantly higher compared to the most widely used value of 50 N/mm². In Görlacher [18] values of rolling shear modulus ranging between 50 N/mm² and 150 N/mm² are found. But it is mentioned that a value ranging between 40 N/mm² and 80 N/mm² is defined as realistic with regard to board cutting and slope of annual rings.

The application of the results of the parameter study for real CLT lay-ups with half-timber-boards or rather sideboards resulted in rolling shear moduli ranging from 80 to 88 N/mm² ([13]). Hence, a ratio between shear- and rolling shear modulus $G_{CLT,mean}/G_{r,CLT,mean}$ of 8.1 ($G_{r,CLT,mean}$ = 80 N/mm²) or 7.4 ($G_{r,CLT,mean}$ = 88 N/mm²), needs to be taken into consideration. Further research is needed with regard to the influence of relieves on the rolling shear modulus. In this context Feichter [13] points out that due to relieves the rolling shear stiffness is reduced significantly.

Additionally, Feichter [13] puts emphasis on the substantial influence of the rolling shear modulus of the basic material on the global modulus of elasticity of CLT. Results of FE-calculations in consideration of various setting of the transverse layer (to be considered in the course of the FE-calculation: width of board, gaps, endless), verified the claim that the rolling shear modulus highly influences the global modulus of elasticity in bending. To confirm, differences up to 20 % in relation to a reference modulus of elasticity (CLT, for example 12,000 N/mm²) could be identified. By considering the adapted equations to determine the shear correction value via assuming a “specific to board” rolling shear modulus it was able to adjust the result and reach the reference value.

3.3 Shear strength for loads in-plane

The shear values declared in section 2.11 are based on the test setups described in section 3.3.1 and section 3.3.2. It should be mentioned that these test setups are also defined in the DRAFT EN 16351:2012 [1]. In the course of conducting these tests the shear- and torsion strengths can be determined, whereas it is only possible to define the related shear stress value by applying the approach described in section 3.3.3.

3.3.1 Mechanism I - shear

In order to be able to determine the shear strength of mechanism I, a test arrangement according to the ÖNORM EN 789:2005 [21], or rather the ÖNORM EN 408:2012 [20], needs to be conducted. This setup has been developed and used by Hirschmann [12] and is also included in the DRAFT EN 16351:2012 [1] (cf. Fig. 5).

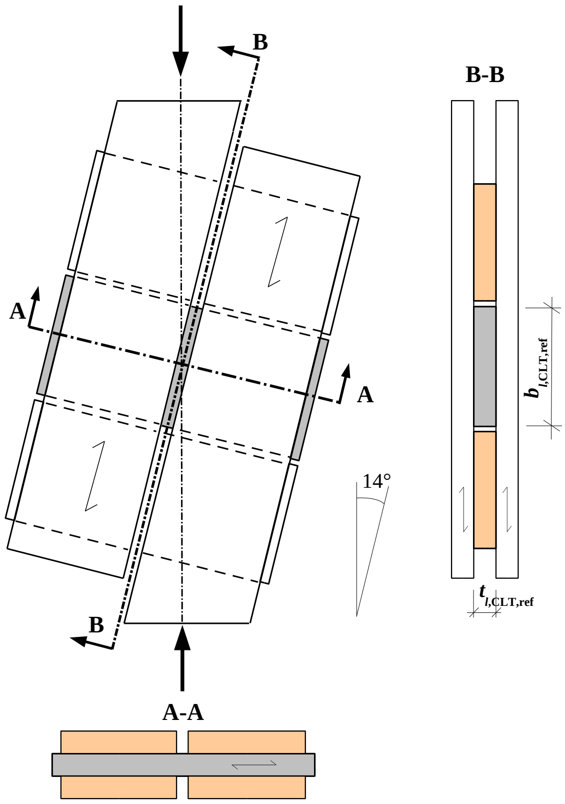

Fig. 5 Test arrangement for determination of the shear strength for mechanism I (load in-plane)

Due to the testing at an angle of 14° lateral supports are totally unnecessary. Hence, the test setup can be substantially simplified and there are no systematic load eccentricities.

This test arrangement is used to test a single layer (with or without gaps). In this context it needs to be mentioned that the greatest board thickness, or rather the greatest gap width, should be implemented. Added to this, it is highly advisable to use the reference cross section of the basic material $b_{l,CLT,ref}$ /$t_{l,CLT,ref}$ = 150/30 mm on the subject of the tested layer.

3.3.2 Mechanism II – torsional shear

The torsional shear strength of mechanism II is determined by conducting a test setup according to Fig. 6 concerning the orthogonal glued interface of two boards. The board thickness $t_{l,CLT,ref}$ = 30 mm and width $b_{l,CLT,ref}$ = 150 mm are defined as reference dimensions. In this context it is of utmost importance to ensure that the specimen is able to longitudinally deform freely, in direction of thickness. An overlap of $a \geq 30$ mm is highly recommended.

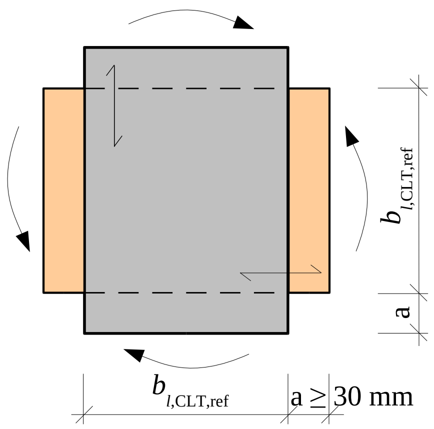

Fig. 6 *Test arrangement for determination of the torsional shear strength in the glued interface of two boards (mechanism II)*

The test setup is also included in the DRAFT EN 16351:2012 [1].

3.3.3 Shear values in-plane by bending test

The CUAP 03.04-06:2005 [22] suggests a four-point-bending test setup similar to the ÖNORM EN 408:2012 [20] for determination of shear values for loads in-plane (cf. Fig. 7). The top layers in longitudinal direction need to have a continuously open gap in the middle of the depth of beam to initiate the shear load transmission through the layer perpendicular to span.

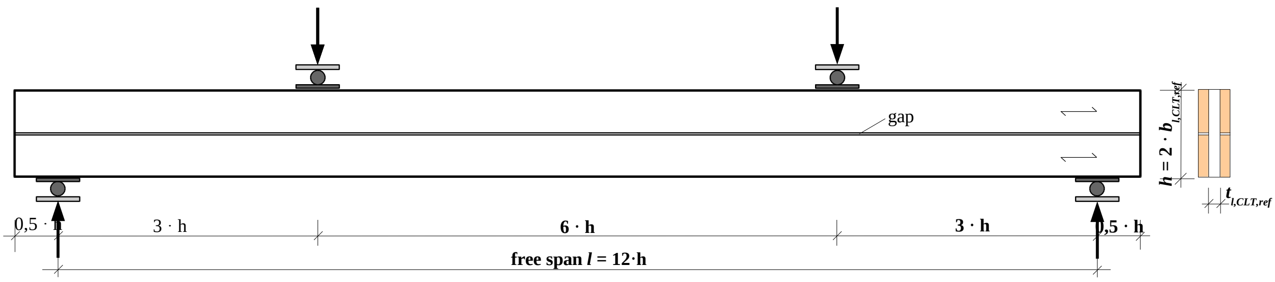

Fig. 7 *Test arrangement for determination of shear values according to CUAP 03.04-06 for loads in-plane*

Due to the fact that many bending failures are caused by this test setup, it is just possible to determine a related shear stress (no shear strength). Hence, it can be assumed that the actual value of shear strength is higher.

The calculation of shear stress is done in consideration of the following points:

- beam theory – rectangular cross section,
- net dimension (A_{net}) or
- gross dimension (A_{gross})

If the net cross section A_{net} is used for the calculation of the shear stress, only the middle layer is taken into account and thus, a higher shear stress value is calculated. This represents the mechanically correct procedure – because of the gap in the middle of the beam depth the longitudinal layers cannot transmit the shear.

When calculating the shear values with the gross cross section A_{gross} smaller shear stresses are determined because of consideration of the top layers in longitudinal direction. The specification of the associated reference cross sections of the shear stress is significant for subsequent verification.

4. Conclusion and summary

This paper attempts to meet requirements for the basis of design, the material properties and the characteristic values for strength, stiffness and density of cross laminated timber (CLT) and to disclose them in a table similar to the strength classes for glued laminated timber (GLT).

The partial safety factor, $\gamma_{M,}$ and the modification factors, $k_{mod,}$ can be set based on the values for glulam (GLT). With regard to the deformation factor, $k_{def,}$ some research work showed that separate values for CLT, with more or less than seven layers, seems reasonable.

An important point in specifying strength classes is to establish reference sections for CLT and for the basic material (boards). Based on GLT and also from tests, a reference section for CLT $b_{CLT,ref}/h_{CLT,ref}$ = 600/150 mm and for the lamella $b_{l,CLT,ref}/t_{l,CLT,ref}$ = 150/30 mm was defined.

For the characteristic bending strength a bearing model can be determined, which is derived from GLT und is a function depending on the base material. Other effects (dispersion of the base material, size effect and effect of homogenisation relating to GLT, system effect of the lamellas in the top layer) are considered by a factor $k_{m,CLT}$. Furthermore, the verification of the tension strength of the finger joint has to be considered. Through the application of the bearing model, several strength classes of CLT can be defined as a function of the used basic material. It should be noted that the present bearing model is valid for certain boundary conditions (lay up: homogeneous, five layers, boards with the same thickness, four lamellas in the top layers). Certainly, there is still a need for research.

The characteristic tensile strength parallel to grain can likewise be determined by a function depending on the tensile strength and the dispersion of the base material. The function is developed from studies regarding the system effect of the parallel acting single lamellas in GLT. This model is also valid for the reference section and refers to the net cross section of the parallel acting layers.

For the characteristic compression strength parallel to grain of CLT, a calculation model in accordance with GLT is given, which takes into account the density and the number of parallel acting boards in the cross section. In the absence of research work concerning this matter it is recommended to define the characteristic compression strength parallel to grain with the characteristic bending strength. More conservative values are achieved with this approach.

Regarding the compression strength perpendicular to grain and the shear strength under load in-plane some research work was done at the Graz University of Technology, which confirm the defined characteristic values.

CLT shows gaps (from production or swelling and shrinkage), which lead to two different mechanisms under shear load in-plane – shear (mechanism I) and torsional shear (mechanism II). For both mechanisms numerical research (FE analysis) and practical considerations (test configurations) were made or executed.

The rolling shear strength is significantly affected by the dimensions of the single board and the CLT lay-up and manufacture. The definition of two different characteristic values, which depend on the ratio of the width of the board to the board thickness b/t, seems useful.

The characteristic values for stiffness and density are mostly based on the requirements for GLT. The rolling shear modulus is given as a function of shear modulus and is slightly higher than the value specified in most approvals. The rolling shear modulus strongly depends on the location of the board in the stem or the slope of the annual rings and has a substantial variation.

To determine the mechanical properties of CLT, appropriate test configurations are set with corresponding reference dimensions. For the determination of the bending properties the test configuration is proposed according to ÖNORM EN 408 with a constant ratio for the free span length to prevent the occurrence of rolling shear failure. It could be shown that the local bending modulus of elasticity is much more stable in comparison to the determination of global modulus of elasticity.

The test configurations, for determination of shear and torsional shear strength of mechanisms I and II, and the test setup according to CUAP 03.04-06 is shown. Using the test configuration according CUAP 03.04-06, it is only possible to establish shear stresses related to bending strength (no shear strength), with attention, in particular, to the reference sections (net/gross). On the one hand, the reference cross section affects the calculation of the shear values and, on the other hand, they are also important for subsequent verification.

5. References

[1] DRAFT EN 16351:2012-01, “*Holzbauwerke – Brettsperrholz – Anforderungen*”.

[2] ÖNORM EN 1995-1-1:2009-07, “*Bemessung und Konstruktion von Holzbauten – Teil 1.1: Allgemeines – Allgemeine Regeln und Regeln für den Hochbau*”.

[3] Jöbstl, R.A., Schickhofer, G., “*Comparative examination of creep of GLT and CLT slabs in bending*”, Proceedings of the 40th meeting of CIB-W18, Bled, Slovenia, 2007

[4] Brandner, R., Schickhofer, G. “*Glued laminated timber in bending: new aspects concerning modelling*”, In: Wood Science and Technology, 42:401-425 (2008)

[5] Jöbstl, R.A., Moosbrugger, T., Bogensperger, T., Schickhofer, G., “*A contribution to the design and system effect of cross laminated timber (CLT)*”, Proceedings of the 39th meeting of CIB-W18, Florence, Italy, 2006

[6] Brandner, R., “*Stochastic System Actions and Effects in Engineered Timber Products and Structures*”, Institute for Timber Engineering and Wood Technology, TU Graz, Dissertation, 2012

[7] FprEN 14080:2012-02, “*Timber structures – Glued laminated timber and glued solid timber- Requirements*”.

[8] Brandner, R., “*TU-Graz_hbf-gmbh Comments on EN 14080*”, Institute for Timber Engineering and Wood Technology, TU Graz and holz.bau forschungs gmbh, 2008

[9] Bogensperger, T., Augustin M., Schickhofer, G., “*Properties of CLT-panels exposed to compression perpendicular to their plane*”, Proceedings of the 44th meeting of CIB-W18, Alghero, Italy, 2011

[10] Technische Universität Graz et al, “*BSPhandbuch – Holzmassivbauweise in Brettsperrholz*”. Institute for Timber Engineering and Wood Technology, TU Graz and holz.bau forschungs gmbh, 2009

[11] Jöbstl, R.A., Bogensperger, T., Schickhofer, G., “*In-plane shear strength of cross laminated timber*”, Proceedings of the 41th meeting of CIB-W18, St. Andrews, Canada, 2008

[12] Hirschmann, B., “*Ein Beitrag zur Bestimmung der Scheibenschubfestigkeit von Brettsperrholz”* Institute for Timber Engineering and Wood Technology, TU Graz, Masterarbeit, 2011

[13] Feichter, I., “*Spannungs- und Traglastberechnungen an ausgewählten Problemen der Holz-*

*Massivbauweise in Brettsperrholz***“**, Institute for Timber Engineering and Wood Technology, TU Graz, Masterarbeit, 2013

[14] Jeitler, G., “*Versuchstechnische Ermittlung der Verdrehkenngrößen von orthogonal verklebten Brettlamellen*“, Institute for Timber Engineering and Wood Technology, TU Graz, Diplomarbeit, 2004

[15] DIN 1052:2008-12, “*Entwurf, Berechnung und Bemessung von Holzbauwerken – Allgemeine Bemessungsregeln und Bemessungsregeln für den Hochbau*”.

[16] ÖNORM EN 338:2009-12, “*Bauholz für tragende Zwecke – Festigkeitsklassen*”.

[17] ÖNORM EN 1194:1999-09, “*Holzbauwerke – Brettschichtholz - Festigkeitsklassen und Bestimmung charakteristischer Werte*”.

[18] Görlacher, R., “Ein Verfahren zur Ermittlung des Rollschubmoduls von Holz”, Universität Karlsruhe, Lehrstuhl für Ingenieurholzbau und Baukonstruktionen, 2002

[19] Reichelt, B., “*Einfluss der Sperrwirkung auf den Ausziehwiderstand selbstbohrender Holzschrauben - eine vergleichende Betrachtung zwischen BSP und BSH*“, Institute for Timber Engineering and Wood Technology, TU Graz, Masterarbeit, 2012

[20] ÖNORM EN 408:2012-09, “*Holzbauwerke – Bauholz für tragende Zwecke und Brettschichtholz – Bestimmung einiger physikalischer und mechanischer Eigenschaften*”.

[21] ÖNORM EN 789:2005-04, “*Holzbauwerke – Prüfverfahren – Bestimmung der mechanischen Eigenschaften von Holzwerkstoffen“*.

[22] CUAP 03.04-06:2005-06, “*Solid wood slab element to be used as a structural element in buildings*”.

Theme II

Design and Construction

DI Dr.techn.

Alexandra Thiel

Institute of Timber Engineering and Wood Technology

Graz University of Technology

Austria

Email: alexandra.thiel@tugraz.at

Alexandra Thiel studied Civil Engineering at Graz University of Technology. She earned a diploma degree in 1999. From 1999 to 2007 she worked as Univ.-Assistant at Institute of Applied Mechanics at Graz University of Technology. She obtained her PhD degree in Civil Engineering Sciences in 2007. Since 2008 she has been a researcher at the Centre of Competence holz.bau-forschungs gmbh in Graz. Her research topics are timber engineering and wood technology, especially concerning solid timber solutions in cross laminated timber.

Dr.-Ing

Philipp Dietsch

Chair for Timber Structures and Building Construction

Technische Universität München

Germany

Email: dietsch@tum.de

Philipp Dietsch studied Civil Engineering at TUM from 1999 – 2005, which included an academic year at McGill University, Montreal/Canada. His Diploma Thesis at the Centre for advanced Wood Processing at UBC, Vancouver/Canada won the prize for outstanding theses, awarded by the Association of German Engineers (VDI). After his studies, Philipp Dietsch became assistant at the Chair of Timber Structures and Building Construction. His focus in structural research lies in wide-span timber structures, e.g. robustness of systems. He contributed to the expertise about the Bad Reichenhall ice-arena collapse and works in the assessment of existing timber structures. In 2012 he was awarded the doctoral degree for his thesis “Design and application of shear reinforcements for glulam timber beams”. Philipp is member of the European scientific COST-network (German delegate in COST Actions FP1004 and FP 1101) and delegate in German and European code commissions (“Mirror Committee - Timber Structures” and CEN TC250/SC5 „Eurocode 5“, leader of the WG “Reinforcement”).

Prof. Dr.-Ing

Thomas Uibel

FH Aachen University of Applied Sciences

Germany

Email: uibel@fh-aachen.de

Thomas Uibel studied Civil Engineering at the University of Hannover between 1997 and 2002. From 2002 to 2012 he worked as Research Scientist at Karlsruhe Institute of Technology (KIT), Versuchsanstalt für Stahl, Holz und Steine (Research Institute for Steel, Timber and Masonry), Timber Engineering and Building Construction. In 2012 he received his Ph.D. in Civil Engineering from KIT. Since July 2012 he has held the position of Professor for Timber Structures and Basics of Structural Engineering at FH Aachen (University of Applied Sciences)

ULS and SLS design of CLT and its implementation in the CLTdesigner

Alexandra Thiel

Research & Development

Centre of Competence holz.bau forschungs gmbh

Graz, Austria

Summary

This contribution deals with the analysis and design of cross laminated timber (CLT), used as wall, floor and roof elements and exposed to common load situations. Different calculation procedures for plates loaded out-of-plane and in-plane are discussed. The determination of required stiffness values is explained and for some load situations, the design procedure at ultimate limit state (ULS) and serviceability limit state (SLS) is given. Furthermore, the concept of reduced cross section for structural fire design is explained. Overall this contribution aims to show the design procedures, as implemented in the software tool CLTdesigner, a software package developed and provided by the Institute of Timber Engineering and Wood Technology of Graz University of Technology and Centre of Competence holz.bau forschungs gmbh.

1. Introduction

Cross laminated timber (CLT) has been established as a load-bearing two dimensional product for use as wall, floor and roof elements. Apart from some National Application Documents, as well as the draft of the European product standard for CLT, prEN 16351 [1], this product has not yet been included in European standards. Thus the design process has to be done according to numerous, product-specific, technical approvals. The harmonisation of these currently available design procedures, and the establishment of a product test and design standard for CLT, is seen as worthwhile for engineers, carpenters and architects in practice. On the basis of the design concept, as established in Eurocodes [2] [3] [4] [5] and numerous research works accomplished in recent years (e.g. BSPhandbuch [6]), a software tool for the design of CLT, the CLTdesigner [7], has been developed at the Institute of Timber Engineering and Wood Technology at Graz University of Technology and the Centre of Competence holz.bau forschungs gmbh in Graz.

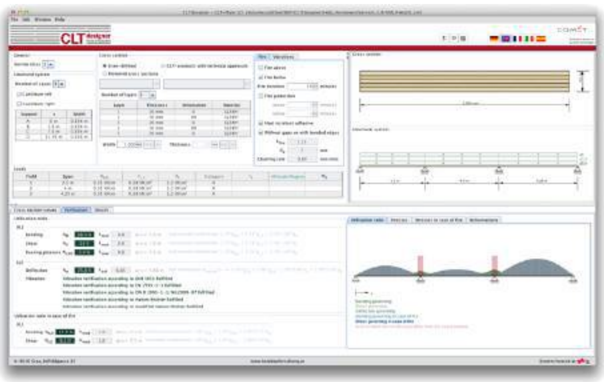

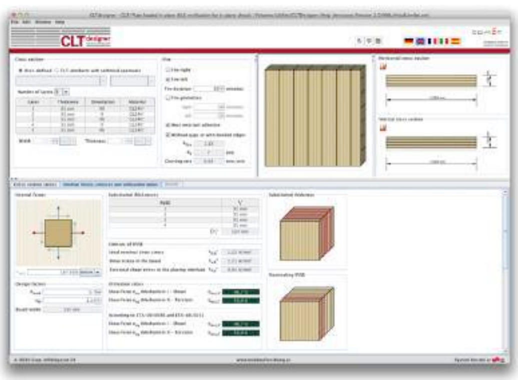

Fig. 1 CLTdesigner – modules: plate loaded out-of-plane (left); plate loaded in-plane (right)

This software tool, structured in modules, is continuously under further development. Currently the design of common wall, floor and roof elements, in regard to ULS and SLS, is provided.

Within the following paper the design of CLT elements, in common load situations, is described with reference to the design approaches implemented in the CLTdesigner.

2. Basic principles

2.1 Methods of calculation

2.1.1 Loads out-of-plane

Currently, numerous procedures for the design of CLT in bending out-of-plane are applied. In particular, the shear flexibility of the transverse layers has to be considered. Well-known procedures are the γ-method (GAMMA) [8] [9] [10] [11] and the shear analogy method (SAV) [12] [13]. These procedures, originally used for the design of fasteners in mechanically joined girders, have been modified for CLT. The transverse shear-flexible beam, according to Timoshenko (TIMO), constitutes an additional approach.

In the framework of a research project at the Centre of Competence holz.bau forschungs gmbh, these three approaches were analysed in detail, which was done by means of six examples of practical relevance (one-, two- and three-span beams of various span ratios) and their outcome compared with the results of a two-dimensional finite element plate calculation (FE_1) [14]. Further comparability studies can be found in [15] [16].

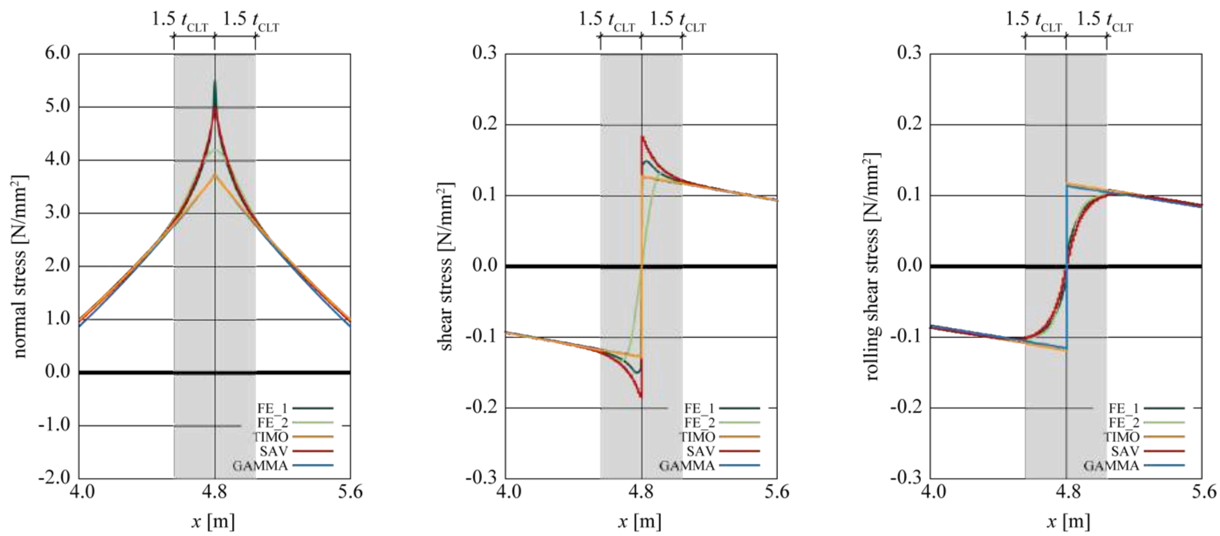

Fig. 2 Normal, shear and rolling shear stresses at the inner support of a two-span beam due to bending out-of-plane: comparison of the different calculation procedures ([14])

To summarise, the field moments found in all three approximate approaches compare well to each other. Of course, only the SAV was able to give good estimates for the peaks in moments and normal stresses at the inner supports, in cases of statically indeterminate continuous beams (- 10 %); GAMMA and TIMO significantly underestimate, although it has to be understood that these deviations occur very locally at the supports (± 1.5 · t_{CLT}) (see Fig. 2).

A more realistic modelling of two-dimensional support conditions (e.g. CLT wall as support; FE_2), instead of a structural line-support (FE_1), reflects smoothed stress peaks and thus lower deviations of GAMMA and TIMO from the finite element solution FE_2.

Overall, all these approaches constitute approximations, with individual pros and cons. For example, although the results of GAMMA and TIMO are compare well, the γ-method, established in technical approvals (e.g. [17] [18] [19]) and Eurocode 5 [2] as well as DIN [13], proves to be much more complex (e.g. the examination of γ-values in cases of different spans) and requires much more effort for application in a two-dimensional plate structure. The shear analogy method enables consideration of arbitrary structural systems and loads and captures the influence of point loads and inner supports well but it is very elaborate and results strongly depend on the dimensions of discretisation. In addition, the shear stresses close to point loads and inner supports, calculated according to SAV are overestimated.

In practice, the design of CLT is seldom governed by stresses but more by the SLS design, and thus, by deflection and vibration. Within the practical relevant range of $l / t_{CLT} \geq 15$, the calculated deflections of all three approximate approaches, GAMMA, SAV and TIMO, compare well to each other and are sufficiently accurate (see Fig. 3). Of course, in cases of short spans, *l*, or rather small ratios of span to depth, l / t_{CLT} , and heavy point loads, a more advanced examination of the stresses at supports and/or close to point loads is advised.

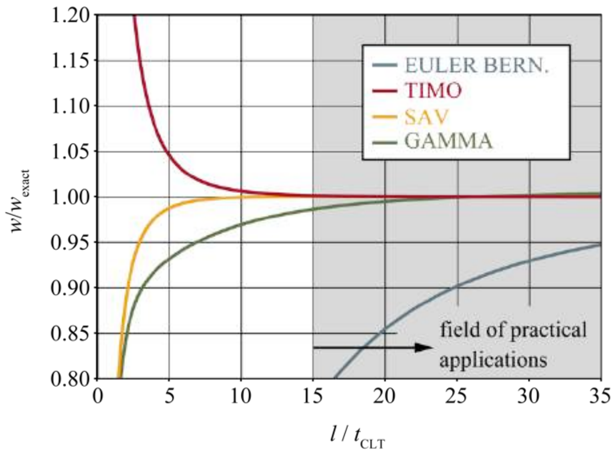

Fig. 3 Deflections calculated by means of various methods in relation to the exact analytical solution [21] of a 5-layer CLT-element with thickness ratio $t_{90} / t_0 = 1.0$

To conclude, within the practical, relevant range of $l / t_{CLT} \geq 15$, all the approximate approaches represented here are applicable. Of course, it is necessary to prove the consistency between the design method used for stiffness and stress calculations and that used for derivation of strength and stiffness properties, based on tests. For calculations in the range $l / t_{CLT} < 15$, exact solutions of shear flexible multilayer plates [20] [21] are recommended.

2.1.2 Loads in-plane

For the calculation of stresses in CLT, caused by loads in-plane, again various procedures are available. Some approvals use (e.g. [22]) the calculation of stresses based on the net cross section, others (e.g. [23]), particularly for shear, strength values are based on the gross cross section. A further approach, as applied in the following section, is based on a “representative volume element, RVE” and the “representative volume sub-element, RVSE”, see [6] [24].

Thus, a CLT element stressed in-plane is divided into RVEs. RVE is defined by a thickness equivalent to the CLT element, t_{CLT}, with a square surface equivalent to a node of crossed boards, with lateral length equivalent to the board’s width plus half of the gap width on both sides. This RVE is further subdivided into RVSEs. These have the same square surface and a thickness, t_i^*, which is composed of the minimum of the adjacent halved board thicknesses on both sides of the adhesive layer, as plane of symmetry (see Fig. 4). Theoretically, the RVSE is based on the assumption of an infinite number of layers of constant thickness. Thus boundary effects, as consequence of a finite number of layers, are neglected. These effects have to be considered in a separate step, which will be explained later on.

The RVE is solely stressed in-plane (normal forces n_x and n_y, shear force n_{xy}), thus stresses and strains are constant over the entire thickness t_{CLT}.

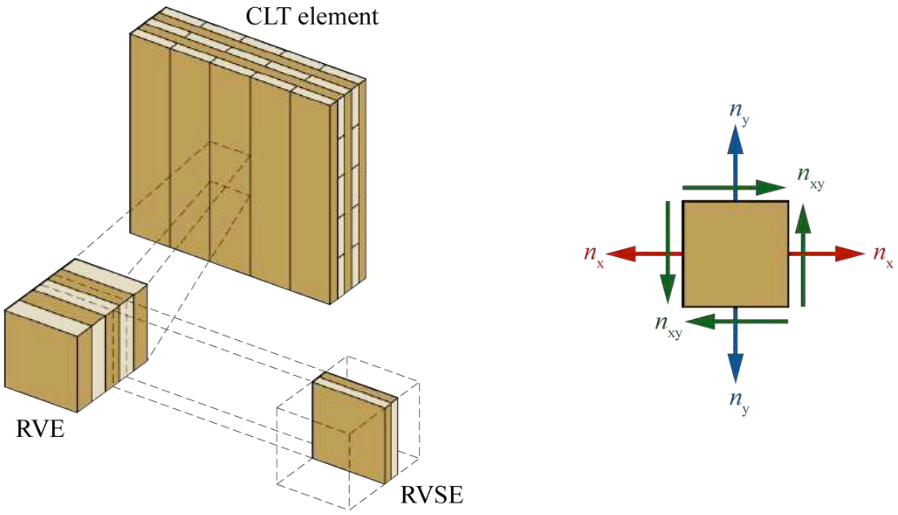

Fig. 4 Definition of RVE and RVSE on a CLT element (left) and acting forces on a RVE (right)

2.2 Stiffness values

2.2.1 Bending stiffness

The bending stiffness of a CLT element, K_{CLT}, is calculated according to eq. (1). In this way, the changing layer orientation and corresponding material parameters, such as the modulus of elasticity, are taken into account. For layers with α = 0°, the $E_{0,mean}$, and, for layers with α = 90° the $E_{90,mean}$ according to the product specification, are be applied. Because of the high ratio $E_{0,mean}$ / $E_{90,mean}$ ≈ 30, the contribution of the cross layers (α = 90°) to K_{CLT} is negligible. Thus for simplicity K_{CLT} can be calculated based on $E_{90,mean}$ = 0.

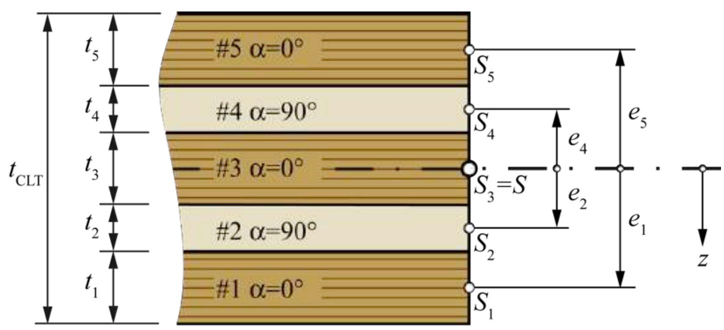

Fig. 5 Cross section of a 5-layer CLT element

$$K_{\mathrm{CLT}} = \sum(E_{\mathrm{i}} \cdot I_{\mathrm{i}}) + \sum(E_{\mathrm{i}} \cdot A_{\mathrm{i}} \cdot e_{\mathrm{i}}^2) \tag{1}$$

I_{i}	moment of inertia of layer *i* in reference to its neutral axis
E_{i}	modulus of elasticity of layer *i*, ($E_{0,\mathrm{i}}$ or $E_{90,\mathrm{i}}$)
A_{i}	cross-sectional area of layer *i*
e_{i}	distance between the centre of gravity S_{i} of layer *i* and the centre of gravity *S* of the CLT element

2.2.2 Axial Stiffness

As for K_{CLT}, the crosswise layered structure of CLT has also to be considered for calculating the axial stiffness. The axial stiffness, $(EA)_{\mathrm{ef}} = D_{\mathrm{x}}$ (stiffness in x-direction) for a linear member, is given in eq. (2).

$$(EA)_{\mathrm{ef}} = D_{\mathrm{x}} = \sum_{i=1}^{n} E_{\mathrm{i}} \cdot A_{\mathrm{i}} \tag{2}$$

In the case of a plate loaded in-plane, with $E_{90} = 0$, the stiffness values, D_{x} (see eq. (3)) and D_{y} (see eq. (4)) of a 1 m wide plate strip, are based on the effective cross section. Consequently, only those boards that are oriented in the specific direction are taken into account.

$$D_{\mathrm{x}} = E_{0,\mathrm{mean}} \cdot \sum_{i=1}^{n} t_{\mathrm{i,x}} \tag{3}$$

$$D_{\mathrm{y}} = E_{0,\mathrm{mean}} \cdot \sum_{i=1}^{n} t_{\mathrm{i,y}} \tag{4}$$

D_{x}	axial stiffness in x-direction
D_{y}	axial stiffness in y-direction
$t_{\mathrm{i,x}}$	thickness of layer *i* with fibre direction parallel to x-direction
$t_{\mathrm{i,y}}$	thickness of layer *i* with fibre direction parallel to y-direction

2.2.3 Shear stiffness for plates loaded in-plane

The shear stiffness of a CLT element loaded in-plane, S_{xy}, is calculated according eq. (5) and is the product of the effective shear modulus, G^*, and the thickness of the CLT element, t_{CLT}. The effective shear modulus is given in eq. (6). The specified adjustment factor, α_{T}, was determined in the course of a finite element study in [25]. It shows a dependence on the ratio $t\,/\,a$. As an approximation for non-constant *a* and/or *t*, a mean value of all boards should be used.

$$S_{\mathrm{xy}} = G^* \cdot t_{\mathrm{CLT}} \tag{5}$$

$$G^* = \frac{G_{0,\mathrm{mean}}}{1 + 6 \cdot \alpha_{\mathrm{T}} \cdot \left(\frac{t}{a}\right)^2} \quad \text{with} \quad \alpha_{\mathrm{T}} = 0.32 \cdot \left(\frac{t}{a}\right)^{-0.77} \tag{6}$$

$G_{0,\mathrm{mean}}$	mean value of shear modulus of the base material (boards)
t	(mean) thickness of layers
a	(mean) board width or (mean) distance of cracks

2.2.4 Shear stiffness for plates loaded out-of-plane

The shear stiffness, S_{CLT}, of CLT elements loaded out-of-plane, as given in eq. (7), is dependent upon the shear stiffness of a rigid composite beam, S_{tot} (see eq. (8)), (without warping of cross-sectional area) and the shear correction coefficient, κ (see eq. (9)). For the longitudinal layers and cross layers, respectively, the shear modulus $G_{\mathrm{CLT,mean}}$ and the shear modulus perpendicular to grain (rolling shear modulus) $G_{\mathrm{r,CLT,mean}}$ apply.

$$S_{\mathrm{CLT}} = S_{\mathrm{tot}} \cdot \kappa \tag{7}$$

$$S_{\mathrm{tot}} = \sum (G_{\mathrm{i}} \cdot b_{\mathrm{i}} \cdot t_{\mathrm{i}}) = \sum (G_{\mathrm{i}} \cdot A_{\mathrm{i}}) \tag{8}$$

$$\kappa = \frac{1}{S_{\mathrm{tot}} \cdot \frac{1}{K_{\mathrm{CLT}}^2} \cdot \int\limits_{t_{\mathrm{CLT}}} \frac{S^2(z, E(z))}{G(z) \cdot b(z)} \mathrm{d}z} \tag{9}$$

G_{i}	shear modulus of layer i (G_{i} or $G_{\mathrm{r,i}}$)
b_{i}	width of layer i
t_{i}	thickness of layer i
$S(z,E(z))$	first moment of area depending on coordinate z
$G(z)$	shear modulus depending on coordinate z
$b(z)$	width of cross section depending on coordinate z

Calculation of the shear correction coefficient, κ , as implemented in the CLTdesigner, is done by numerical integration over the entire cross section, analogous to eq. (9). Fig. 6 shows the shear correction coefficient, dependent on the ratio t_0 / t_{CLT}. Results of all available CLT-products are compared with the analytical solutions of 3-, 5- and 7-layer elements. Due to the influence of the transverse shear-flexible cross layers, the shear correction coefficient for a CLT element, in the current product-range, is nearly constant and about ¼ of that for a uni-directional rectangular cross section.

The calculation of the shear correction coefficient, according to eq. (9), does not consider the influence of different board widths or gaps between the boards of the same layer. In [26] it is shown that these two parameters lead to a reduction, in the shear correction coefficient, by approximately 10 % to 15 %.

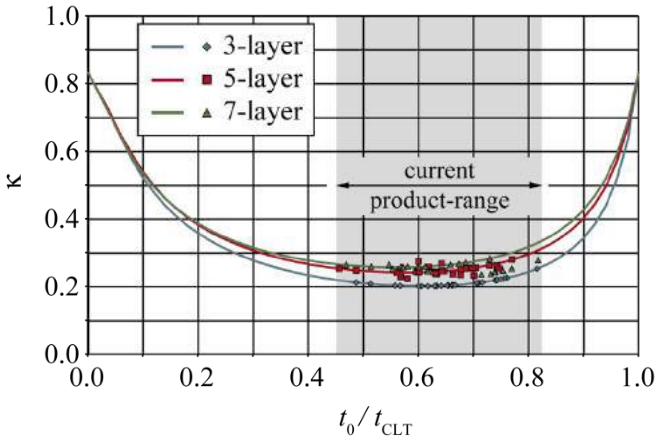

Fig.6 *Shear correction coefficient κ for the ratio $G_0 / G_r = 10$ depending on depth ratio t_0 / t_{CLT} – analytical solutions and values of current products evaluated by means of the CLTdesigner, where t_0 is the sum of thicknesses of all layers with $\alpha = 0°$*

2.2.5 Twisting stiffness

In [25] the twisting stiffness, D_{xy}, of a homogenous plate with orthotropic material, is defined according to eq. (10). For validity this equation, the shear modulus, G_{xy}, must be taken as constant over the entire thickness, t_{CLT}. This equation is only valid for CLT elements composed of boards with adhesive bonding on their narrow faces and without cracks. If these requirements are not fulfilled, the twisting stiffness has to be reduced following eq. (11) and (12) (see also [25]). The number of layers and the geometry of the boards are found to be the influencing parameters. Parameters p and q, based on a numerical study [25], are listed in Tab. 1. In case of varying board widths and thicknesses, mean values for a and t should be used.

$$D_{xy} = G_{xy} \cdot \frac{t_{CLT}^3}{12} \tag{10}$$

$$D_{xy}^* = G_{xy}^* \cdot \frac{t_{CLT}^3}{12} = \kappa_{CLT,P} \cdot G_{xy} \cdot \frac{t_{CLT}^3}{12} = \kappa_{CLT,P} \cdot D_{xy} \tag{11}$$

$$\kappa_{CLT,P} = \frac{1}{1 + 6 \cdot \alpha_{FIT} \cdot \left(\frac{t}{a}\right)^2} \qquad \text{with} \quad \alpha_{FIT} = p \cdot \left(\frac{t}{a}\right)^q \tag{12}$$

D_{xy}	twisting stiffness of a homogenous plate with orthotropic material or of CLT elements glued together at their narrow sides and without cracks
D_{xy}^*	reduced twisting stiffness of CLT elements without bonding on their narrow sides and/or with cracks
G_{xy}^*	reduced shear modulus for CLT elements without bonding on their narrow sides and/or with cracks
$\kappa_{CLT,P}$	reduction factor for twisting stiffness
t	thickness of the board
a	width of the board

Tab. 1 Parameters p and q for 3-, 5- and 7-layer CLT elements

parameter	3-layer	5-layer	7-layer
p	0.89	0.67	0.55
q	-0.67	-0.74	-0.77

The influence of the parameter ratio t / a and the number of layers on $\kappa_{CLT,P}$ is shown in Tab. 2.

Tab. 2 Reduction factor $\kappa_{CLT,P}$

t / a	$\kappa_{CLT,P}$		
	3-layer	5-layer	7-layer
1:6	0.67	0.70	0.73
1:5	0.61	0.65	0.69
1:4	0.54	0.59	0.63
1:3	0.45	0.50	0.54

The ratio t / a = 1:4 and the shear modulus G_{xy} = 650 N/mm^2 will lead to the following values for reduced shear modulus G_{xy}^*, as shown in Tab. 3.

Tab. 3 Determined reduced shear modulus G_{xy}^* *for t / a = 1:4 and* G_{xy} *= 650 N/mm*^{2}

t / a	G_{xy}^* [N/mm^2]		
	3-layer	5-layer	7-layer
1:4	~ 350	~ 380	~ 410

2.3 Structural fire design

CLTdesigner uses structural fire design as described by Frangi in [6], which is based on the method of reduced cross sections according to EN 1995-1-2 [4]. Therefore, the information about the charring depth over the time is decisive. The charring depth, d_{char}, depends on the charring rate β (regulated for layers with or without gaps between boards), the type of adhesive applied (in particular their behaviour if exposed to high temperature - high temperature-proofed or not) and on the availability of fire protection.

The charring rate is defined as follows:

- CLT without gaps or gaps up to 2 mm: β = 0.65 mm/min
- CLT with gaps up to 6 mm: β = 0.80 mm/min

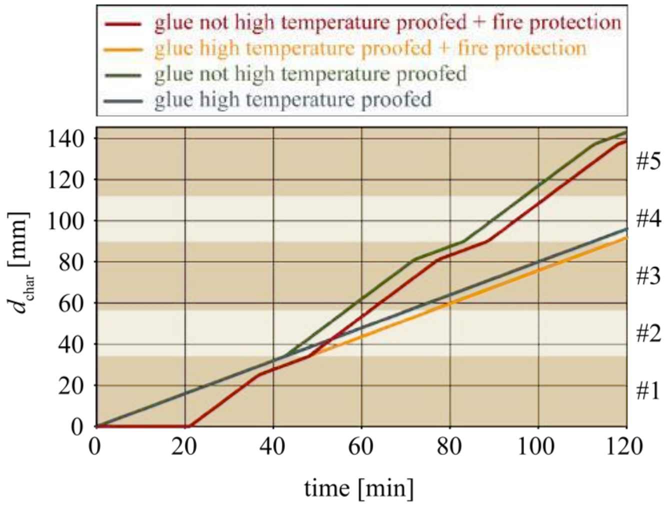

Fig. 7 Charring depth in time-dependency of a 5-layer CLT element: different scenarios on type of adhesive and availability of fire protection

Fig. 7 shows the charring depth depending on the charring time for different scenarios. It can be recognised that, from failure of the fire protection up to the time where the protecting charcoal layer is formed, a double charring rate has to be considered. The same applies in cases where adhesives are used which are not proofed to resist high temperatures. In fact during fire tests performed on CLT elements, loaded out-of-plane, detachment of charred layers was observed (see [27]). Of course this is not the case for CLT wall elements loaded in-plane.

Definitions of the reduced cross section are given in Fig. 8. The depth is reduced by the effective charring depth, d_{ef}, according to eq. (13), where k_0 increases linearly from 0 to 1 in the first 20 minutes of fire exposure. Consequently, after a charring time t of 20 min, the full additional thickness of d_0 = 7 mm, which accounts for the zone of thermally modified material, is added to the charring depth, d_{char}.

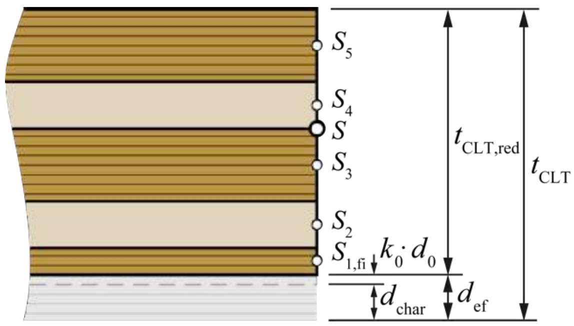

Fig. 8 Definitions concerning the reduced cross section due to fire

$$d_{ef} = d_{char} + k_0 \cdot d_0 \quad \text{with} \quad k_0 = \min\begin{cases} t/20 \\ 1.0 \end{cases} \tag{13}$$

By using the method of reduced cross section, the verification process in case of fire can be done as usual, but with the design strength in fire, $f_{d,fi}$ according to eq. (14). In doing so, the 20%-quantile of strength f_{20} (with k_{fi} = 1.15; according to GLT due to the assumption of equal dispersions), the modification factor $k_{mod,fi}$ = 1.0 and the partial safety factor $\gamma_{M,fi}$ = 1.0 can be applied.

$$f_{\mathrm{d,fi}} = k_{\mathrm{mod,fi}} \cdot \frac{f_{20}}{\gamma_{\mathrm{M,fi}}} \quad \text{with} \quad f_{20} = k_{\mathrm{fi}} \cdot f_{\mathrm{k}} \tag{14}$$

3. Ultimate Limit State (ULS) Design

In the following, the procedures, relevant for ultimate limit state design for the most common load situations of wall, ceiling and roof CLT elements, are presented.

In general, the verifications are restricted to CLT elements of uniform material in all layers. This is because the underlying load bearing models, and therefore the published and used strength values, are based on that.

3.1 Bending (loads out-of-plane)

For CLT elements loaded out-of-plane, the maximum design bending stress on the edge has to be less than the design value of the bending strength for CLT (see eq. (15)).

$$\frac{\sigma_{\mathrm{max,d}}}{f_{\mathrm{m,CLT,d}}} \leq 1.0 \tag{15}$$

The calculation of stresses (see eq. (16)) is based on the Timoshenko beam theory. In this theory, Bernoulli's hypothesis of cross sections that remain plane, even during deformation, is still valid. Therefore, the bending stress distribution over the cross section remains linear. Because of (regular) gaps (cracks) between the boards, within each layer, a transfer of normal stresses in the cross layers (tension and compression perpendicular to grain) is not (always) possible. Thus the calculation can be made with $E_{90} = 0$. In doing so, the stresses in longitudinal layers increase and are therefore on the safe side.

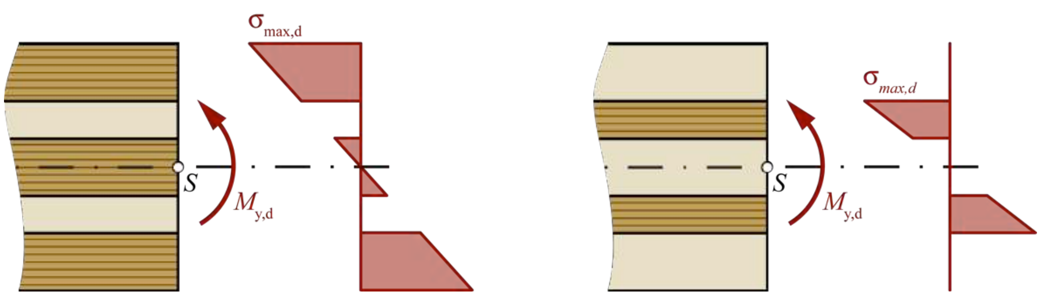

Fig. 9 Normal stress distribution over the cross section of a CLT-plate due to a bending moment out-of-plane (E_{90} = 0): exterior longitudinal layers (left); exterior cross layers (right)

$$\sigma(z) = \frac{M_{\mathrm{y}}}{K_{\mathrm{CLT}}} \cdot z \cdot E(z) \tag{16}$$

The characteristic bending strength, $f_{\mathrm{m,CLT,k}}$, can be based on either the tensile strength of the base material (boards), according to eq. (17) (see [28] [6]) or the characteristic bending strength of glued laminated timber (GLT), $f_{\mathrm{m,GLT,k}}$, of the appropriate strength class and with a reference depth of 600 mm according to eq. (18) (see [6] [17] [18] [19]). Currently the CLTdesigner uses eq. (18).

$$f_{m,CLT,k} = k_{m,CLT} \cdot f_{t,0,l,k}^{0.8} \tag{17}$$

$$f_{m,CLT,k} = k_l \cdot f_{m,GLT,k} \tag{18}$$

The system strength factor, k_l, takes into account the parallel effect of interacting components. This can be calculated according to eq. (19) and is thus dependent on the number of parallel interacting boards, n, in the outer layer of the bending tension zone.

$$k_l = \min\begin{cases} 1.1 \\ 1 + 0.025 \cdot n \end{cases} \quad \text{for } n > 1 \tag{19}$$

The number of parallel interacting boards can be determined on the specified limits for the board width, within technical approvals. The width of a board usually varies between 80 mm and 250 mm. Considering these limits, it can be assumed that a 1 m wide CLT element has at least four interacting boards, thus the system factor $k_l = 1.1$ applies.

The specified strength value refers to a reference depth for CLT of $t_{CLT,ref} = 150$ mm. Due to a lack of systematic investigations, a correction factor for the depth, k_h, is not currently applied.

In consideration of modification factor, k_{mod}, and partial safety factor $\gamma_M = 1.25$, the design value of the bending strength is:

$$f_{m,CLT,d} = \frac{k_{mod} \cdot f_{m,CLT,k}}{\gamma_M} \tag{20}$$

3.2 Tension (loads in-plane)

Under the assumption that the modulus of elasticity parallel-to-grain, $E_{0,mean}$, of all layers is equal, the verification of tensile stresses of CLT elements, loaded in-plane, is carried out according to eq. (21). For determining the effective net area, $A_{net,ef}$, only parallel layers oriented in the force direction are considered. With the system factor, $k_{sys,t,0}$, the system effect of parallel interacting boards is taken into account. Currently, in CLTdesigner, this factor is set equal to 1.0.

$$\frac{N_d}{A_{net,ef}} \le f_{t,0,CLT,net,d} = \frac{k_{mod} \cdot f_{t,0,CLT,net,k}}{\gamma_M} = k_{sys,t,0} \cdot \frac{k_{mod} \cdot f_{t,0,l,k}}{\gamma_M} \tag{21}$$

3.3 Compression (loads in-plane)

For members loaded concentrically and axially in compression eq. (22) should be fulfilled.

$$\frac{N_d}{A_{net,ef} \cdot f_{c,0,CLT,net,d}} \le 1.0 \tag{22}$$

However, for slender members in compression, the possibility of lateral buckling has to be considered. For this case, two design methods are available:

- proof according to equivalent beam method

- proof according to theory of 2nd order

3.3.1 Equivalent beam method

Using the method of an equivalent beam, eq. (23) has to be fulfilled.

$$\frac{N_{\mathrm{d}}}{k_{\mathrm{c}} \cdot A_{\mathrm{net,ef}} \cdot f_{\mathrm{c,0,CLT,net,d}}} \leq 1.0 \tag{23}$$

Here the compressive strength is reduced by the instability factor, k_{c}, according to eq. (25). This instability factor is a function of the relative slenderness, λ_{rel}, the shape of the cross section and the quality of manufacturing (straightness factor, β_{c}, see eq. (27)). The relative slenderness, λ_{rel}, (eq. (28)) is dependent on the ideal elastic buckling load, n_{cr}, according to eq. (24). This equation also considers the shear flexibility, an important parameter in the case of CLT. The 5 %-quantile of the bending stiffness $K_{\mathrm{CLT,05}}$ and of the shear stiffness $S_{\mathrm{CLT,05}}$ is calculated according to eq. (1) and (7), by means of 5 %-quantiles instead of mean values ($E_{0,05}$, $G_{\mathrm{CLT,05}}$ and $G_{\mathrm{r,CLT,05}}$).

$$n_{\mathrm{cr}} = \frac{K_{\mathrm{CLT,05}} \cdot \pi^2}{l_{\mathrm{k}}^2 \cdot \left(1 + \frac{K_{\mathrm{CLT,05}}}{S_{\mathrm{CLT,05}} \cdot l_{\mathrm{k}}^2}\right)} \tag{24}$$

$$k_{\mathrm{c}} = \min \left[\begin{array}{c} 1.0 \\ \dfrac{1}{k + \sqrt{k^2 - \lambda_{\mathrm{rel}}^2}} \end{array} \right] \tag{25}$$

$$k = 0.5 \cdot \left(1 + \beta_{\mathrm{c}} \cdot \left(\lambda_{\mathrm{rel}} - 0.3\right) + \lambda_{\mathrm{rel}}^2\right) \tag{26}$$

$$\beta_{\mathrm{c}} = 0.1 \tag{27}$$

$$\lambda_{\mathrm{rel}} = \sqrt{\frac{A_{\mathrm{net,ef}} \cdot f_{\mathrm{c,0,CLT,net,k}}}{n_{\mathrm{cr}}}} \tag{28}$$

3.3.2 Theory of 2nd order

If second order analysis (equilibrium on the deformed system) is used, then the effects of induced deflection on internal forces and moments are considered and thus a combined load situation with a normal force and a bending moment occurs. Eq. (29) shall be satisfied.

$$\left(\frac{N_{\mathrm{d}}}{A_{\mathrm{net,ef}} \cdot f_{\mathrm{c,0,CLT,net,d}}}\right)^{2} + \frac{M_{\mathrm{d}}^{\mathrm{II}}}{W_{\mathrm{ef}} \cdot f_{\mathrm{m,CLT,d}}} \leq 1.0 \tag{29}$$

3.4 Compression (loads out-of-plane)

The design of CLT elements, stressed in compression perpendicular to-the-plane is according to EN 1995-1-1 [2]. The verification has to fulfil eq. (31).

$$\sigma_{\mathrm{c,90,CLT,d}} = \frac{F_{\mathrm{c,90,d}}}{A_{\mathrm{c,90}}} \tag{30}$$

$$\sigma_{\mathrm{c,90,CLT,d}} \leq k_{\mathrm{c,90,CLT}} \cdot \frac{k_{\mathrm{mod}} \cdot f_{\mathrm{c,90,CLT,k}}}{\gamma_{\mathrm{M}}} = k_{\mathrm{c,90,CLT}} \cdot f_{\mathrm{c,90,CLT,d}} \tag{31}$$

$f_{\mathrm{c,90,CLT,k}}$	characteristic compressive strength perpendicular to the plate plane of a CLT cube
$k_{\mathrm{c,90,CLT}}$	factor taking into account the load configuration, possibility of splitting and degree of compressive deformation
$A_{\mathrm{c,90}}$	real area of contact, which transmits load into CLT

The compressive strength of CLT perpendicular-to-plane is influenced by many parameters; in [29] the following parameters were investigated on CLT cubes under laboratory conditions: (i) width of annual growth rings, (ii) the position of the pith, (iii) the number of layers, and (iv) the thickness ratio of adjacent layers (parallel to perpendicular). Salzmann [30] investigated 5-layer CLT test specimens of different depth (from 150 mm to 197 mm), which were produced by one single manufacturer. These test specimens, of dimensions 160 mm x 160 mm, were tested under point load at different positions. Serrano [31] tested 3-layer CLT elements with a depth of 120 mm and constant layer thickness stressed uniformly by a line load (50 mm x 300 mm) at different positions.

Based on these investigations, the characteristic compressive strength value perpendicular-to-plane of a CLT cube is proposed, with $f_{\mathrm{c,90,CLT,k}} = 2.85$ N/mm^2. This value is affected by the plate thickness and the layup factor but the proposed value neglects this influence and is on the safe side. The values of $k_{\mathrm{c,90,CLT}}$ have been determined by tests and finite element analysis. Depending on the load situation, the values are between 1.0 and 1.8. The proposed values are given in Tab. 4 and Tab. 5.

Note: According to EN 1995-1-1 the effective contact area perpendicular-to-plane, A_{ef}, should be determined taking into account the effective contact length parallel to grain, whereby the actual contact length is increased by 30 mm on each side. Please note that the proposed values of $k_{\mathrm{c,90,CLT}}$ are based on the real contact area $A_{\mathrm{c,90}}$.

Tab. 4 *Proposed values of $k_{c,90,CLT}$ for plates under point load based on a characteristic strength value for compression perpendicular-to-plane of a CLT cube of $f_{c,90,CLT,k}$ = 2.85 N/mm^2 and the real contact area $A_{c,90}$ ([30] [32])*

load situation		$k_{c,90,CLT}$
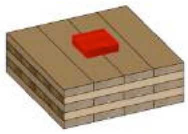	central	1.8
	boundary, parallel to fibre direction of surface layer	1.5
	boundary, perpendicular to fibre direction of surface layer	1.5
	edge	1.3

Tab. 5 *Proposed values of $k_{c,90,CLT}$ for plates under line load based on a characteristic strength value for compression perpendicular-to-plane of a CLT cube of $f_{c,90,CLT,k}$ = 2.85 N/mm^2 and the real contact area $A_{c,90}$ ([31])*

load situation		$k_{c,90,CLT}$
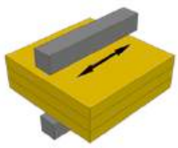	central parallel to main direction	1.3
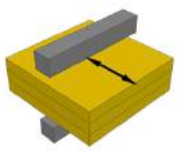	central, perpendicular to fibre direction of surface layer	1.8
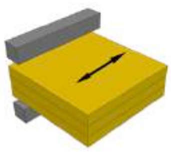	boundary, parallel to fibre direction of surface layer	1.0
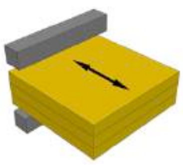	boundary, perpendicular to fibre direction of surface layer	1.5

Currently a master thesis is carried out at Graz University of Technology concerning further investigations on CLT elements under compression line load perpendicular-to-plane. Real load situations, for example CLT wall on a CLT slab, are also being tested.

3.5 Shear (loads in-plane)

Not all CLT products use boards glued on the narrow faces. Even so, the occurrence of cracks due to swelling and shrinkage cannot be prevented. Thus shear stresses can only appear in end-grain sections, narrow faces are free of those stresses. Therefore shear forces can only be transferred indirectly across the crossing of two boards in adjacent layers. Due to shear forces acting in different planes, torsional stresses in the glued interface occur (see Fig. 10).

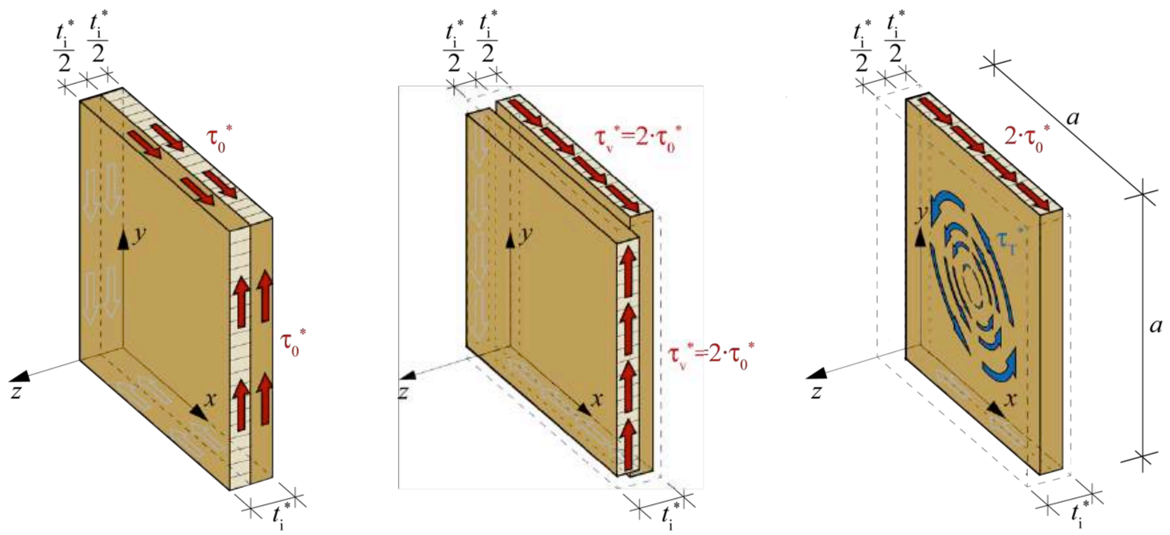

Fig. 10 Stresses in one RVSE: glued on narrow faces and completely free from cracks (left); mechanism I (centre); mechanism II (right) ([6])

The case of shear stresses in end-grain sections is denoted by mechanism I – shear, and the case of torsional stresses in the glued interface by mechanism II – torsion. Both mechanisms (see Fig. 11, mechanism I – shear, mechanism II – torsion) have to be verified separately.

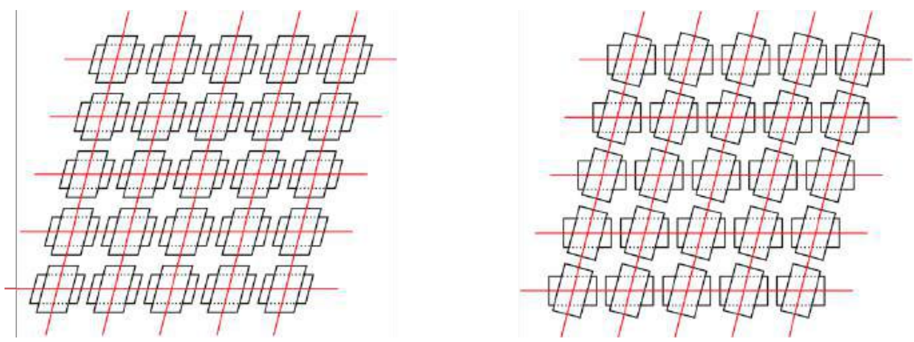

Fig. 11 Mechanism I – shear (left); mechanism II – torsion (right) ([6])

The design method, which is according to [6] [24], is based on the use of representative volume elements (RVE) and representative volume sub-elements (RVSE) and is generally applicable for two-dimensional plane CLT elements loaded in-plane. If CLT is used as linear element loaded in-plane, different considerations have to be made (see [33]). One RVSE has the dimensions of two crossing boards of adjacent layers, with gaps included, times the ideal thickness, t_i^*, according to the scheme shown in Tab. 6. With this scheme the edge effect of a finite number of layers and varying thicknesses of layers are also considered. Of course, this approach might deliver conservative results. This is due to the fact that, in cases of different thicknesses of adjacent layers, only the thinner layer is taken into account.

Tab. 6 Scheme for the determination of the ideal thickness t_i^* of a n-layer CLT element

node 1 (= node on the top)	layer 1 (top) layer 2 (core)	$t_1^* = \min(2 \cdot t_1, t_2)$
node *i* (= core node)	layer *i* (core) layer *i*+1 (core)	$t_i^* = \min(t_i, t_{i+1})$
node *n*–1 (= node on the top)	layer *n*–1 (core) layer *n* (top)	$t_{n-1}^* = \min(t_{n-1}, 2 \cdot t_n)$

The overall thickness, t^*, of all ideal RVSEs, is denoted as the sum of the ideal thicknesses, t_i^* (see eq. (32)), and thus is always smaller than or equal to the geometric overall thickness, t_{CLT}, of the CLT element.

$$t^* = \sum_{i=1}^{n-1} t_i^* \leq t_{CLT} \tag{32}$$

The proportionate shear force, $n^*_{xy,RVSE(i)}$, in a n-layer CLT element, can be determined by eq. (33).

$$n^*_{xy,RVSE(i)} = \frac{n_{xy}}{t^*} \cdot t_i^* \tag{33}$$

The ideal nominal shear stress, $\tau^*_{0,RVSE(i)}$, of the i^{th} RVSE, can be calculated by dividing the proportionate shear force through the thickness, t_i^*. This leads to a constant nominal shear stress, τ_0^*, for all RVSEs (see eq. (34)).

$$\tau^*_{0,RVSE(i)} = \frac{n^*_{xy,RVSE(i)}}{t_i^*} = \frac{n_{xy}}{t^*} = \tau_0^* \tag{34}$$

3.5.1 Mechanism I – shear

For mechanism I, the size of effective shear stress, τ_v^*, of a RVSE in the cross sectional area, can be calculated with eq. (35). It is twice the ideal nominal shear stress and equal for all RVSEs.

$$\tau_v^* = 2 \cdot \tau_0^* \tag{35}$$

To fulfil eq. (36), the design stress has to be less or equal the design resistance.

$$\left|\tau^*_{\mathrm{v,d}}\right| \leq f_{\mathrm{v,CLT,d}} = \frac{k_{\mathrm{mod}} \cdot f_{\mathrm{v,CLT,k}}}{\gamma_{\mathrm{M}}} \tag{36}$$

Note: For determination of the shear stress a constant distribution over width of the board, contrary to a quadratic distribution as well known from rectangular cross sections of a linear element (τ_{max} is of a factor 3/2 higher than the constant supposed value), is assumed. This can be expected because the assumptions of the beam theory (constant shear force distribution as well as free shear warping on the boundary) is not satisfied. Instead, it can be assumed that interference by the locked structure of the CLT plate will lead to a rather constant shear stress distribution.

In contrast to the previously mentioned method, in some technical approvals the verification of mechanism I is based on the net cross section area. In case of constant layer thicknesses, both methods produce identical results but, for varying layer thicknesses, differences can occur.

3.5.2 Mechanism II – torsion

For mechanism II each node (glued interface) of the RVE has to be verified. The RVSE with the largest ideal thickness, t_i^*, is decisive, because there the maximum torsional moment, $M_{T,i}$, appears (see eq. (37)).

$$M_{\mathrm{T,i}} = \tau^*_0 \cdot t^*_{\mathrm{i}} \cdot a^2 \tag{37}$$

The torsional stress, $\tau^*_{T,i}$ (see eq. (38)), is defined by dividing the torsional moment, $M_{T,i}$, by the polar moment of resistance, W_P, see eq. (39).

$$\tau^*_{\mathrm{T,i}} = \frac{M_{\mathrm{T,i}}}{W_{\mathrm{P}}} = \frac{\tau^*_0 \cdot t^*_{\mathrm{i}} \cdot a^2}{\frac{a^3}{3}} = 3 \cdot \tau^*_0 \cdot \frac{t^*_{\mathrm{i}}}{a} \tag{38}$$

$$W_{\mathrm{P}} = \frac{I_{\mathrm{P}}}{a/2} = \frac{a^3}{3} \tag{39}$$

The polar moment of resistance, W_P, is composed of the polar moment of inertia of the glued interface, I_P according to eq. (40), and the edge distance, $a/2$ (assumption: dimension of the glued interface $a \cdot a$).

$$I_{\mathrm{P}} = I_{\mathrm{y}} + I_{\mathrm{z}} = \frac{a \cdot a^3}{12} + \frac{a^3 \cdot a}{12} = \frac{a^4}{6} \tag{40}$$

For verification of mechanism II eq. (41) should be satisfied.

$$\left|\tau^*_{\mathrm{T,d}}\right| \leq f_{\mathrm{T,CLT,d}} = \frac{k_{\mathrm{mod}} \cdot f_{\mathrm{T,CLT,k}}}{\gamma_{\mathrm{M}}} \tag{41}$$

Also mechanism II is regulated in some technical approvals. However, the specified equations in the approvals are only valid for rectangular CLT elements, with constant layer thickness, without openings, under constant shear. In that case, the approach proposed here and that given in the approvals lead to identical results. If there is a large variation in layer thicknesses, significant differences will occur.

3.6 Shear (loads out-of-plane)

The distribution of shear stress over the cross section, resulting from loads out-of-plane, can be calculated with eq. (42). The assumption of $E_{90} = 0$ leads to a constant value instead of a quadratic distribution of shear stress in cross layers. The maximum shear stress occurs at the height of the centre of gravity. However, due to different layer orientation, in CLT of uniform material two verifications are required (see eq. (43)). In longitudinal layers, a proof of shear stress vs. shear strength, $f_{v,CLT,d}$, and, in cross layers, a proof of shear stress vs. rolling shear strength, $f_{r,CLT,d}$, has to be done.

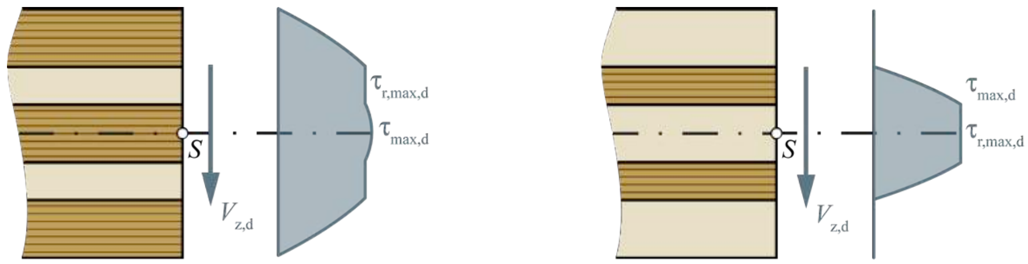

Fig. 12 Shear stress distribution over the cross section of a CLT plate due to shear force ($E_{90} = 0$): exterior longitudinal layers (left); exterior cross layers (right)

$$\tau(z_0) = \frac{V_z \cdot \int_{A_0} E(z) \cdot z \cdot \mathrm{d}A}{K_{\mathrm{CLT}} \cdot b(z_0)} \tag{42}$$

$$\frac{\tau_{\mathrm{max,d}}}{f_{\mathrm{v,CLT,d}}} \leq 1.0 \quad \text{and} \quad \frac{\tau_{\mathrm{r,max,d}}}{f_{\mathrm{r,CLT,d}}} \leq 1.0 \tag{43}$$

4. Serviceability Limit State (SLS) Design

4.1 Deflections (loads out-of-plane)

For CLT elements loaded out-of-plane, it is important to check deflections. Due to shear-flexible cross layers, it is essential to also include deformations caused by shear (see eq. (44)).

$$w_{\mathrm{ges}} = \frac{1}{K_{\mathrm{CLT}}} \int \left(M \cdot \overline{M} \right) \mathrm{d}x + \frac{1}{S_{\mathrm{CLT}}} \int \left(V \cdot \overline{V} \right) \mathrm{d}x \tag{44}$$

The maximum deflection, at midspan, of a single-span beam under uniform distributed load, can be calculated with eq. (45).

$$w(l/2) = \frac{5 \cdot q \cdot l^4}{384 \cdot K_{\mathrm{CLT}}} + \frac{q \cdot l^2}{8 \cdot S_{\mathrm{CLT}}} \tag{45}$$

The stiffness values, K_{CLT} and S_{CLT}, can be computed according to eq. (1) and (7), using mean values of elasticity (modulus of elasticity and shear moduli).

As well as the instantaneous deflections at time $t = 0$, the final and net final deflections at $t = \infty$ have to be checked. Final and net final deflections take into account the longterm effects due to creep. Due to the cross layers, and consequently rolling shear, in CLT the deformation factor, k_{def}, is higher than for solid wood or glued laminated timber (GLT). [34] and prEN 16351 [1] give values of k_{def} for 3- to 7-layer CLT elements, depending on the service class (SC). For SC 1 and SC 2, respectively, values of $k_{def} = 0.85$ and 1.10 are proposed. For CLT elements with more than 7 layers the values for plywood can be applied.

The combinations of actions can be taken from EN 1995-1-1 [2] and from the National Application Documents.

4.2 Vibrations (loads out-of-plane)

For CLT elements with spans larger than 4 m, vibration usually governs the design. Currently there are a variety of methods and limit values. In the framework of a research project [35] at the Centre of Competence holz.bau forschungs gmbh, the following methods were analysed and compared: (i) the method for verifying vibration according to Eurocode 5, (ii) the suggestions of Hamm / Richter, (iii) a modified version of it, and (iv) the Canadian approach of Hu [36]. Added to this, on the basis of a parametric study on a single-span beam (with spans ranging from 3 m to 7 m under self weight, permanent load and exposed to imposed load of category A) the influence of significant parameters has been investigated. The conclusion is that, if these procedures are compared, then decisively different results occur. This is because the limit values are based on the highly subjective opinion of the person conducting the test. Therefore, it is currently impossible to define which approach would be best suited to verifying vibrations. Thus, it is considered worthwhile to compare available results from measurements with the prevailing methods and their limit values. Another highly important aspect is seen to be the quantification of the influence of support conditions (e.g. hinged, partly fixed, fixed, slabs supported by a floor beam, the influence of the upper floor loads transmitted through walls on the degree of clamping). Currently such investigations with regard to this are in progress at the Centre of Competence holz.bau forschungs gmbh.

The CLTdesigner provides the following procedures:

- verification according to EN 1995-1-1 [2]
- suggestions of Hamm / Richter in [6]
- modified version of Hamm / Richter (see [35])

Primarily these methods check the natural frequency, the stiffness criteria and the vibration acceleration. Following [2], the vibration velocity should also be checked. This verification is mainly required for light floors and therefore not considered for CLT floors.

4.2.1 Natural frequency

The natural frequency of a single-span beam, $f_{m,beam}$, follows eq. (46).

$$f_{m,beam} = \frac{k_m}{2\pi \cdot l^2} \sqrt{\frac{(EI)_{l,ef}}{\bar{m}}} \; [Hz] \tag{46}$$

$(EI)_{l,ef}$ effective bending stiffness in longitudinal direction

The effective bending stiffness, in the longitudinal direction, consists of the bending stiffness of the CLT element, K_{CLT}, and the bending stiffness of a possible final screed, but without the composite action (just as its own moment of inertia, without the Steiner parts). Furthermore, the shear flexibility may be taken into account by using the effective apparent bending stiffness (based on bending and shear deformations) instead of K_{CLT}.

The factor, k_m, takes different support conditions and Eigenmodes into consideration. In [37] the following values are given for the 1st Eigenmode ($m = 1$):

Tab. 7 Factor, k_m, to consider different support conditions for the 1st Eigenmode ([37])

support condition	k_m
hinged at both ends	$\pi^2 = 9.87$
fixed at both ends	22.4
fixed / free (cantilever)	3.52

For multi-span systems, the continuous beam effect can be considered. Factor k_{f2} , according eq. (47), can be used. Depending on the ratio l_{min} / l_{max}, this factor is between 1.0 and 1.5.

$$k_{f_2} = -5.3828\left(\frac{l_{min}}{l_{max}}\right)^6 + 16.6637\left(\frac{l_{min}}{l_{max}}\right)^5 - 19.7305\left(\frac{l_{min}}{l_{max}}\right)^4 + 10.3840\left(\frac{l_{min}}{l_{max}}\right)^3 - 1.9017\left(\frac{l_{min}}{l_{max}}\right)^2 - 0.5879\left(\frac{l_{min}}{l_{max}}\right) + 1.5537 \quad (47)$$

In the CLTdesigner, the natural frequency is calculated according to the method of Morleigh, see [38]. Additionally to the bending effects, this method also includes influences such as shear flexibility or elastic clamping. As, in context of CLT, the shear flexibility is of crucial importance, it is highly advisable to also take it into consideration in the context of vibrations.

If the slab is hinged at four sides, the transverse load-carrying effect can be taken into account. Therefore the natural frequency is calculated with eq. (48). Both the twisting stiffness, according to eq. (11), and the effective bending stiffness, in the transverse direction, can be considered. The increase of the natural frequency very much depends on the span to width ratio of the slab, l / b.

$$f_{1,plate} = f_{1,beam} \cdot \sqrt{1 + \frac{2 \cdot D_{xy}^*}{(EI)_{l,ef}} \cdot \frac{l^2}{b^2} + \frac{(EI)_{b,ef}}{(EI)_{l,ef}} \cdot \frac{l^4}{b^4}} \; [Hz] \quad (48)$$

The calculated natural frequency should be higher than the critical frequency, f_{crit}. The critical frequencies for normal and high requirements are shown in Tab. 8.

Tab. 8 Critical frequency f_{crit} for high and normal requirements

applied method	high requirements	normal requirements
EN 1995-1-1	8 Hz	
Hamm / Richter	8 Hz	6 Hz
Hamm / Richter modified	8 Hz	6 Hz

4.2.2 Stiffness criterion

In the examination of the criterion for stiffness, the maximum instantaneous vertical deflection caused by a vertical concentrated static force, F = 1 kN, at any point of the floor taking the load distribution into account, should be calculated and compared with the limit value $w_{\text{crit,1kN}}$.

Again, the shear flexibility should be taken into account when calculating the deflection. For a single-span beam, the maximum deflection, $w(F,b_{\text{F}})$, can be calculated with eq. (49). The load distribution will be considered by the effective width, according to eq. (50).

$$w(F,b_{\text{F}}) = \frac{F \cdot l^3}{48 \cdot (EI)_{l,\text{ef}} \cdot b_{\text{F}}} + \frac{F \cdot l}{4 \cdot (GA)_{\text{ef}} \cdot b_{\text{F}}} \tag{49}$$

$$b_{\text{F}} = \frac{l}{1.1} \cdot \sqrt[4]{\frac{(EI)_{\text{b,ef}}}{(EI)_{l,\text{ef}}}} \tag{50}$$

Tab. 9 Limit values for the stiffness criterion $w_{\text{crit,1kN}}$, for high and normal requirements

applied method	high requirements	normal requirements
EN 1995-1-1*)	1 mm	2 mm
Hamm / Richter	0.25 mm	0.5 mm
Hamm / Richter modified		

*) EN 1995-1-1 allows variable limit values for the stiffness criterion, but it is highly advisable to stay within the limit values

4.2.3 Vibration acceleration

If the natural frequency, f_1, is between the critical frequency f_{crit} and the minimum frequency f_{min} = 4.5 Hz, the vibration acceleration a should also be checked. This vibration acceleration should be less than a critical acceleration, a_{crit}. The critical accelerations, for normal and high requirements, are shown in Tab. 12.

The vibration acceleration is calculated according to eq. (51) and depends on the effective (generalised) mass, M_{gen}, of the slab, the excitation frequency, f_{f}, the natural frequency, f_1, the Fourier coefficient of the prevailing harmonic partial oscillation, $\alpha_{\text{i,f1}}$, and the self weight of the excitatory person, F_0 = 700 N, as well as on the modal damping ratio, ζ.

$$a = \frac{0.4 \cdot \left(\frac{F_0 \cdot \alpha_{\text{i,f}_1}}{M_{\text{gen}}} \right)}{\sqrt{\left(\left(\frac{f_1}{f_{\text{f}}} \right)^2 - 1 \right)^2 + \left(2 \cdot \zeta \cdot \frac{f_1}{f_{\text{f}}} \right)^2}} \quad [m/s^2] \tag{51}$$

For the calculation of modal (generalised) mass, M_{gen}, different information can be found in literature. To consider the influence of the orthotropic material, the use of eq. (52) with b_{F} from eq. (50) is proposed. Of course, for a more realistic consideration of the orthotropic material, further research is needed.

$$M_{gen} = M \cdot \frac{l}{2} \cdot b_F \ \left[\text{kg/m}^2\right] \quad \text{with } b_F \leq \text{half room width } \frac{b}{2} \tag{52}$$

In fact published values of Fourier coefficients and excitation frequencies do not agree. Tab. 10 shows the values as given in [39].

Tab. 10 Fourier coefficients and excitation frequencies according to [39]

natural frequency f_1 [Hz]	Fourier coefficient $\alpha_{i,f1}$	excitation frequency f_f [Hz]
$4.5 < f_1 \leq 5.1$	0.20	f_1
$5.1 < f_1 \leq 6.9$	0.06	f_1
$6.9 < f_1 \leq 8.0$	0.06	6.9

The damping ratio ζ for CLT floors is between 2.5 % and 3.5 %, depending on the type of floor construction and support conditions, see [40].

Tab. 11 Recommended values for damping ratio, ζ, dependent on the type of floor construction

type of floor construction	damping ratio ζ	
	supported on 2 sides	supported on 4 sides
CLT floors with a light or without floor construction	2.0 %	2.5 %
CLT floors with heavy floor construction	2.5 %	3.5 %

Tab. 12 Critical values of vibration acceleration, a_{crit}, for high and normal requirements

applied method	high requirements	normal requirements
EN 1995-1-1	0.05 m/s²	0.10 m/s²
Hamm / Richter		
Hamm / Richter modified		

5. Discussion and Conclusions

This paper sets out the calculation and design of cross laminated timber used as wall, floor and roof elements and exposed to common load situations. Different calculation procedures for plates loaded out-of-plane and in-plane are discussed. The determination of the required stiffness values is explained and, for some load situations, the design procedures at ultimate limit state (ULS) and serviceability limit state (SLS) are cited. Furthermore, the concept of the reduced cross section for structural fire design is demonstrated.

The methods shown are, in principle, limited to homogeneous CLT elements, composed of base material of one strength class. Of course for optimising the layup, for example, with regard to bending moments out-of-plane and the use of higher grades for the outer layers, it is necessary to adopt current load bearing and design models, as already available for combined glued laminated timber.

Some less common load situations, such as bending and shear of linear beam elements loaded in-plane as well as plates loaded in tension out-of-plane are not included in this paper. A detailed discussion about CLT elements used as linear elements can be found in [33]. Currently, at the Institute of Timber Engineering and Wood Technology at Graz University of Technology, a master thesis is in progress, the subject of which is the topic of door and window lintels (the remaining parts of CLT plates after door and window openings have been cut out). These lintels are tested in stiffness and strength. From tests, with different remaining wall strips on the side of the openings, the degree of clamping will be determined.

Concerning CLT elements loaded in tension perpendicular to-the-plane, there is currently no recognised systematic investigation. Amongst other issues, there is need for research regarding the load distribution. Both timber and adhesive show poor resistance when exposed to tension perpendicular to grain. Therefore, it is recommended that this load situation be avoided.

It is seldom the case that a CLT element is exposed to only one type of load. More often, different load combinations occur. For this reason the establishment of relevant interaction equations for stresses of combined actions is required. As part of the new COMET K-project "focus_sts" at the Centre of Competence holz.bau forschungs gmbh, there are investigations scheduled on this topic.

To stimulate the application of the solid timber construction technique in CLT further, it is necessary to make scientific findings available for engineers, architects and carpenters in practice as quickly and effectively as possible. Amongst other methods, this is enabled by a constant further development of the software tool CLTdesigner.

Furthermore, at present, new media play a significant role. Currently the mobile phone and the tablet PC are almost always available. Therefore the Institute of Timber Engineering and Wood Technology of Graz University of Technology has started the development of CLT Apps. The first App deals with the design of CLT floor and roof elements, loaded in bending out-of-plane. Another will follow.

Figure 13 CLT App for the iPhone

Acknowledgement: Thanks are due, for support for this work, to the Centre of Competence holz.bau forschungs gmbh.

6. References

[1] prEN 16351:2011-11, Timber structures – Cross laminated timber – Requirements.

[2] EN 1995-1-1:2004-11, Eurocode 5: Design of timber structures – Part 1-1: General – Common rules and rules for buildings.

[3] ON B 1995-1-1:2010-08, Eurocode 5: Bemessung und Konstruktion von Holzbauten – Teil 1-1: Allgemeines – Allgemeine Regeln für den Hochbau, (German).

[4] EN 1995-1-2:2004-11, Eurocode 5: Design of timber structures – Part 1-2: General – Structure fire design.

[5] EN 1990:2002-04, Eurocode – Basis of structural design.

[6] Schickhofer G., Bogensperger T., Moosbrugger T. (ed.): *BSPhandbuch: Holz-Massivbauweise in Brettsperrholz – Nachweise auf Basis des neuen europäischen Normen-konzepts*, Verlag der Technischen Universität Graz, 2010, ISBN 978-3-85125-109-8 (German).

[7] CLTdesigner, www.cltdesigner.at, 10.4.2013.

[8] Schelling W., *Die Berechnung nachgiebig verbundener zusammengesetzter Biegeträger im Ingenieurholzbau*, Dissertation, TH Karlsruhe, 1968 (German).

[9] Schelling W., Zur Berechnung nachgiebig zusammengesetzter Biegeträger aus beliebig vielen Einzelquerschnitten, In: Ehlbeck J., Steck G. (editors): *Ingenieurholzbau in Forschung und Praxis*, Bruderverlag Karlsruhe, 1982 (German).

[10] Schelling W., Genauere Berechnung nachgiebig verbundener Holzbiegeträger mit dem γ-Verfahren, In: *Festschrift E. Csiesielski*, Werner-Verlag, S. 10, April 1998 (German).

[11] Blaß H. J., Görlacher R., Bemessung im Holzbau – Brettsperrholz: Berechnungsgrundlagen, In: *Holzbaukalender*, Bruderverlag, S. 580-598, 2003 (German).

[12] Kreuzinger H., Platten, Scheiben und Schalen – Ein Berechnungsmodell für gängige Statikprogramme, In: *Bauen mit Holz 1/1999*, 1999 (German).

[13] DIN 1052:2008-12: Entwurf, Berechnung und Bemessung von Holzbauwerken – Allgemeine Bemessungsregeln und Bemessungsregeln für den Hochbau (German).

[14] Bogensperger T., Silly G., Schickhofer G., Comparision of Methods of Approximate Verification Procedures for Cross Laminated Timber, Research Report, holz.bau forschungs gmbh, 2012.

[15] Mestek P., *Punktgestützte Flächentragwerke aus Brettsperrholz (BSP) – Schubbemessung unter Berücksichtigung von Schubverstärkungen*, Dissertation TU München, 2011 (German).

[16] Winter S., Kreuzinger H., Mestek P., *Holzbau der Zukunft: Teilprojekt 15 – Flächen aus Brettstapeln, Brettsperrholz und Verbundkonstruktionen*. Reihe Holzbauforschung, Band H 007/15, ISBN 978-3-8167-7875-2, 2009 (German).

[17] European Technical Approval ETA-08/0242, Deutsches Institut für Bautechnik, 11.3.2009.

[18] Allgemeine bauaufsichtliche Zulassung Z-9.1-559, Deutsches Institut für Bautechnik, 5.2.2008 (German).

[19] Allgemeine bauaufsichtliche Zulassung Z-9.1-680, Deutsches Institut für Bautechnik,

10.1.2007 (German).

[20] Guggenberger W., Moosbrugger T., *Mechanics of Cross-Laminated Timber Plates under Uniaxial Bending*, WCTE 2006, 9th World Conference on Timber Engineering, 2006.

[21] Moosbrugger T. Elastomechanik von Stäben mit komplexem Querschnittsaufbau und verallgemeinerter Querschnittskinematik, Dissertation, Graz University of Technology, 2013 (German)

[22] Allgemeine bauaufsichtliche Zulassung Z-9.1-721, Deutsches Institut für Bautechnik, 30.9.2008 (German).

[23] European Technical Approval ETA-11/0189, Deutsches Institut für Bautechnik, 10.6.2011.

[24] Bogensperger T., Moosbrugger T., Silly G., *Verification of CLT-plates under loads in plane,* WCTE 2010, 11th World Conference on Timber Engineering, Riva del Garda, 2010.

[25] Silly G., *Numerische Studien zur Drill- und Schubsteifigkeit von Brettsperrholz (BSP)*, Diploma Thesis, Graz University of Technology, 2010 (German).

[26] Feichter I., *Spannungs- und Traglastberechnungen an ausgewählten Problemen der Holz-Massivbauweise in Brettsperrholz (BSP)*, Master Thesis, Graz University of Technology, 2013 (German).

[27] Frangi A., Fontana M., Hugi E., Jöbstl R. A., Experimental analysis of cross-laminated timber panels in fire. *Fire Safety Journal*, 44:1078–1087, 2009; DOI: 10.1016/j.firesaf.2009.07.007

[28] Jöbstl R. A., Bogensperger T., Moosbrugger T., Schickhofer G., *A contribution to the Design and System Effect of Cross Laminated Timber (CLT)*, CIB-W18, 39-12-4, Florence, 2006.

[29] Halili Y., *Versuchstechnische Ermittlung von Querdruckkenngrößen für Brettsperrholz*, Diploma Thesis, Graz University of Technology, 2008 (German).

[30] Salzmann C., *Ermittlung von Querdruckkenngrößen für Brettsperrholz (BSP)*, Master Thesis, Graz University of Technology, 2010 (German).

[31] Serrano E., Enquist B., *Compression strength perpendicular to grain in cross-laminated timber (CLT)*, WCTE 2010, 11th World Conference on Timber Engineering, Riva del Garda, 2010.

[32] Bogensperger T., Augustin M., Schickhofer G. , *Properties of CLT-Panels Exposed to Compression Perpendicular to their Plane*, CIB-W18, 44-12-1, Alghero, 2011.

[33] Blaß H. J., Flaig M., Stabförmige Bauteile aus Brettsperrholz, *Karlsruher Berichte zum Ingenieurholzbau Band 24*, ISBN 978-3-86644-922-0, 2012 (German).

[34] Jöbstl R. A., Praxisgerechte Bemessung von Brettsperrholz. In: *Ingenieurholzbau – Karlsruher Tage 2007*, 50-61, 2007 (German).

[35] Thiel A., Schickhofer G., Design Methods of Cross Laminated Timber concerning Floor Vibrations: A Comparability Study, Research Report, holz.bau forschungs gmbh, 2012.

[36] Gagnon S., Pirvu C. (editors), *CLT Handbook: cross-laminated timber*, Library and Archives Canada Cataloguing in Publication, Canadian Edition 2011.

[37] Smith A. L., Hicks S. J., Devine P. J., *P354: Design of Floors for Vibration: A new Approach*, (Revised Edition, February 2009), Ascot 2009.

[38] Petersen C., *Dynamik der Baukonstruktionen*, Friedr. Vieweg & Sohn Verlagsgesellschaft mbH, Braunschweig / Wiesbaden, 2000 (German).

[39] Lignum Holzwirtschaft Schweiz (editor), *Holzbau: Bemessungsbeispiele zur Norm SIA 265*, Schweiz 2003 (German).

[40] Fitz M., *Untersuchung des Schwingverhaltens von Deckensystemen aus Brettsperrholz (BSP)*, Diploma Thesis, Graz University of Technology, 2008 (German).

[41] Zimmer S., *Ein Beitrag zur Aufarbeitung der Schwingungsthematik für die Holz-Massivbauweise in Brettsperrholz*, Master Thesis, Graz University of Technology, 2013 (German).

Design concept for CLT - reinforced with self-tapping screws*

Peter Mestek

Dr.-Ing., Structural Engineer

Sailer Stepan und Partner GmbH

Munich, Germany

Philipp Dietsch

Dr.-Ing., Research Associate, Academic Director

Lehrstuhl für Holzbau und Baukonstruktion, TU München

Munich, Germany

Summary

Concentrated loads on Cross Laminated Timber elements (CLT) in areas of point supports or load applications cause high local shear stresses. Inclined self-tapping screws with continuous threads have turned out to be an effective reinforcement. As neither the German design standard DIN 1052 [2] nor technical approvals cover this construction method a research project funded by the AiF [3] was conducted to gather basic information for its application. These basics include the determination of shear stresses next to concentrated loads, the interaction of compression perpendicular to the grain and rolling shear stresses as well as theoretical and experimental examinations of the load bearing behaviour of reinforced CLT-elements. This paper presents the main research results. A design concept validated by means of the test results is proposed [4].

1. Introduction

Ceilings of CLT are generally simply supported on two sides so that uniaxial load transfer is activated parallel to the lamellas of the top layers. Due to the composition of the CLT-elements, with an orthogonally alternating orientation of neighbouring board layers, the slabs are also suitable for constructions with point supports. These systems profit from the biaxial load transfer and the possibility of the prefabrication of large-scale elements.

Concentrated loading causes high shear stresses in these areas (Fig. 1). Since the rolling shear capacity of timber is considerably lower than its shear capacity parallel to the grain, shear-fracture appears in the cross layers of CLT elements. First tests within the scope of pilot projects revealed that reinforcement with inclined self-tapping screws noticeably enhance the shear capacity of the CLT-elements [5]. As this reinforcement is not covered by the current design standards, a research project funded by the AiF [3] was conducted to gather basic information for their application.

* The contents of the paper have first been presented at the CIB W18 Meeting 2011 in Alghero, Italy [1]

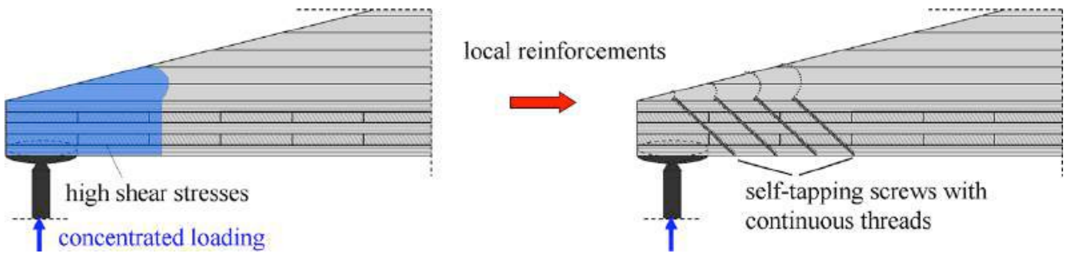

Fig. 1 Local reinforcement by self-tapping screws with continuous threads

2. Experimental tests

Within the scope of the project various experimental tests were carried out. Some small-scale tests were necessary to determine material and system parameters for the FEM-simulations carried out in parallel. Tests with CLT-elements supplied basic information for the interaction of rolling shear and compression perpendicular to the grain as well as for the load bearing behaviour and the strengthening effect of CLT-elements reinforced by self-tapping screws.

2.1 Material and fabrication

The cross section of the test specimens consisted of seven layers, the total thickness of the elements was 119 mm (7 x 17 mm) and 189 mm (7 x 27 mm). The base plates were built up of spruce boards of grade S10 (visual grading according to DIN 4074-1 [6]) that were not glued along their edges. The density of the boards for the cross layers ranged between 440 kg/m^3 and 480 kg/m^3. Due to the fabrication process by vacuum gluing, the lamellas of the test series “Type 119” and “Type 189” had relief grooves parallel to the grain as shown in Fig. 2.

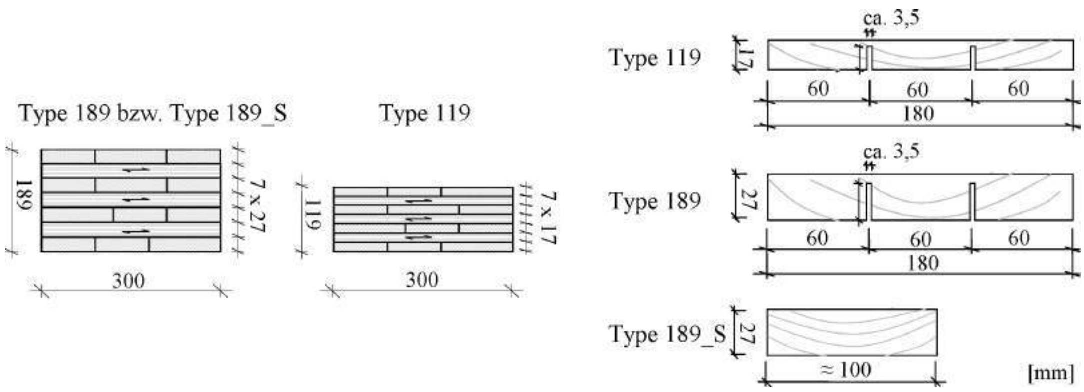

Fig. 2 Cross sections and dimensions of the single boards

2.2 Interaction of rolling shear stresses and compression perpendicular to the grain

Concentrated loading in CLT elements causes a combination of high shear stresses and compression perpendicular to the grain (Fig. 3). The positive effect of compression on the shear capacity parallel to the grain is an established fact and has been the object of various investigations [7], [8]. However, comparable evaluations concerning the interaction of rolling shear strength and compression perpendicular to the grain are not yet available. Hence experimental tests were carried out to gather first information on the increase in rolling shear capacity due to this stress interaction. Therefore shear elements inclined against the vertical by 10° were stressed by a shear force. The shear force was induced into the layers parallel to the primary direction (Fig. 4). The initiation of the compression was developed by lateral steel profiles (HEA 100) coupled with exterior rods. The rods in combination with the head plates and the impression cylinder enabled the initiation of a specific compression that could be controlled by the load cell. Friction minimizing teflon plates between the test specimens and the steel profiles avoided any transfer of shear forces by the framework and guaranteed free shear deformation of the test samples. The base elements had a width of 300 mm. As shown in Fig. 4, five base elements of each section type were separated into three test specimens. To minimize the variation of the results, one test specimen per base element was assigned to each test series. In order to determine a reference value one series (i = 0) of each section type was tested without external pre-stressing.

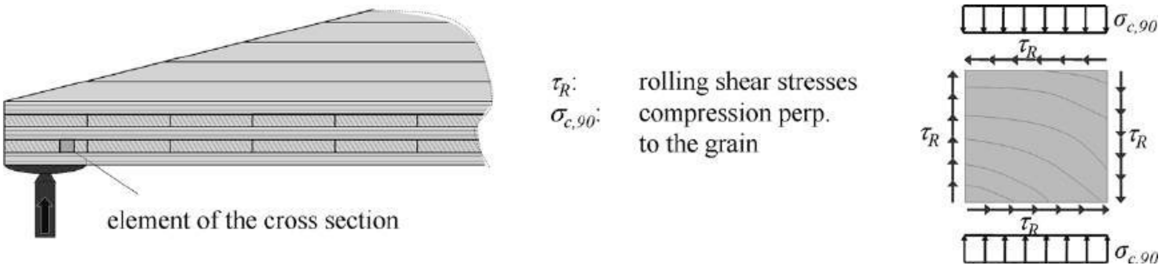

Fig. 3 Interaction of rolling shear and compression perp. to the grain caused by concentrated loading

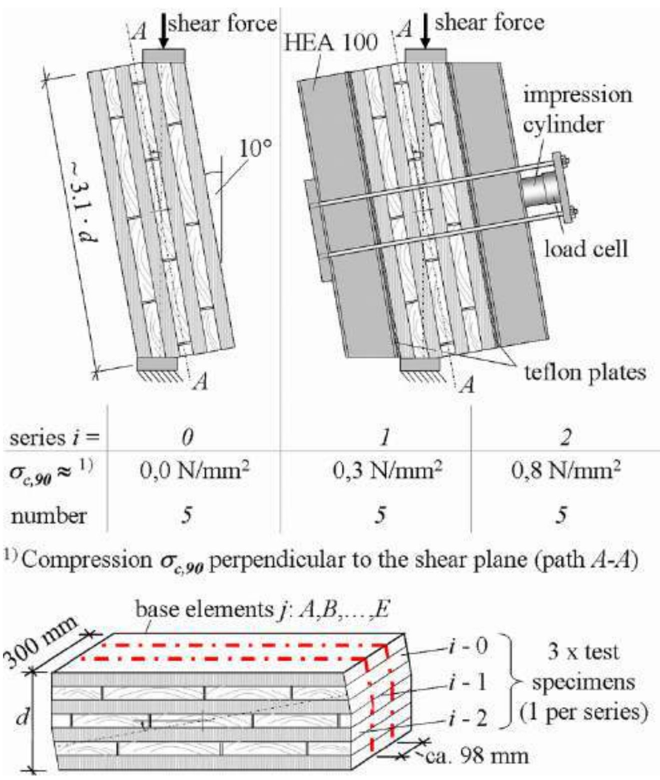

Fig. 4 Test configuration

The simulation of the test configuration by using an FEM-shell-model [9] shows that due to the inclined load initiation compression perpendicular to the shear plane is mainly located in the boundary region (Fig. 5). Because of its rapid decrease it was neglected in the course of further evaluations. The force component parallel to the shear plane causes an almost constant distribution of rolling shear stresses and so the rolling shear capacity was calculated on the assumption of a constant stress distribution. The mean values in Tab. 1 indicate that not only the material but also the geometric relations of the board dimensions, particularly the arrangements of the relief grooves, influence the level of resistance. It appeared that the smaller the ratio of the distance between the gaps or relief grooves to the thickness of the layers, the smaller the rolling shear capacity.

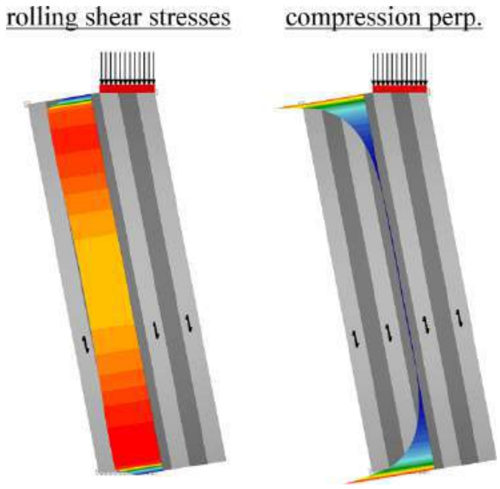

Fig. 5 Distribution of stresses

Tab. 1 Mean values of the rolling shear capacity

Elements		Type 119-*i*		Type 189-*i*		Type 189_S-*i*	
Series *i*	$\sigma_{c,90}$ [N/mm²]	$f_{R,mean,i}$ [N/mm²]	*COV* [-]	$f_{R,mean,i}$ [N/mm²]	*COV* [-]	$f_{R,mean,i}$ [N/mm²]	*COV* [-]
$i = 0$	0,00	1,47	0,08	0,90	0,09	1,42	0,06
$i = 1$	≈ 0,30	1,52	0,07	1,10	0,09	1,61	0,04
$i = 2$	≈ 0,80	1,84	0,07	1,27	0,06	1,83	0,04

As the reference for comparison was from tests without external pre-stressing, the main focus was directed to the increase of the strength and not on the value of the rolling shear strength itself. The increase in the rolling shear capacity can be described by the parameter, $k_{R,90}$, according to equation (1). The evaluation was carried out separately for each base element to minimize the influence of the material properties.

$$k_{R,90} = \frac{f_{R,i,j}}{f_{R,i=0,j}} \qquad \text{with} \quad i = 1,\, 2 \text{ and } j = A, \ldots, E \text{ (see Fig. 4)} \tag{1}$$

The chart in Fig. 6 illustrates the evaluation of the parameter $k_{R,90}$ according to equation (1) and the corresponding regression curves of each element type. It appears that the ratio of the distance between the gaps to the thickness of the layer affects the parameter $k_{R,90}$ as well. Nevertheless it does not seem useful to consider this geometrical ratio within a practical design concept, since the influence of the ratio on the resistance is already taken into account by the characteristic rolling shear capacity in the technical approvals. In addition the design engineer generally does not know the exact dimension of the boards and even less the arrangement of the relief grooves. So, for the final proposal, the parameter $k_{R,90}$ was derived on the basis of a regression curve including all results without differentiation of the element types (Fig. 7). It represents a conservative criterion for the stress interaction that allows a maximum increase of 20 % of the rolling shear capacity. The parameter $k_{R,90}$ should be applied within the stress verification as shown in the following equations:

$$\tau_{R,d} \le k_{R,90} \cdot f_{R,d} \qquad \text{with} \quad k_{R,90} = \min \begin{cases} 1 + 0{,}35 \cdot \sigma_{c,90} \\ 1{,}20 \end{cases} [-] \quad \text{and } \sigma_{c,90} \text{ in N/mm}^2 \qquad (2) \text{ and } (3)$$

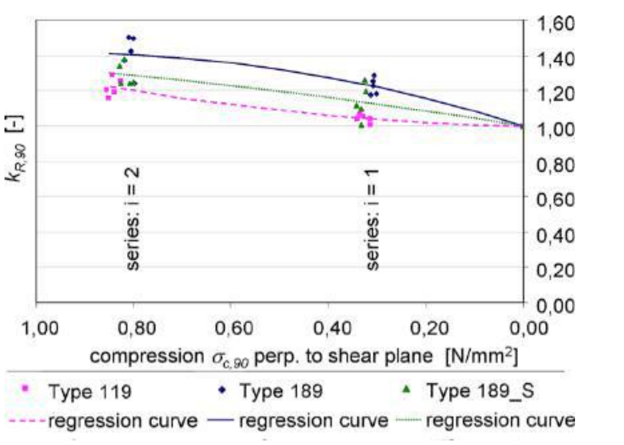

Fig. 6 Evaluation of kR,90 for each element type

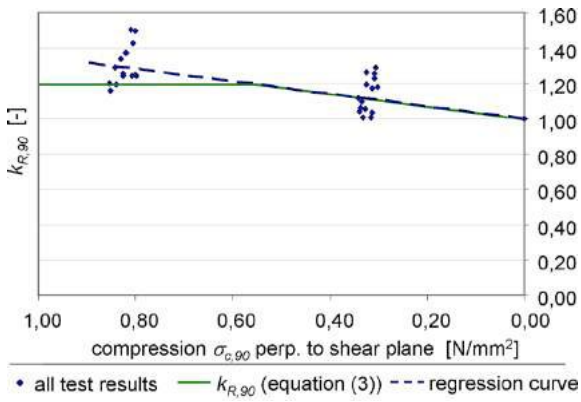

Fig. 7 Proposal for the calculation of kR,90

2.3 Reinforcement – uniaxial load transfer

The load bearing behaviour of reinforced CLT elements was analysed by means of various test configurations. Tests with shear elements that were inclined against the vertical by 10° (analogous to Fig. 4, without pre-stressing) are described and evaluated in [3]. In addition the following four-point-bending tests according to CUAP 03.04/06 [10] were carried out. The test configuration and main dimensions are shown in Fig. 8. First one unreinforced series of each element type was tested to determine a reference value of the rolling shear capacity. Tab 2 contains the calculated mean and characteristic values. Then the elements of the remaining series were reinforced with self-tapping screws with continuous threads (Spax-S [11], d = 8,0 mm).

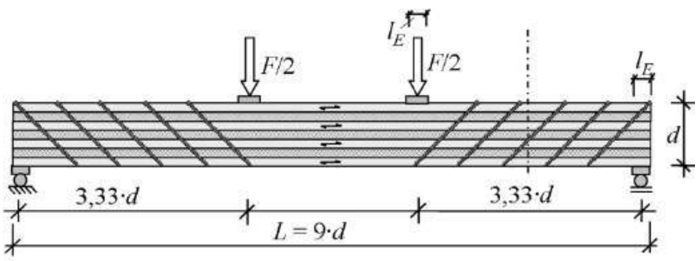

	d	L	l_E	width b	
Type 119	119	1070	50	300	[mm]
Type 189 / 189_S	189	1700	80	300	[mm]

Fig. 8 Configuration of four-point-bending tests

Tab. 2: Rolling shear capacity of the unreinforced elements

Element Type	Type 119	Type 189	Type 189_S	
$f_{R,mean,0}$	1,35	0,97	1,34	[N/mm²]
$f_{R,k,0}$	1,13	0,77	1,08	[N/mm²]
$f_{R,k}$ (acc. to abZ)	0,70	0,70	0,70	[N/mm²]

The primary criterion to describe the influence of the reinforcement on the structural behaviour is the strengthening factor $\eta_{mean,i}$. It is defined by the ratio of the proof loads of the reinforced elements to the proof loads of the unreinforced reference series:

$$\eta_{mean,i} = \frac{F_{mean,i}}{F_{mean,0}} \quad \left(= \frac{F_{mean,\,reinforced\ specimens}}{F_{mean,\,unreinforced\ specimens}} \right) \tag{4}$$

Tab. 3 to Tab. 5 give a general view of the tested arrangements of screws for each element type and also contain the strengthening factor $\eta_{mean,i}$, calculated on the basis of the test results. Each series consisted of five test specimens. The results reveal that the application of screws increases the load-carrying capacity by up to 64 %. Even comparatively few screws cause an increase of more than 25 %. So the structural behaviour is affected positively by a growing number of screws. Consequently the failure mode changes and the elements partially fail by bending and not by shear fracture.

Tab. 3: Type 119 – $\eta_{mean,i}$

Arrangement of the screws (d = 8,0 mm) in mm	Type	$\eta_{mean,i}$ [-]	COV [-]
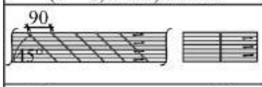	119-1	**1,25**	0,03
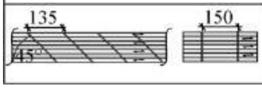	119-2	**1,30**	0,09

Tab. 4: Type 189 – $\eta_{mean,i}$

Arrangement of the screws (d = 8,0 mm) in mm	Type	$\eta_{mean,i}$ [-]	COV [-]
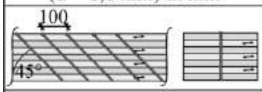	189-1	**1,31**	0,05
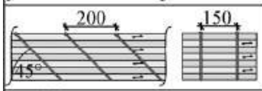	189-2	**1,38**	0,06
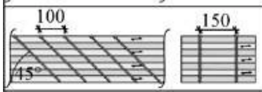	189-3	**1,64**	0,08
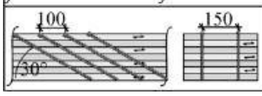	189-4	**1,59**	0,04

Tab. 5: Type 189_S – $\eta_{mean,i}$

Arrangement of the screws (d = 8,0 mm) in mm	Type	$\eta_{mean,i}$ [-]	COV [-]
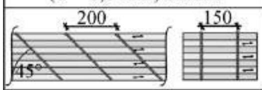	189_S-2	**1,34**	0,02
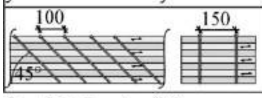	189_S-3	**1,46***	0,10*

*partially bending failure

2.4 Reinforcement – biaxial load transfer

Shear tests with plate elements were carried out to gain preliminary experience with reinforcement by self-tapping screws under biaxial load transfer. Plate elements supported along all sides and stressed by concentrated loading as well as elements with point supports in the corner regions were used according to the configurations shown in Fig. 10. A first test revealed intense indentations in the area of loading (Fig. 9). As a consequence, self-tapping screws, under the steel plates of the load application and at the point supports, were applied vertically to serve as reinforcement. Further information on this kind of reinforcement is given in [12].

Fig. 9 Intense indentations in the area of the load application

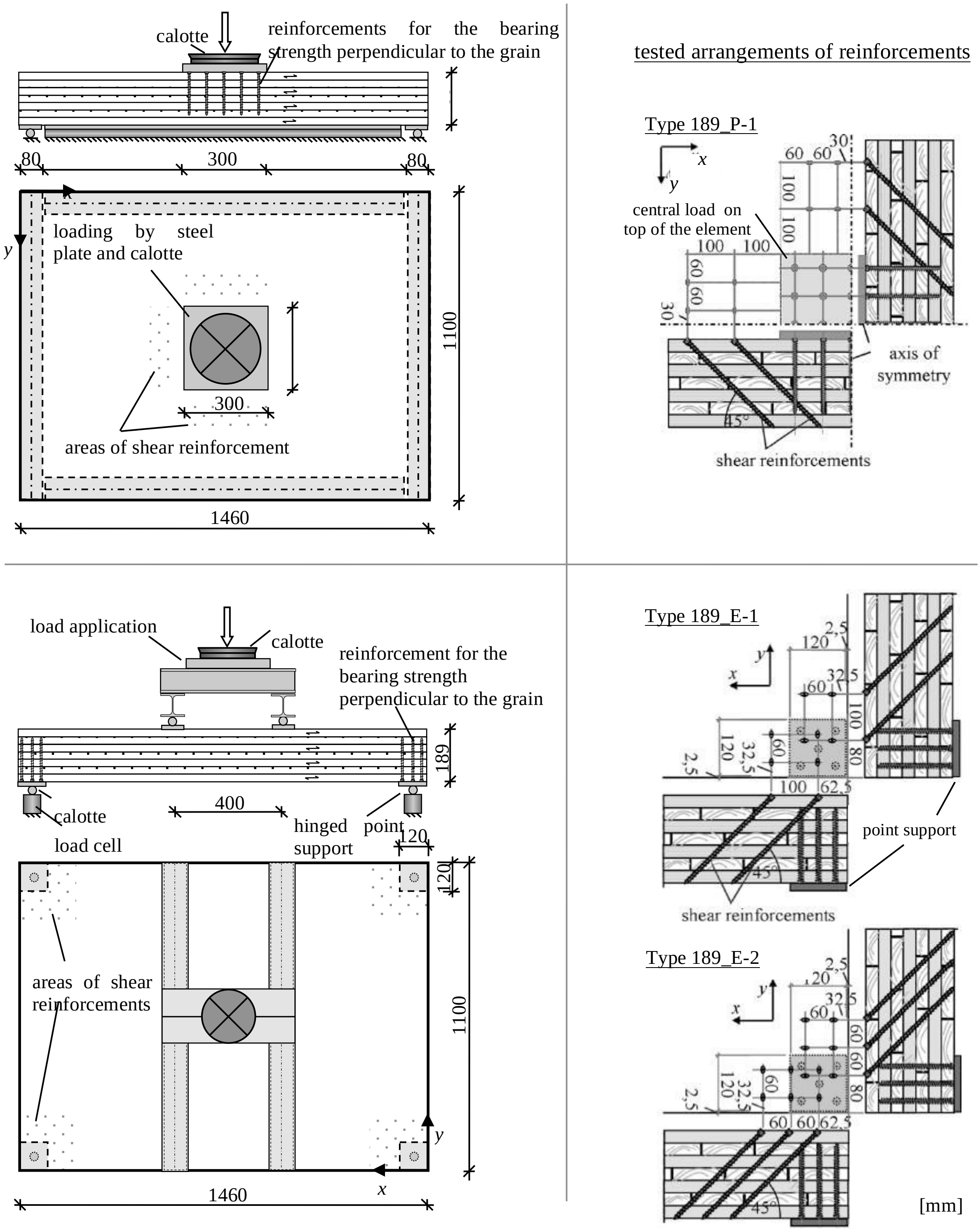

Fig. 10 Test configurations and arrangements of reinforcement

One unreinforced series of each configuration was tested to determine the reference values of the shear capacity. Then the series of reinforced elements shown in Fig. 10 were carried out. The series “Type 189_E-2” consisted of two, all others of three test specimens. Table 6 shows the strengthening factors $\eta_{mean,i}$ calculated by means of the proof loads according to equation (1) analogous to the tests on beam elements. The increase in load-carrying capacity ranged between 26 % and 49 %.

Tab. 6 Mean values of proof loads and strengthening factor ηmean,i

test configuration	central load Type 189_P-i		point support in corner region Type 189_E-i		
series i =	0 (unreinforced)	1 (reinforced)	0 (unreinforced)	1 (reinforced)	2 (reinforced)
mean value of proof loads $F_{mean,i}$ [kN]	381,1	479,4	304,9	409,7	455,6
COV [-]	0,05	0,02	0,04	0,05	0,01
strengthening factor $\eta_{mean,i}$ [-]	-	**1,26**	-	**1,34**	**1,49**

Due to the biaxial load transfer it is not possible to analytically calculate the rolling shear capacity by means of the proof loads. FEM-simulations were necessary to evaluate the rolling shear stresses at the time of failure. The simulations were done with the program ANSYS [13] using a solid model taking into account the symmetrical conditions (Fig. 11). The rolling shear stresses determined by the simulations exceed the rolling shear capacity according to the four-point-bending tests by up to 70 %. Further examinations revealed that this cannot be explained only by the stress interaction. Hence it may be assumed, that in case of biaxial load transfer additional effects like dispersion and redistribution of stresses or dowelling effects caused by less stressed areas get activated and thus lead to these comparatively high strength values.

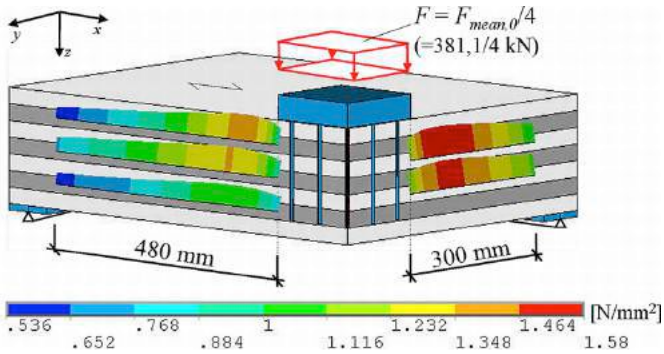

Fig. 11 Distribution of rolling shear stresses of the series "Type 189_P-0" (unreinforced element)

3. Calculation of internal forces and stresses

In contrast to simply supported CLT slabs with uniformly distributed loads there are no calculation toolkits or design charts for constructions with point supports or concentrated loads available that guarantee a cost-effective and safe design. In the case of shear-design it is first of all necessary to evaluate the distribution of shear forces in primary and secondary supporting direction to be able to calculate the critical shear stresses. Hence different influencing factors concerning the distribution of shear forces were examined by means of a parametric study in order to find an approach for the simple estimation of shear stressing. The calculations of this study were carried out using girder-grid-models in order to avoid stress peaks caused by concentrated loads and to minimize the computational effort. The required stiffnesses were calculated according to annex D.3 of the German design code DIN 1052 [2] using the material constants of boards of the strength class C 24.

Different influencing variables concerning the distribution of shear forces were evaluated. Detailed descriptions can be found in [3] and [4]. The significant variables and considered limits were:

- Thickness d of the elements: $0{,}10\ \text{m} < d < 0{,}22\ \text{m}$
- Ratio of the spans l/b: $1 < l/b < 3$
- Number of layers n: $5 < n < 11$
- Square support (Fig. 13/14) $b_{A,x} = b_{A,y}$

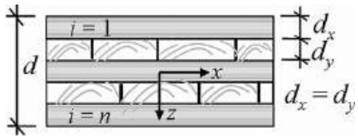

Fig. 12 Examined section type

The following structural systems were analysed:

- Central point support respectively concentrated loading
- Point support in the corner region

The results reveal that in the analysed systems the distribution of shear forces is predominantly influenced by the number of layers. Other parameters, like the ratio l/b of the element dimensions or its thickness can be neglected. So the shear force in the primary direction can be calculated by applying the following equations and the shear force in the secondary direction by the equilibrium of the forces.

- Central point support / concentrated loading (Fig. 13): $V_{xz} \approx 0{,}33 \cdot n^{-0{,}1} \cdot F_k$ (5)
- Point support in the corner region (Fig. 14): $V_{xz} \approx 0{,}67 \cdot n^{-0{,}1} \cdot F_k$
  (6)

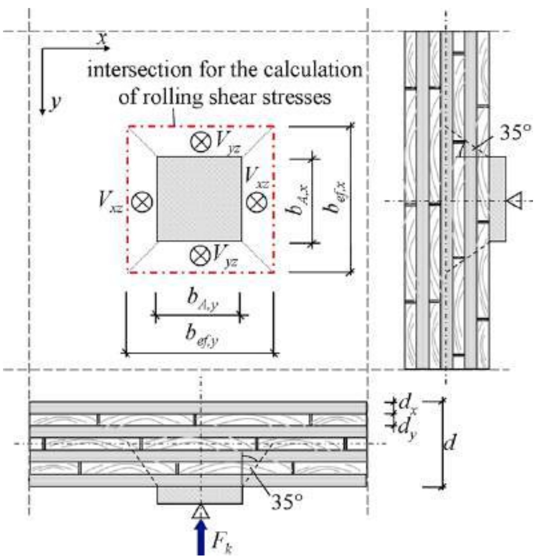

Fig. 13 Central point support / concentr. loading

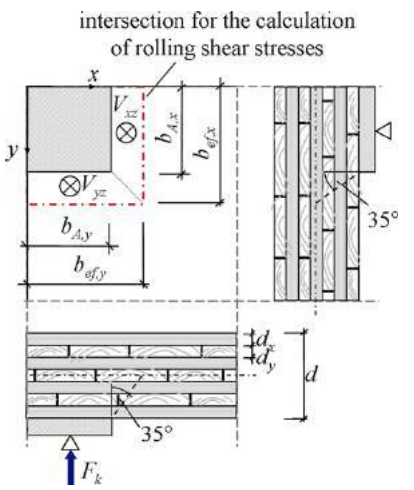

Fig.14 Point support in the corner region

The calculation of the rolling shear stresses along the edges of the support leads to conservative but inefficient results. Hence different approaches of the load distribution were analysed by FEM-simulations using solid models [4]. It appeared that for the analysed systems and conditions the load distribution can be assumed at an angle of 35° to the centre line of the CLT elements. So the governing rolling shear stresses can be calculated by using the effective width shown in Fig. 13 and Fig. 14.

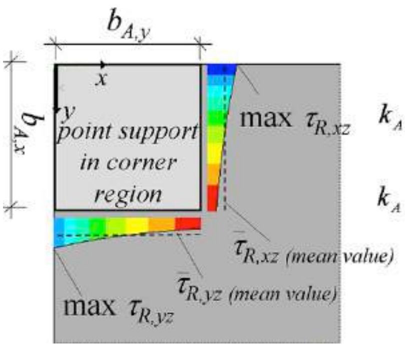

$$k_A = \frac{\max \tau_{R,xz}}{\bar{\tau}_{R,xz}} \quad (7)$$

$$k_A = \frac{\max \tau_{R,yz}}{\bar{\tau}_{R,yz}} \quad (8)$$

Fig. 15 Distribution of stresses

In addition the simulations show that there is a relatively constant distribution of shear stresses along the edges of central point supports. In contrast to this an increase of shear stresses in direction of the edges can be observed along the support edges of point supports in the corner regions (Fig. 15). This increase is according to the calculations in [4] more distinctive with growing ratio of the width of the supports to the thickness of the element. But the analyses of the effective width were based on the assumption that there is a constant distribution of shear stresses. Therefore it was necessary to determine a parameter k_A that considers the increase mentioned. Taking all results into account the rolling shear stresses can be calculated by the following simplified equations:

$$\tau_{R,xz} = \frac{V_{xz} / b_{ef,x}}{k_{R,x} \cdot (d_x + d_y)} \cdot k_A \quad (9)$$

$$\tau_{R,yz} = \frac{V_{yz} / b_{ef,y}}{k_{R,y} \cdot (d_x + d_y)} \cdot k_A \quad (10)$$

Tab. 7 Parameter kR,x and kR,y [-]

number of layers n	5	7	9	11
$k_{R,x}$	2,00	2,50	3,33	3,89
$k_{R,y}$	1,00	2,00	2,50	3,33

Tab. 8 Parameter kA [-]

ratio of $b_{A,x}/d$ or $b_{A,y}/d$		≤ 1,0	≤ 1,5	≤ 2,0
point support in corner region	k_A=	1,35	1,50	1,65
central point support / concentrated loading	k_A=	1,00		

The equations can also be used for beam elements under uniaxial load transfer. In this case the effective width corresponds with the width of the beam and k_A is k_A = 1,0.

<u>Note:</u> In the equations (9) and (10) there is no differentiation of the shear forces of plane A and B according to the shear analogy (annex D.3 of DIN 1052 [2]), because this simplified assumption was taken as the basis within the determination of the effective width.

4. Design concept

The FEM-models described in [3] and [4] on the basis of shell or volume elements are mainly suited for academic research or the analysis of special constructional details. But these simulations are comparatively complex and error-prone because of the great number of input parameters. For a general design concept it makes more sense to use a strut and tie model, which describes the structural behaviour of the composite section of CLT and self-tapping screws in a simplified manner. So it needs considerably fewer input parameters.

The following conditions, for limits of application, were defined to guarantee the verification by the results of the experimental tests and to realize a practical design concept.

- Symmetrical cross section
- Inclination of 45° of the screws
- Arrangements of the screws according to Fig. 16

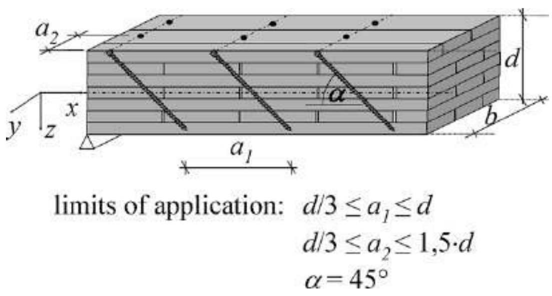

Fig. 16 Arrangements of the screws

4.1 Uniaxial load transfer

According to this design concept the load-carrying capacity under shear stresses of reinforced CLT elements is composed of the rolling shear capacity of the cross layer itself and the proportionate load-carrying capacity of the screws. The assumption of this simultaneous effect is justified, because the experimental tests show that, despite the small shear deformation of the CLT elements, tension forces are activated in the screws. For the calculation of the proportionate load-carrying capacity of the screws, the model shown in Fig 17 can be used. The screws, symbolised by the diagonal struts, bear forces parallel to the shear plane. Due to the fact, that it is mainly a shear model the influence of bending is neglected. The screws in tension additionally cause compression perpendicular to the shear plane which affects the rolling shear capacity positively. In Fig. 17, springs symbolize the transfer of the compression forces. The influence of the stress interaction is considered by the parameter $k_{R,90}$ determined in chapter 2.2.

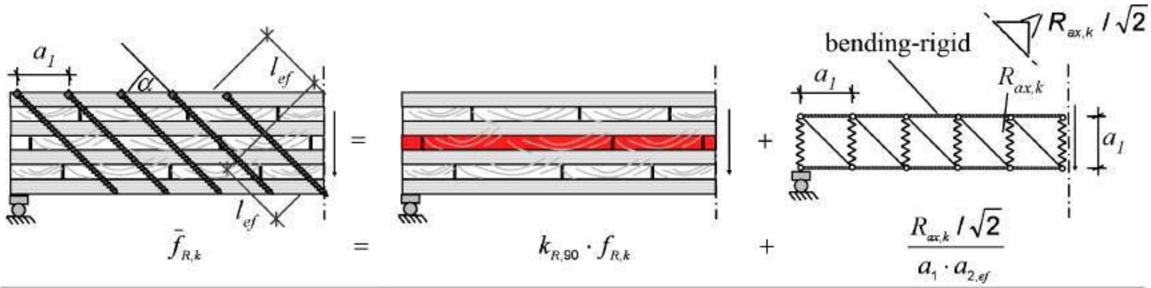

$\bar{f}_{R,k}$	charact. load-carrying capacity of the reinforced CLT under shear stresses	[N/mm²]
$f_{R,k}$	charact. rolling shear capacity (according to technical approvals)	[N/mm²]
$R_{ax,k}$	charact. load-carrying capacity of a screw parallel to its axis	[N]
a_1	distance of the screws parallel to the load bearing direction	[mm]
$a_{2,ef}$	effective distance of the screws perpendicular to the load bearing direction	[mm]
l_{ef}	effective embedment length of the screws for the calculation of $R_{ax,k}$	[mm]
$k_{R,90}$	parameter for the consideration of the stress interaction	[-]

Fig. 17 Design concept on the basis of a strut and tie model

In this case the capacity of the screws is essentially dependent on their withdrawal strength. Universal equations for its calculation are currently not available for an inclination of 45°. However, the investigations within this research project revealed that on the basis of the result of BLAß & UIBEL [14] the withdrawal strength $R_{ax,k}$ of the screws can be calculated approximately according to equation (11).

$$R_{ax,k} = \min\begin{cases} 24{,}8 \cdot d^{0{,}8} \cdot \ell_{ef}^{0{,}9} \\ R_{t,u,k} \end{cases} \quad [\mathrm{N}] \tag{11}$$

d	diameter of the screws in mm
l_{ef}	effective embedment length of the screws in mm
$R_{t,u,k}$	tensile capacity (according to technical approvals)

The effective embedment length l_{ef}, according to equation (12) is dependent on the position of the layer. It results from the minimal penetration length of the screws, based on the centre line of the decisive layer. Fig. 18 shows typical geometric relations.

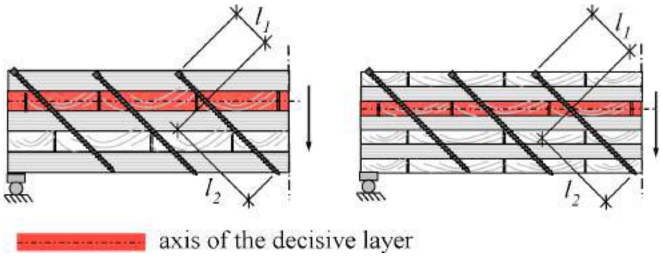

$$l_{ef} = \min\begin{cases} l_1 \\ l_2 \end{cases} \tag{12}$$

Fig. 18 Definition of the effective embedment length l_{ef} of the screws

The compression perpendicular to the grain should be determined by the vertical force component of the screws and the distances between them. Equation (14) delivers the effective distance $a_{2,ef}$, which is the minimum of the real distance a_2 and the quotient of the element width b and the number of screw lines $n_{\perp}$ perpendicular to the load bearing direction.

$$\sigma_{c,90} = \frac{R_{ax,k} / \sqrt{2}}{a_1 \cdot a_{2,ef}} \qquad \text{with} \qquad a_{2,ef} = \max\begin{cases} a_2 \\ b / n_{\perp} \end{cases} \qquad \text{(13) and (14)}$$

The influence of the stress interaction should be considered by the parameter $k_{R,90}$:

$$k_{R,90} = \min\begin{cases} 1 + 0{,}35 \cdot \sigma_{c,90} \\ 1{,}20 \end{cases} \quad [-] \qquad \text{with } \sigma_{c,90} \text{ in N/mm}^2 \tag{15}$$

This finally leads to the following shear verification for reinforced CLT according to the design model shown in Fig. 17.

$$\tau_{R,d} \le k_{\mathrm{mod}} \cdot \frac{\bar{f}_{R,k}}{\gamma_M} \qquad \text{with} \qquad \bar{f}_{R,k} = k_{R,90} \cdot f_{R,k} + \frac{R_{ax,k} / \sqrt{2}}{a_1 \cdot a_{2,ef}} \qquad \text{(16) and (17)}$$

4.2 Biaxial load transfer

Even unreinforced CLT elements show high compressive stresses perpendicular to the grain in areas of point supports or concentrated loading. So the positive influence of the stress interaction on the rolling shear capacity should be considered in the shear design of CLT elements without reinforcement. The compression $\sigma_{c,90}$ perpendicular to the grain and the governing rolling shear stress $\tau_{R,d}$ have to be determined by capable computation programs. In standard cases the stresses can also be estimated by the effective width $b_{ef,x}$ and $b_{ef,y}$, which result from the load distribution at an angle of 35° to the centre line of the elements (Fig. 19 and Fig. 20).

$$\sigma_{c,90} = \frac{F_k}{b_{ef,x} \cdot b_{ef,y}} \qquad \text{with} \quad F_k\text{:} \quad \text{charact. support force or concentrated load} \tag{18}$$

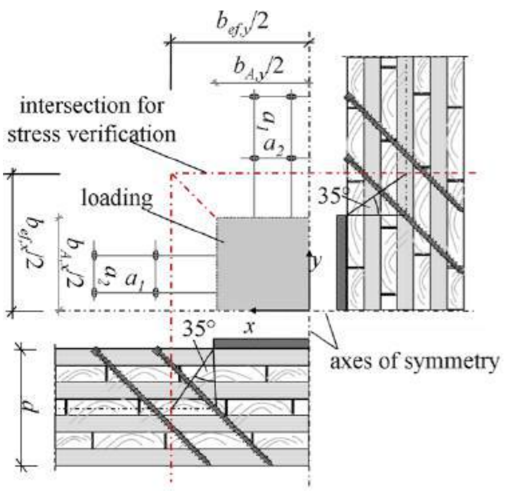

Fig. 19 Central point support / concentr. loading

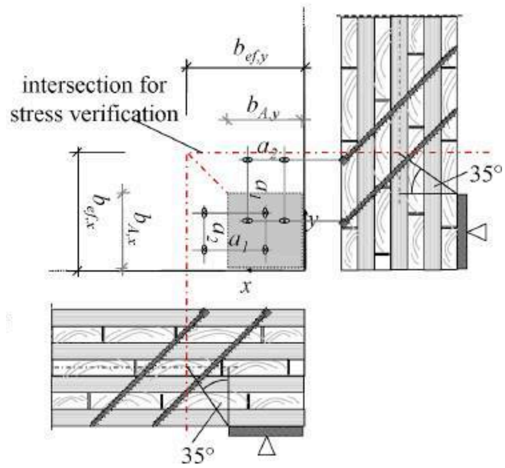

Fig. 20 Point support in the corner region

Again in the course of the stress verification the influence of the stress interaction ought to be considered by the parameter $k_{R,90}$ according to equation (15):

$$\tau_{R,d} \leq k_{\text{mod}} \cdot \frac{k_{R,90} \cdot f_{R,k}}{\gamma_M} \tag{19}$$

The design concept for reinforced CLT elements under biaxial load transfer is also generally based on the strut and tie model for beam elements shown in Fig. 17. However, in this case there is no clearly definable element width. So instead of the beam width b the effective width $b_{ef,x}$ or $b_{ef,y}$ has to be used to determine the effective distance of the screw lines $a_{2,ef}$ perpendicular to the load bearing direction. In primary direction $a_{2,ef}$ is:

$$a_{2,ef} = \max \begin{cases} a_2 \\ b_{ef,x} / n_{\perp} \end{cases} \tag{20}$$

with $n_{\perp}$: number of screw lines $n_{\perp}$ perpendicular to the load bearing direction

The total compression $\sigma_{c,90}$ perpendicular to the grain, needed for the determination of the parameter $k_{R,90}$, is the result of the superposition of the compression components caused by the concentrated loading and vertical force component of the screws:

$$\sigma_{c,90} = \frac{F_k}{b_{ef,x} \cdot b_{ef,y}} + \frac{R_{ax,k} / \sqrt{2}}{a_1 \cdot a_{2,ef}} \tag{21}$$

In the course of the shear verification in equation (22) the shear stress $\tau_{R,d}$, determined on the basis of an unreinforced cross section, has to be compared with the load-carrying capacity of the reinforced elements according to the strut and tie model. Again the rolling shear stresses have to be calculated by capable computation programs or can be estimated by the simplified method using an effective width as described in chapter 3.

$$\tau_{R,d} \leq k_{\text{mod}} \cdot \frac{\bar{f}_{R,k}}{\gamma_M} \quad \text{with} \quad \bar{f}_{R,k} = k_{R,90} \cdot f_{R,k} + \frac{R_{ax,k} / \sqrt{2}}{a_1 \cdot a_{2,ef}} \qquad \text{(22) and (23)}$$

4.3 Verification of the design concept

In order to verify the proposal of the design concept the charts in Fig. 21 contain the characteristic load-carrying capacity according to the strut and tie model as well as the proof loads, the mean values and the 5%-quantile values of the four-point-bending test.

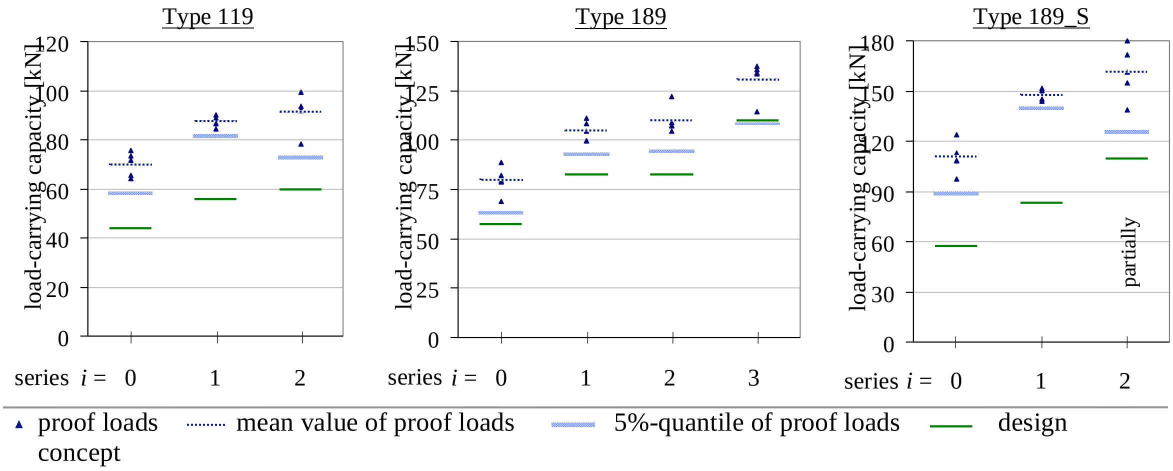

Fig. 21 Comparison of the test results (four-point-bending test) with the design concept

The charts in Fig. 22 show the analogical comparison of the design concept with the results of tests on biaxial load transfer. This time the design concept delivers two components of the load-carrying capacity. Hence the values $F_{max,x,i}$ and $F_{max,y,i}$ indicate the load-carrying capacity according to the strut and tie model in primary and secondary direction. The stresses were calculated according to the simplified method described in chapter 3.

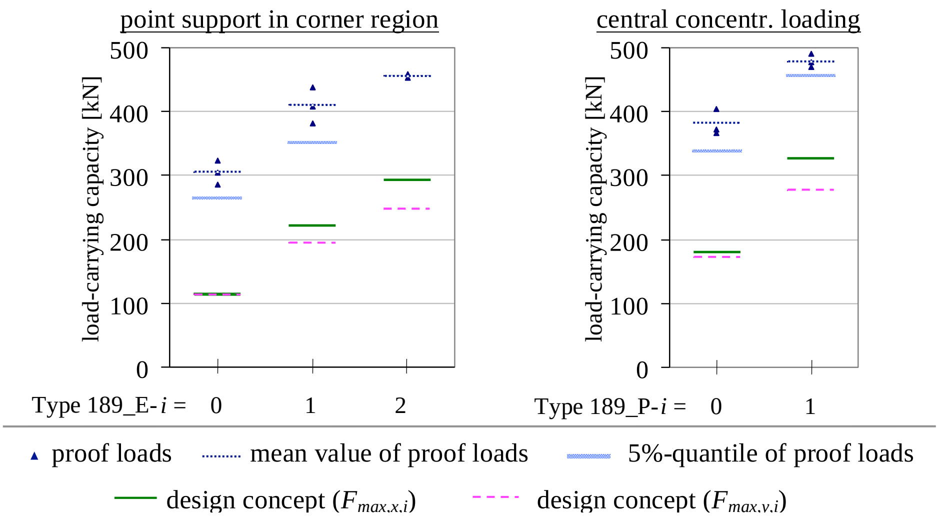

Fig. 22 Comparison of the test results with the design concept – biaxial load transfer

The comparisons verify that the proposed design model represents a conservative approach for the shear design of reinforced CLT. The difference between the values of the design concept and the mean values remains quite constant for each element type. This signifies that the increase in load-carrying capacity, as a result of the reinforcement, is covered fairly well by the design concept. But, especially under biaxial load transfer, the base level, which means the design value of the unreinforced series, is considerably underestimated. This corresponds to the results of the FEM-simulations, which also delivered, for the unreinforced series, considerably higher rolling shear stresses than the rolling shear capacity determined by tests on beam elements under uniaxial load transfer.

5. Conclusion

The results presented in this paper allow the shear design of CLT under concentrated loading, considering reinforcement by inclined self-tapping screws with continuous threads. The main conclusions delivered by the described research project are:

- Concentrated loading in CLT elements causes a combination of high shear stresses and compression perpendicular to the grain. By means of experimental tests, the positive effect of this stress interaction on the rolling shear capacity was verified and a design concept is proposed.
- Self-tapping screws with continuous threads are a simple and efficient reinforcement. They allow a cost-effective shear design of CLT structures, as they can be applied systematically in localised areas with high shear stresses. Thus they increase the load-carrying capacity in the decisive areas. A simplified design concept validated by means of test results is recommended. It is based upon a strut and tie model and can be used for beam elements as well as plate elements under concentrated loading.
- In the case of a biaxial load transfer, additional effects are activated, leading to an increase in the rolling shear capacity compared to that of beam elements. For economic reasons it should be analysed how far the redundant structural behaviour may be considered for the shear verification. One approach might be the use of increased values for the rolling shear capacity in cases of biaxial load transfer.

6. Acknowledgement

The research project was kindly supported by the German Society of Wood Research (DGfH) and the International Association for Technical Issues related to Wood (iVTH). Special gratitude is extended to the German Federation of Industrial Research Associations (AiF) for funding the project with financial means of the German Federal Ministry of Economics and Technology (BMWi).

7. Literature

[1] Mestek, P.; Winter, S.: Design Concept for CLT - reinforced with Self-Tapping Screws. International Council for Research and Innovation in Building and Construction - Working Commission W18 - Timber Structure (CIB-W18); Alghero, Italy, 08/2011.

[2] DIN 1052:2008-12: Entwurf, Berechnung und Bemessung von Holzbauwerken. Allgemeine Bemessungsregeln und Bemessungsregeln für den Hochbau.

[3] Mestek, P.; Winter, S.: Konzentrierte Lasteinleitung in Brettsperrholzkonstruktionen - Verstärkungsmaßnahmen. Schlussbericht zum AiF-Forschungsvorhaben Nr. 15892, TU München, 2011.

[4] Mestek, P: Punktgestützte Flächentragwerke aus Brettsperrholz (BSP) - Schubbemessung unter Berücksichtigung von Schubverstärkungen. Dissertation, TU München, 10/2011.

[5] Colling, F.; Bedö, S.: Prüfbericht Nr.: H06-01/1-ZE-PB; Kompetenzzentrum Konstruktiver Ingenieurbau, Abteilung Holzbau, Fachhochschule Augsburg, unpublished, 2007.

[6] DIN 4074-1:2008-12: Sortierung von Holz nach der Tragfähigkeit – Teil 1: Nadelschnittholz.

[7] Spengler, R.: Festigkeitsverhalten von Brettschichtholz unter zweiachsiger Beanspruchung, Teil 1 - Ermittlung des Festigkeitsverhaltens von Brettelementen aus Fichte durch Versuche. Hrsg.: Laboratorium für den Konstruktiven Ingenieurbau (LKI), Berichte zur Zuverlässigkeitstheorie der Bauwerke H.62/1982.

[8] Hemmer, K.: Versagensarten des Holzes der Weißtanne (Abies Alba) unter mehrachsiger Beanspruchung. Dissertation, TH Karlsruhe, 1984.

[9] Sofistik 2010 Statik. Sofistik AG, Oberschleißheim, 2009.

[10] Common Understanding of Assessment Procedure: “Solid wood slab element to be used as a structural element in buildings”; ETA request No 03.04/06, Austria, 2005.

[11] abZ. Nr. Z-9.1-519 vom 07. Mai 2007; SPAX-S Schrauben mit Vollgewinde als Holzverbindungsmittel; ABC Verbindungstechnik GmbH & Co. KG, Ennepetal, Deutschland; Deutsches Institut für Bautechnik, Berlin, 2007.

[12] Bejtka, I.: Verstärkungen von Bauteilen aus Holz mit Vollgewindeschrauben. Dissertation erschienen in: Karlsruher Berichte zum Ingenieurholzbau 2, Universitätsverlag Karlsruhe, 2005.

[13] ANSYS, Finite Elemente Programm, Release 12.0.

[14] Blaß, H.J.; Uibel, T.: Bemessungsvorschläge für Verbindungsmittel in Brettsperrholz. Bauen mit Holz, Heft 2, 2009.

Joints with Dowel Type Fasteners in CLT Structures

Thomas Uibel

Professor for Timber Structures and Basics of Structural Engineering

Timber Engineering Group, Faculty of Civil Engineering, FH Aachen

Aachen, Germany

Hans Joachim Blaß

Professor for Timber Engineering and Building Construction

Versuchsanstalt für Stahl, Holz und Steine, Karlsruhe Institute of Technology (KIT)

Karlsruhe, Germany

Summary

The load carrying capacity of joints with dowel type fasteners in cross laminated timber (CLT) was the focus of a research project [1], [2], [3] conducted by the authors at Karlsruhe Institute of Technology (KIT). To examine the influence of load duration and climate variation on the load carrying capacity, these studies were complemented by long-term tests with screws in CLT, started in 2007 and finished at the end of 2012.

In this paper the results of embedment tests, withdrawal tests and connection tests are discussed and proposals for the calculation of characteristic values are given. On this basis, calculation models for the load carrying capacity of joints with dowel type fasteners, in the plane side of cross laminated timber and for edge joints, were developed. Furthermore long-term tests with screws are presented.

1. Introduction

Cross laminated timber (CLT) has been used more and more frequently in timber engineering in recent years. Their use in construction requires their connection with each other and with other components of the construction. To that purpose dowel type fasteners can be used. It is possible to position the fasteners perpendicular to the plane of the CLT panels or in the edges (Fig. 1). To calculate the load carrying capacity of dowel type fasteners according to Johansen's yield theory, [4], [5], [6], [7] the yield moment of the fasteners and the embedding strength are needed. The withdrawal strength is necessary to calculate the load carrying capacity of axially loaded screws. In addition, the withdrawal strength is important for estimating the rope effect of laterally loaded connections. In the edges of CLT, the fasteners can be positioned parallel to the grain direction. The embedment strength and the withdrawal strength are also influenced by gaps and grooves.

The aim of the research project at the KIT [1], [2], [3] was to develop proposals for calculating the load carrying capacity of joints with dowel type fasteners in solid wood panels. Furthermore the long-term behaviour of edge joints with self-tapping screws was examined.

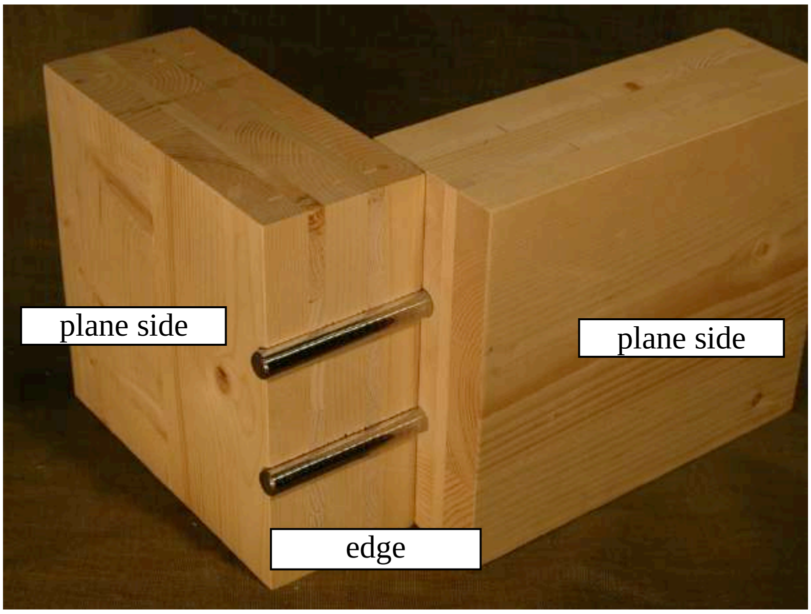

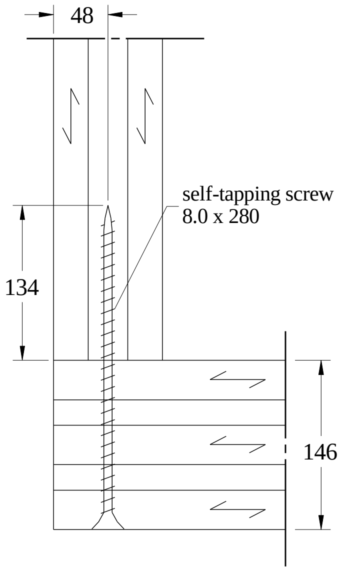

Fig. 1 Opened connection with dowels in cross laminated timber (left), example for an edge joint with self-tapping screws in cross laminated timber (right)

2. Test material

Cross laminated timber panels consist of boards crosswise laminated with a minimum of three layers. Some panels are produced with gaps between the edges of the boards. For these studies CLT made of European spruce (Picea abies) from 4 manufactures with altogether 13 different build-ups were used. For the used products the maximum width of gaps is limited to 6 mm. In addition, grooves with a width of about 2,5 mm are sawn into the boards of some products. Fig. 2 shows cross-sections of different CLT products. Table 1 gives some statistic information about the gaps.

Fig. 2 Cross-sections of panels without and with gaps between boards and grooves

Tab. 1 Width of gaps between boards of one layer for some different products

Manufacturer/product	Build-up	Width (in mm) of gaps in								
		Outer layers			Interlayers			Centre layer		
		mean	max.	95% fractile	mean	max.	95% fractile	mean	max.	95% fractile
1	17-17-17-17-17	0,6	2,1	1,6	1,6	7,3	3,4	1,0	3,0	2,3
2	19-22-19	0,4	2,0	1,3	-	-	-	0,5	2,2	1,8
2	34-13-34-13-34	0,2	1,0	1,0	1,4	6,8	3,3	2,0	6,7	4,5
4	9,5-6,8-9,5-6,8-9,5	0	0	0	0,6	5,4	3,5	0	0	0

The characteristic density (at normal climate, 20°C/65% RH) of cross laminated timber was determined by analysing altogether 2299 test specimens out of a range of products from different manufacturers (Table 2). This revealed a minimum 5th percentile density of 400 kg/m³ for product 2. Taking this result into account, a characteristic density of 400 kg/m³ is proposed for cross laminated timber panels made of European spruce (Picea abies).

Table 3 shows the statistical summary of the density of the specimens for withdrawal tests with self-tapping screws in CLT. Table 4 gives this information for the test specimens of embedment tests with dowel type fasteners positioned in the edges of CLT. This table gives also a comparison between the density of the whole cross section and the density of the relevant layer in which the fastener is positioned.

Tab. 2 Density of cross laminated timber panels at normal climate, 20°C/65% RH

Manufacturer/ product	n	ρ_{mean} kg/m³	ρ_{min} kg/m³	ρ_{max} kg/m³	Coefficient of variation	$\rho_{0,05}$ kg/m³
1	515	470	415	630	5,11 %	430
2	906	437	372	578	6,02 %	400
3	208	458	406	507	5,18 %	423
4	670	459	397	558	5,75 %	419

Tab. 3 Density of the specimens for withdrawal tests with screws in cross laminated timber panels at normal climate, 20°C/65% RH

Manufacturer/ product	Density of the specimen for withdrawal tests							
	Plane side (hole cross section)				Edge (relevant layers)			
	n	ρ_{mean} kg/m³	Coefficient of variation	$\rho_{0,05}$ kg/m³	n	ρ_{mean} kg/m³	Coefficient of variation	$\rho_{0,05}$ kg/m³
1	24	454	4,48 %	423	57	448	8,21 %	374
2	73	426	5,44 %	384	159	404	11,9 %	335
3, 4	22	445	3,34 %	420	52	435	8,29 %	382

Tab. 4 Density of the specimens for embedment tests with dowel type fasteners in the edges of cross laminated timber panels at normal climate, 20°C/65% RH

Manufacturer/ product	n	Density of the whole cross section			Density of the relevant layers		
		ρ_{mean} kg/m³	Coefficient of variation	$\rho_{0,05}$ kg/m³	ρ_{mean} kg/m³	Coefficient of variation	$\rho_{0,05}$ kg/m³
1	184	474	5,76 %	434	481	9,54 %	412
2	292	439	7,65 %	391	417	12,2 %	345
3, 4	233	452	5,55 %	413	461	9,89 %	401

3. Axially loaded self-tapping screws

3.1 Set-up for withdrawal tests

To determine the withdrawal strength of self-tapping screws in CLT 119 tests with screws placed perpendicular to the plane of CLT and 268 tests with screws in the edges of CLT were carried out according to EN 1382 [8]. In the tests the positions of screws were varied, as shown in Fig. 3 and 4. In the plane side they were positioned in areas without gaps (position 1.1) and placed in gaps (position 1.2 to 1.4). Screws driven perpendicular (position C) and parallel (positions A, B) to the grain were considered in the edge withdrawal tests. Furthermore, tests with screws placed in gaps (positions B.1, B.2) were taken into consideration to derive the withdrawal capacity.

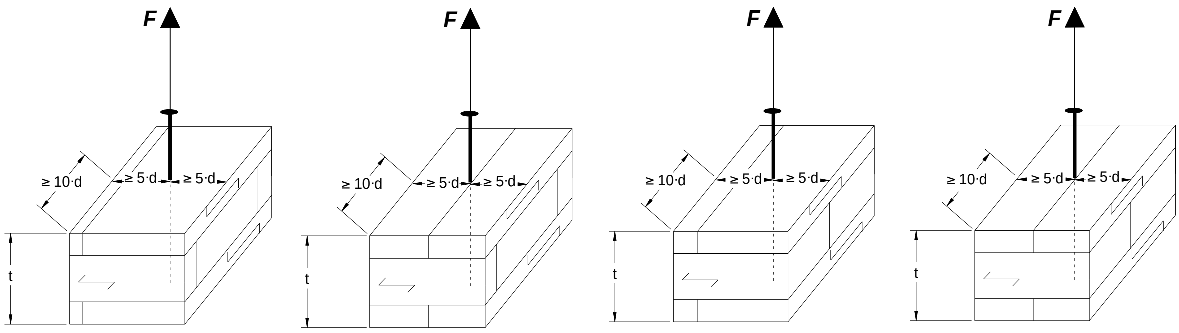

Position 1.1 1.2 1.3 1.4

Fig. 3 Set-up for withdrawal tests with screws positioned perp. to the plane of CLT

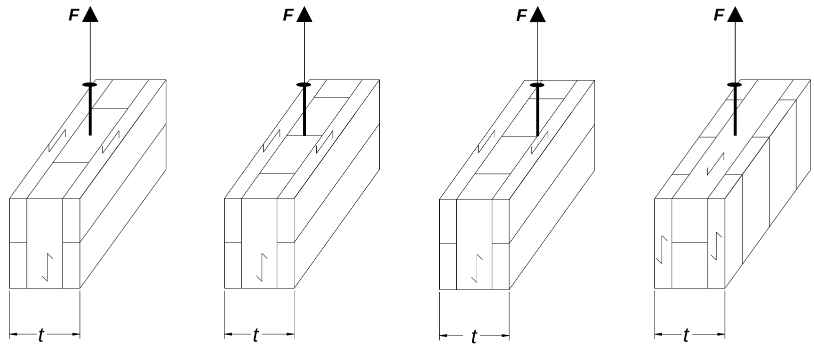

Position A B.1 B.2 C

Fig. 4 Set-up for edge withdrawal tests with screws in CLT

3.2 Results of withdrawal tests

The best correlation between test results and predicted values can be achieved if the withdrawal capacity of self-tapping screws in CLT is calculated according to the following expression:

$$R_{ax,s,pred} = \frac{0,44 \cdot d^{0,8} \cdot l_{ef}^{0,9} \cdot \rho^{0,75}}{1,25 \cdot \cos^2\varepsilon + \sin^2\varepsilon} \quad \text{in N} \qquad (1)$$

$r = 0,91$

with

d nominal or outer diameter of the screw in mm

ℓ_{ef} effective pointside penetration length in mm

ε joints in the plane side of CLT: ε = 90°, edge joints: ε = 0°

ρ for joints in the plane side of CLT: density of CLT (whole cross section) in kg/m³

for edge joints in CLT: density of the relevant layer(s) in kg/m³

Fig. 5 (left) shows the test results vs. the predicted values. The correlation coefficient r is equal to 0,91. To simplify equation (1) the characteristic density of CLT is inserted and the denominator is increased up to 1,5. A further adaptation results in equation (2) for the characteristic withdrawal capacity. The right diagram in Fig. 5 shows the verification of the characteristic values.

$$R_{ax,s,k} = \frac{0,35 \cdot d^{0,8} \cdot l_{ef}^{0,9} \cdot \rho^{0,75}}{1,5 \cdot \cos^2\varepsilon + \sin^2\varepsilon} = \frac{31 \cdot d^{0,8} \cdot l_{ef}^{0,9}}{1,5 \cdot \cos^2\varepsilon + \sin^2\varepsilon} \quad \text{in N} \qquad (2)$$

with

ε joints in the plane side of CLT: ε = 90°, edge joints: ε = 0°

ρ characteristic density of CLT (400 kg/m³)

The given equations are only valid for self-tapping screws, for which the characteristic withdrawal strength in solid wood (C24) exceeds $f_{ax,k} = 80 \cdot \rho_k^2 \cdot 10^{-6} = 9,8$ N/mm².

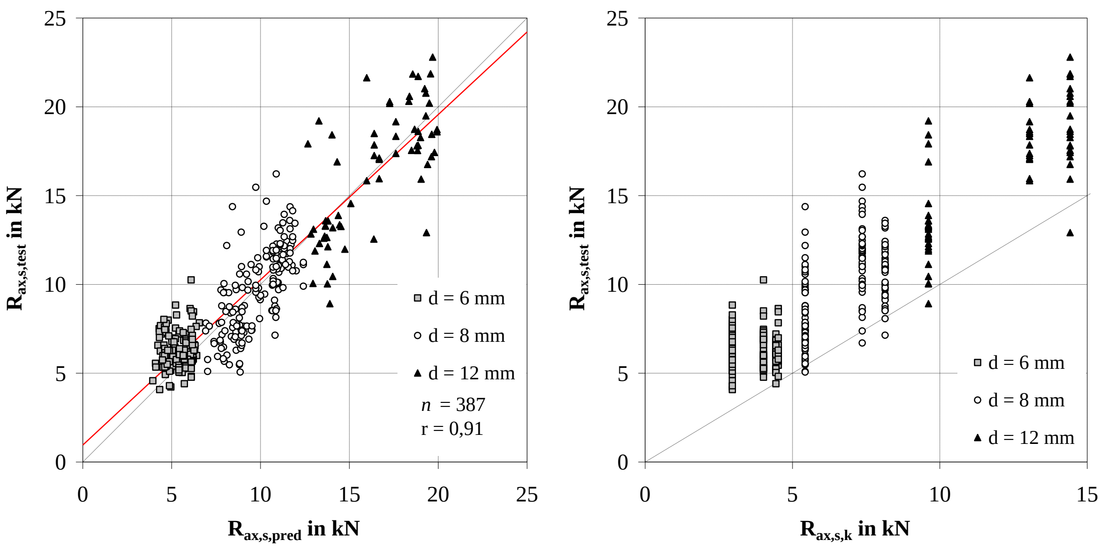

Fig. 5 Withdrawal strength - test results over predicted or characteristic values, resp.

3.3 Proposals for the characteristic withdrawal capacity

The following proposals for the characteristic withdrawal capacity are only valid for self-tapping screws for which the characteristic withdrawal strength in solid wood (strength class C24, according to EN 338) exceeds $f_{ax,k} = 80 \cdot \rho_k^2 \cdot 10^{-6} = 9{,}8$ N/mm². Furthermore the maximum width of gaps and grooves has to be limited to 6 mm. The minimum diameter of screws has to be 6 mm for connections in the plane side of the panels and 8 mm for edge joints.

For axially loaded screws in the plane side of CLT ($\rho_k \geq 400$ kg/m³) the withdrawal capacity can be calculated by inserting $\varepsilon = 90°$ in equation (2):

$$R_{ax,s,k} = 31 \cdot d^{0,8} \cdot l_{ef}^{0,9} \quad \text{in N} \qquad (3)$$

In [1], [3], [6] and [7] the authors assert that it is necessary to examine the influence of load duration and climate variation on the load carrying capacity of edge joints in CLT, (see paragraph 6). Hence screws should not be positioned parallel to the grain until the long-term behaviour is determined. For edge joints with screws positioned perpendicular to the grain the withdrawal capacity can be calculated as follows.

$$R_{ax,s,k} = 28 \cdot d^{0,8} \cdot l_{ef}^{0,9} \quad \text{in N} \qquad (4)$$

4. Laterally loaded dowel type fasteners

4.1 Embedding strength for fasteners positioned in the plane side

4.1.1 Test set-up

To determine the embedding strength of solid wood panels with cross layers 620 embedment tests according to EN 383 [9] were carried out, involving tests with a load under 0°, 45° and 90° to the grain of the outer layers. Furthermore the position of fasteners was varied, as shown in Fig. 6. They were placed in areas without gaps (position 1), placed in gaps (position 2 to 4) or over gaps (position 5).

For tests with fasteners loaded parallel and perpendicular to the grain direction of the outer layers, it was possible to apply the geometry of test specimens as specified in EN 383. To carry out embedment tests with fasteners loaded under 45° to the grain the size of test specimens had to be increased due to plug shear failure in outer layers.

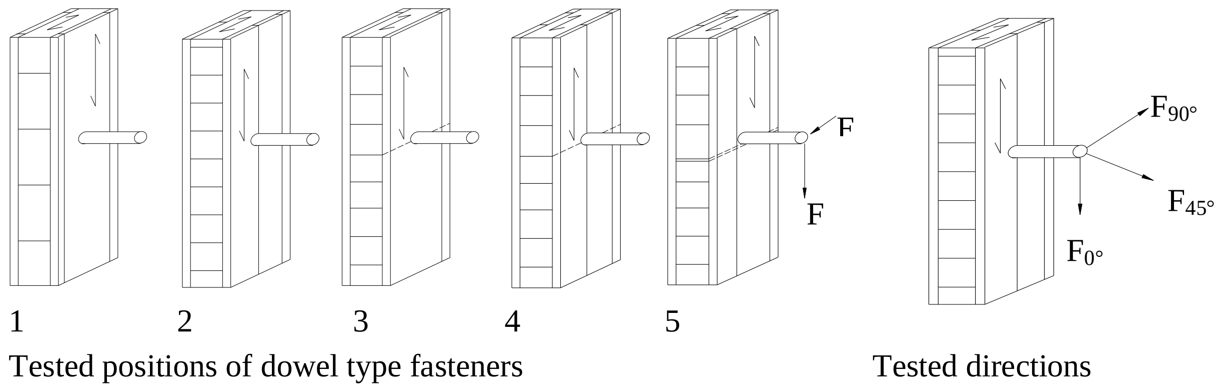

Fig. 6 Positions of fasteners and load direction in embedment tests, schematic sketch

4.1.2 Results for dowels

For dowels it was possible to develop the following two models for embedment strength on the basis of a multiple regression analysis of 438 test results. In the first model the embedment strength, as given in equation (5), is independent of the build-up of the panels. The correlation coefficient r is equal to 0,75. The embedment strength depends on the diameter d of the dowel, the density ρ of the solid wood panel and the angle α between load and grain direction of the outer layer.

$$f_{h,pred} = \frac{0,035 \cdot (1 - 0,015 \cdot d) \cdot \rho^{1,16}}{1,1 \cdot \sin^2\alpha + \cos^2\alpha} \quad \text{in N/mm}^2 \qquad (5)$$

$r = 0,75$

Additionally the second model (eq. (6)) takes into account the build-up of the panels as defined in Fig. 7.

$$f_{h,pred} = 0,032 \cdot (1-0,015 \cdot d) \cdot \rho^{1,20} \cdot \left[\frac{\sum_{i=1}^{n} t_{0,i}}{t \cdot \left(1,6 \cdot \sin^2\alpha + \cos^2\alpha\right)} + \frac{\sum_{j=1}^{n-1} t_{90,j}}{t \cdot \left(1,6 \cdot \cos^2\alpha + \sin^2\alpha\right)} \right]$$

$$r = 0,77 \qquad (6)$$

$$\left[f_{h,pred}\right] = \frac{N}{mm^2}$$

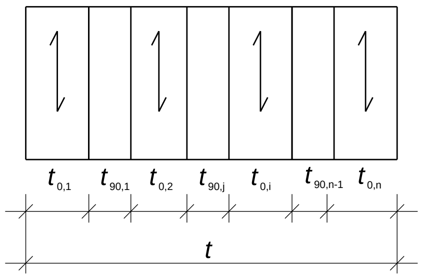

Fig. 7 Definition of thickness of layers for eq. (6) and (7)

The validity of equation (5) and (6) is limited to panels which fulfil the following conditions:

- Maximum thickness of one layer: 40 mm
- Ratio ζ of layers with different grain directions as defined in Fig. 7:

$$0,95 < \zeta < 2,1 \qquad \zeta = \frac{\sum t_{0,i}}{\sum t_{90,j}} \qquad (7)$$

with

$t_{0,i}$ thickness of layer, parallel to the grain direction of the outer layers

$t_{90,i}$ thickness of layer, perpendicular to the grain direction of the outer layers

Fig. 8 shows the results of embedment tests over the predicted values for model 1. The characteristic embedment strength on basis of equation (5) for a characteristic density of 400 kg/m³ can be calculated according to the following expression:

$$f_{h,k} = \frac{0,031 \cdot (1-0,015 \cdot d) \cdot \rho_k^{1,16}}{1,1 \cdot \sin^2\alpha + \cos^2\alpha} = \frac{32 \cdot \left(1-0,015 \cdot d\right)}{1,1 \cdot \sin^2\alpha + \cos^2\alpha} \qquad \text{in N/mm}^2 \qquad (8)$$

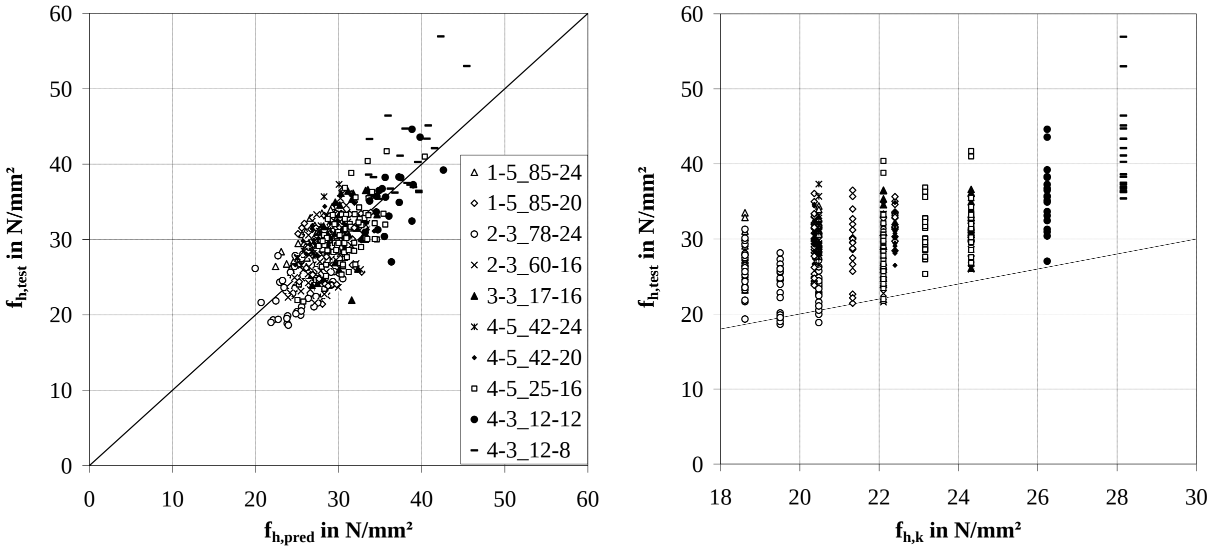

Fig. 8 Comparison of test results and predicted resp. characteristic values for dowels

4.1.3 Results for screws and nails

On the basis of a regression analysis of 179 tests the embedment strength for screws and nails in CLT with a maximum thickness of each layer of 9 mm ($t_i \leq 9$ mm) can be derived as:

$$f_{h,pred} = 0{,}13 \cdot d^{-0{,}53} \cdot \rho^{1{,}05} \qquad \text{in N/mm}^2 \qquad (9)$$
$$r = 0{,}83$$

A comparison of predicted values and test results is shown in Fig. 9. The correlation coefficient was determined as r = 0,83. In equation (9) the embedding strength is independent of the angle α. This result corresponds to the research results of Blaß and Bejtka [10], [11] for self-tapping screws.

By inserting a characteristic density of 400 kg/m³ in equation (9) the characteristic embedment strength can be proposed as:

$$f_{h,k} = 0{,}112 \cdot d^{-0{,}5} \cdot \rho_k^{1{,}05} = 60 \cdot d^{-0{,}5} \qquad \text{in N/mm}^2 \qquad (10)$$

The validity of equation (10) is limited to panels with layers of 9 mm in maximum thickness.

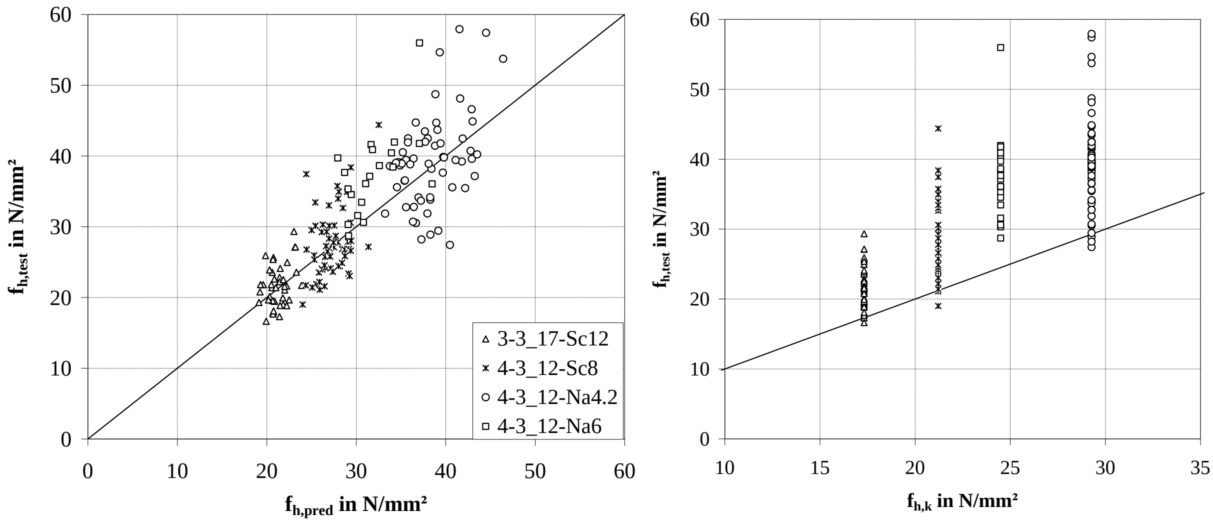

Fig. 9 Comparison of test results and predicted resp. characteristic values (screws/nails)

4.2 Embedding strength for fasteners positioned in the edges

4.2.1 Test set-up

The embedment tests with dowels, screws and nails in CLT were carried out according to EN 383 [9]. To avoid splitting of test specimens, tensile reinforcement was required in some cases [3].

The test programme includes tests with two different load directions as shown in Fig. 10 (direction A and B). In the edges of CLT many positions of fasteners are possible. Fig. 11 shows five possible positions of fasteners with different diameters in relation to the thickness of the layers and in relation to the grain direction. The examined positions of fasteners in relation to gaps and grooves are displayed in Fig. 12. It was not possible to determine the relevant configuration before the tests. Thirteen different combinations of load direction and fastener position were considered in the tests with dowels while in the tests with screws and nails seven combinations were included. For the tests CLT made of European spruce (Picea abies) from four different manufacturers with seven different build-ups were used. Table 4 in paragraph 2 gives some statistical information about the density of the test specimens.

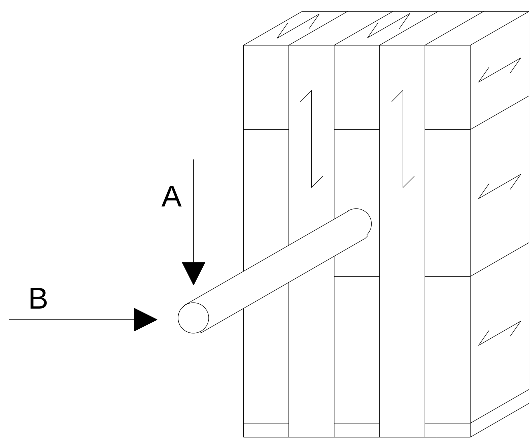

Fig. 10 Tested load directions, schematic sketch of a test specimen

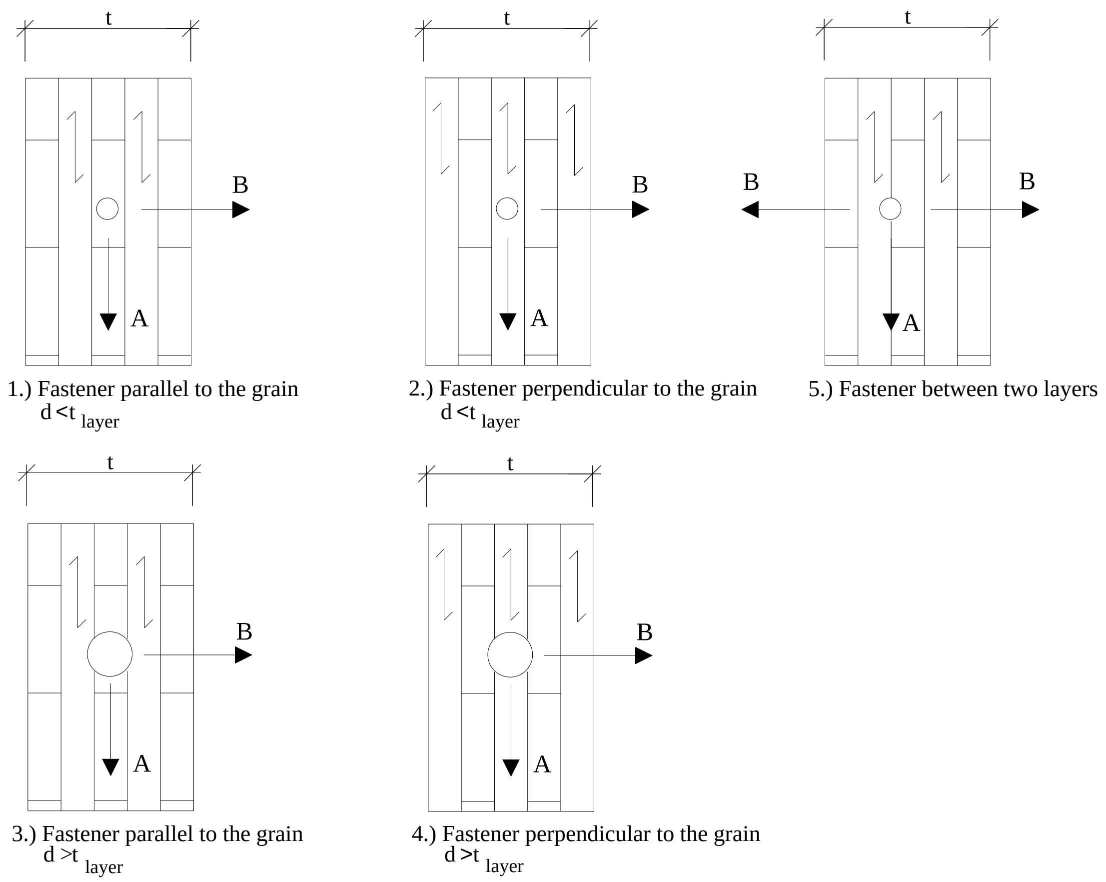

Fig. 11 Possible positions of fasteners in the edges, schematic sketch

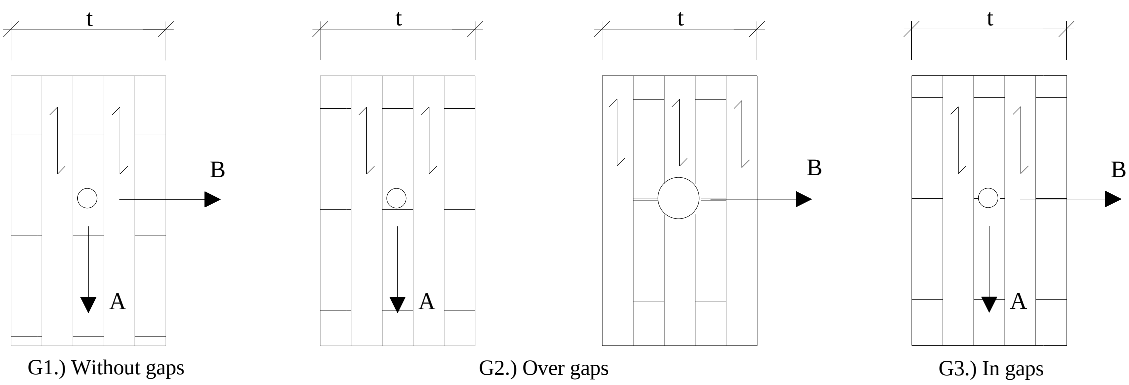

Fig. 12 Possible positions of the fasteners in relation to gaps, schematic sketch

4.2.2 Results for dowels

To determine the embedding strength of cross laminated timber 390 tests with dowels were evaluated. For the tests dowels with 24, 16, 12, 8 and 6 mm in diameter were used. The test results in the different test configurations were analysed to reveal the relevant position. Fig. 13 shows the ratio $f_{h,test}/\rho$ over the diameter for the tested dowel positions. The test configurations are named after the combination of load direction (A, B as shown in Fig. 10) and the position of the fasteners (1 to 5 as shown in Fig. 11). The tests carried out in position A1 result in the lowest values for the embedment strength.

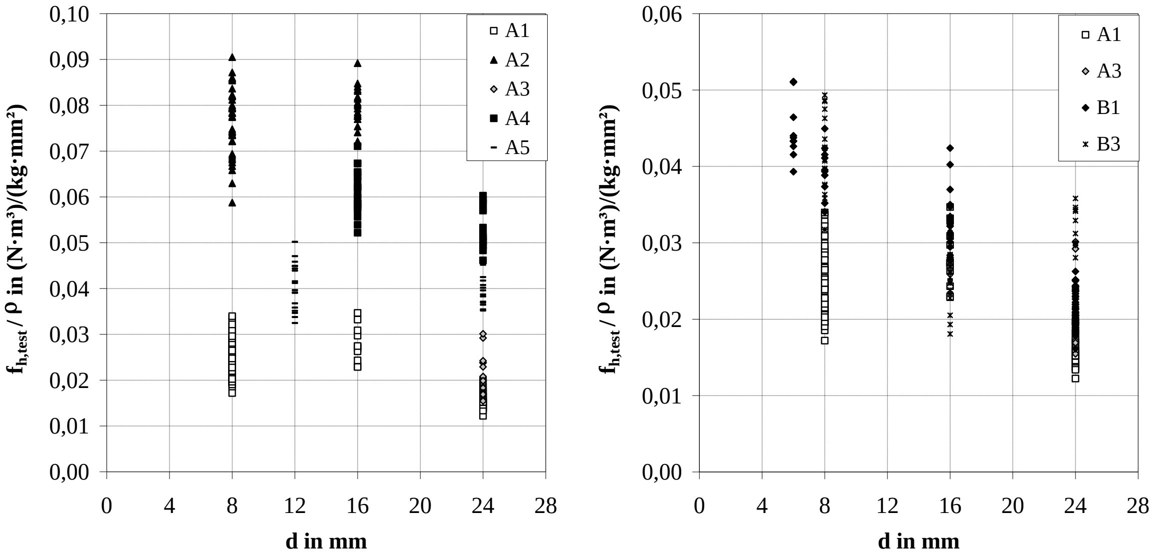

Fig. 13 Ratio $f_{h,test}/\rho$ over diameter d for the different tested positions of dowels

For dowels it was possible to develop the model for the embedment strength given in equation (11). It is based on a multiple regression analysis of 100 embedment tests carried out in the relevant test position A1. The embedment strength depends on the diameter d of the dowel and the density ρ_{layer} of the layer or the layers in which the dowel is placed. A comparison of predicted values and test results is shown in Fig. 14. The correlation coefficient r is equal to 0,63. The diagram shows also the results for the non-relevant positions.

$$f_{h,pred} = 0{,}049 \cdot (1 - 0{,}017 \cdot d) \cdot \rho_{layer}^{0{,}91} \qquad \text{in N/mm}^2 \quad (11)$$

$$r = 0{,}63$$

with

d diameter of the fastener

ρ_{layer} density of the relevant layer(s)

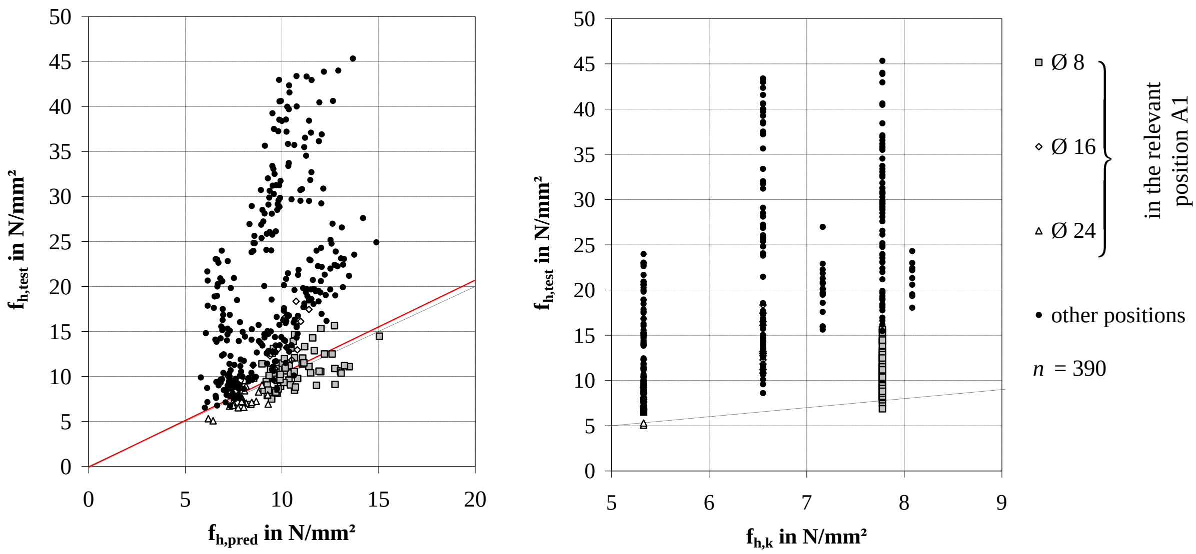

Fig. 14 Comparison of test results and predicted values, resp. characteristic values of the embedment strength, influence of the dowel position

By inserting the characteristic density of the relevant layer, which complies with the density of the raw material (350 kg/m³ for C24) in equation (11), the characteristic embedment strength can be proposed as:

$$f_{h,k} = 0{,}0435 \cdot \left(1 - 0{,}017 \cdot d\right) \cdot \rho_{layer,k}^{0,91} = 9 \cdot \left(1 - 0{,}017 \cdot d\right) \quad \text{in N/mm}^2 \quad (12)$$

4.2.3 Results for screws and nails

Altogether 319 embedment tests with nails (d = 4,2 mm) and screws (d = 6, 8, 12 mm) in seven different combinations of load direction and fastener positions were carried out. On the basis of a regression analysis of 117 tests with screws and nails in the relevant test configuration A1 the embedment strength can be derived as:

$$f_{h,pred} = 0{,}8622 \cdot d^{-0,46} \cdot \rho_{layer}^{0,56} \quad \text{in N/mm}^2 \quad (13)$$
$$r = 0{,}68$$

A comparison of predicted values and test results is shown in Fig. 15. The correlation coefficient was determined as r = 0,68. Having inserted the characteristic density of the layers ($\rho_{layer,k}$ = 350 kg/m³) in (11), simplified and adapted the equation the characteristic embedment strength can be proposed as:

$$f_{h,k} = 0{,}862 \cdot d^{-0,5} \cdot \rho_{layer,k}^{0,56} = 20 \cdot d^{-0,5} \quad \text{in N/mm}^2 \quad (14)$$

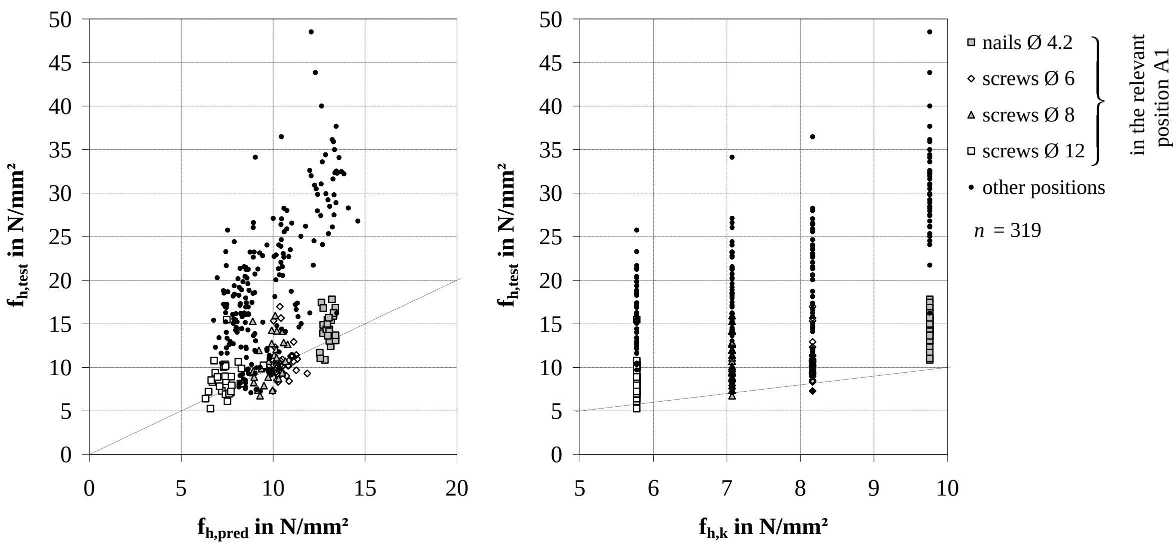

Fig. 15 Comparison of test results and predicted or characteristic values (screws/nails) resp.

5. Load carrying capacity of connections in CLT

5.1 Joints in the plane side

The load carrying capacity of joints in CLT under lateral load can be determined according to Johansen's yield theory.

For connections with screws and nails in the plane side of panels with thin layers ($t_i \leq 9$ mm) it is possible to use the characteristic embedment strength as given in equation (10) for the calculation. In case of products with layers of more than 9 mm in thickness the embedment strength of solid wood can be used (s. paragraph 8.3.1.1 in EN 1995-1-1). For this calculation the characteristic density of the raw material (350 kg/m³ for C24) is decisive. The characteristic embedment strength for self-tapping screws can also be calculated according to the following proposal of Blaß and Bejtka [11]:

$$f_{h,s,k} = 0,019 \cdot \rho_{layer,k}^{1,24} \cdot d^{-0,3} \quad \text{in N/mm}^2 \qquad (15)$$

In other cases the embedment strength depends on the angle between load and grain direction so that additional investigations are necessary. Here obviously the embedment strength of a layer loaded in grain direction is larger than of one loaded perpendicular to the grain, s. paragraph 4.1. In many cases, which are dependent on the type of connection, the build-up of the solid wood panels and the diameter and yield moment of the fastener, a simplified calculation of the load carrying capacity using the embedment strength given in paragraph 4.1.2 is possible. For some configurations the yield moment develops in the outermost layers. This allows direct use of their embedment strength for the calculation. In conclusion, the limits for the application of simplified calculations have to be defined for different build-ups of solid wood panels.

For multiple fastener joints in the plane side of CLT the effective number of fasteners in a row is equal to the actual number of fasteners ($n_{ef} = n$).

5.2 Edge joints

For calculating the load carrying capacity of edge joints according to Johansen's yield theory the embedding strength for dowels, screws and nails is given in paragraph 4.2.3. For the design of multiple fastener joints it is suggested to consider the effective number of fasteners.

5.3 Recommendations for the design of connections

For laterally and axially loaded joints in CLT the defined requirements on the minimum diameters of fasteners have also to be fulfilled (s. paragraph 3.3 and [6], [7]). Further requirements are defined for spacings and distances as well as for the geometry of edge joints (minimum thickness of CLT panels, minimum thickness of the relevant layer, minimum embedded length), see [1], [3], [6] and [7].

6. Long-term tests with edge joints

To examine the influence of load duration and climate variation on the load carrying capacity of edge joints with screws in CLT, long-term tests were set up. The test programme contains 48 tests with axially loaded self-tapping screws driven into the middle layer of the test specimens parallel to the grain. The long-term behaviour of laterally loaded edge joints with self-tapping screws is also examined. To this purpose, tests with single and double shear CLT-to-CLT-connections are included in the test programme. The test set-up is shown in Fig. 16. The environmental conditions comply with Service Class 2. The design resistance of the test specimens was determined from the characteristic values with the modification factor $k_{mod} = 0,8$ and the partial factor γ_M = 1,3. The laterally loaded screws were loaded with the full design resistance while the axially loaded screws were loaded with 70 % of the design resistance. The long term-tests were started in 2007 and were finished in 2012. During the test duration the climate was recorded and the displacements of laterally loaded specimens were measured periodically. Fig. 17 shows a displacement-time curve of one specimen. The tests with laterally loaded screws were finished in April 2012, after a conditioning in normal climate (20°C/65% RH) the remaining load carrying capacity was examined in the end of 2012.

In the long-term tests with axially loaded screws 19 withdrawal failures were observed during the test duration. After *conditioning at 20/65 t*he other specimens were tested in a short-term test to determine the remaining withdrawal capacity. The results of the long-term tests will be published in a few months.

Fig. 16 Long term tests with screwed edge joints in CLT under lateral load and axial load

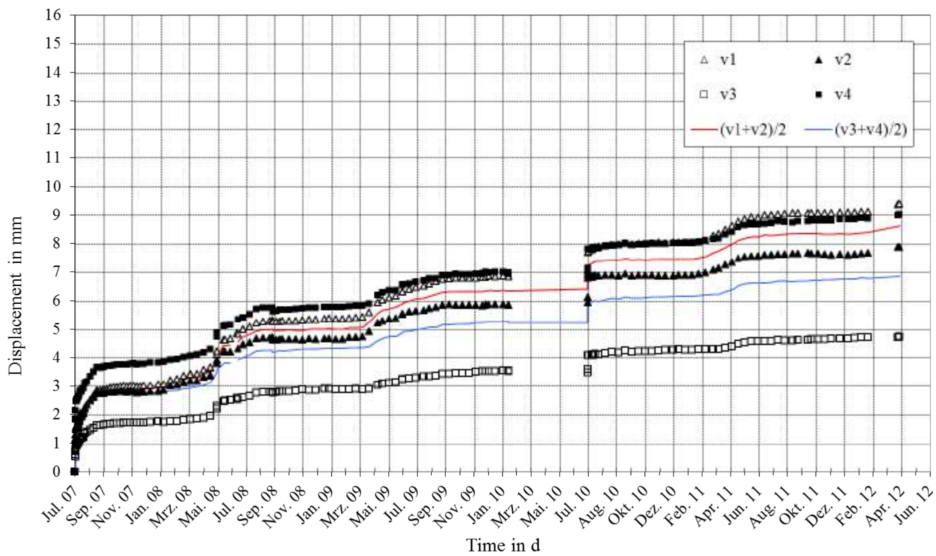

Fig. 17 Displacement-time curve for one specimen of the long-term tests with screwed edge joints in CLT under lateral load (four measurement points)

7. Conclusions

The parameters of cross laminated timber for calculating the load carrying capacity of dowel type fasteners were examined. For the characteristic density of solid wood panels made of European spruce a value of 400 kg/m³ is proposed. It was possible to determine the embedment strength of cross laminated timber for dowel type fasteners positioned in the plane sides or in the edges of the panels. Furthermore for these cases calculation models for the withdrawal capacity of self-tapping screws were proposed.

Long-term tests revealed that the withdrawal capacity of axially loaded screws driven into layers of the edge parallel to the grain is much less than assumed. For this application further research is necessary.

8. References

[1] Blaß, H. J.; Uibel, T., „Tragfähigkeit von stiftförmigen Verbindungsmitteln in Brettsperrholz“, Karlsruher Berichte zum Ingenieurholzbau, Band 8, Lehrstuhl für Ingenieurholzbau und Baukonstruktionen (Ed.), Universität Karlsruhe (TH), 2007

[2] Uibel, T.; Blaß, H. J., “Load carrying capacity of joints with dowel type fasteners in solid wood panels”, in: *Proceedings*, *CIB-W18 Meeting 2006*, Florence, Italy 2006, Paper 39-7-5

[3] Uibel, T.; Blaß, H. J., “Edge joints with dowel type fasteners in cross laminated timber”, in: *Proceedings*, *CIB-W18 Meeting 2007*, Bled, Slovenia 2007, Paper 40-7-2

[4] Hilson, B. O., "Verbindungen mit stiftförmigen Verbindungsmitteln – Theorie", in: Blaß, H. J.; Görlacher, R.; Steck, G. (Ed.): *Holzbauwerke STEP1 – Bemessung und Baustoffe*, Fachverlag Holz, Düsseldorf, 1995

[5] Johansen, K. W., "Theory of timber connections", International Association of bridge and structural Engineering, Bern, 1949, p. 249-262

[6] Uibel, T., „Brettsperrholz – Verbindungen mit mechanischen Verbindungsmitteln“, *Tagungsband: Ingenieurholzbau - Karlsruher Tage 2007*, Bruderverlag, Köln 2007

[7] Blaß, H. J.; Schickhofer, G.; Traetta, G.; Uibel, T., “Verbindungstechnik – Tragfähigkeitsnachweise von stiftförmigen Verbindungsmitteln in BSP (Kapitel E 4)“, *BSPhandbuch, Holz-Massivbauweise in Brettsperrholz*. Ed.: G. Schickhofer, Verlag d. Tech. Univ. Graz, Graz 2009, p. E-7 - E-22

[8] EN 1382: 1999 - Timber structures - Test methods - Withdrawal capacity of timber fasteners

[9] EN 383: 1993 - Timber structures; Test methods; Determination of embedding strength and foundation values for dowel type fasteners

[10] Bejtka, I., „Verstärkungen von Bauteilen aus Holz mit Vollgewindeschrauben“, Karlsruher Berichte zum Ingenieurholzbau, Band 2, Lehrstuhl für Ingenieurholzbau und Baukonstruktionen (Ed.), Universität Karlsruhe (TH), Karlsruhe, 2005

[11] Blaß, H. J., Bejtka, I., Uibel, T., „Tragfähigkeit von Verbindungen mit selbstbohrenden Holzschrauben mit Vollgewinde“, Karlsruher Berichte zum Ingenieurholzbau, Band 4, Lehrstuhl für Ingenieurholzbau und Baukonstruktionen (Ed.), Universität Karlsruhe (TH), Karlsruhe, 2006

Theme III

Seismic

Prof.

Roberto Tomasi

Department of Civil, Environmental and Mechanical Engineering

University of Trento

Italy

Email: Roberto.Tomasi@unitn.it

Roberto Tomasi received his MSc in Civil Engineering in 2000 and is PhD in Structural Engineering in 2004 at University of Trento. Since 2005, as member of the Department of Civil, Environmental and Mechanical Engineering of University of Trento, he is involved in teaching activity in the Timber Engineering and Structural Rehabilitation courses of the Civil Engineering and Architectural Degree Programs. He is co-author of more than 40 papers published in Peer Reviewed International Journals and International Conference Proceedings, and of a manual on Timber Engineering (in Italian). His current and recent research activity includes the ductile design of timber joints, glued in rods, analysis of the interaction between timber floor and masonry, seismic behavior of multi-storey timber buildings. Since 2004, for the the Association of Timber and Mills Italian and Austrian Industries, he is involved as teacher in professional courses, and as coordinator in an Help Desk Website specifically directed to professional designers.

Univ-Prof. Dr.-Ing

Werner Seim

Department of Civil Engineering and Environmental Engineering University of Kassel

Germany

Email: wseim@uni-kassel.de

Dr. Werner Seim is professor on Timber Engineering in the Department of Civil Engineering and Environmental Engineering at the University of Kassel (Germany), where he has served as a faculty member since 1999. He received his Dipl.-Ing. from University of Stuttgart (1988), and his Dr.-Ing. from University of Karlsruhe (1994). In 1998 he spent one year as a postdoc at University of California, San Diego and in 2008 he was visiting professor at University of British Columbia, Vancouver. Dr. Seim's research is directly related to timber engineering with a focus on earthquake resistance, composite structures and form fitting connections as well as to innovative structures in masonry. He has authored several refereed research papers in high quality engineering and scientific journals such as Journal of Structural Engineering, Engineering Structures and Construction & Building Materials. Dr. Seim works as a consulting engineer since 1989 with special interest in Timber Engineering and Building Rehabilitation.

Assoc. Prof.

Massimo Fragiacomo

Department of Architecture, Design and Urban Planning

Univsersitá degli Studi di Sassari

Italy

Email: fragiacomo@uniss.it

Massimo Fragiacomo is Associate Professor of Structural Design at the University of Sassari, Italy, since 2007. Past work experiences include almost three years at the University of Canterbury, New Zealand, and six years at the University of Trieste, Italy. He holds a PhD in Design and Preservation of Structures and a Degree in Structural Engineering at the University of Trieste, Italy. He is author of about 220 papers, 67 published on peer reviewed International Journals. His main areas of expertise include Timber, Earthquake and Fire Engineering. He has been Principal Investigator in several national and international research projects. For his research activity he has received prestigious awards including the Frederick Palmer Prize offered by the Institution of Civil Engineers – UK in 2012. He is member of the Eurocode 5 and Eurocode 8 Technical Committees, and the corresponding Italian mirror groups.

Seismic behavior of connections for buildings in CLT

Roberto Tomasi

Assistant Professor

University of Trento

Trento, Italy

1. Introduction

CLT is one of the most efficient wood engineered products available as an alternative to concrete or masonry buildings, and it is now increasing in popularity. CLT panels have been manufactured in Europe for more than ten years, and they are now widely used throughout the continent, with good results in terms of structural behavior, building speed, and quality housing. In these systems, resistance to horizontal actions - wind and earthquakes - is entrusted to metal connector systems arranged in such a way as to absorb the horizontal forces and to prevent the uplift effects of the wall. Shear-type connectors (such as screws or angle brackets) are used to ensure the transfer of shear actions, and so called “hold-downs” are adopted in order to counteract the tense actions causing the wall’s rocking behavior. Moreover, metal connection systems of other types are usually adopted in between vertical and horizontal diaphragms to ensure a “box like” behavior. This paper illustrates the types of structural connection system commonly adopted in multi-storey buildings and presents recent research carried out at the University of Trento on the seismic behavior of connections for buildings in CLT.

2. Structural connection systems in CLT buildings

2.1 A possible classification of structural joints in CLT

The main joint systems in a CLT building are illustrated in fig 1, where three categories are defined: a) joint between vertical panels and horizontal diaphragms (see Fig. 1, joint 1, 2 and 3); b) joint between vertical panels (see Fig. 1, joint 5 and 6); c) joint between horizontal elements in a diaphragm (see Fig. 1, joint 7).

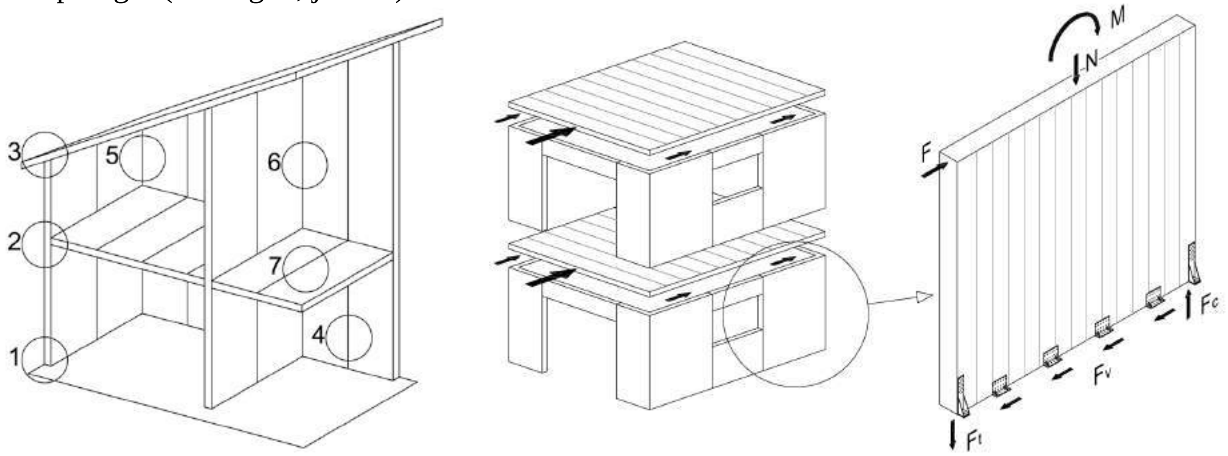

Fig. 1 Main joints in a CLT building, horizontal force distribution in a CLT building and in the single wall [1]

2.1.1 Case A: Joint between vertical panels and horizontal diaphragms

A modern CLT system is a prefabricated system where construction elements are stacked storey by storey. As a consequence, structural continuity among vertical elements must be achieved by means of connectors able to transmit vertical and horizontal forces. Typically, two different types of connections are used according to the force transmitted to the ground, as in the scheme of force transmission illustrated in Fig. 3c: Devices (usually termed 'hold-downs') are designed to resist the tensile force due to the overturning moment; other devices (e.g. angle brackets) transfer the horizontal shear to the ground. Alternatively, a single device, designed to resist both vertical and horizontal forces, can be used, as shown in Fig. 3b.

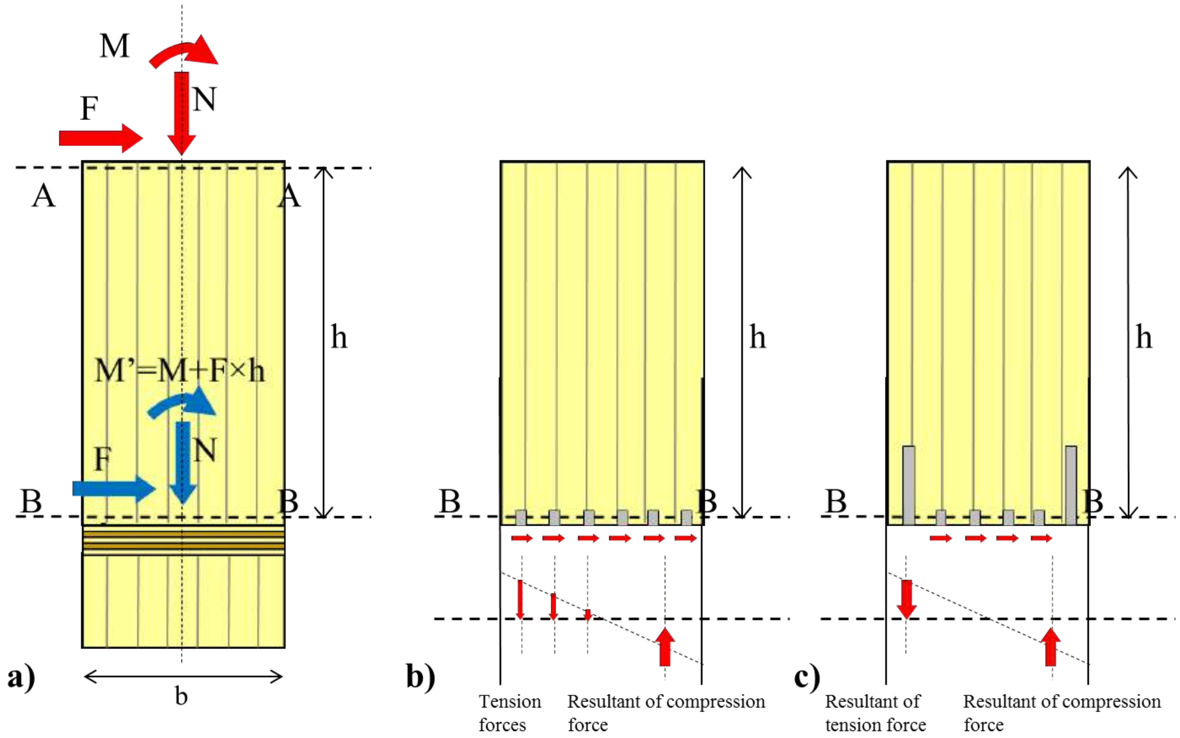

Fig. 2 a) External forces acting on the A-A and B-B sections of a generic CLT wall; b) internal forces with connections working both in shear and in tension; c) internal forces with angle brackets prevent sliding, and hold-downs prevent rocking of the CLT wall.

2.1.2 Case B: Joint between vertical panels

The lateral dimensions of CLT panels often have to be limited owing to production or transportation problems. It may therefore be necessary to joint them along the vertical narrow edges in order to produce longer timber walls, as illustrated in Fig. 3a. If the vertical joints are suitably designed, the composite wall can be considered a single element: otherwise, the panels aligned without these vertical connections should be considered as not collaborating, and therefore treated as independent elements (Fig. 3b). Fig. 4 illustrates some possible joint configurations for vertically connected CLT.

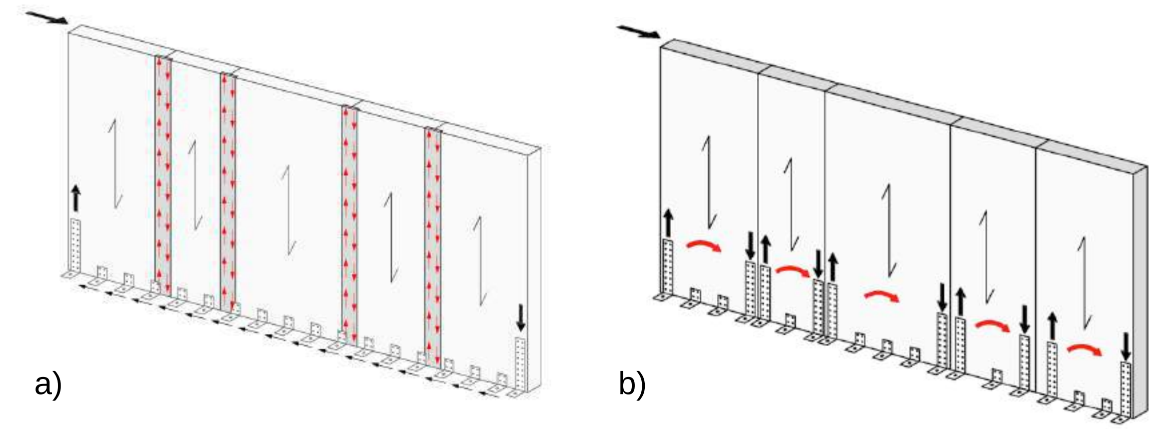

Fig. 3 Internal force distribution and connection system in a single wall composed by different CLT panels connected by vertical joints a), or not connected by vertical joints b)

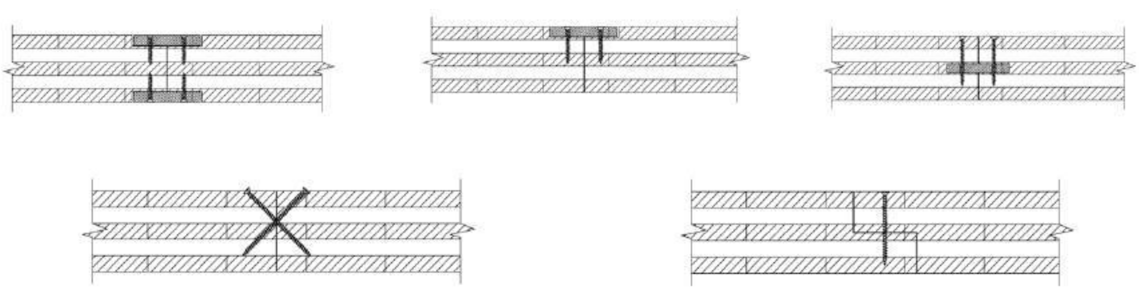

Fig. 4 Possible joint configuration for CLT panel connected to the narrow edges

2.1.3 Case C: Joint between horizontal panels

Also in the case of floor jointed between the narrow edges of CLT panels, connections have great importance in guaranteeing adequate diaphragm behavior in buildings subject to lateral load, as illustrated in Fig. 5. The possible joint configurations are comparable to those illustrated in Fig. for case B.

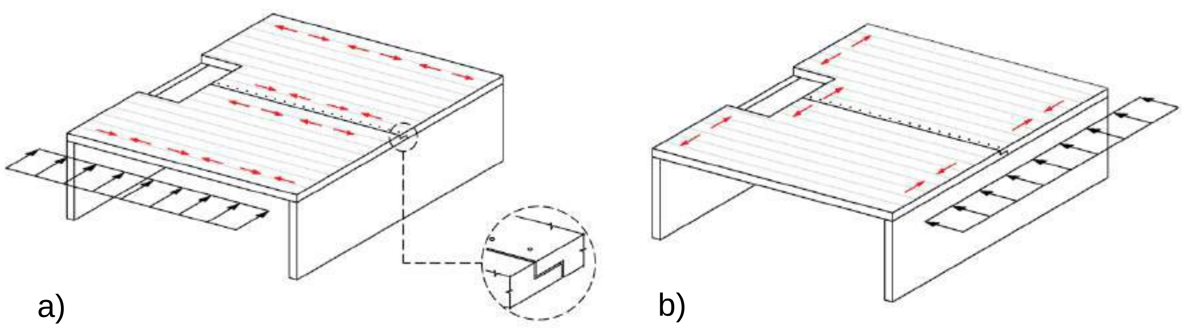

Fig. 5 Internal force distribution in floor diaphragms of a CLT building

2.2 Type of connectors

2.2.1 L-shaped steel elements

In order to prevent sliding and up-lift of the wall, a solution commonly adopted is the use of L-shaped steel elements nailed to the CLT panels (usually only to one side, in an unsymmetrical configuration, see Fig. 6a). As illustrated above, two different types of devices are used according to the force transmitted to the ground. Hold-downs are designed with a particular geometry in order to resist vertical forces and to offer negligible rigidity to lateral loads. L-shape metal plates have a narrow flange base with a central hole for connection of the anchor bolt to the foundation or to the floor level, and a long perforated vertical flange endowed with ribs to be nailed to the CLT. Angle brackets are designed to offer greater rigidity to lateral forces. They therefore have larger flange bases for a greater number of anchors and nails aligned horizontally: in some cases they can also have reinforcement such as ribs or corrugations in order to resist vertical loads as well.

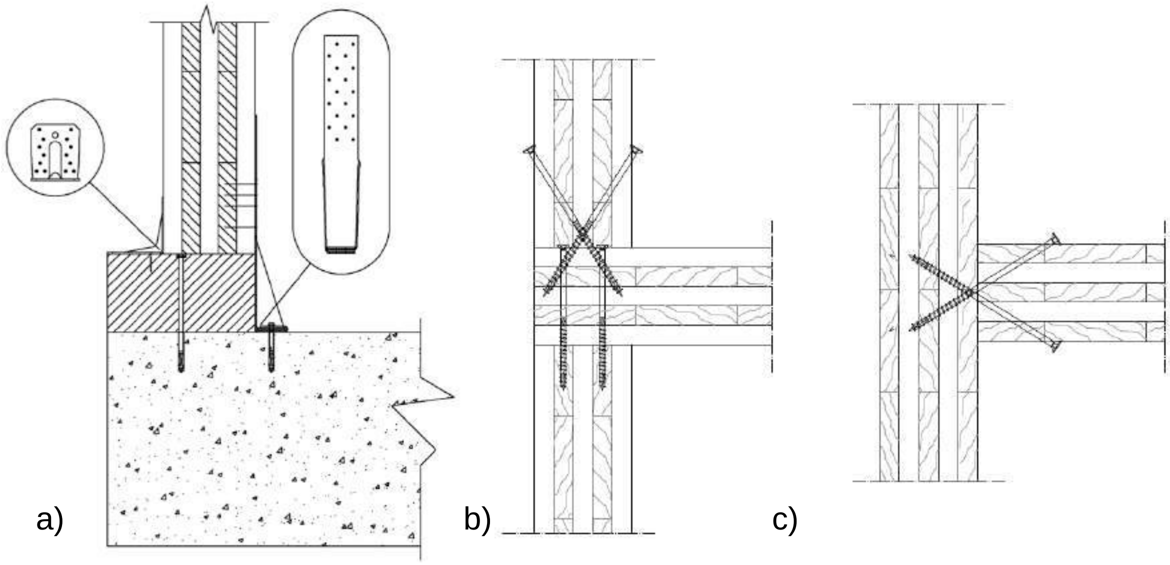

Fig. 6 Possible joint configurations in a CLT building for: a) section of a joint between vertical panel and foundation; b) section of a joint between vertical panel and horizontal floor diaphragms; c) plan of a joint between vertical panels

2.2.2 Dowel type connectors in CLT

Self-tapping screws can be an alternative type of connection system adopted to transmit both vertical and horizontal forces through the building. Fig. 6b and Fig. 6c show possible solutions for respectively joint 2 and joint 6 described in Fig. 1.

The design rules adopted in the current version of the standard to calculate the mechanical properties of dowel-type connections under lateral or axial load assume, in the case of solid wood or glued laminated timber, homogenous mechanical parameters such as embedding strength or withdrawal capacity of the screws. In the case of CLT, dowel-type connectors may be positioned perpendicularly to the plane of cross laminated timber, traversing different layers with non-homogenous mechanical parameters, or on the narrow side of the CLT panel. Modified calculation models based on Johansen's classic yield theory for dowel-type connections, which also takes into account the stratigraphy of the CLT panel, have been proposed and validated by some authors for these cases ([2] and [3]).

3. Experiments on the behavior of CLT walls under lateral load

The goal of experiments performed at the University of Trento was to study the behavior of the CLT starting from analysis of the mechanical properties of connection systems depending on different variables considered in the experimental campaign (type of connection system, vertical load, presence of openings, etc.). The preliminary tests were devoted to different types of angle brackets and hold-downs [4]. In a second phase, the capacity of an entire CLT wall subjected to lateral and vertical load was tested.

3.1 Test on connections between foundation and CLT panels

3.1.1 Test on single connections: materials

The ***angle bracket*** and ***hold-down*** elements were manufactured cold bending or welding perforated metal sheets with a variety of ribs or corrugations intended to increase rigidity. Each type of connection tested differed from the others in element typology, length of nails, and number of anchors. The joint configurations were usually unsymmetrical, because they were fixed to only one side of the CLT walls.

The ***angle bracket*** elements are usually adopted to prevent sliding of the wall from the foundation or wooden floor. Hence their geometry should be optimized to this function. Five types of commercial angle brackets (65, 90, 90_CR, 110, 65-135) and two types of new type angle brackets specifically designed for this campaign (200, 200CR), were tested. Because the ***hold-down*** element prevents the uplift and rotation of the panel, it is designed with a particular geometry to resist vertical forces. The action line of the load follows the symmetry axis of the vertical nailed flange. The base is connected to the concrete slab through a standard anchor positioned with thick washers (10 or 20 mm), so as to prevent the negative effects caused by prying action mechanisms and to distribute the compression on a larger surface. Each element was tested adopting two fastener types (Anker 4.0x40 and 4.0x60 nails).

Tab. 1 and Tab. 2 respectively report the geometry of the angle bracket and hold-down system and the type of fastener.

3.1.2 Test on single connections: set-up

The specimen and the test set-up geometry were designed in order to reproduce as accurately as possible the actual shear force pattern between wall and foundation: the non-symmetric set-up configuration reproduced the actual on-site geometry (see Fig. 7). For both connection system types, three-layer type CLT panels were used with a total thickness of 98 mm (32+34+32 mm).

For the angle bracket specimen, a 500 x 500 mm wooden panel was fixed to a steel base reaction frame by 2 UPN 120 profiles counteracting the vertical displacement, and to the hydraulic jack by means of a rigid vertical steel plate which simulated the foundation slab. The connection system, nailed to the CLT panel with 4.0x40 or 4.0x60 annularly threaded nails, jointed the vertical steel plate with 1 or 2 bolts.

In the case of the hold-down specimen, a 500 x 700 mm CLT panel was used with two lateral notches at the bottom in order to provide the anchoring point for the vertical bar linked to the head of the actuator through an horizontal HEB 260 profile. The wooden panel was linked to the steel base reaction frame only by the hold-down, nailed to the CLT specimen with 4.0x40 or 4.0x60 annularly threaded nails and connected to the ground with one steel anchor. The assembly configuration contemplated a thick washer only for HD 340 and HD 620 type elements, while for all the other elements no further washers were present.

Tab. 1 *Angle bracket elements geometry and test configurations*

Type			65	90	90_CR	110	65-135	200_N	200_CR_N
Geometry Angle Brackets	t	[mm]	2,5	3	3	3	4	3	3
	b	[mm]	65	90	90	110	65	200	200
	h	[mm]	90	100	100	90	135	100	100
	r	[mm]	90	100	100	50	90	60	60
	rib		yes	no	yes	yes	yes	no	yes
Fasteners	Type		Anker	Anker	Anker	Anker	Anker	Anker	Anker
	Vertical plate								
	Φ_{holes}	[mm]	5	5	5	5	5	5	5
	$\Phi_{connector}$	[mm]	4	4	4	4	4	4	4
	$L_{connector}$	[mm]	40 or 60	40 or 60	40 or 60	40 or 60	40 or 60	40 or 60	40 or 60
	$n_{connector}$		8	12	12	15	13	30	30
	Horizontal plate								
	Φ_{holes}	[mm]	11	11	11	13	13,5	12	12
	Φ_{anchor}	[mm]	10	10	10	10	10	10	10
	$n_{anchors}$		1	1 or 2	1 or 2	2	1	2	2

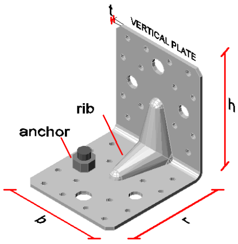

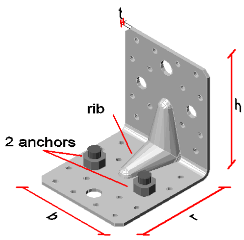

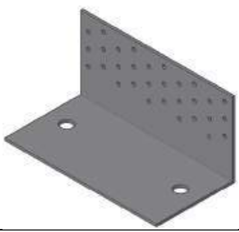

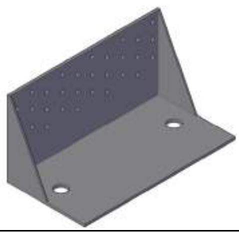

Tab. 2 *Hold-down elements geometry and test configurations*

Type			HD 406	HD 559	HD 285	HD 340	HD 620
Geometry Hold-down	t	[mm]	2,5	2,5	3	3	3
	b	[mm]	60	60	65	60	80
	h	[mm]	406	559	285	340	620
	r	[mm]	61	61	90	63	83
	rib		yes	yes	yes	yes	yes
Fasteners	Type		Anker	Anker	Anker	Anker	Anker
	Vertical plate						
	Φ_{holes}	[mm]	5	5	5	5	5
	$\Phi_{connector}$	[mm]	4	4	4	4	4
	$L_{connector}$	[mm]	40 or 60	40 or 60	40 or 60	60	60
	$n_{connector}$		18	32	17	20	52
	Horizontal plate						
	Φ_{holes}	[mm]	17	17	13,5	17	21
	Φ_{anchor}	[mm]	16	16	12	16	20
	$n_{anchors}$		1	1	1	1	1

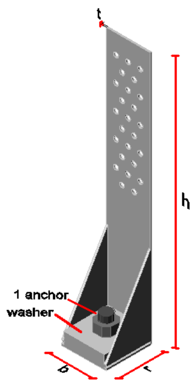

Fig. 7 shows the instrumentation layout adopted in the test: the applied force was measured by a load cell placed between the jack actuator and the specimen; the displacements were measured using L.V.D.T. - linear variable differential transducers - placed on both sides of the specimens, along the shear planes, using specific steel supports for the measuring equipment. Moreover, inclinometers were placed in order to measure the rotation referred to the vertical nailed plate. By means of this configuration it was possible to evaluate the following: relative sliding (nailed vertical plate – wood specimen); relative rotation (nailed vertical plate – wood specimen); and global displacement of the connection (vertical displacement of the head of the jack). The tests were implemented with a displacement control method; in monotonic tests, the loading was applied under displacement control up to failure at a constant rate of 0.05 mm/sec, according to the provisions of EN 26891 [5].

a)  b) 

Fig. 7 Test set up for angle brackets a) and for hold-down connectors b)

3.1.3 Test on single connections: test results and discussion

A total amount of 115 tests were carried out on different configurations of ***angle brackets elements*** (77 monotonic tests and 38 cyclic tests, with a minimum of two tests being performed for each configuration), taking account of the possibility of different fastener types (4.0x40 and 4.0x60 deformed nails) and assembly configurations (1 or 2 bolts). Some of the results are shown by the graphs in Fig. 9a) and Fig. 9b), which respectively compare the influence on the mechanical properties of the angle bracket geometry and of the number of steel anchors (single or double). The most efficient elements, in terms of strength and stiffness, are those where the eccentricities e_x (between the barycentre of the nailed vertical plate and the base plate, measured in the vertical plane) and e_y (between this barycentre and the steel anchors, measured on the base plate plane) illustrated in Fig. 8b are minimized. Furthermore, increasing the parameter c (spacing between the anchors in the horizontal flange) reduces the stress state of the steel connectors. The presence of a single anchor in the horizontal flange does not ensure a correct shear force transmission from the element to the ground; in this case, the fastener also undergoes a rigid rotation mechanism, causing a lower level of joint strength and stiffness, as shown in Fig. 9b. Taking these considerations into account, angle brackets with a larger width b and two anchor bolts (see Fig. 9a) will provide higher values in term of strength and stiffness. In Fig. 9b, the experimental test results are compared with the characteristic strength values determined according to EN 1995-1-1 [6], Johansen classic modified theory ([2] and [3]), and European technical approvals. The global stiffness of the connection K_{el} was determined according to EN 1995-1-1 taking account only of the nail deformation contribution. In the test performed on angle brackets, the ratio between the stiffness K_{el} and the experimental global stiffness $K_{s,el}$ reached values in the range of 10-30. This observation underlines the fact that a calculation of the global connection stiffness based only on the contribution of the nailed connections overestimates the real stiffness of the system. In the global deformation, account should also be taken of the part due to the connection systems, such as nails and steel anchors, and of the specific contribution made by the metal element. This is the consequence of the fact that a simplified calculation, based on the classic rules, does not consider the deformability of the metal element, which is on the contrary very significant.

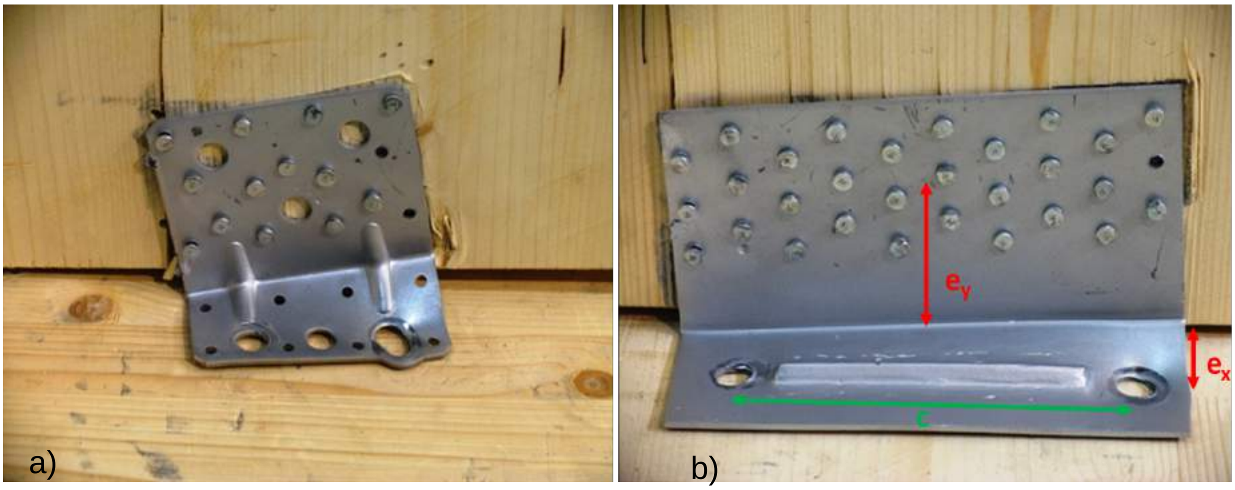

Fig. 8 Influence of the geometry of the connection on the type of failure for AB-110 a) and AB 200 b)

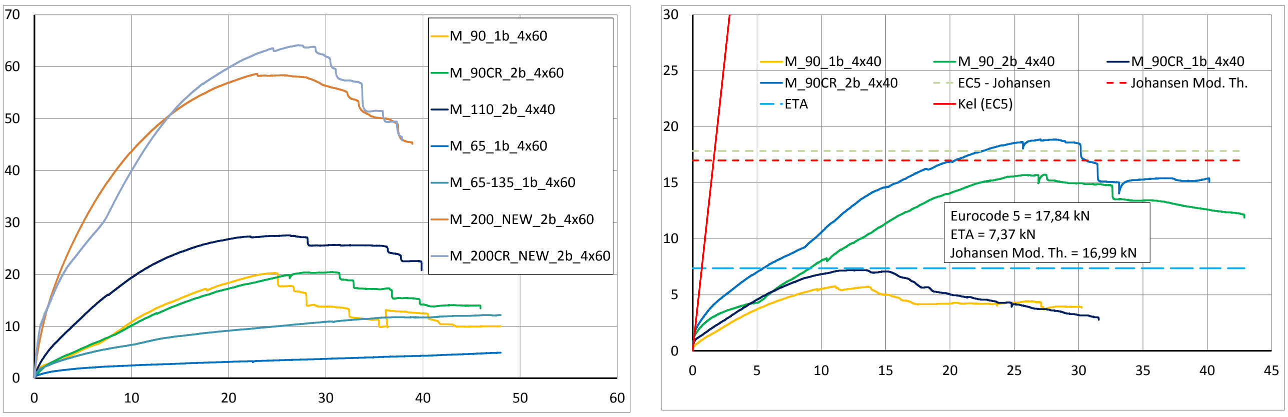

Fig. 9 Experimental F-v curve (kN-mm) of some steel angle brackets (4.0x60 nails - 1 or 2 steel anchors) a), experimental F-v curve (kN-mm) of 90 and 90R type elements (4.0x40 nails – 1 or 2 steel anchors) compared with characteristic values b);

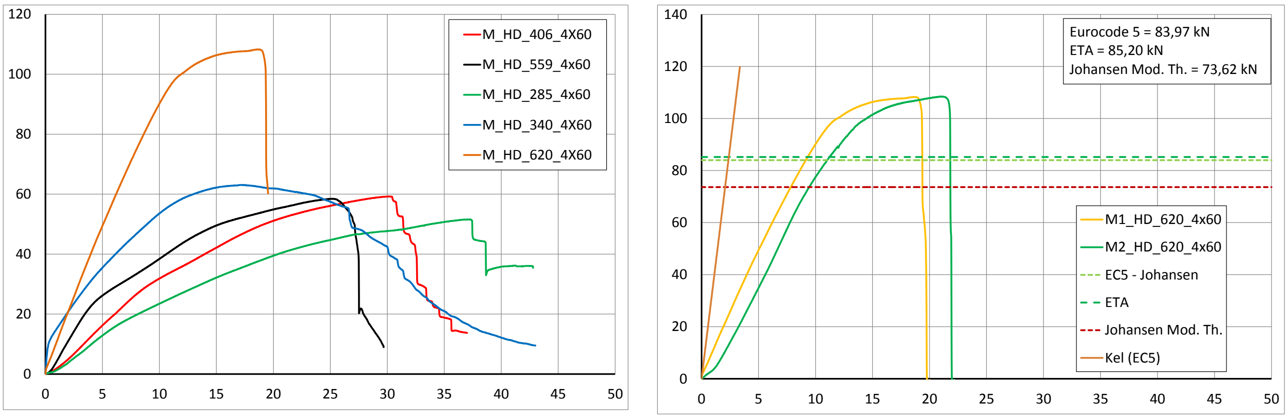

Fig. 10 Comparison between experimental F-v (kN-mm) curves for all hold-downs a); Experimental F-v curve for HD 620 elements b)

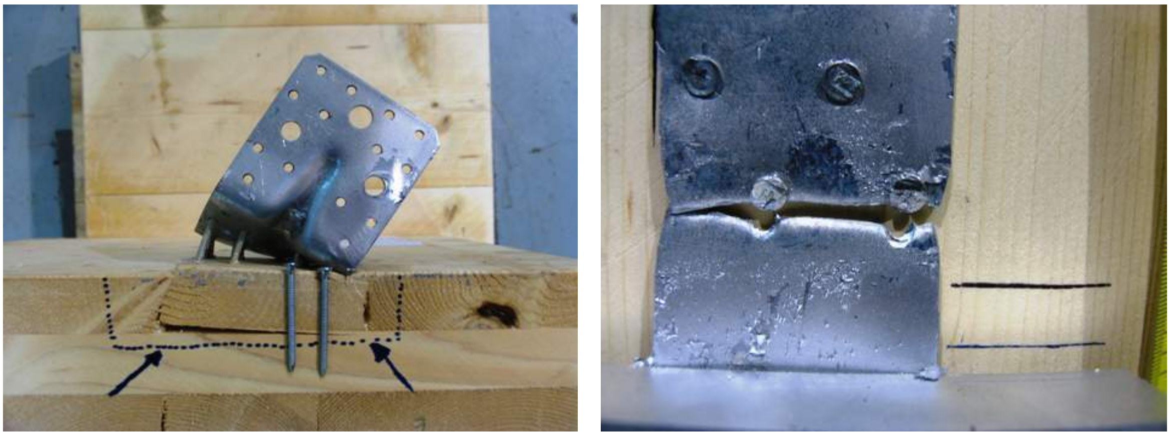

Fig. 11 a) Typical failure modes for configurations with one basic steel anchor only in angle brackets test; b) brittle failure of vertical steel plates

Overall, 36 tests were carried out on **hold-down** systems (22 monotonic tests and 14 cyclic tests). For elements of this type, the principal stress is a tension acting on the vertical axis. In this case, the global resistance values are not affected by the length of the nails, but depends mainly on the number of fasteners (nails) and on the ultimate tensile load of the steel vertical plate. As observed for angle brackets, the ratio between the stiffness K_{el} (carried out from standard as the product $K_{ser} \cdot n_{nails}$) and the experimental global stiffness $K_{s,el}$ reaches values in the range of 2-5.

HD 406, HD 559, HD 285 and HD 620 types showed, in the cases of both monotonic and cyclic tests, collapse due to the tensile fracture of the vertical plate. The fracture always happened on the first section with the minimum net area. This phenomenon occurred for values lower than the total bearing capacity of the nailed connection. In order clearly to understand the phenomenon of a collapse really affecting the nailed connection, some tests were carried out with a not "fully nailed" configuration but also with a lower number of metal fasteners. For these elements, and only in these cases, a ductile collapse due to the failure of nails was observed. The HD 340 type hold-down, by contrast, showed the most efficient behaviour. These elements appeared to be the most optimized because a brittle failure of the vertical steel plate was never observed.

3.2 Test on single CLT walls

3.2.1 Test on CLT wall: materials and set-up

The goal of the experimental campaign was to evaluate the behaviour of CLT shear walls subjected to both static and cyclic lateral load, in function of variables such as entity of vertical load, type of connections, presence of openings, presence of intermediate floors, etc. Test specimens were square wall segments 2.50 m by 2.50 m, 3-layer CTL panels, and they were used for all the tests. The total thickness of the panels was 90 mm, each layer being 30 mm thick. The main variables characterizing the specimens are described in Tab. 3. For all the tests standard commercial hold-down elements were used; for the shear connection with angle brackets both standard and new, specially developed elements were used. They were connected to CLT panels with 4.0 mm x 60 mm (d x L) annular ring nails. All metal connection devices were placed on only one side of the wall, in an asymmetric configuration.

Tests in two different main configurations were performed: the first one to simulate the connection between the walls and the concrete slab used for the first floor, and the second one simulating the floor/wall connection used for the upper floors in CLT building. In this latter case, the brackets were connected to the floor panel with nails fixed on the base flange. The CLT panels used to simulate the floor were rigidly connected to the base beam. To prevent relative sliding between the floor panel and the base beam, a special counter-plate reinforced by welded ribs was fixed at the ending of the base beam using 6 M20 bolts. With this configuration only the relative displacement between the wall and the floor was measured.

Tab. 3 CLT test: geometry and test configurations

n°	Type of wall	CLT	L	AB		HD		Protocol	Foundation	Notes
		[mm]		*n°*	*type*	*n°*	*type*			
1	***L0_AB90CR_HD340***	*30-30-30*	*0 kN*	*3*	*90CR*	*2*	*340*	*M/C*	*concrete*	
2	***L20_AB90CR_HD340***	*30-30-30*	*20 kN*	*3*	*90CR*	*2*	*340*	*M/C*	*concrete*	
3	***L20_AB90CR_HD340-1***	*30-30-30*	*20 kN*	*3*	*90CR*	*2*	*340*	*C*	*concrete*	*1 anchor for AB*
4	***L20_AB200_HD340***	*30-30-30*	*20 kN*	*3*	*200NEW*	*2*	*340*	*M/C*	*concrete*	
5	***L20_AB200***	*30-30-30*	*20 kN*	*3*	*200NEW*	*-*	*-*	*C*	*concrete*	
6	***L0_AB200_HD620***	*30-30-30*	*0 kN*	*3*	*200NEW*	*2*	*620*	*M/C*	*concrete*	
7	***L20_AB200_HD620***	*30-30-30*	*20 kN*	*3*	*200NEW*	*2*	*620*	*M/C*	*concrete*	
8	***L0_AB200CR_HD620***	*30-30-30*	*0 kN*	*3*	*200NEW_CR*	*2*	*620*	*M/C*	*concrete*	
9	***L20_AB200CR_HD620***	*30-30-30*	*20 kN*	*3*	*200NEW_CR*	*2*	*620*	*M/C*	*wooden floor*	
10	***L0_AB90CR_HD340-f***	*30-30-30*	*0 kN*	*3*	*90CR*	*2*	*340*	*C*	*wooden floor*	
11	***L20_AB90CR_HD340-f***	*30-30-30*	*20 kN*	*3*	*90CR*	*2*	*340*	*C*	*wooden floor*	
12	***L0_AB200_HD620-f***	*30-30-30*	*0 kN*	*3*	*200NEW*	*2*	*620*	*C*	*wooden floor*	
13	***L20_AB200_HD620-f***	*30-30-30*	*20 kN*	*3*	*200NEW*	*2*	*620*	*C*	*wooden floor*	
14	***L20_AB90CR_HD340-w***	*30-30-30*	*20 kN*	*3*	*90CR*	*2*	*340*	*C*	*concrete*	*window*
15	***L20_AB90CR_HD340-d***	*30-30-30*	*20 kN*	*3*	*90CR*	*2*	*340*	*C*	*concrete*	*door*

Legend*: L: load; AB: angle bracket; HD: hold down; Protocol: monotone or cyclic test; Foundation: connection type from wall to floor; Notes: if there are holes in the walls (windows or doors) or the type of anchor with angle brackets*

The set-up used during the experimental campaign allowed the simultaneous application of vertical load and horizontal displacement (Fig. 12a). The application of the vertical loads was obtained by counterweights suspended from horizontal levers hinged on a fixed frame. Spherical hinges were used to allow the three-dimensional independent free displacement of the beams. The position of the points of suspension of counterweights on the levers could be translated to apply different load levels. The horizontal displacement at the top of the wall was provided by a hydraulic actuator with a special device. This allowed relative rotation and the vertical scroll between the plate against the wall and actuator fixed to the contrast wall. In order to enable cyclic tests, fixed on the opposite side of the wall was a plate attached with four threaded bars to the head of the actuator. Vertical pads connected to the fixed frame were placed to prevent overturning of the wall in the direction orthogonal to the test. To minimize the friction forces between the wall and set–up, the pads were covered with sheets of plastic material with a low friction surface (PTFE). Angle brackets and hold-downs that constrained the sample were fixed to a base made of steel and filled with concrete. This structure was made of two UPN profiles spaced with steel traverses internally to which concrete was cast. Threaded bushes were welded on the traverses to allow screwing bolts of the sill beam, while holes were made in the wings of UPN profiles for the insertion of the angle brackets and hold-down bolts. Using these components, it was possible to reproduce the real fixing between the CLT wall and the foundation, and it was also possible to replace the sample quickly without making a new hole in the concrete base.

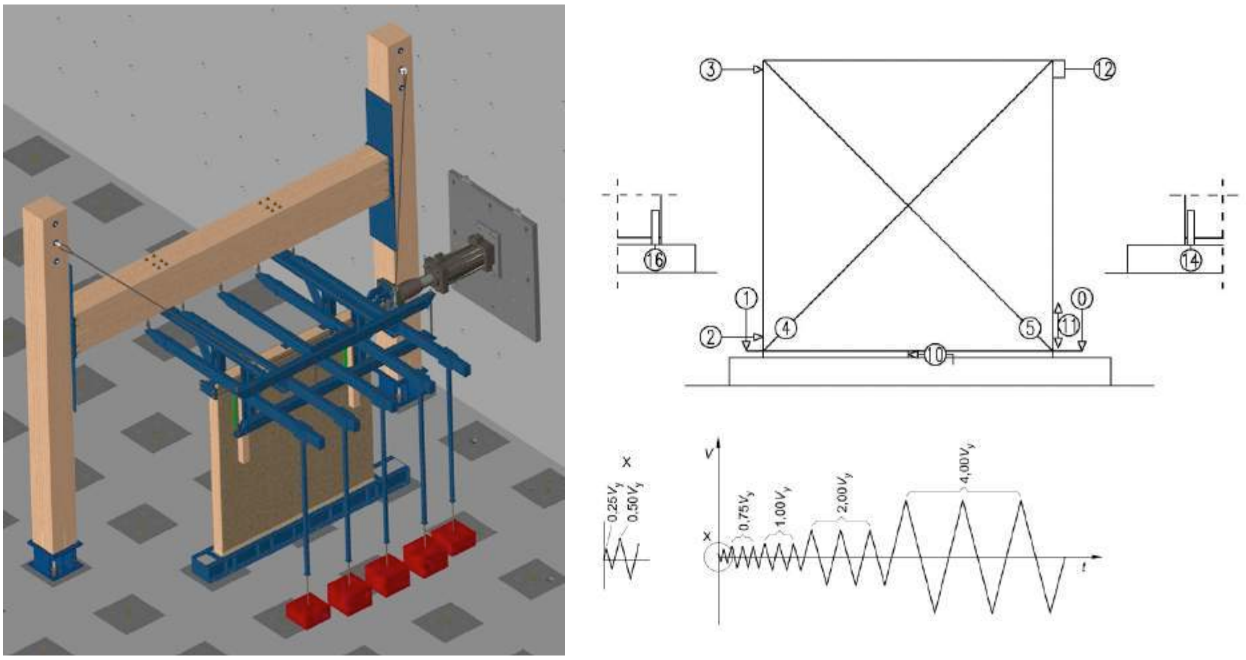

Fig. 12 a) test set-up, designed to apply to the shear wall monotonic and cyclic lateral load, and vertical fixed load; b) instrument position and cyclic procedure according to EN 12512

Different measurement devices were positioned on the wall, as shown in Fig. 12b. LVDT transducers measured the uplift of the wall (L0 for monotonic/cyclic tests, L1 measured only for the cyclic tests), the horizontal relative displacement between the ground and the bottom surface (L2), the horizontal displacement at the upper top plate (L3). Wire potentiometers measured the shear deformation in the plane of the panel (L4 and L5). The load cell of the hydraulic jack measured the force applied at the top (LC12). Load cells incorporated in the hold-down bolts measured the vertical reactions under the wall (LC14 and LC15). The horizontal load was applied by monotonically advancing the actuator until the specimen’s failure, with a rate of loading selected equal to 0.05 mm/s. The cyclic test procedure was formulated in accordance with EN 12512 [7].

3.2.2 Test on CLT wall: test-results and discussion

The in-plane shear deformation of the CLT panels could be considered negligible compared with the other displacement contributions correlated to the connection devices. This was observed for all specimen configurations in Tab. 3, since a low in-plane deformation of the panel was measured by the L4 and L5 wire potentiometers.

In regard to the failure of specimens, it was observed that collapse never occurred on the panel itself but involved the capacity of base connections in different ways depending on the test. Failure mechanisms never involved the maximum shear capacity of the angle brackets, even in the case of the less resistant type AB-90CR. In all cases, it was observed that failure started from the nailed connection of the vertical plate of the hold-down in tension: two different types of ultimate failure were observed, depending on the type of hold-down used. In the case of HD-340 hold-downs, failure occurred with a composite mechanism that involved the shear-withdrawal capacities of the vertical nailed connection. The bending deformation on the base plate around the bolt used for connection to the ground was limited by the use of a 20 mm thick steel washer. Type HD-340 hold-downs never had failure on the vertical steel plate itself. A marked difference with the case of the stronger HD-620 hold-down was observed. In all those tests, whatever the type of the bracket and the load configuration, a brittle fracture on the vertical steel plate occurred because of the higher total strength of the nailed connection compared with the axial strength in tension of the plate itself. A brittle fracture on the external layer of the CLT was rarely observed, probably due to imperfect gluing, with a group tear-out failure mechanism occurring around the fasteners. Fig. 13a illustrates the strong influence of the hold-down configuration on the behaviour of the wall under lateral load, in terms of both stiffness and ultimate load. To be noted is that the three different cases analysed (no hold-down, HD-340, HD-620) present a similar initial stiffness. It may therefore be supposed that, during the first steps of the test, friction and axial stiffness of the brackets played a significant role. As the horizontal imposed displacement increased, the role of the hold-down grew stronger not only in terms of stiffness but also in regard to the ultimate load.

Fig. 13b shows the experimental results for tests on the connection between panel and base beam (concrete slipping surface) and the connection with CLT floor panel. In the case of tests with the same connection device, the maximum force and the shapes of diagrams did not strongly depend on the type of base adopted. Moreover, the failure of the system was always related to the failure of the hold-down in tension, which caused a sudden fall in terms of strength. Some behaviour differences should be noted when horizontal displacement is considered.

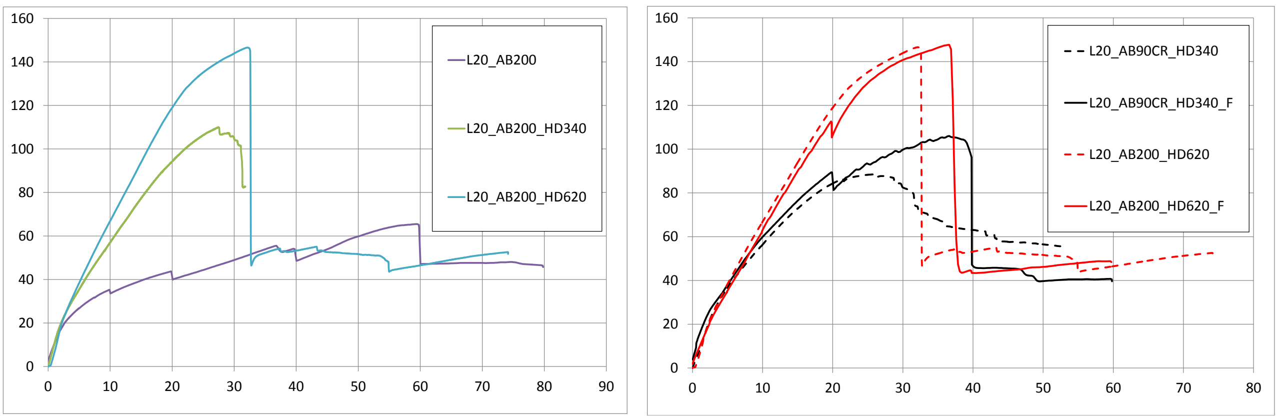

Fig. 13 Comparison between experimental F-v curves (kN-mm)in function of the type of hold-down a) and of the type of basement (concrete or wood) b)

The vertical load acting at the top of the panel did not influence the behaviour of the walls in terms of the ultimate collapse mechanism, which was always related to the hold-down (the weakest link in the chain of resisting elements). But its effect in terms of increase in maximum horizontal load-carrying capacity and global stiffness is clearly visible from the experimental curves reported in Fig. 14a, where two levels of loads (0-10 kN/m) are considered. As a matter of fact, the rocking mechanism is strongly influenced by the level of vertical forces, which allow for reduction of the traction force absorbed by the hold-down.

Openings in walls, like windows or doors, inevitably entail a decrease in strength and stiffness compared with walls without openings. In two specimens, a 1 x 1 m window and a 0.8 x2,1 m door were cut into the CLT wall: the experimental results of walls with and without openings are compared in Fig. 14b; they show a evident decrease of performance in the case of the door opening.

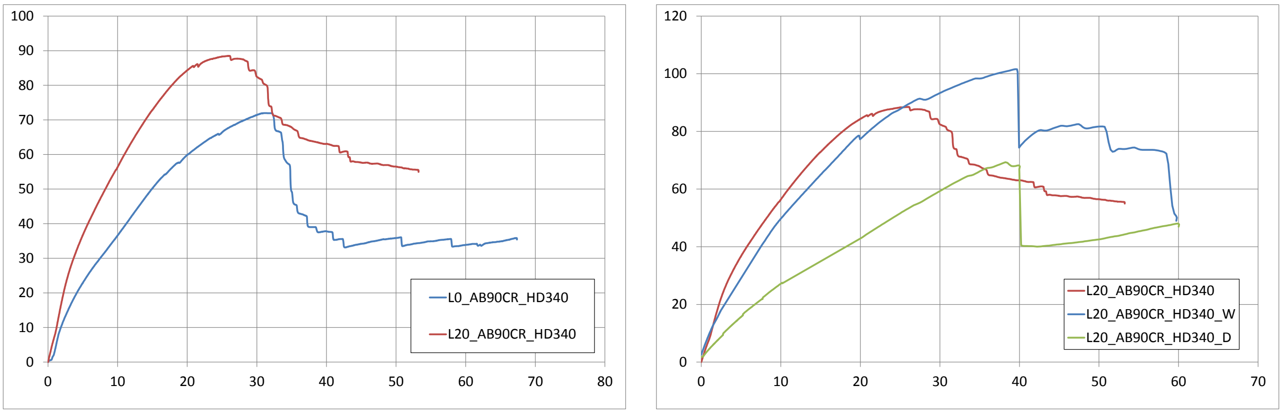

Fig. 14 Comparison between experimental F-v curves (kN-mm)in function of the load level a) and of the presence of opening b)

4. Conclusion and future work

The role of connection systems in the performance of CLT buildings under lateral load has been discussed and investigated. The primary experimental outcome of the research is that, for the tested configuration of the CLT wall, the overall mechanism should always be referred to the failure of the connection device, especially for the elements placed to prevent the in-plane uplift. The research presented is part of broader investigation performed at the University of Trento on the seismic behavior of timber multi-storey buildings. The project comprises the coordination of shaking table tests performed on different real size specimens with the same geometry but built with different timber technology (log house, platform frame, CLT), within the framework of the Series Project (Seismic Engineering Research Infrastructures for European Synergies). On the basis of this wide experimental database, future work will be devoted to proposing and validating possible design approaches for multi-storey buildings in seismic zones.

5. Acknowledgements

The author wishes to thank former students Ermanno Acler, Paolo Endrizzi and Michele Webber for their valuable contribution to the research. Moreover, Gianluca Mischi is thanked for his help in revising the paper.

6. References

[1] Tomasi R, *Joint and connection in CLT: theory and practice* (*in Italian*) www.promolegno.com

[2] Blaas, H.J., Uibel, Th., Forschung an der Universität Karlsruhe –Stiftförmige Verbindungsmittel in Brettsperrholz, In: 5. Grazer Holzbau Fachtagung- Tagungsband,

ISBN: 3-90-2020-32-6, Graz, 2006

[3] Pirnbacher, G., Traetta, G., Schickhofer, G., Forschung an der TU Graz – Anwendung der Johansen-Theorie für gekreuzt geschichtete Strukturen, In: 5. Grazer Holzbau Fachtagung-Tagungsband, ISBN: 3-90-2020-32-6, Graz, 2006

[4] Acler E., Piazza M., Tomasi R, Webber M. *Experimental investigation of the behavior of different types of connections between the XLAM panels and the concrete slab*. In: Structural engineeringworld congress, Villa Erba, Cernobbio, Como, Italy; 2011

[5] EN 26891:1991. Timber structures – joints made with mechanical fasteners: general principles for the determination of strength and deformation. CEN, European Committee for Standardization, Brussels, Belgium; 1991.

[6] EN1995-1-1:2004. Design of timber structures Part 1-1: General-common rules and rules for building. CEN, European Committee for Standardization, Brussels, Belgium; 2004. 416

[7] EN12512:2001/A1:2005. Timber structures – test methods – cyclic testing of joints made with mechanical fasteners. CEN, European Committee for Standardization, Brussels, Belgium; 2005.

CLT Wall Elements Under Cyclic Loading – Details for Anchorage and Connection

Johannes Hummel
Chair of Timber Engineering
University of Kassel, Germany

Georg Flatscher
Institute of Timber Engineering and Wood Technology
TU Graz, Austria

Werner Seim
Chair of Timber Engineering
University of Kassel, Germany

Gerhard Schickhofer
Institute of Timber Engineering and Wood Technology
TU Graz, Austria

Summary

This paper presents the results of experimental studies on the behaviour of CLT walls under cyclic loading carried out at the University of Kassel and TU Graz with focus on the influence of different configurations of anchorage and connection. Results of a case study – performed to identify realistic loading conditions of wall elements for testing – are presented first. A brief introduction on data processing is given to evaluate parameters like ductility and hysteretic damping. The influence of vertical load, support conditions and loading protocol is also discussed.

1. Introduction

For building structures under earthquake impact, various approaches have been developed to assess safety levels and to properly design structural elements and details. Force-based design (lateral force method), non-linear static (pushover) analysis and non-linear time history (dynamic) analysis [1] have different level of accuracy to represent geometrical details and material behaviour. Even though it might be questionable whether a higher level of input accuracy always leads to more accurate results, it is undisputable that there is a minimum amount of information needed to design properly the lateral load-resisting system. All different modelling techniques are characterized by the need to disassemble a structural system into several, simpler subsystems. Therefore knowing the behaviour of subsystems like wall and slab elements under cyclic loading considering their interaction is the basis for every calculation method.

It is widely accepted that hysteresis loops from cyclic testing of elements under reverse horizontal loading provide the most comprehensive information. Load vs. deflection curves can be converted directly to multi-linear approximations to be used in time history analyses (e.g. FRAGIACOMO & RINALDIN [2]). Moreover, element stiffness and ductility, which are basic parameters for force-based design, can be derived simple by simple data processing (e.g. SEIM & VOGT [3]).

According to modern design criteria for seismic resistance, CLT buildings are designed for a specific performance level, which goes from completely elastic (see DUJIC & AL. [4],[5]) to specific post-elastic deformations providing a certain amount of energy dissipation.

As the energy dissipation of the CLT-element itself is negligible, the potential for ductile behaviour must be assigned to the connections. In this context the complete understanding of the interaction between wall and slab elements resp. foundation is indispensable. Valuable basic information has already been published by POPOVSKI & KARACABEYLI [6] with a focus on connections and details commonly used in North America.

To account for European construction practice, two research studies have been performed at University of Kassel and TU Graz. In the context of construction practice, the following issues were identified as the most important ones.

1) Anchoring of the wall-element: a quasi-rigid restraint exists only at the first level of a multi-storey building where the basement or the foundation is mostly a reinforced concrete structure. At all other levels the interconnection of wall elements for vertical and horizontal forces is through a slab element. Tie-downs and angle brackets are commonly used for these details, however connection with only self-tapping screws is also possible. In all cases deformation and energy dissipation is affected by the contribution of the slab.
2) Contact area where compression forces are transferred: the situation might vary from timber-to-timber with comparatively high potential for friction to plastic interlayers attached for air tightness resulting in near zero-friction.
3) Size of the panels: construction practice requires large elements for speed and quality control on site. Therefore the cutting of wall elements into substructures should be avoided even if this would increase the potential for ductility. As a consequence of that, load transfer around openings must be ensured to avoid brittle anticipated failure in these areas.

At the beginning of the following sections, some basic considerations about loading conditions will be presented first, and the data processing will be explained. The test setup will then be documented, and the most important results will be presented.

Fig. 1 Test set-up for wall element testing

2. Testing conditions and data processing

2.1 Pre-calculations on wall-slab interaction

First of all, it was necessary to identify realistic loading conditions for the test set-up (Fig. 1). Consequently, pre-investigations with representative multi-storey timber buildings (e.g. see Fig. 2) were performed under various seismic actions representing different earthquake-prone areas in Europe. These buildings have different floor plans and differ in the number and location of shear walls, and the presence and location of a reinforced concrete core. Aspects of building physics and fire safety were considered in the assembly of walls and slabs (see Fig. 3).

A common seismic analysis method used by engineers in practice – the response spectrum (or linear dynamic analysis) method – was applied for the seismic analysis of the three dimensional models. Different types of models were considered in this analysis where the connection flexibility plays an essential role; for example, modelling was enhanced from rigid (type 1) to elastic (type 2) connections, where the latter ones were modelled with linear elastic springs between structural elements.

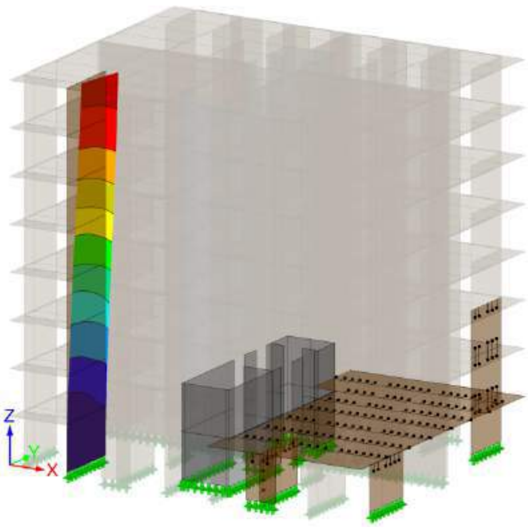

Fig. 2 Model of an 8-storey building and reference wall (left); connections modelled with springs (detail)

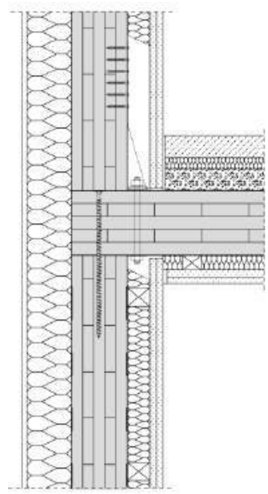

Fig. 3 Wall-slab connection detail

The level of modelling even in the elastic range influences the dynamic behaviour of the FE model, which can be seen in Fig. 4. If the model is more accurate, the natural vibration period shifts to the descending branch of the elastic response spectrum, which leads to a substantial reduction of the seismic action (base shear).

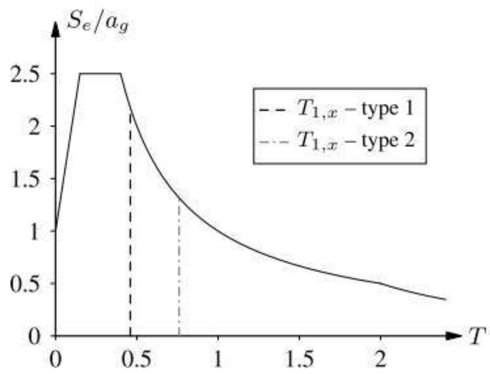

Fig. 4 Maximum acceleration depending on the natural vibration period for types 1 and 2 models

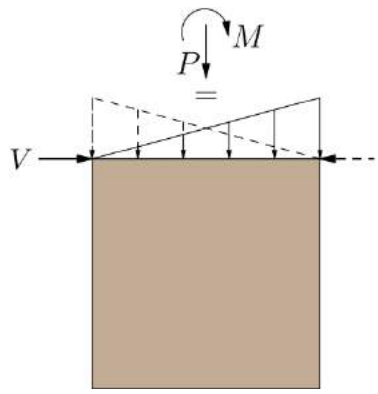

Fig. 5 Relation between horizontal and vertical loading (schematic)

The pre-investigations also show a clear interaction between horizontal and vertical loads (see Fig. 5). It was found that the loading condition of a certain wall, e.g. the wall depicted in Fig. 2, is a combination of vertical load and overturning moment. The vertical load (axial force) on the wall increases in the direction of the seismic excitation. This applies especially for walls in the lower storeys, whereas the distribution of the vertical load on walls in the middle and high storeys remains approximately constant. It was also found that the stiffness of the slab influences the distribution of horizontal loads due to in-plane stiffness and the distribution of the vertical loads due to their flexural stiffness. For more details see Hummel & Seim [7].

2.2 Data processing

Ductility μ and equivalent viscous damping v_{eq} are widely used to describe the characteristics of monotone and cyclic behaviour of structural elements and derive information for seismic design from testing. In general, the ductility factor μ is defined as the ratio between the ultimate deformation and the yield deformation, see equation (1).

$$\mu = \frac{D_u}{D_y} \tag{1}$$

To evaluate the yield point, there are different methods but there is no commonly accepted definition. A frequently used approach is the method described in EN 12512 [8]. The yield point according to EN 12512 is defined as the intersection point of the dashed lines displayed in Fig. 6. A widely accepted definition of the ultimate displacement D_u is to use the point of 0.8 F_{max} in the softening branch.

For data processing of cyclic tests, the value v_{eq} gives an amount of the damping behaviour of a structural element due to energy dissipation (see CHOPRA [9]). The equivalent viscous damping v_{eq} is defined as the ratio between the dissipated energy E_d and the potential energy E_p (divided by 4π) [9], see equation (2).

$$v_{eq} = \frac{E_d}{4\pi \cdot E_p} \tag{2}$$

The dissipated energy E_d is represented by the enclosed area of a cycle as shown in Fig. 4. The potential energy E_p is determined from the current stiffness corresponding to the maximum amplitude displacement u per hysteresis loop (see CHOPRA [9]).

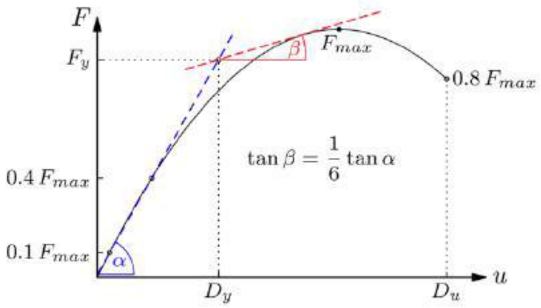

Fig. 6 Definition of yield point and ductility according to EN 12512 [8]

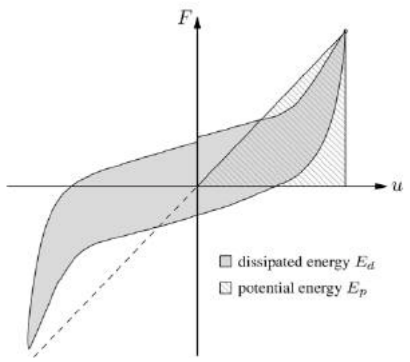

Fig. 7 Definition of equivalent viscous damping

3. Test results

3.1 Series W-CLT – University of Kassel

At the University of Kassel the seismic performance of timber structures is studied within the research project OPTIMBERQUAKE. Besides light-frame timber walls and moment-resisting frames, a main focus was placed on CLT-wall elements.

3.1.1 Configurations

Twelve wall elements (dimensions 2.50 m × 2.50 m) were tested under various conditions as shown in Tab. 1. The varied parameters are vertical load, support conditions and loading protocol. In almost all tests the combination with 2 hold-downs and 3 angle brackets (one-sided) was chosen. One test was carried out without angle brackets (only with hold downs). Two tests were performed with an elastomeric interlayer (sylodyn), and in one test a plastic interlayer (PE) used in construction practice to improve building physics was employed. The aim of these tests was to observe the influence of friction.

Tab. 1 Testing program, University of Kassel

test	vertical load	connection	support	loading protocol
W-CLT-1.1	10 kN/m	2 HD, 3 AB	rigid (steel)	monotonic ISO 21581
W-CLT-1.2	10 kN/m	2 HD, 3 AB	rigid (steel)	cyclic ISO 21581
W-CLT-1.3	10 kN/m	2 HD, 3 AB	rigid (steel)	cyclic CUREE
W-CLT-2.1	50 kN/m	2 HD, 3 AB	rigid (steel)	monotonic ISO 21581
W-CLT-2.2	50 kN/m	2 HD, 3 AB	rigid (steel)	cyclic ISO 21581
W-CLT-2.3	50 kN/m	2 HD, 3 AB	rigid (steel)	cyclic CUREE
W-CLT-3.1	10 kN/m	2 HD, 3 AB	CLT	monotonic ISO 21581
W-CLT-3.2	10 kN/m	2 HD, 3 AB	CLT	cyclic ISO 21581
W-CLT-3.3	50 kN/m	2 HD, 3 AB	CLT	cyclic ISO 21581
W-CLT-3.4	50 kN/m	2 HD, 3 AB	CLT + sylodyn	cyclic ISO 21581
W-CLT-3.5	50 kN/m	2 HD, 3 AB	rigid (steel)+ 2×PE	cyclic ISO 21581
W-CLT-3.6	10 kN/m	2 HD	CLT + sylodyn	cyclic ISO 21581

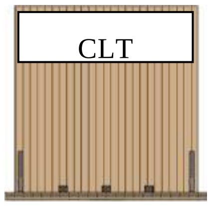

HD - hold down, AB - angle bracket, sylodyn - elastomeric interlayer, PE - PE sheet

3.1.2 Results

Tab. 2 presents the main results from data processing (according to section 2.2). For evaluation of cyclic tests the first backbone curve (e.g. Fig. 8 and Fig. 9) was used to determine the maximum load F_{max}, the ductility factor μ and the stiffness K_{ser} and the third envelope curve to calculate the equivalent viscous damping ν_{eq}. Although the connector configurations are basically the same, the results are significantly different. This applies for maximum load, stiffness, ductility and damping ratio.

Tab. 2 Results from post-processing of monotonic and cyclic tests

test	F_{max} [kN]	K_{ser} [kN/mm]	μ [-]	v_{eq} [-]	contribution to deflection CLT	Slip	Rocking
W-CLT-1.1	102.1	4.72	3.2	–	5%	28%	67%
W-CLT-1.2	89.1	4.53	4.2	0.103	4%	24%	72%
W-CLT-1.3	94.1	4.08	3.5	0.141	6%	24%	70%
W-CLT-2.1	133.3	8.02	6.6	–	7%	33%	60%
W-CLT-2.2	122.4	11.40	9.1	0.162	3%	44%	53%
W-CLT-2.3	126.4	12.17	12.1	0.269	5%	34%	61%
W-CLT-3.1	74.7	4.53	9.3	–	3%	17%	80%
W-CLT-3.2	63.2	5.80	14.9	0.084	4%	22%	74%
W-CLT-3.3	92.5	15.51	21.4	0.091	7%	17%	76%
W-CLT-3.4	98.9	5.93	5.2	0.085	4%	23%	73%
W-CLT-3.5	106.3	7.01	4.7	0.127	5%	46%	49%
W-CLT-3.6	39.9	1.86	4.9	0.152	4%	43%	53%

mechanism

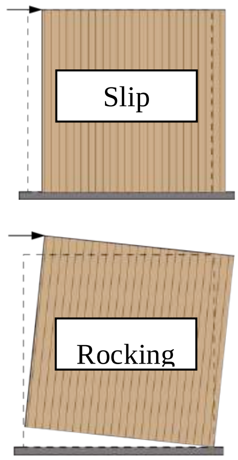

'CLT' stands for the inherent deformation of the CLT-element due to bending and shear.

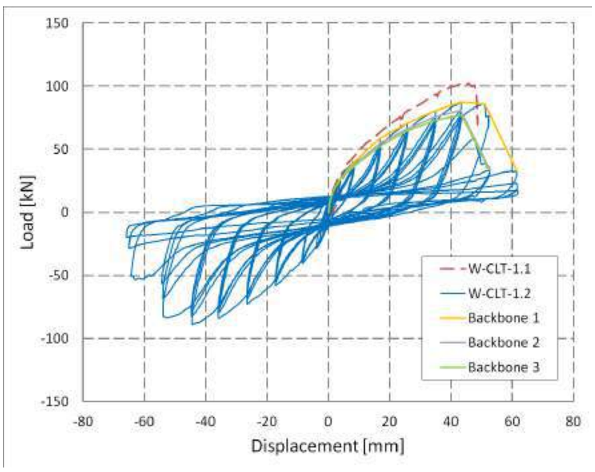

Fig. 8 Load-displacement curve of tests W-CLT-1.1 (monotonic) and W-CLT-1.2 (cyclic) and backbone curves from cyclic test

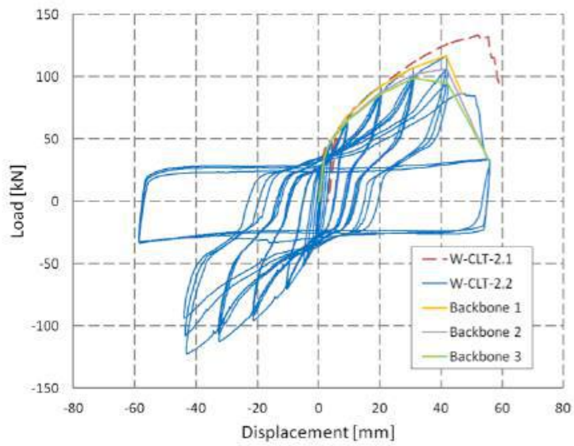

Fig. 9 Load-displacement curve of tests W-CLT-2.1 (monotonic) and W-CLT-2.2 (cyclic) and backbone curves from cyclic test

Failure modes

The failure modes of monotonic and cyclic tests are quite different. The monotonic tests failed mainly due to rocking (failure of the hold down – fracture of nail heads), whereas the cyclic tests exhibited a failure of the angle brackets resulting from a combination of slip (mainly) and rocking of CLT-element. In most cases, hold-downs did not fail under cyclic loading. However, a large uplift of the hold-downs due to a high indentation of the washer (∅ 68 mm) on the underside of the floor element was observed for hold-downs anchored to the CLT slab element. The different failure modes are documented in Fig. 10.

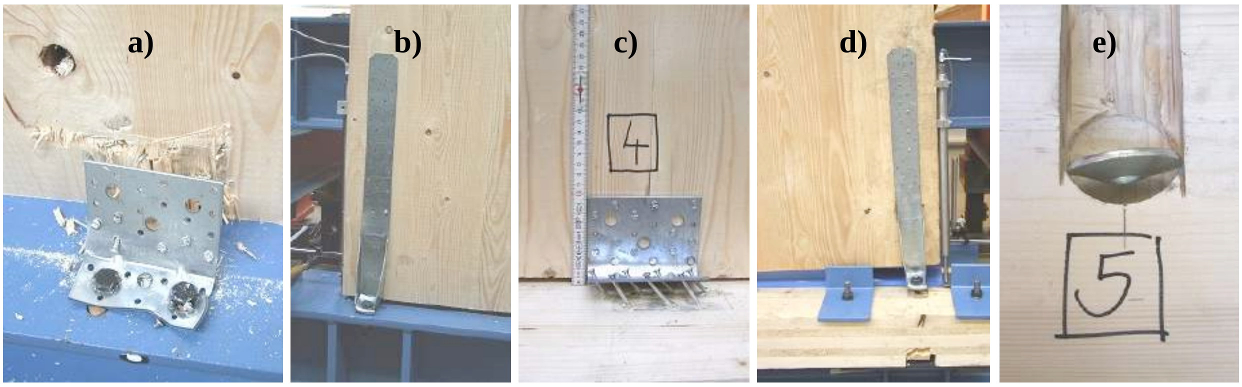

Fig. 10 Failure modes of connections
a) angle bracket (rigid support) – steel failure of the short leg and pull out of the ring shanked nails;b) hold down (rigid support) – uplift and fracture of the nail heads;
c) angle bracket (on CLT) – pull out of the ring shanked nails of the bottom leg;
d) hold down (on CLT with sylodyn) – high uplift due to indentation of the washer, see e); e) washer underneath the CLT-floor element – indentation and deformation of the washer

Load-bearing capacity – maximum horizontal forces

Tab. 2 makes it clear that parameters like vertical load and support conditions have a considerable influence on the load-bearing capacity of a wall. The comparison of the tests W-CLT-1.1 to W-CLT-1.3 versus W-CLT-2.1 to W-CLT-2.3 show an increase of the maximum forces by approximately 30 kN resulting from a higher vertical load (see Tab. 1). A similar effect is noticed in tests W-CLT-3.1 vs. W-CLT-3.4 where the difference between maximum forces is not that high. On the other hand the influence of the loading protocol on maximum force can be considered as negligible. However, the achieved horizontal loads in the test according to the CUREE protocol lie between the values of the monotonic and cyclic tests according to ISO 21581.

Test W-CLT-3.5 – with two PE sheets representing a double interlayer for air tightness – exhibit a lower maximum force because of a reduction in friction. Surprisingly, a maximum load of almost 40 kN was reached with the configuration without angle brackets (W-CLT-3.6) for which the calculated load bearing capacity according to design provisions would be actually zero.

Stiffness and ductility

A correlation between the initial stiffness K_{ser} and the ductility seems to exist, since both values were influenced by the vertical load and support conditions in a similar manner. From W-CLT-1.1 to W-CLT-2.3 tests, it can be also seen that initial stiffness and ductility increase when the vertical load increases. The type of interlayer rather than the support condition also influences the stiffness K_{ser} and ductility, as the use of an interlayer reduced the initial stiffness as shown in Tab. 2.

Hysteretic damping

The equivalent viscous damping is highly affected by the vertical load and support conditions. Higher vertical loads maximize the damping value for the rigid support condition due to the effect of friction, whereas the vertical load has no substantial influence for bearing on CLT. This conclusion is also supported by the results of test W-CLT-3.5. Reasons for the comparatively low damping values of W-CLT-3.2 – W-CLT-3.4 tests are different failure modes of the angle brackets (see Fig. 10c). Due to pull out of the nails in the lower leg, the capacity of the angle brackets to dissipate energy is significantly reduced. Surprisingly, configuration W-CLT-3.6 without angle brackets exhibits a comparatively high damping capacity. That is caused by a high slip contribution to the total deflection and thus high energy dissipation due to friction in combination with a relatively low stiffness. This leads to the conclusion that there must be an interaction between predominant contribution to the total deflection – either slip or rocking – and hysteretic damping and, therefore, energy dissipation. The equivalent viscous damping is also influenced by the loading protocol. It can be seen from Tab. 2 that the use of the CUREE protocol yields to higher damping values in comparison with the ISO protocol.

3.2 Series WA – TU Graz

Research at the Graz University of Technology Institute of Timber Engineering and Wood Technology regarding the cyclic behaviour of CLT-buildings has been structured in three steps: (i) single joint tests, (ii) tests on wall elements, and (iii) shaking table tests on a three storey building. This paper focuses on step (ii).

The tests on single wall elements carried out at the University of Kassel in summer 2012 and presented in the previous sections, were designed based on the preliminary results of the single joint tests (see [10]).

3.2.1 Configurations

Tab. 3 and Fig. 11 give information on the tested wall configurations and basic parameters. Angle brackets and hold-downs were only mounted on one side of the wall. The aim of these tests was to analyse the influence of various connections, vertical loads and wall geometries on the monotonic and cyclic behaviour of in plane horizontally loaded CLT walls.

Tab. 3 Testing program, TU Graz

ID	vertical load	connections	geometries
WA_A	20.8 kN/m | 0 kN/m	4 angle brackets	2.5 m × 2.5 m
WA_B	20.8 kN/m | 5.0 kN/m	2 angle brackets | 2 hold downs	2.5 m × 2.5 m
WA_C	20.8 kN/m	4 angle brackets and ∅ 6.0×100 mm screws	2 pieces 1.25 m × 2.5 m
WA_D	20.8 kN/m | 5.0 kN/m	∅ 8.0×280 mm	2.5 m × 2.5 m
WA_E	20.8 kN/m | 5.0 kN/m	2 angle brackets | 2 hold down	2.5 m × 2.5 m with a door opening

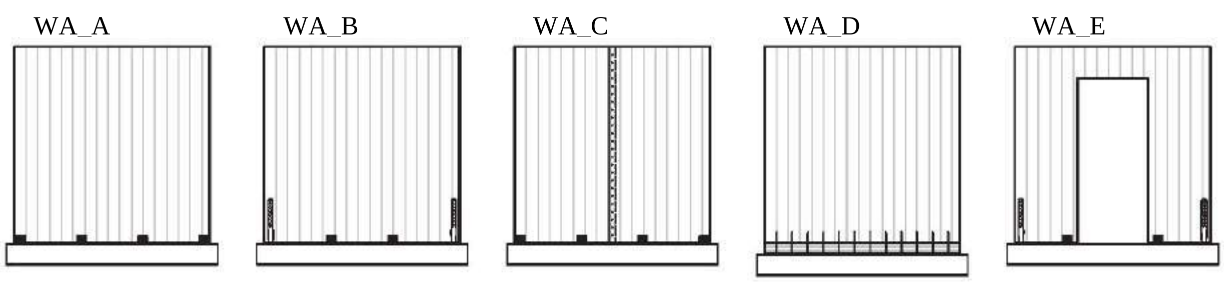

Fig. 11 Test configurations of wall, TU Graz

Each configuration was at least tested once under both monotonic and cyclic loading according to ISO 21581:2010 [11].

3.2.2 First results

Tab. 4 gives a brief overview of the results only of tests with a vertical load of 20.8 [kN/m]. Moreover the total deflection is given as a sum of deformation of CLT (due to shear and bending), slip and rocking of the wall. These contributions were calculated based on average values of the whole test. More details are shown in [12].

Data processing was done in two steps: step one comprises a so called ‘standard analysis’ and includes the description of failure modes and specific values like maximum force, stiffness and ductility; step two includes the analysis of the contributions to the total deflection. In this analysis the calculation of the stiffness K_{ser} is based on EN 26891:1991 [13] (calculation of stiffenes based on F_{est}). For ductility, the formulas given in EN 12512 [8] were used as reference (see section 2.2).

Tab. 4 Test results (mean values) of monotonic and cyclic tests

ID	**standard analysis**				**deflection contributions**		
	F_{max} [kN]	K_{ser} [kN/mm]	μ [-]	ν_{eq} [-]	CLT	slip	rocking
WA_A_M02	62.77	9.928	18.7	–	4 %	14 %	82 %
WA_A_Z01	63.00	9.623	13.9	0.169	10 %	22 %	68 %
WA_B_M01	77.36	7.754	8.3	–	5 %	41 %	54 %
WA_B_Z01	71.70	4.992	5.5	0.202	11 %	41 %	48 %
WA_C_M02	64.80	9.298	18.0	–	6 %	19 %	75 %
WA_C_Z01	62.80	14.994	26.0	0.151	9 %	25 %	66 %
WA_D_M01	51.07	13.918	14.9	–	7 %	8 %	85 %
WA_D_Z01	60.40	14.403	13.3	0.159	11 %	9 %	80 %
WA_E_M01	74.62	4.290	5.4	–	26 %	34 %	40 %
WA_E_Z01	75.80	4.293	6.0	0.161	43 %	26 %	31 %

Failure modes

The failure modes of angle brackets were found to be highly dependent on their position within the wall. If the bracket was situated at the end of the wall, then a significant deformation was attained and failure of the metal part of the angle bracket was the main failure mechanism (Fig. 12a). If the brackets were placed in the middle of the wall, then a mixed failure mechanism as expected for combined shear and axial loads was observed. Especially in cyclic tests, a shear failure was documented (Fig. 12b).

In hold-downs, the dominant failure mode was fracture of nail heads (Fig. 12c). Rotation of the metal part of the hold down caused by shear load was also observed (Fig. 12d).

In configuration D, failure for screw withdrawal was primary observed in the wall panel, but partly also in the slab elements. None of the screws showed steel failure.

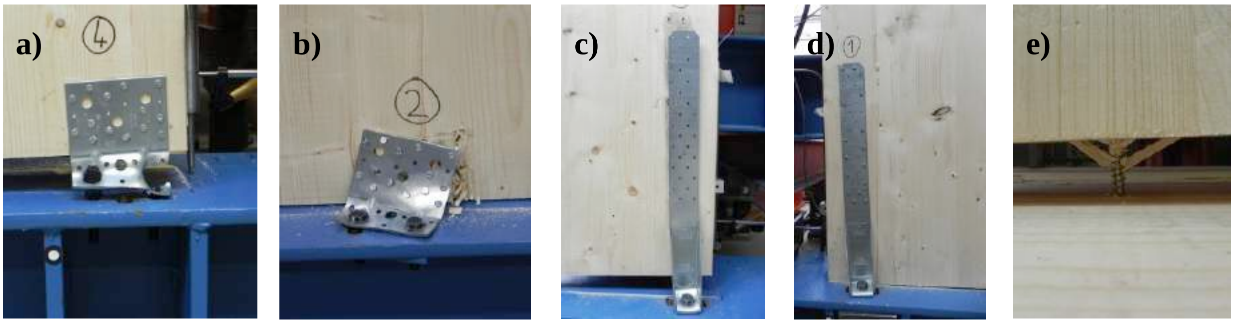

Fig. 12 failure modes of connections
a) metal sheet deformation; b) shear failure; c) fracture of nail heads;
d) rotation of metal part of hold down; e) screw withdrawal failure

Loads

With the maximum loads of configuration A considered as a reference, comparable loads in configuration C were found. Conversely, the loads of Configuration B were slightly higher due to: (i) the number of nails in the hold downs (one more nail (15) with respect to the brackets (14)), and (ii) the higher axial stiffness of the hold-downs compared to angle brackets. Based on the comparable results of configuration B and E, it can be concluded that the door opening did not affect the maximum load. The results of configuration D have to be analysed separately as the behaviour of screws is completely different from that of the other types of connections. Nevertheless, the same maximum loads as in the other configurations were reached.

Stiffness

In contrast to the maximum loads, a clearly different behaviour in terms of stiffness can be noticed among the different configurations. In configuration D and in the cyclic test of configuration C, the highest stiffness was observed. A possible reason is seen in the interaction with friction, which occurs already at small shear deformations of the wall and screws, respectively.

The higher stiffness of configuration A compared to configuration B is seen as a consequence of the low shear stiffness of the hold-downs.

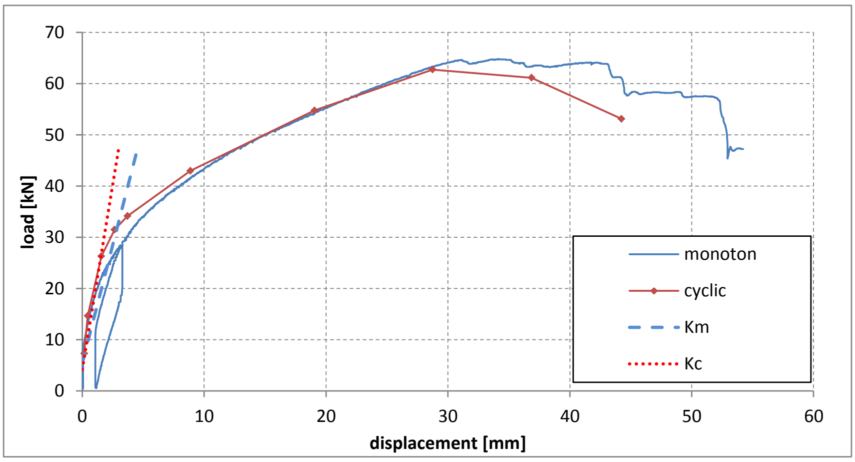

Surprisingly, an increase in stiffness of 60% from the monotonic to the cyclic loading appears in configuration C. However, analysis of the overall load-displacement curves reveals only minor differences (see Fig. 13).

Fig. 13 monotonic and cyclic backbone curve of configuration C

Ductility

In general the ductility observed is relatively high. Of course a more detailed investigation is required.

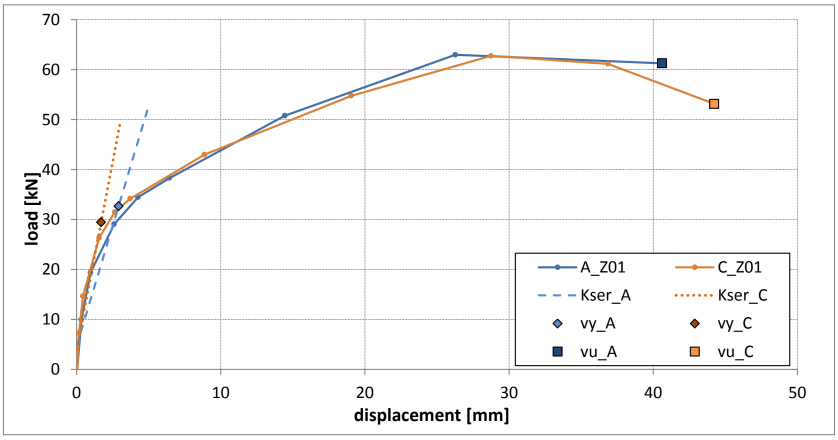

Fig. 14 cyclic backbone curve of configurations A and C

By comparing the ductility (and stiffness) ratios of cyclically tested configurations A and C may lead to the conclusion that their behaviour is different. However, a qualitative analysis of the load-displacement graph in Fig. 14 does not necessarily confirm this result.

Contributions to the total deflection

Tab. 4 gives average percentages obtained from the whole tests. The CLT-elements without openings were very stiff (including bending and shear deformations) and their contribution to the overall deflection can be estimated as 5-10 %. The contributions of slip (translation) and rocking (rotation) depend more on the type and design of joints. Overall, a higher contribution of rocking was observed in all configurations.

4. Summary and Conclusions

To summarize the results of wall elements tested at the University of Kassel and TU Graz, additional diagrams will be discussed. As mentioned above, there is a relation between initial stiffness and ductility. Fig. 15 illustrates that there is an increasing ductility for higher values of stiffness K_{ser}. The significant contribution of the connectors in terms of stiffness and ductility can be noticed if test W-CLT-1.1 to W-CLT-2.3 and WA_A_M02 to WA_A_C_Z01 are compared. Tests W-CLT-2.1 to W-CLT-2.3 have been used for wall-foundation connection with a vertical load of 50 kN/m, whilst tests WA_A_M02 and WA_A_Z01 have been used as alternative configurations (angle brackets only) with a vertical load of 20.8 kN/m. The second configuration shows only a slightly lower stiffness, but a much higher ductility.

From Fig. 16, it appears that there might be an influence between the slip contribution on the total deflection and the equivalent viscous damping. For test W-CLT-1.2 to W-CLT-2.3 and WA_A_Z01 to WA_E_Z01 there is a higher damping value if the slip contribution increases. This effect is similar for the support on CLT (W-CLT-3.2 to W-CLT-3.6) where the equivalent viscous damping is lower compared to the configuration with a rigid support. A possible reason for this relation could be that the energy dissipation increases due to a higher amount of friction.

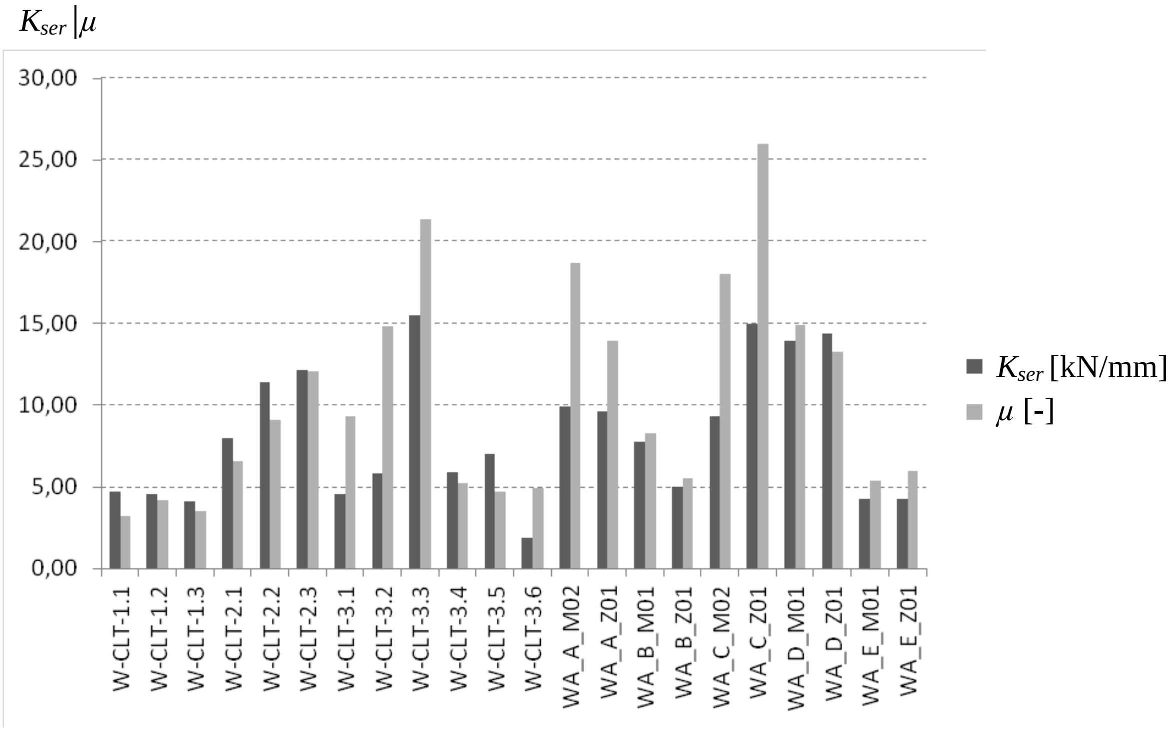

Fig. 15 Stiffness K_{ser} and ductility μ of series W-CLT and series WA

As mentioned above, also the loading protocol has a main effect on the equivalent viscous damping (see also [14]). This is shown by the comparison of test W-CLT-1.2 (ISO) with W-CLT-1.3 (CUREE) as well as by W-CLT-2.2 (ISO) with W-CLT-2.3 (CUREE).

In addition, it should be noted that the coupled wall specimen (WA_C_Z01) did not show a higher damping value than the single wall test WA_A_Z01.

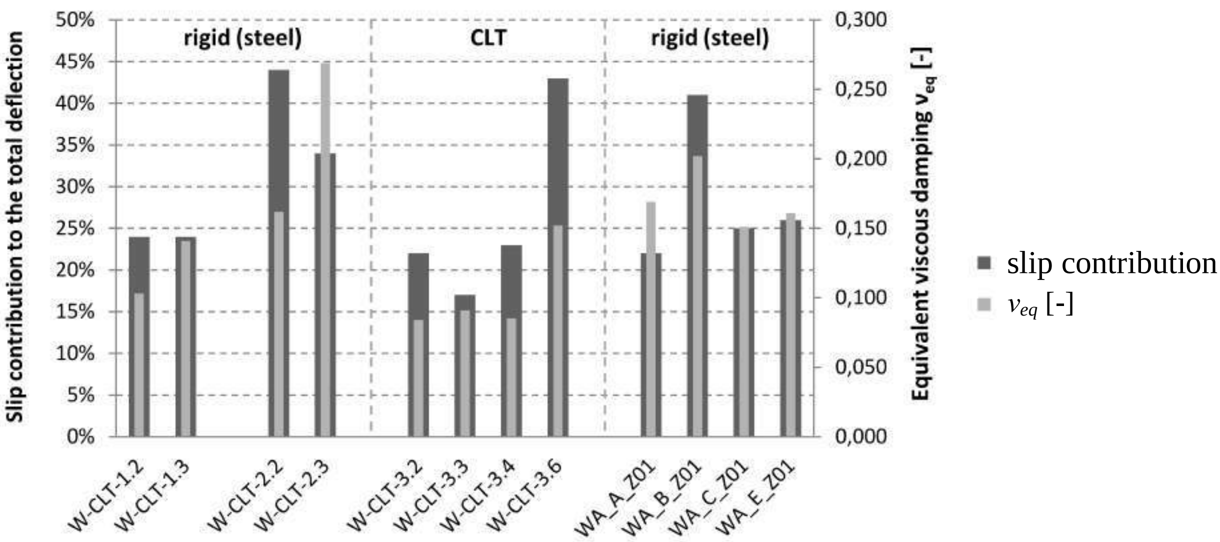

Fig. 16 Slip contribution and equivalent viscous damping from cyclic test of series W-CLT and series WA

In conclusion, the following recommendations can be made:

- Building physics requirements on support detailing can also have a direct influence on the cyclic behaviour, since elastomeric interlayers raise the friction into the connection between wall and slab, whereas plastic interlayers (for air tightness) reduce friction. For the plastic interlayer, this leads to a reduction of damping, stiffness and ductility. For the elastomeric interlayer, the ductility ratio decreases due to a lower initial stiffness caused by the soft interlayer. Here, the damping value remains nearly constant.

- The slip and rocking contributions on the overall deflection affect the damping capacity of the wall element under cyclic loading. If rocking dominates, then the equivalent viscous damping reduces. If slip dominates, then the hysteretic damping increases.
- Cutting of wall elements into smaller sections does not really help increase the hysteretic damping but may increase the ductility.

5. References

[1] DIN EN 1998-1: *Eurocode 8: Design of structures for earthquake resistance – Part 1: General rules, seismic actions and rules for buildings; German version EN 1998-1:2004*. April 2006.

[2] FRAGIACOMO, M.; RINALDIN, G.: *Advanced models for seismic analyses of timber buildings*, 9. Grazer Holzbau-Fachtagung, pp. J-1 – J-28, September 2011

[3] SEIM, W.; VOGT, T.: *OPTIMBERQUAKE: Deliverable 2B – Timber framed wall elements – monotonic and cyclic testing*, Department of Structural Engineering, Chair for Building Rehabilitation and Timber Engineering, University of Kassel, 2012.

[4] DUJIC, B.; STRUS, K.; ZARNIC, R.; CECCOTTI, A.: *Prediction of dynamic Response of a 7-storey Massive XLam Wooden Building tested on a Shaking Table.* 11th World Conference on Timber Engineering, Trentino, 2010.

[5] *Seismic test on a 7-storey building (movie)*, on http://www.ivalsa.cnr.it/en/photo-video/foto/progetto-sofie-test-sismico-2007.html, Institute IVALSA of the National Research Council and the Autonomous Province of Trento, 2007

[6] POPOVSKI, M.; KARACABEYLI, E.: *Seismic Performance of Cross-Laminated Wood Panels. INTERNATIONAL COUNCIL FOR RESEARCH AND INNOVATION IN BUILDING AND CONSTRUCTION, WORKING COMMISSION W18 - TIMBER STRUCTURES*, 2011. CIB-W18/44-15-7.

[7] HUMMEL, J.; SEIM, W.: *OPTIMBERQUAKE: Deliverable 1 – Preliminary design and testing program*, Department of Structural Engineering, Chair for Building Rehabilitation and Timber Engineering, University of Kassel, 2011.

[8] EN 12512: *Timber structures – test methods – cyclic testing of joints made with mechanical fasteners*, 2001.

[9] CHOPRA, A. K.: *Dynamics of Structures*. Prentice Hall, 3 edition, 2006.

[10] FLATSCHER, G.; SCHICKHOFER, G.: *Verbindungstechnik in BSP bei monotone und zyklischer Beanspruchung – Statusbericht TU Graz*, 9. Grazer Holzbau-Fachtagung, pp. G-1 – G-22, September 2011

[11] ISO 21581: *Timber structures – Static and cyclic lateral load test methods for shear walls,* 2010

[12] FLATSCHER, G.: *Versuchstechnische Betrachtung zyklisch beanspruchter Wandelemente in der Holz-Massivbauweise*, 18. Internationales Holzbau-Forum 2012, Prolog IV, Garmisch-Partenkirchen Dezember 2012

[13] EN 26891: *Holzbauwerke – Verbindungen mit mechanischen Verbindungsmitteln –*

Allgemeine Grundsätze für die Ermittlung der Tragfähigkeit und des Verformungsverhaltens, 1991, equal to ISO 6891:1983

[14] VOGT, T.; HUMMEL, J.; SEIM, W.: *Timber framed wall elements under cyclic loading*. *12th World Conference on Timber Engineering, Auckland*, 2012.

Seismic Behaviour of Cross-Laminated Timber Buildings: Numerical Modelling and Design Provisions

Massimo Fragiacomo

Associate Professor of Structural Design

Dept. of Architecture, Design and Urban Planning, University of Sassari

Alghero, Italy

Summary

The paper discusses the numerical modelling of Cross-Laminated Timber (CLT) buildings subjected to seismic actions. After pointing out some important features of a correct modelling, which include the need for a proper schematization of the connection flexibility, an advanced non-linear hysteretic spring implemented in Abaqus is introduced and used to schematize a CLT wall subassembly, demonstrating excellent accuracy. Provisions for seismic design are then given, including behaviour factors, capacity based design rules, and overstrength factors, which are needed to ensure dissipative behaviour of CLT buildings and prevent any brittle failure.

1. Introduction

Cross-Laminated Timber (CLT) buildings are being increasingly used in Europe, North America, Japan and Australasia. Their advantages of sustainability, light weight and rapidity of construction make them an excellent alternative to reinforced concrete and steel for multi-storey low and medium rise buildings. The improved dimensional stability achievable by laminating layers of boards, placed at a right angle, and the possibility to use low grade timber boards are additional benefits compared to traditional light frame and glulam construction. The increased fire resistance is another advantage which is crucial in multi-storey buildings.

The seismic resistance of timber buildings is an important issue, particularly when multi-storey buildings are built in medium to high seismicity regions. Timber structures are lightweight (about 1/5th to 1/4th of the weight of a reinforced concrete structure), therefore also the seismic actions are lower, as they are very much dependent on the building mass. However, possible issues are the low ductility exhibited by timber as a structural material, and the presence of several joints and discontinuity among the prefabricated timber members used to construct the building, which may lead to loss of stability if they are not sufficiently connected. Structural ductility is a key property to ensure good seismic behaviour, as it allows energy dissipation and consequently reduction of the seismic actions compared to the case of a brittle structure [1].

In a timber structure, ductility can be attained either by introducing steel members (for example steel fuses, U-shaped flexural plates, etc.) specifically designed to plasticize during the earthquake [2], or by designing some connections between the structural members to behave in a ductile manner [3]. In either case, the development of a ductile global failure mechanism must be ensured, by locating the ductile elements/connections in a suitable location within the structure and designing all the remaining connections/members for the strength demand calculated from equilibrium, when the plastic element is subjected to the product of its actual strength capacity and its overstrength ratio. The overstrength ratio of the plastic element is conventionally defined as the ratio between the 95th percentile of its peak strength $F_{0.95}$, and its design capacity F_d [3]:

$$\gamma_{Rd} = \frac{F_{0.95}}{F_d} \tag{1}$$

This design method, also known as 'Capacity Based Design' [1], aims to prevent anticipated brittle failures, which would impede the development of a proper ductile global failure mechanism, by oversizing the brittle members and forcing the weaker (and ductile) elements to plasticize. Fig. 1 displays the application of these concepts to a simple case: a multi-storey timber moment-resisting frame with elasto-plastic joints. By oversizing beams and columns with respect to the beam-column connection, and ensuring the column-foundation connection can plasticize simultaneously with the beam-column joints, a global ductile failure mechanism (often referred to as 'strong column, weak beam') is obtained (Fig. 1a). Conversely, if the plasticization occurs within the columns, for example due to the discontinuity of the column in the connection region, a global brittle failure mechanism (often referred to as 'storey mechanism' or 'strong beam, weak column) is obtained, as can be easily observed from Fig. 1d where the base shear vs. top floor displacement is plotted in black and compared to the red curve obtained for the previous case. By assuming the same moment-rotation relationship for the beam-column connection (case (a)) and for the column (case (b)), the top floor deflection is about four times larger in the former case compared to the latter one. It should be pointed out, however, that the failure of a timber column is in general brittle, therefore case (b) would actually exhibit an even smaller deflection and global ductility.

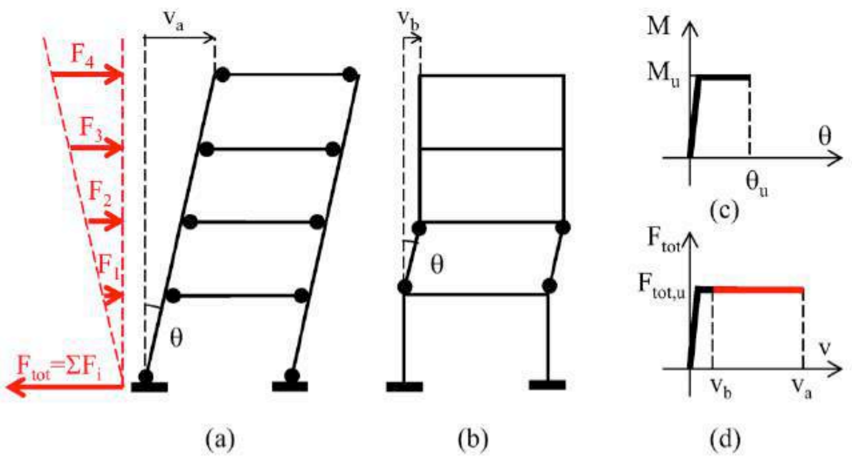

Fig. 1 Ductile (a) and non ductile (b) failure mechanisms of a moment-resisting timber frame with elasto-plastic moment-rotation relationship in the connections and columns (c), and corresponding base shear-top floor displacement curves (d)

To make the method fully applicable, information on the ductile failure mechanism and on the values of the overstrength factors should be provided to designers. Current codes of practice such as the Eurocode 8 [4] provide little information on the failure mechanism, and no values for the overstrength factors.

This paper provides this information for cross-laminated (CLT) multi-storey timber buildings based on some recent experimental and numerical research. Furthermore, provisions for numerical modelling of these types of buildings are given, and an advanced finite element (FE) model recently developed for seismic analysis is presented and briefly discussed.

2. Numerical Modelling of the Seismic Behaviour of CLT Buildings

A CLT building is constructed by assembling CLT wall and floor panels. Typical connection systems include hold-downs, tie-downs, angle brackets, and self-drilling screws. Hold-downs and angle brackets are shaped metal plates connected to the timber panels using nails and to the foundation using bolts (see Fig. 2). The former mostly resist axial force (uplifting) whereas the latter mostly resist shear. Tie-downs are metal plates connecting an upper wall to a lower wall with the aim of resisting mostly axial force. Nails are usually employed to connect it to the wall panels. Self-drilling screws are used to connect adjacent wall and floor panels, floor panels to wall panels, and perpendicular wall panels [6].

Fig. 2 CLT wall panel at the end of the cyclic tests, near to the failure condition [5]

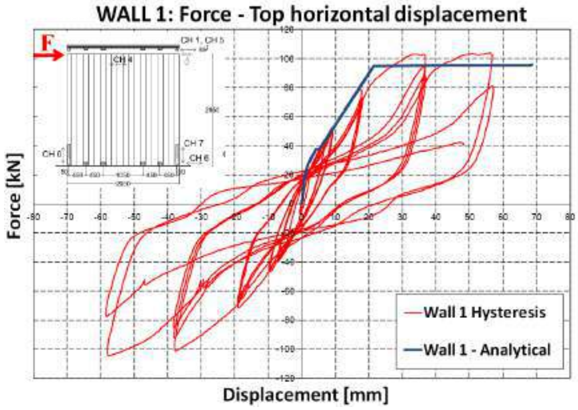

Fig. 3 Results of experimental cyclic tests carried out on single CLT wall panel [5]

2.1 Experimental Cyclic Behaviour of CLT Wall Subassemblies

Extensive testing carried out on CLT wall subassemblies [5,6,7] and entire buildings [8,9] subjected to static, cyclic, and seismic loading has demonstrated the excellent seismic performance, which is characterized by significant energy dissipation, limited damage of the building at the end of the seismic event, and by the possibility to survive strong earthquakes. Fig. 3 depicts the typical cyclic behaviour of a single CLT wall panels without opening connected to the foundation with two hold-downs and four angle brackets and tested in accordance with the EN12512 loading protocol [10]. The hysteresis loops are characterized by significant energy dissipation, pinching behaviour, stiffness and strength degradation from the first to the following cycles at the same target displacement, and a softening branch after the attainment of the peak strength. Hardly any damage was observed in the panel itself during the test, and all energy dissipation occurred in the connections, which plasticized and eventually failed (Fig. 2). The most important deflection components were due to the flexibility (in shear and axial force) of the connections, whereas the flexural deformation and shear distortion of the wall itself were generally negligible (Fig. 4). Cyclic tests carried out on CLT wall panels with openings showed similar results, in particular no sign of failures in the panel itself were detected, unless with very large openings cut in it [11].

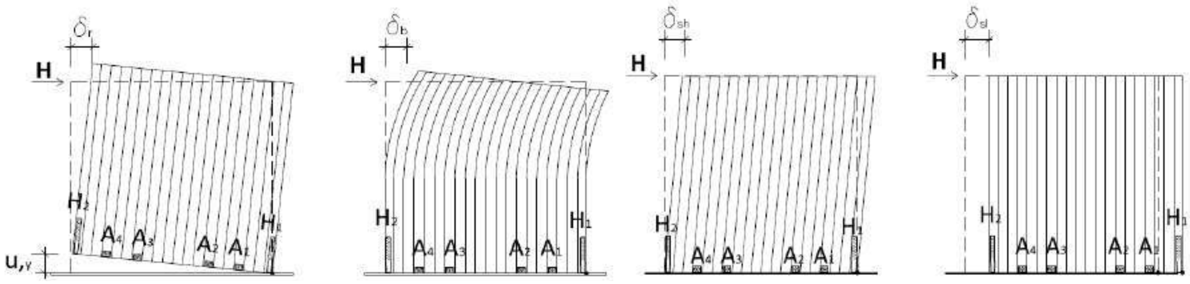

(a) (b) (c) (d)

Fig. 4 Deflection components of a CLT wall panel: (a) rocking due to stretching of base connection, (b) bending, (c) shear distortion, (d) slip of base connections

2.2 FE Modelling of CLT Wall Subassemblies

The results of the experimental cyclic tests carried out on CLT wall subassemblies suggest that a proper modelling of the connections is crucial, whereas the CLT panel itself can be modelled as linear-elastic or even as rigid when significant openings are absent.

2.2.1 FE Modelling of CLT Panels

The CLT panels can be modelled using: (i) rigid elements; (ii) diagonal springs (Fig. 5); or (iii) 2D plane stress (shell) elements (Fig. 6). Modelling (i) does not allow for flexural and shear deformation of the panel, whilst modelling (ii) only allows for shear distortion of the panel, as usually rigid links pinned-connected at their ends are used to frame the panel. Alternatively, diagonal springs can be calibrated to also account for the flexural deformation of the panel, by simply imposing the same horizontal deflection of the model as in the real panel [12]. Modelling (iii) allows for both flexural and shear deformation of the panel.

Unless large openings are present, the panels can be modelled as linear elastic. The layered structure of the panel can be taken into account in approach (iii) using the transformed section method, namely by transforming the layered panel into a homogeneous, orthotropic panel with different stiffness properties in the two directions [13]. Alternatively, some software packages such as SAP2000 [14] and Abaqus [15] allows the user to implement multilayer/composite shell elements where each layer is characterized by different mechanical properties.

The presence of large openings may reduce the stiffness of the wall – criteria for calculating the actual stiffness of the wall with opening and for implementing it in the model with diagonal springs (approach (ii)) are provided by Sustersic and Dujic [16].

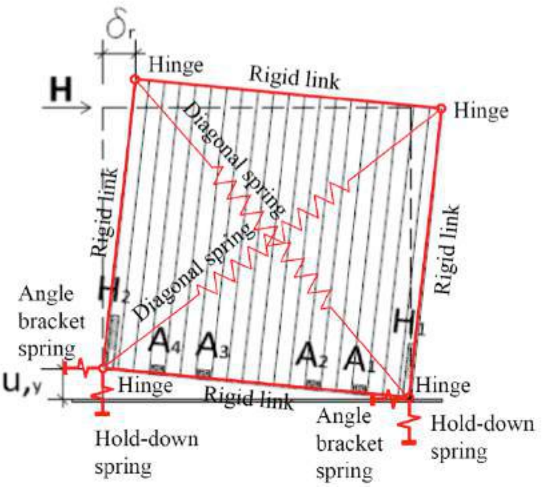

Fig. 5 Modelling of CLT subassembly using diagonal and lumped springs

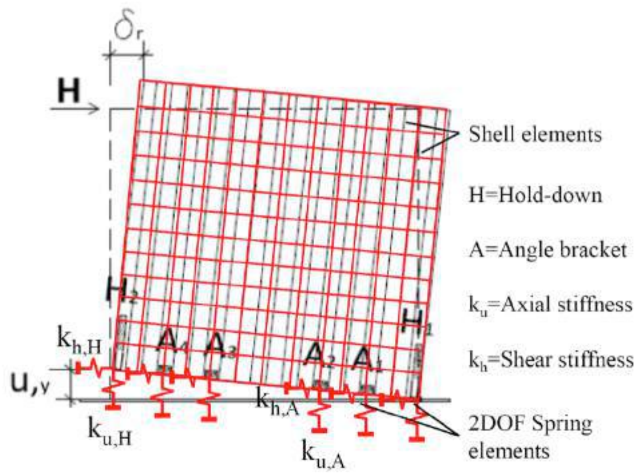

Fig. 6 Modelling of CLT subassembly using 2D shell elements and concentrated 2DOF springs

2.2.2 FE Modelling of CLT Connections – Kinematic Behaviour

The connections play a key role in accurate modelling of CLT buildings. Most of connections used in CLT construction do not restrain rotations but only translation. In a plane subassembly, they can therefore be schematized with 2 degree-of-freedom (DOF) translational springs. Since several connectors are generally used in a CLT subassembly, the 2DOF springs can either be concentrated at the actual connector location (Fig. 6) or be lumped in a couple of primary nodes (Fig. 5). In the latter schematization, the mechanical properties of the lumped springs are calculated from the properties of the real connections – for example in Fig. 5 the two angle bracket springs have a stiffness obtained by summing up the shear stiffness of all angle brackets and hold-downs, whilst the stiffness of the two hold-down springs depends on the location and axial stiffness of all hold-downs and angle-brackets. It is important to point out that in general both shear and axial stiffness should be considered for CLT typical connections. For example, analytical studies recently carried out [5,17] proved the significant influence of the axial behaviour of angle brackets on the cyclic response of CLT wall subassemblies. The simplified assumption of considering only the shear behaviour of angle brackets and neglecting their axial stiffness would lead to significant underestimation of strength and stiffness capacity of CLT wall panels.

2.2.3 FE Modelling of CLT Connections – Mechanical Behaviour

The mechanical behaviour of the springs schematizing the connections can be modelled with different degrees of complexity, depending on the type of analysis carried out. According to Eurocode 8 [4], four types of seismic analyses can be performed: (i) linear static; (ii) linear dynamic (eigenvalue); (iii) non-linear static (push-over); and (iv) non-linear dynamic (time-history).

For linear static (i) and linear dynamic (ii) analyses, the springs should be regarded as linear-elastic. The stiffness of the spring can be assessed either via experimental testing carried out on the connections (see for example Fig. 7 and Fig. 8, which refer to a hold-down loaded in tension and to an angle bracket loaded in shear, respectively [5]), or using empirical formulas such as those proposed by the Eurocode 5 – Part 1-1 [18] for timber-timber and steel-timber connections with mechanical fasteners.

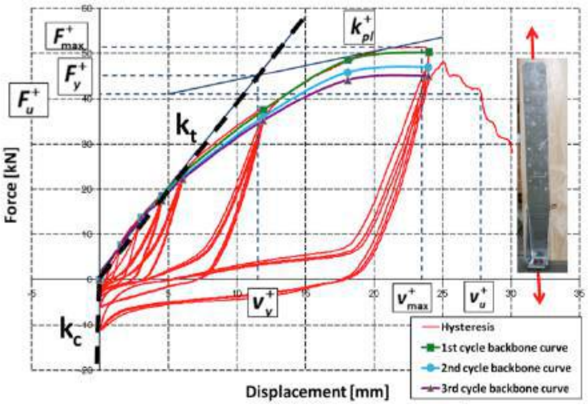

Fig. 7 Experimental force-displacement hysteretic behaviour of hold-down in tension

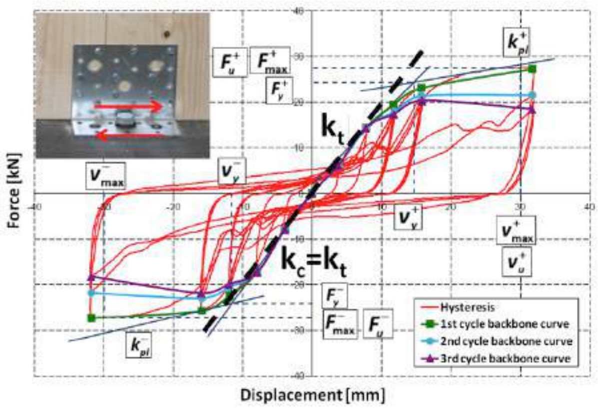

Fig. 8 Experimental force-displacement hysteretic behaviour of angle bracket in shear

If the results of experimental testing carried out on each connector (hold-down, angle bracket, screwed wall-wall joint, etc.) loaded in shear and axial force are available, the stiffness to consider should be calculated as a secant value at 40% of the peak strength (thick black dashed line in Fig. 7 and Fig. 8 [19,20]). It should be noted that the behaviour under axial force of the metal connections (hold-downs and angle brackets) is non-symmetric, as they are flexible in tension (k_t) and very stiff (almost rigid) in compression due to the contact with the foundation or with the supporting floor panel (k_c) (Fig. 7). This lack of symmetry ($k_t \neq k_c$) is an issue in linear static and dynamic analyses, where only one value of stiffness should be used.

For linear static analyses, if the structure is reasonably simple and the sign of the axial force (tension or compression) can be predicted in the metal connectors, the different tensile and compressive stiffness could be used. In linear dynamic analyses, however, only one value of stiffness can be used, as in a modal response spectrum analysis, the vibrations of the buildings are investigated and, therefore, the same connector is loaded in both directions (compression and tension). An equivalent axial stiffness k_e must therefore be determined for the connectors. This can be done via non-linear modelling of each wall using gap elements (namely nonlinear elements almost rigid in compression with zero tensile stiffness) and elastic links for hold-downs/angle brackets, with the actual tensile and shear stiffness, so as to simulate the exact boundary conditions of contact in compression and elastic flexible behaviour in tension and shear. The wall model must then be recalibrated so that only the elastic links and no gap elements are used, and the target horizontal displacements for the nonlinear and linear cases are the same under the same horizontal load (Fig. 9 [16,21]).

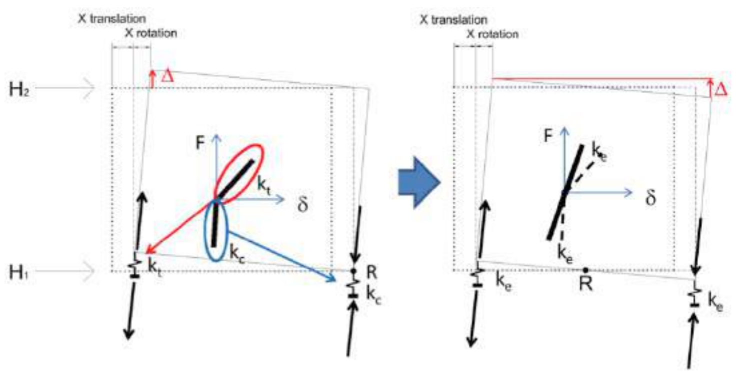

Fig. 9 Evaluation of an equivalent axial stiffness of metal connectors for linear dynamic analyses

In non-linear static (pushover) analyses, a non-linear elastic force-displacement relationship is considered for each connector. If results from cyclic tests are available, it is suggested that reference to the 3rd cycle backbone curve is made (violet curves in Fig. 7 and Fig. 8). In this way, the effects of cumulative damage of a seismic (cyclic) load are considered, and conservative results are obtained [19,20]. In this case, the non-symmetric behaviour of the connectors, when subjected to axial force, can be fully considered. These non-linear curves can be easily implemented in software packages such SAP2000 and ABAQUS by approximating the actual non-linear curves with piecewise linear curves. The non-linear static response of CLT subassemblies or CLT buildings is then used within the N2 method, as recommended by the Eurocode 8 – Part 1 [4], to assess the safety of the structure for seismic actions [19,20,21].

Far more complex is the case of non-linear dynamic (time-history) analyses. In this case, the connections should be modelled as non-linear springs with the hysteresis rules typical of timber connections (Fig. 7 and Fig. 8), namely: (i) non-linear symmetric (in shear) or non-symmetric (in axial load) backbone curve with softening under reversal load; (ii) pinching behaviour; and (iii) strength and stiffness degradation for consecutive load cycles. Additional phenomena that should be considered are (iv) the effect of friction at the wall panel-to-foundation interface and at the interface between wall and supporting floor panel, and (v) the interaction for each connector between shear and axial degrees of freedoms. In this case, a non-linear time-history analysis is carried out, where the CLT subassembly is subjected to a certain generated or recorded earthquake ground motion, and the motion equations are solved by the software which returns all relevant quantities (deformations, stresses, energies, accelerations, velocities, etc.) at every step. An important issue is to identify software packages for non-linear dynamic analyses with hysteresis rules suitable for timber connections.

2.2.4 Software Packages for Non-linear Time-history Analysis of Timber Structures

The widespread software package SAP2000 [14] does not have a specific hysteretic rule for timber connections. However, the pivot rule can be used [19,20] to schematize with some approximations the connection behaviour (phenomena (i) and (ii) in the previous Section).

Fig. 10 and Fig. 11 display the screenshots of multi-linear plastic pivot link in SAP2000, used for modelling the axial behaviour of hold-down and shear behaviour of angle brackets, respectively. Fig. 12 and Fig. 13 plot the comparison between experimental and approximating cycling curves of hold-down in tension and angle bracket in shear, respectively. The pivot rule overestimates the dissipated energy.

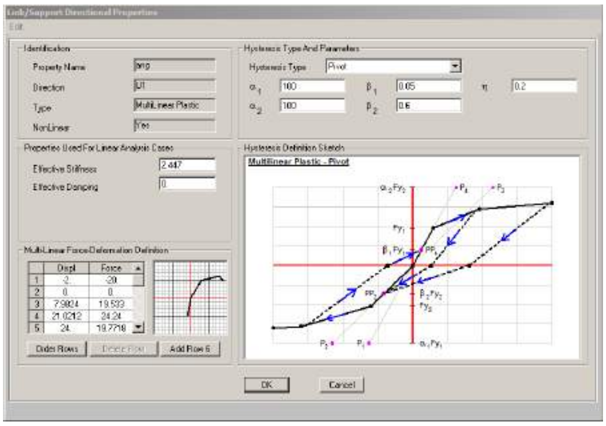

Fig. 10 Screenshot of multilinear plastic pivot link in SAP2000 used for modelling the axial behaviour of hold-down

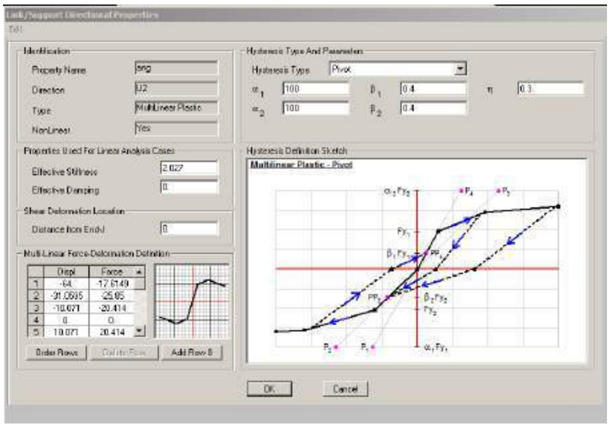

Fig. 11 Screenshot of multilinear plastic pivot link in SAP2000 used for modelling the shear behaviour of angle bracket

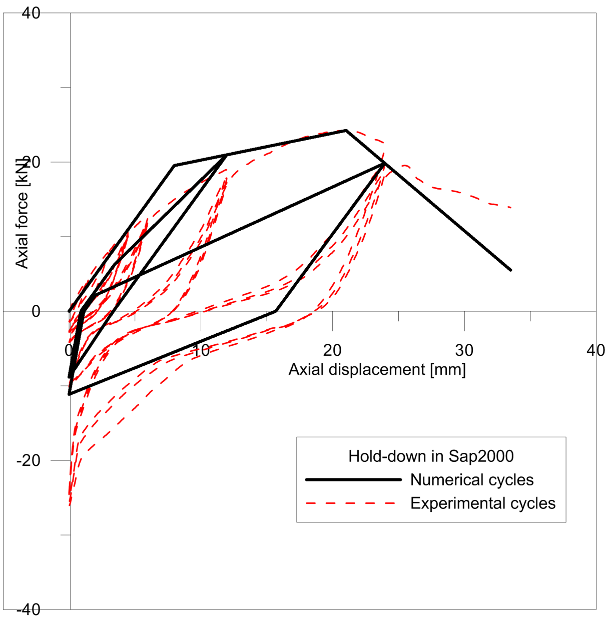

Fig. 12 Comparison between experimental and approximating cycling curves of hold-down in tension

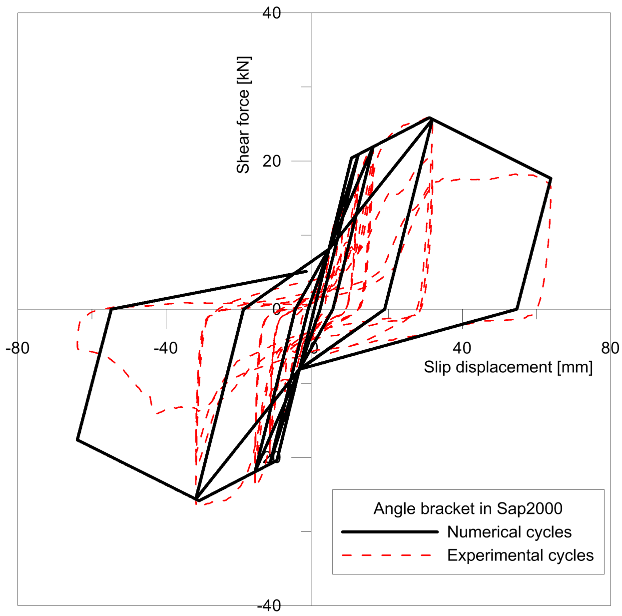

Fig. 13 Comparison between experimental and approximating cycling curves of angle-bracket in shear

Better approximation of the hysteretic behaviour can be obtained using the SAPWood V2.0 software [22], which was originally developed for lightframe timber construction. In this case, phenomena (i), (ii) and (iii) described in the previous Section can be adequately represented. Other authors used Straus7 software package to implement the cyclic behaviour of the connections. In this case, since an appropriate hysteretic rule is not available, the connections were schematized using macro-springs obtained by combining elastic and plastic only-tension and only-compression springs [23]. Phenomena (i) and (ii) described in the previous Section could be modelled, even though no softening branch can be followed on the backbone curve.

A further possibility is to implement the proper behaviour of the timber connections in existing software packages using external subroutines. A cyclic behaviour was first implemented in DRAIN-2DX [24,25] and then in DRAIN-3DX [26] where phenomena (i) and (ii) described in the previous Section could be both modelled properly. By using this model, the test results of a three-storey CLT building tested on a shaking table in Japan [8] could be accurately reproduced.

2.2.5 Advanced Model for Non-linear Time-history Analysis of Timber Structures

With the aim to develop a rigorous FE model for seismic analyses of CLT buildings, a user subroutine was implemented in Abaqus to schematize the cyclic behaviour of the connections [20,27]. Phenomena (i), (ii) and (iii) listed in Section 2.2.3 are all considered, with the 1st backbone curve being schematized with a tri-linear curve. Fig. 14 and Fig. 15 display the adopted schematization for connections (hold-downs and angle brackets) loaded under axial and shear forces, respectively. The screwed connections between adjacent wall panels can be schematized using the model for shear behaviour (Fig. 15).

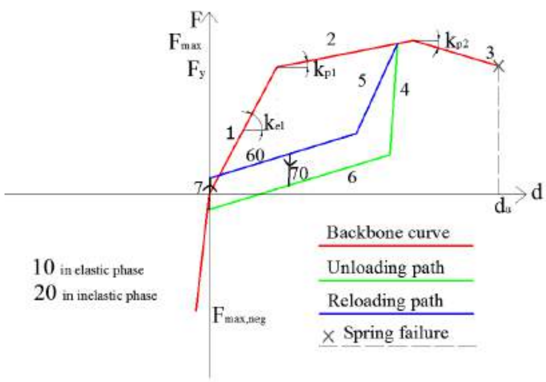

Fig. 14 Schematization of the connection hysteretic behaviour under axial load [27]

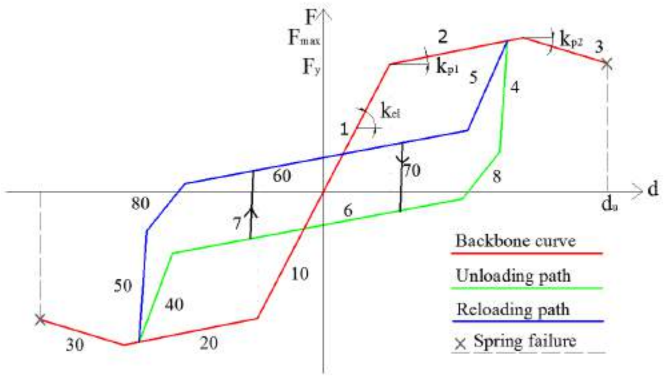

Fig. 15 Schematization of the connection hysteretic behaviour under shear load [27]

These hysteretic models need calibration on experimental cyclic tests carried out on connections loaded in shear and tension. To aid in the calibration process, which would be quite difficult and time consuming if carried out only visually, a software for automated calibration was developed, and is freely available on the Internet [28]. This software evaluates automatically the slopes of branch #1 and #2 and the yielding force according to EN 12512 [10]. Then the user can specify unloading/reloading stiffnesses and the slope of branch #3 through some parameters that characterise the cyclic paths and the softening branch. Every time that a parameter is changed, the program recalculates the total energy according to the developed hysteresis model, imposing the same displacement used in the experimental test. After that, the software looks for an optimum value for the parameters governing the strength degradation by minimising the standard deviation of the difference between experimental and numerical (spring) energy values using an iterative process. The calibration process stops when the difference in total energy is lower than 5%. Fig. 16 – Fig. 19 compare the experimental results of the cyclic tests on hold-downs and angle-bracket connections loaded in tension and shear [5] with the model schematization.

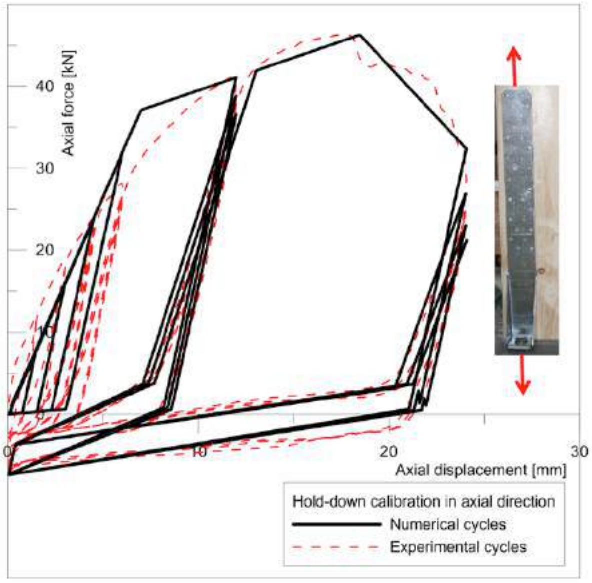

Fig. 16 Schematization of the hold-down hysteretic behaviour under axial load

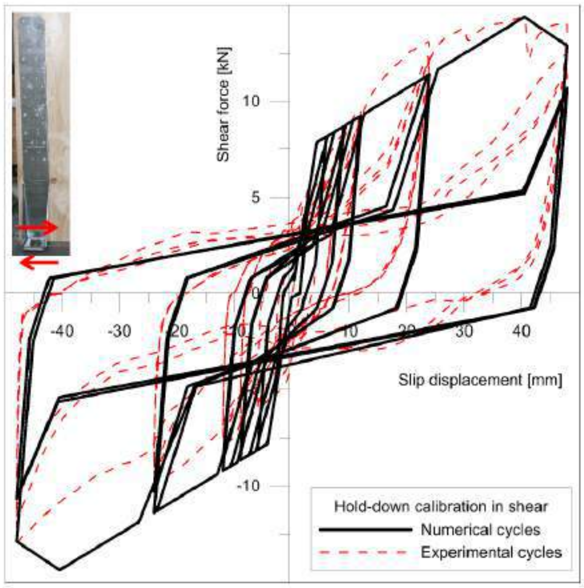

Fig. 17 Schematization of the hold-down hysteretic behaviour under shear load

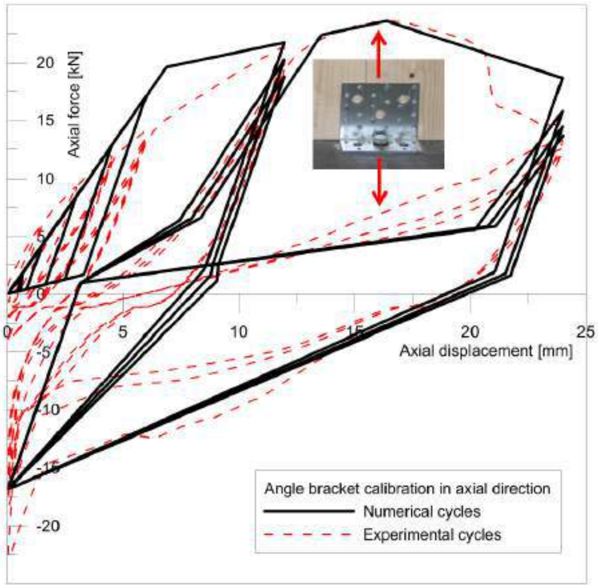

Fig. 18 Schematization of the angle bracket hysteretic behaviour under axial load

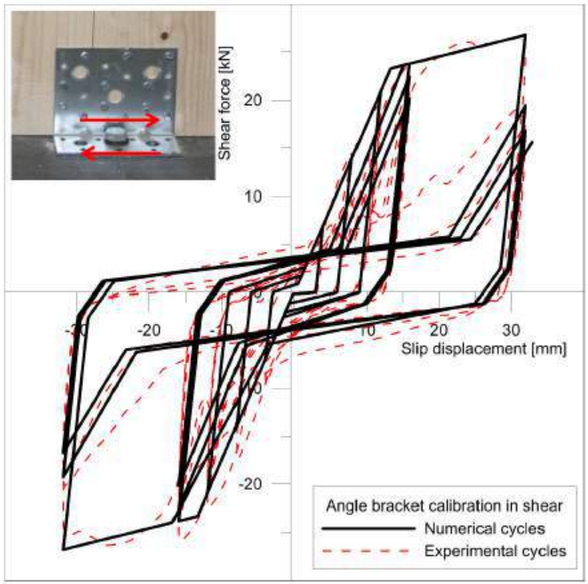

Fig. 19 Schematization of the angle bracket hysteretic behaviour under shear load

The model also considers an interaction between the axial and shear resistance of the connectors. The domain formulation is taken from a European Technical Approval document for CLT connections [29], and has the following form:

$$\left(\frac{F_N}{R_N}\right)^2 + \left(\frac{F_V}{R_V}\right)^2 \leq 1 \tag{2}$$

where F_N, F_V, R_N and R_V are the axial force and shear force at the current analysis steps, and the yielding axial and shear strength, respectively [30,31].

The contribution of static friction at the wall-foundation and wall-supporting floor panel interface can be lumped in every spring schematizing the connections, and is taken into account by Eq. (3):

$$F_f = k_f \cdot F_N \tag{3}$$

where F_N, k_f and F_f signify the axial force, the static friction coefficient, and the static friction force in the connection spring. When the shear force exceeds the friction resistance, the panel starts moving, and the friction force is assumed proportional to the axial force [30,31].

This model has been used to calculate the cyclic response of CLT subassemblies (single and coupled walls) that were experimentally tested at CNR IVALSA Trees and Timber Institute [5]. The hold-down and angle bracket connections were also separately tested at IVALSA, and the experimental cyclic results were approximated with the model (see Fig. 16 – Fig. 19) and then used to predict the response of the subassemblies. Fig. 20 and Fig. 21 compare experimental and numerical lateral force-top wall deflection curves, and the time histories of the total energies, respectively [30,31]. An excellent agreement can be noticed, proving the accuracy of the model developed. The same model was used to reproduce the behaviour of a one-storey CLT building subjected to pseudo-dynamic test at the University of Trento, obtaining excellent accuracy [31], and is being used to reproduce the shaking table tests carried out by CNR IVALSA Timber and Trees Institute on three- [8] and seven-storey CLT buildings [32].

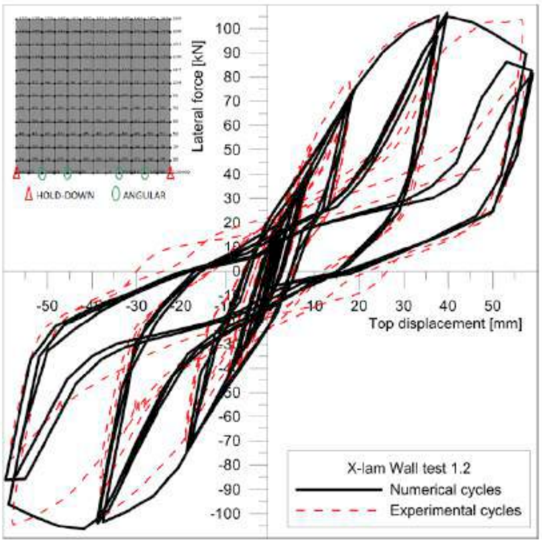

Fig. 20 Experimental-numerical comparison of the cyclic behaviour of a CLT wall subassembly – Force-displacement curves

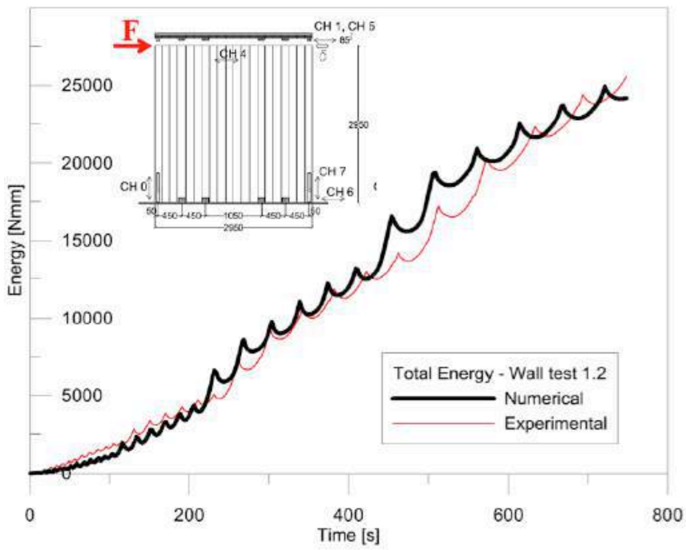

Fig. 21 Experimental-numerical comparison of the cyclic behaviour of a CLT wall subassembly – Time history of the total energy

3. Design Provisions for Seismic Design of CLT Buildings

As mentioned in the Introduction, only little information is available in the current version of the Eurocode 8 - Part 1 [4] for seismic design of timber buildings. CLT buildings are not even mentioned, therefore there is a need to provide some guidance with particular regards to the values of the behaviour factor, and the concepts of capacity based design and overstrength.

3.1 Energy Dissipation in CLT Buildings and Subassemblies

Experimental seismic tests carried out on entire CLT buildings [8,9,32], subassemblies [5,6,7,11] and typical connections [5,17,19] have proved the ability of these structures to dissipate a significant amount of energy. A behaviour factor q of 3 was recommended [8] for CLT buildings with walls composed of several panels having heights equal to the inter-storey height and widths not greater than 2.6 m, connected together by means of vertical joints made with mechanical fasteners (screws or nails) (see Fig. 22). In this case, the dissipative elements were mainly the screwed connections between adjacent CLT wall panels, and the nailed connections between CLT wall panels and metal connector devices (angle brackets, hold-downs, tie downs). No experimental and numerical results exist, however, for the q factor of CLT buildings with walls having the same height as the interstorey height and made of a single element up to the maximum transportable length. At this stage, the use of a q factor no greater than 2 is recommended for this type of CLT buildings [34].

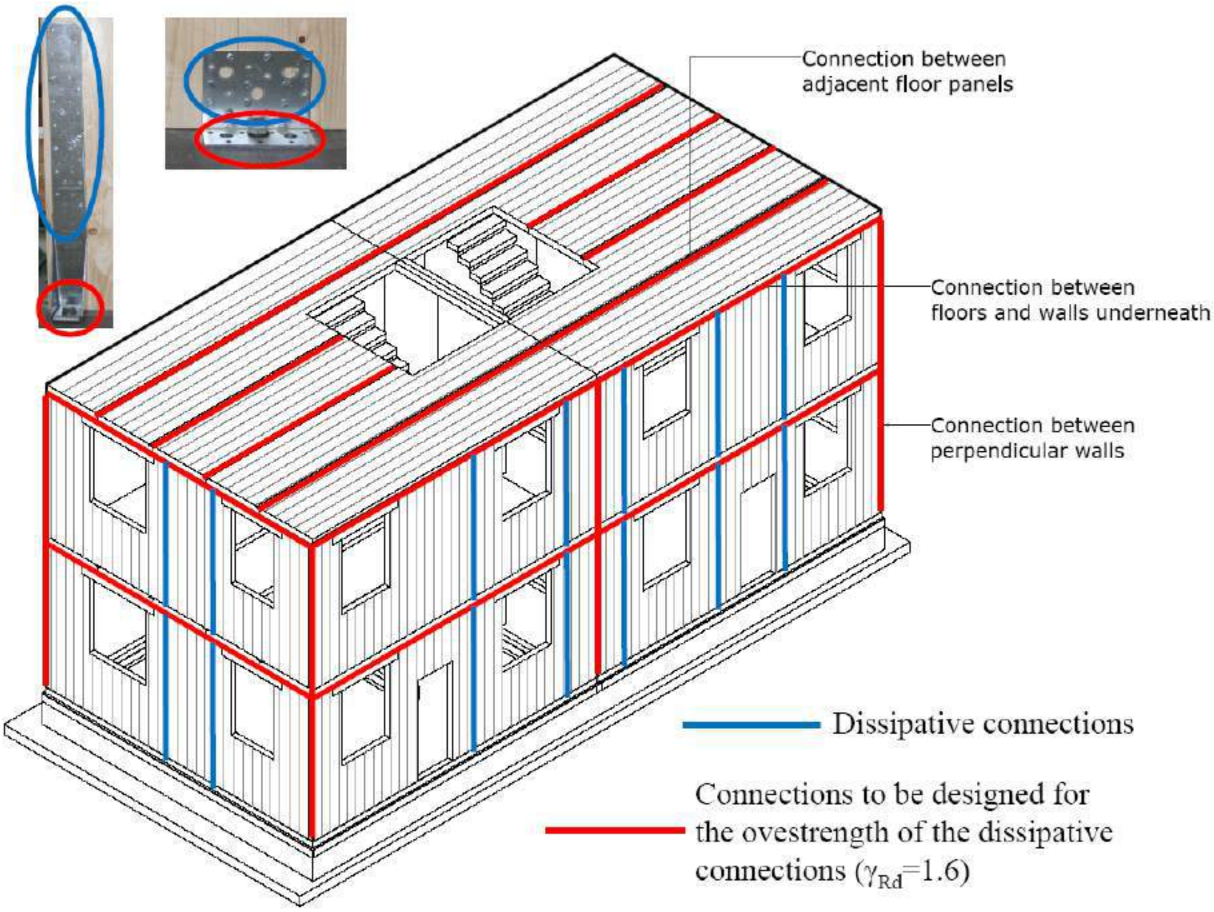

Fig. 22 CLT building with walls composed of several panels, and connections that must be designed with overstrength criteria in order to comply with capacity based design

3.2 Provisions for Ductile Behaviour of CLT Connectors

Experimental tests carried out on single metal connectors for CLT buildings have shown the possibility of undesired brittle failure mechanisms. Fig. 23 shows some of these brittle failures that should be avoided by applying capacity design principles within the connector itself.

These brittle failure mechanisms are avoided by designing the steel parts of metal connectors (angle-brackets, hold-downs and tie-downs) and the connections with the foundation/supporting floor panel (labelled with ‘b’ as ‘brittle’ in Fig. 23) for the overstrength of the connections with the wall panels (labelled with 'd' as 'ductile' in Fig. 23). The purpose is to ensure the plasticization can occur in the connections 'd' and is not prevented by anticipated brittle failures of connections 'b' and of the metal parts (Fig. 23). If $F_{Rd,d}$, $F_{Rd,b}$, and $F_{Rd,m}$ signify the design shear strengths of the dissipative connection, the design strength of the brittle connection, and the design strength of the metal part, respectively, and γ_{Rd} is the overstrength ratio of the ductile connection, i.e. the connection to the wall panel, the design of the metal connectors shall satisfy the conditions:

$$\gamma_{Rd} \cdot F_{Rd,d} \leq F_{Rd,b} \tag{4}$$

$$\gamma_{Rd} \cdot F_{Rd,d} \leq F_{Rd,m} \tag{5}$$

The overstrength ratio of the ductile connections lays in the range 1.3 to 1.6 [3,19,34]. Some of the metal connectors currently manufactured do not comply with these conditions; they could be improved by following the capacity based design rules provided above, to avoid the undesired brittle failures shown in Fig. 23.

Fig. 23 Undesired failures of CLT connections: yielding of steel part of angle bracket with nails withdrawal (left), failure of steel part of hold-down (middle), pull-through of bolt in the angle bracket (right)

Further provisions must be given to ensure the dissipative connections behave in a ductile way and dissipate energy, otherwise the use of the behaviour factors q=3 and 2 for buildings with walls made of several CLT panels or made of a single, long panel, respectively, is not justified. To this aim, brittle failure mechanisms of the timber part such as splitting, shear plug, fracture of wood in tension, and tear out must be avoided (Fig. 24). The only allowed failure mechanism of wood is crushing, which should occur together with the formation of one or two plastic hinges in the fasteners (Fig. 25). In accordance with the Eurocode 5 – Part 1-1 [18] notations, only failure mechanisms b, d and e are allowed in the dissipative connections. Using the EC5 design formulas for connections with metal fasteners, is then possible to control the failure mechanism and ensure, during the design process, that the connection will be dissipative. This design criterion applies to metal connectors and the screwed connections between adjacent wall panels, which are considered as dissipative, to ensure only the ductile failure mechanisms, with at least one plastic hinge formation in the mechanical fasteners, can take place.

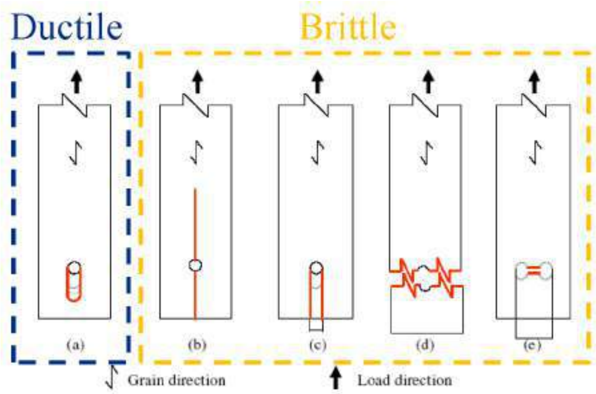

Fig. 24 Possible failure modes of timber in a connection with mechanical fasteners

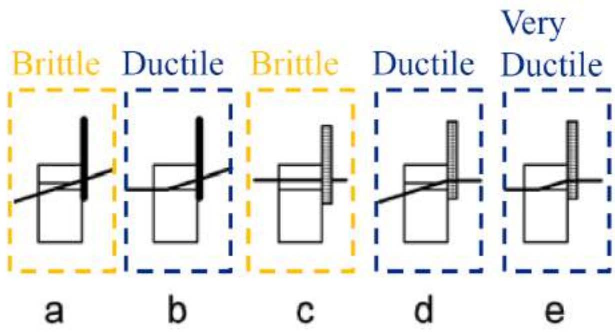

Fig. 25 Failure mechanisms of steel-to-timber connections with mechanical fasteners

3.3 Capacity Design Rules for CLT Buildings

CLT timber buildings should act, to the greatest possible extent, as box-type structures. To achieve this, it is important to prevent any local failures which may compromise the box-type behaviour.

The connections devoted to the dissipative behaviour in a CLT building are [34]: (i) vertical (screwed) connections between wall panels in case of walls composed of more than one element; (ii) connections between CLT walls and angle brackets placed along the wall to resist mostly shear; and (iii) connections between CLT walls and anchoring elements (hold-down and tie-down) placed at wall ends and at wall openings against uplift.

In order to ensure the development of cyclic yielding in the dissipative zones, all other structural members and connections shall be designed with sufficient overstrength so as to avoid anticipated brittle failure. This overstrength requirement applies especially to (Fig. 22):

- metal parts of hold-downs, tie-downs, and angle brackets, to ensure no plasticization and brittle failure can occur in these parts;
- connections of hold-downs, tie-downs, and angle brackets to foundation or supporting floor panel, to ensure no loss of stability can occur in the connected wall panel;
- connections between adjacent floor panels in order to limit, to the greatest possible extent, the relative slip and to assure a rigid in-plane behaviour;
- connection between floors and walls underneath thus assuring that, at each storey, there is a rigid floor to which the walls are rigidly connected;
- connection between perpendicular walls, particularly at the building corners, so that the stability of the walls and of the structural box is always assured;
- wall panels under in-plane vertical action due to the earthquake and floor panels under diaphragm action due to the earthquake.

The seismic resistance of shear walls should be higher at lower storeys and should decrease at higher storeys proportionally to the decrease of the storey seismic shear, thus leading to the simultaneous plasticization of the ductile connections in order to maximize the energy dissipation of the whole building.

The overstrength factors to use in design were found to be in the range 1.3-1.6 [5,19,34]. The recommended values are 1.3 for buildings with walls made of only a long CLT panel, and 1.6 for buildings with walls made shorter CLT panels connected to each other with screwed connections.

4. Conclusions

CLT buildings are characterized by excellent seismic behaviour, which has been demonstrated by full scale shaking table tests carried out on entire buildings, and by cyclic tests performed on wall subassemblies and connections. However, little information on seismic design is provided in the Eurocode 8 – Part 1, and not much about numerical modelling can be found in literature either. This paper discusses, extensively, criteria for numerical modelling of CLT buildings and subassemblies. It is highlighted that a proper modelling of the connections is crucial, whereas an accurate schematization of the CLT panels is less important, due to their large stiffness, provided they have reduced openings. The metal connectors such as hold-downs and angle brackets should be modelled as two degree-of-freedom springs, with stiffness properties calculated based either on experimental results or on the empirical formulas of the Eurocode 5 – Part 1-1. Non-linear static and dynamic analyses can be carried out once the non-linear static and cyclic behaviour of the connectors is properly modelled. Widespread software package such as SAP2000 can be used where the multilinear plastic pivot hysteretic rule is available and can approximate the actual experimental behaviour of CLT timber connections. A more advanced model, that considers all the features of CLT connections and, in addition, the interaction between the two degrees-of-freedom and the effect of friction, was implemented in Abaqus and used to predict the experimental cyclic behaviour of wall subassemblies and CLT buildings, showing excellent accuracy.

This paper also provides information on the use of capacity based design. A behaviour factor of 3 and 2 was recommended for CLT buildings with short walls and several vertical screwed joints, and for CLT buildings with long entire walls without vertical screwed joints, respectively. The dissipative elements are: (i) the vertical (screwed) connection between wall panels in case of walls composed of more than one element; (ii) the connections between CLT walls and angle brackets; and (iii) the connections between CLT walls and anchoring elements (hold-down and tie-down). All the other connections, metal elements and CLT panels are designed for the overstrength of the dissipative elements, which can be estimated as 1.6 for CLT buildings with short walls and several vertical screwed joints, and 1.3 for CLT buildings with long entire walls without vertical screwed joints. The dissipative connections must be designed to ensure no brittle failure occurs in wood, and one or more plastic hinges occur in the metal fasteners.

5. References

[1] Pauley T., and Priestley M.J.N., *Seismic design of reinforced concrete and masonry buildings*, Wiley Ed., 1992.

[2] Buchanan A., Deam B., Fragiacomo M., Pampanin S., and Palermo A., “Multi-storey prestressed timber buildings in New Zealand”, *IABSE Structural Engineering International*, Vol. 18, No. 2, 2008, pp. 166-173.

[3] Jorissen A., and Fragiacomo M., “General notes on ductility in timber structures”, *Engineering Structures*, Vol. 33, No. 11, 2011, pp. 2987-2997.

[4] European Committee for Standardization (CEN), *Eurocode 8—Design of structures for earthquake resistance, Part 1: General rules, seismic actions and rules for buildings*, Brussels, Belgium, 2004.

[5] Gavric I., Ceccotti A., and Fragiacomo M., “Experimental cyclic tests on cross-laminated timber panels and typical connections”, *14th ANIDIS Conference*, September 18-22, 2011, 12 pp., CD.

[6] Ceccotti A., Lauriola M.P., Pinna M., and Sandhaas C., “SOFIE project – Cyclic tests on cross-laminated wooden panels”, *9th World Conference on Timber Engineering WCTE 2006*, Portland (U.S.A.), August 6-10, 2006, CD.

[7] Dujic B., and Zarnic R., *Report on evaluation of racking strength of KLH system*, University of Ljubljana, Faculty of Civil and Geodetical Engineering, Slovenia, 2005.

[8] Ceccotti A., Follesa M., and Lauriola M.P., “Quale fattore di struttura per gli edifici multipiano a struttura di legno con pannelli a strati incrociati?”,12th ANIDIS Conference, Pisa, Italy, 2007.

[9] Hristovski V., Dujic B., Stojmanovska M., and Mircevska V., “Full-scale shaking-table tests of Xlam panel systems and numerical verification – Part 1: Specimen 1”, *ASCE Journal of Structural Engineering*, posted ahead of print, 2013, doi: 10.1061/(ASCE)ST.1943-541X.0000754.

[10] European Committee for Standardization (CEN), *Timber structures – Test methods – Cyclic testing of joints made with mechanical fasteners*, *EN12512*, 2001, Brussels, Belgium.

[11] Dujic B., Klobcar S., and Zarnic R, *Influence of openings on shear capacity of wooden walls*, Research Report, 2005, University of Ljubljana and CBD Contemporary Building Design Ltd., Slovenia.

[12] Sustersic I., Fragiacomo M., and Dujic B., “Influence of the connection behaviour on the seismic resistance of multi-storey crosslam buildings”, *12th World Conference on Timber Engineering WCTE 2012*, Auckland, New Zealand, July 16-19, 2012, Vol. 3, pp. 402-410.

[13] Blass H.J., and Fellmoser P., “Design of solid wood panels with cross layers”, *8th World Conference on Timber Engineering, WCTE 2004*, June 14-17, 2004, Lahti, Finland, pp. 543-548.

[14] Computers & Structures Inc., *SAP2000—Integrated finite element analysis and design of structures*, Berkeley, CA, 2000.

[15] Simulia, *ABAQUS User’s Manuals – Version 6.9-1*, 2011.

[16] Sustersic I., and Dujic B., “Simplified cross-laminated timber wall modeling for linear-elastic seismic analysis”, *Meeting forty-five of the Working Commission W18-Timber Structures, CIB*, International Council for Research and Innovation, Växjö, Sweden, August 26-30, 2012, 7 pp.

[17] Gavric I., *Seismic Behaviour of Cross-Laminated Timber Buildings*, Ph.D. Thesis, 2013, University of Trieste, Italy.

[18] European Committee for Standardization (CEN), *Eurocode 5 – Design of timber structures – Part 1-1: General rules and rules for buildings*. 2004.

[19] Fragiacomo M., Dujic B., and Sustersic I., “Elastic and ductile design of multi-storey crosslam massive wooden buildings under seismic actions”, *Engineering Structures*, Vol. 33, No. 11, 2011, pp. 3043-3053.

[20] Fragiacomo M., and Rinaldin G., “Advanced models for seismic analyses of timber buildings”, *Außergewöhnliche Einwirkung - Erdbeben - im Holzbau*, *Workshop on*

crosslam construction "Grazer Holzbau-Fachtagung – 9. Gra FHT'11", Technical University of Graz, Austria, 2011, pp. J-1 – J-28.

[21] Sustersic I., Fragiacomo M., and Dujic B., "Influence of connection properties on the ductility and seismic resistance of multi-storey cross-lam buildings", *Meeting forty-four of the Working Commission W18-Timber Structures, CIB*, International Council for Research and Innovation, Alghero (Italy), August 29-September 1, 2011, 11 pp.

[22] Pei S., Popovski M., and van de Lindt J.W., "Seismic design of a multi-story cross laminated timber building based on component level testing", *12th World Conference on Timber Engineering WCTE 2012*, Auckland, New Zealand, July 16-19, 2012, CD.

[23] Pozza L., Scotta R., and Vitaliani R., "A non linear numerical model for the assessment of the seismic behavior and ductility factor of X-Lam timber structures", *International Symposium "Timber Structures from Antiquity to the Present"* edited by J. Chilton and I. Mungan, Istanbul, Turkey, June 25-27, 2009, pp. 151-162.

[24] Ceccotti A., and Vignoli A., "A hysteretic behavioural model for semirigid joint", *European Earthquake Engineering*, 1989, Vol. 3/89, pp. 3-9.

[25] Ceccotti A., Lauriola M., and Vignoli A., "About the seismic resistance of the Hamar Hall", International Wood Engineering Conference IWEC, 1996, New Orleans (USA) Vol.1 pp. 203-210.

[26] Ceccotti A., Follesa M., and Karacabeyli E., "3D seismic analysis of multi-storey wood frame construction", World Conference on Timber Engineering, 2000, Whistler Resort (Canada), Proceedings 1.2.3.

[27] Rinaldin G., Amadio C., and Fragiacomo M., "A component approach for non-linear behavior of cross-laminated solid timber panels", *14th ANIDIS Conference*, Bari, Italy, September 18-22, 2011, 10 pp., CD.

[28] Rinaldin G., So.ph.i. software version 4, *http://giovanni.rinaldin.org/*, 2011.

[29] ETA Danmark A\S. European Technical Approval ETA-06/0106. Technical Approval for Simpson Strong-Tie Angle Bracket 90, *http://www.strongtie.dk/* (in Danish).

[30] Gavric I., Rinaldin G., Amadio C., Fragiacomo M., and Ceccotti A., "Experimental-numerical analyses of the seismic behaviour of cross-laminated wall systems", *15th World Conference on Earthquake Engineering (15WCEE)*, Sept. 24-28, 2012, Lisbon, Portugal.

[31] Rinaldin G., Amadio C., and Fragiacomo M., "A component approach for the hysteretic behaviour of connections in cross-laminated wooden structures", *Earthquake Engineering and Structural Dynamics*, in review.

[32] Okabe M., Ceccotti A., Yasumura M., Minowa C., Kawai N., Sandhaas C., and Shimizu H., "Comparison with measuring method of internal storey drift on shaking table test of 7-storey X-lam building", *11th World Conference on Timber Engineering WCTE 2010*, June 20-24, 2010, Riva del Garda, Italy, CD.

[33] Ceccotti A., Follesa M., Kawai N., Lauriola M.P., Minowa C., Sandhaas C., and Yasumura M., "Which seismic behaviour factor for multi-storey buildings made of cross-laminated wooden panels?" *Meeting thirty-nine of the Working Commission W18-Timber Structures, CIB*, Intern. Council for Research and Innovation, Florence, Italy, August 28-31, 2006.

[34] Follesa M., Fragiacomo M., and Lauriola M.P., "A proposal for revision of the current timber part (Section 8) of Eurocode 8 Part 1", *Meeting forty-four of the Working*

Commission W18-Timber Structures, CIB, International Council for Research and Innovation, Alghero, Italy, August 29-September 1, 2011, 13 pp.

Theme IV

Building Physics and Examples

Nic Clark

Managing Director

KLH UK

London

UK

Email: nic.clark@klhuk.com

Nic Clark has over 27 years' experience within the construction industry, working with Main Contractors. As well as responsibility for commerciality and cost management of construction projects he works with innovative products, programme and logistical solutions. Nic joined KLH UK in 2012 to continue to raise awareness of CLT within the construction industry and promote its use as a modern method of construction.

Dipl.-Ing

Andreas Ringhofer

Institute of Timber Engineering and Wood Technology

Graz University of Technology

Austria

Email: andreas.ringhofer@tugraz.at

Andreas Ringhofer studied Civil Engineering Sciences with Environment and Construction Management (bachelor programme) and Civil Engineering Sciences and Structural Engineering (master programme) at Graz University of technology. He earned a diploma degree in 2010. From 2011 to 2012 he worked as Project-Assistant and since 2012 he has been Univ.-Assistant at the Institute of Timber Engineering and Wood Technology at Graz University of Technology. His research topics are timber engineering and wood technology, especially connection techniques with self-tapping screws. This is also the topic for his PhD, which he is working on.

Dipl.-Ing.

Heinz J. Ferk

Institut für Hochbau

Labor für Bauphysik

Technische Universität Graz

Austria

Email: ferk@tugraz.at

Heinz Ferk completed a degree in civil engineering at the Graz University of Technology in Austria. Until 1995 he was Research and Teaching Assistant at the Institute for Building and Industrial Construction with a focus on building physics and building science. He founded an office for building engineering and consulting and pioneered work for the multistory wood-based building market, e.g. the first 3 story wood-frame-based building with laminated timber ceilings in Styria, the first 3-story CLT based building in Austria, the first 4+ CLT based building Vienna. Since 2000 he has been head of the Laboratory of Building Physics at the Institute of Building Construction of the Graz University of Technology, and, since 2006, Vice Head oft the Institute. He is a member of several national and international standardization committees and other building science and building regulation related institutions.

Timber-in-Town – current examples for residential buildings in CLT and tasks for the future

Andreas Ringhofer

Univ.-Assistant

Institute of Timber Engineering and Wood Technology
Graz University of Technology

Graz, Austria

Gerhard Schickhofer

Professor for Timber Engineering and Wood Technology, Director of the Insitute[1)]

Institute of Timber Engineering and Wood Technology
Graz University of Technology[1)]

Graz, Austria

Summary

Solid timber construction (STC) with Cross Laminated Timber (CLT), which was presented for the first time to an international audience of specialists in the context of the concluding conference of the COST Action E5 "Timber frame building systems" in September 2000 [10], can be definitely regarded as one of the most significant innovations in timber engineering within recent decades. Worldwide sales figures of about 500,000 m3 and a wide area of application, which includes not only modern one-family houses, multi-storey buildings, but also office- and administration buildings, hall systems and bridge structures, prove this statement. However, the motto "everything is possible", which goes along with this rapid development, and the legitimate concentration on the feasibility in static-constructive terms (ULS, SLS, fire, earthquake, etc.) lead to the problem that interdisciplinary issues are considered insufficiently; this is in the context of multi-storey buildings with questions concerning qualitative building services adapted to this type of construction.

Therefore, the aim of this report can be seen in dealing with these interdisciplinary problems. In concrete terms this means facing them and offering possible solutions in the context of solid timber construction out of Cross Laminated Timber. Due to the local processes on the subject of using Cross Laminated Timber, this report is based on a number of selected and partly completed projects in the Graz (AT) conurbation.

1. Introduction

"Is timber coming to town?" This question, asked at the 8th International sawmilling Congress in 2013, can definitely be answered in the affirmative. Timber has always been an essential building material in construction and probably one of the first and most important building materials in structural engineering. Due to fire disasters it was banned from the cities and replaced by reinforced concrete at the end of the nineteenth century.

Series events ("timber to town"), completions ("timber construction in the city"), research and development projects ("Low Carbon Future Cities", "Timber in Town"), as well as marketing projects ("Wood Growing Cities"), have contributed to the fact that timber returns to the front line in the cities as for example Vienna (6F), Zurich (6F), London (8F, 9F), Oslo (8F), Växjö (8F), Bad Aibling (8F), Milan (9F) and Melbourne (10F). Forerunner for this development has been the 25 years existence of Cross Laminated Timber and its associated solid timber construction techniques.

Fig. 1 Project "Wohnbau Wagramerstraße", Vienna, AT (left) [18]
Project "Murray Grove", London, UK (middle) [19]
Project "Via Cenni" / „Legno in Citta", Mailan, IT (top right) [20]
Project "Bridport House", London, UK (down right) [21]

Despite the understandable enthusiasm for multi-storey residential buildings constructed of Cross Laminated Timber, it should not be forgotten that other fields of application in urban space are of significant importance as well. Such fields of application are, for instance, the possibility not only of adding further storeys and construction extensions but also the use of timber, in particular of Cross Laminated Timber, for the construction of office and education buildings in urban space. Several projects under the UK government "Building Schools for the Future" programme pioneered the concept of "education builds on wood". In this context numerous kindergarten and schools have been built in UK using the solid timber construction technique, many of them in urban space. Approaches to this concept can also be found in Austria, however based and implemented on the initiative of some individuals.

Fig. 2 Project „Open Academy", Norwich, UK (left) [8]
Project "Bautechnikzentrum TU Graz", Graz, AT (middle)
Project "Kinderkrippe Schönbrunngasse", Graz, AT (right), (Foto: Paul Ott)´

Returning to multi-storey residential buildings, it cannot be ignored that, especially in this category, the human being desires nowadays to get ‘always wider, longer and higher’[14]. But for the construction of multi-storey residential buildings in timber, it is also valid that, before thinking of comparative and superlative, the basics have to be known. The competition to maximize dimensions (heights) should not be the centre of attention when building with timber (and in particular when it concerns multi-storey residential buildings) but rather an integral way to reach optimization, combined with aspects like

- wider in application
- longer in period of use and
- higher in quality.

After all, the point is to create living space in a way that saves resources on the one hand and complies with minimum requirements, remains affordable and meets the criterion of sustainability on the other hand. This is a challenge that every method of construction has to respond to. And it is not an easy one when prices of land, building costs and rents rise continuously. M. Linz describes in his publication “Neither lack nor excess”[17] the “three steps to sustainability” and calls them

- efficiency (small input of material and energy per product or service),
- consistency (ecologically harmless technologies; compatibility between nature and technique) and
- sufficiency (low consumption of recourses by reduction of demand).

What does this have to do with solid timber construction technique in Cross Laminated Timber? Over the last two decades the solid timber construction technique has succeeded in gaining such a level that it can be offered to architects and engineers as a safe, robust and reliable building method. However the response after the first use was quite often that it is interesting but too expensive for the customer. S. Smith and T. Wallwork address this topic in their contribution “CLT – **C**ross **L**aminated **T**imber or **C**onsumes **L**ots of **T**imber”[16] and make a comparison with steel and concrete. Their contribution deals with efficiency-raising measures around the product Cross Laminated Timber and results in the conclusion that the “CLT product needs to evolve”. This proclaimed improvement in efficiency can only be achieved by research and development. The necessity of such measures is beyond question. Examples of this are:

- Use of the diversity of wood species combined with deploying regional wood resources
- Reduction of the demand on the wood resource by cross-section optimization
- Effort to standardize according the slogan
  “one system – one element – one product”
- Improved production process and coordinated machinery use
- Design and planning principles combined with standardized verification methods

All the above-mentioned measures can be assigned to the aspect ‘efficiency’. Measures of this type are indispensable for a continuous development of the solid timber construction technique. The second aspect ‘consistency’, which in this context refers to appropriateness, is already inherent in the material, wood, due to it being a renewable resource that has potential for recycling combined with many low emission products. To act according the slogan ‘reduce – reuse – recycle’ comprises the three aspects ‘efficiency’, ‘consistency’ and ‘sufficiency’ and – applied to constructions in Cross Laminated Timber - is able to lead to improved and optimized construction systems (e.g. housing).

The next parts of this paper present examples of structural engineering with solid timber construction technique in Cross Laminated Timber, built in recent years or are actually planned in and around the City of Graz. The reader’s attention should be turned to the implementation of the measures listed above in improving the efficiency of building activities with CLT. The aim is not only to contribute to a further spreading of this building method but also to show constructive principles to guarantee a high quality and durability of buildings in the solid timber construction technique. These principles, underlying quotations of Professor H. Gamerith [3] (Emeritus at the Institute of Building Construction at Graz University of Technology), should emphasize the necessity of interdisciplinary thinking and acting within the framework of planning a realisation of multi-storey building constructions.

2. Completed or planned construction projects with solid timber construction technique in Cross Laminated Timber in Greater Graz

2.1 Project „social housing Wittenbauerstraße“, Graz

Fig. 3 Top view building 1 (left picture); building 2 (right picture)

2.1.1 Project description

This construction project, completed in autumn 2012, consists of 22 housing units in total (between 60 and 90 m² of living space) that are split up into two buildings (see Fig. 5). In these units, the main structure is constructed in solid timber construction technique with Cross Laminated Timber. They are arranged as separate three-storey structures and made with access via a central situated staircase made of reinforced concrete. In order to enable largely green space underground parking was planned for its inhabitants. The total of the obstructed surface is 2600 m² out of which 1600 m² (approx. 60 %) can be identified as living area.

Project duration was about three years divided into a planning phase of 20 months and a construction phase of 16 months (one of those was the assembly of CLT-elements). Timber construction (specification ‘carpentry’) , at a cost of €0.7 million, represents a small proportion

(20%) of the total project cost of €3.3 million. For cost estimation, therefore, this amounts to approximately €2000 per m² of living area.

After consultation with the constructor and the sponsors of this social housing (the City of Graz and the province of Styria), it was possible, within the framework of the project, to construct the bearing walls of one of the units with CLT made of birch. Because the use of hardwood as a basic material is very innovative in multi-storey building construction, special attention was paid, by the Institute of Timber Engineering and Wood Technology, to production, assembly and the use of these elements in their form of finished wall structure.

This was achieved by issuing an "approval on an individual basis"; within this framework, material tests of the basic material, as well as tests of the finished products, were conducted at Graz University of Technology [15]. For further quality control, spot core samples were taken from completed wall elements (see Fig 4). The samples were subsequently tested for delamination according to EN 391:2001 [11].

Fig. 4 Test configuration for bending test birch-CLT (top left) [15]
Taking of core samples on the spot for delamination tests (down left)
Wall of birch-CLT – visual quality (right)

To evaluate the building physics behaviour of the walls, the Institute of Timber Engineering and Wood Technology of Graz University of Technology scheduled two control cross-sections (one in birch and a one meter wall strip in spruce-CLT for reference); these were used to monitor and record, by means of installed sensor technology, the change of the relative humidity (thus wood moisture) and temperature across the entire cross-section of the wall. First results are published [9] and a more detailed investigation will be presented at the "RILEM International Symposium on Materials and Joints in Timber Structures" taking place in October 2013.

The aim of using birch wood for the production of CLT was to demonstrate the potential of wood species that are available locally and/or in abundance to become new resources for the production of CLT.

2.1.2 Principle of the structural system

As already mentioned in chapter 2.1.1, CLT elements were mainly used for the load transfer beside the components made of reinforced concrete (foundation and staircases). Because these elements, used for walls and floors, are able to carry both horizontal and vertical loads into the foundation and the floor plan and elevation of the separate units fulfil all principles of stability, the three-storey buildings, are paced around cores but form independent load bearing structures. The central core serves only for access to the units and as the position for “cellar” storage for the units. Using this, it was possible to de-couple the units from each other and from the unheated staircase, acoustically and thermally. Movement joints between the CLT frame and the concrete core are used where necessary to allow differential horizontal movement.

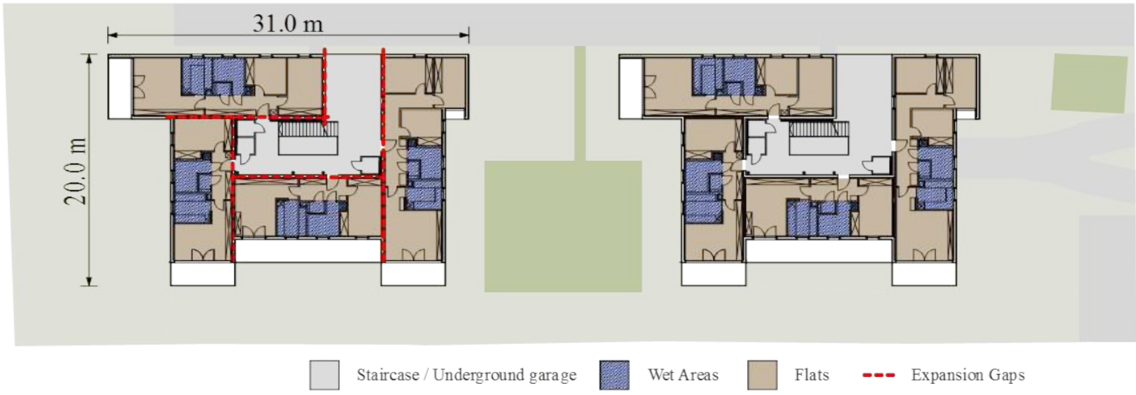

Fig. 5 Floor plan of the plot with function sharing in different colours

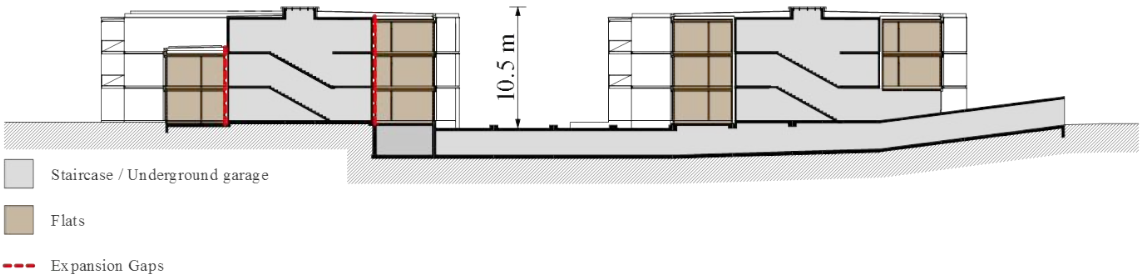

Fig. 6 Cross section of both buildings

A one-span system with a width of about 5 m for all units considerably simplified the structural design, as well as the construction (see Fig. 7). The verification of vibrations at serviceability limit state (SLS) was the decisive factor for dimensioning the necessary thickness of elements (5-layered, 198 mm, l/h ~ 26). With a calculated eigenfrequency of f_1 = 6.1 Hz, according to ÖNORM B 1995-1-1/NA:2009-07, verification for the chosen element was not fulfilled and, as the maximum depth for 5-layered elements is 200mm, the problem had to be investigated in more detail (this was to avoid the use of more expensive 7-layered elements). An initial new calculation according to the Hamm/Richter method [7] gave a result of f_1 = 7.2 Hz. The main reason for the difference, between the two first eigenfrequencies, is that the active vibrating mass is ascertained for both methods in a different way (ÖNORM B 1995-1-1/NA:2009-07: gravity loads incl. quasi-permanent parts of imposed loads; Hamm/Richter: gravity loads only). Because the newly calculated eigenfrequency was between “normal” (6 Hz) and “high requirement“ (8 Hz) [7], the next step was to make an agreement with the building owner to carry out vibration tests during and at the end of the construction progress, in order to verify the calculated eigenfrequency in situ. This was made within the scope of a master thesis at Graz University of Technology [6]. In the master thesis vibration characteristics of CLT-floors were examined on the basis of this construction project. The lowest (measured in different parts of the bearing structure in the building), and therefore essential first eigenfrequency, resulted to 12.9 Hz and exceeded, by more than twice, the 6.1 Hz according to ÖNORM B 1995-1-1/NA:2009-07. This indicates the discrepancy between calculation-verification and measurement and points to the need to continue to research on the vibration behaviour of CLT-floors, especially when taking into consideration the clamping effect caused by wall loads.

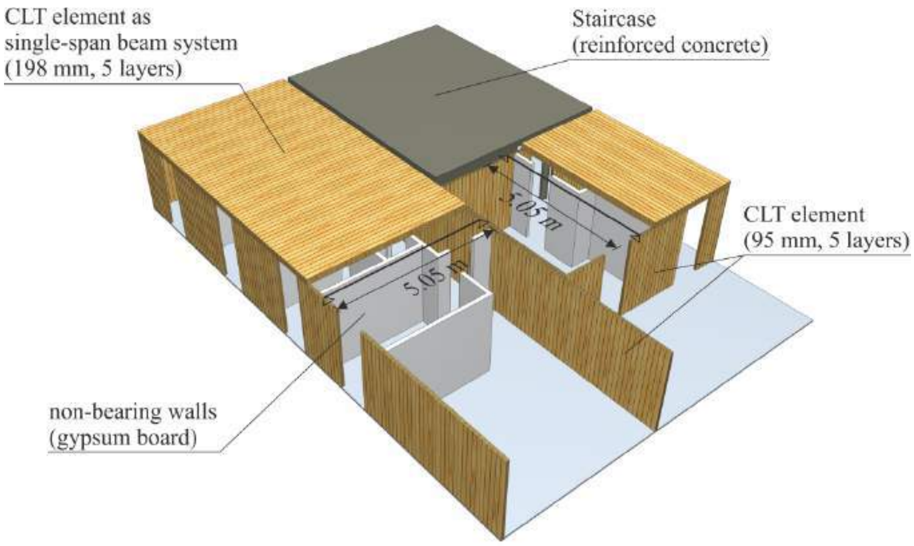

Fig. 7 Floor plan with span proportions

In considering the load, g_k , for the floor assembly shown in Fig. 11 a traffic load of q_k = 3.00 kN/m² (incl. gravity loads of removable separating walls) and is used in the Hamm/Richter method ("normal requirement") for the calculation of vibration for CLT assumed to be single-span beam systems, with the ratio of span to thickness is generally l/h = 25 to 30**.** The range of validity for this ratio is limited to spans of around 6.50 m, which should be sufficient for spans in housing.

In addition to floor and roof systems, the construction of all bearing walls (according Fig. 7 only external walls are bearing) was made with CLT. Because of the advantages, with air tightness and fire behaviour, the choice was taken to use a five-layered CLT-element. The smallest possible thickness of element with 95 mm (5 x 19 mm) from the producer was decisive, not the ULS or fire (REI 60) behaviour.

In view of raising efficiency when building with CLT, when positioning of the load-bearing walls at the planning stage, two essential principles were obeyed. All wall elements should be designed without large openings of full storey height, with the effect that the offcut during production could be reduced to a minimum (see Fig. 8). Positioning of the walls on top of each should ensure that horizontal loads (wind, earthquakes) are transmitted directly to the foundations, thus significantly reducing the loads on fastening the elements, and easing their design.

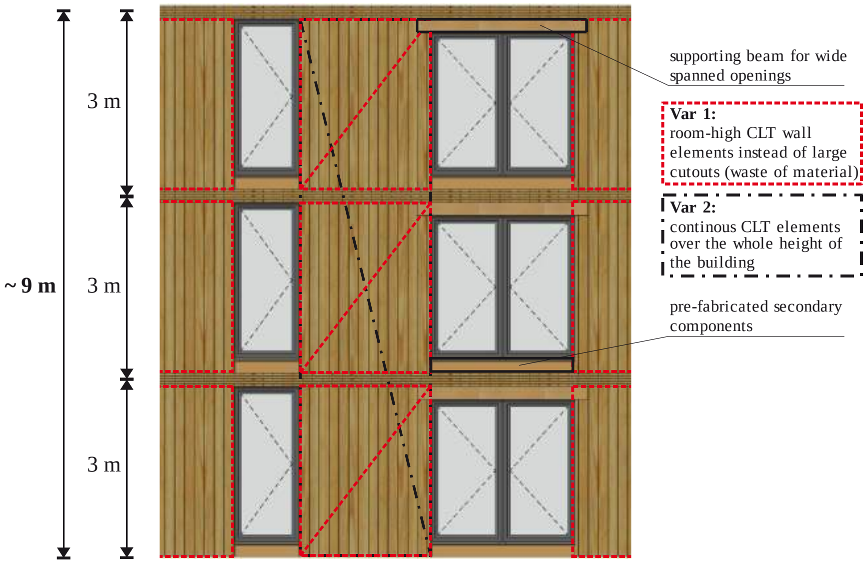

Fig. 8 Positioning of wall elements in elevation

As shown in Fig 3 and Fig. 5, a balcony or a terrace was planned for each unit. In contrast to the widespread use of cantilever floors serving to support balconies, for this project it was decided to make all extensions in form of secondary constructions (in this case made of steel). On the one hand, this was for reasons of building physics (to avoid thermal bridges respectively moisture and air transfer into the structure), and on the other hand it was for structural reasons (due to different life cycles of balcony/floor allowing the possibility of replacement and having no requirement for height compensation because of the assembly of the floor). Or with the words of H. Gamerith [3]:

„The faster a part erodes, is used up or can be damaged the easier it should be reachable to repair or replace "

Fig. 9 gives an overview of the balcony system. It's a prefabricated element and connected selectively with self-tapping screws to the primary supporting structure, entirely in line with the idea to mount and demount quickly.

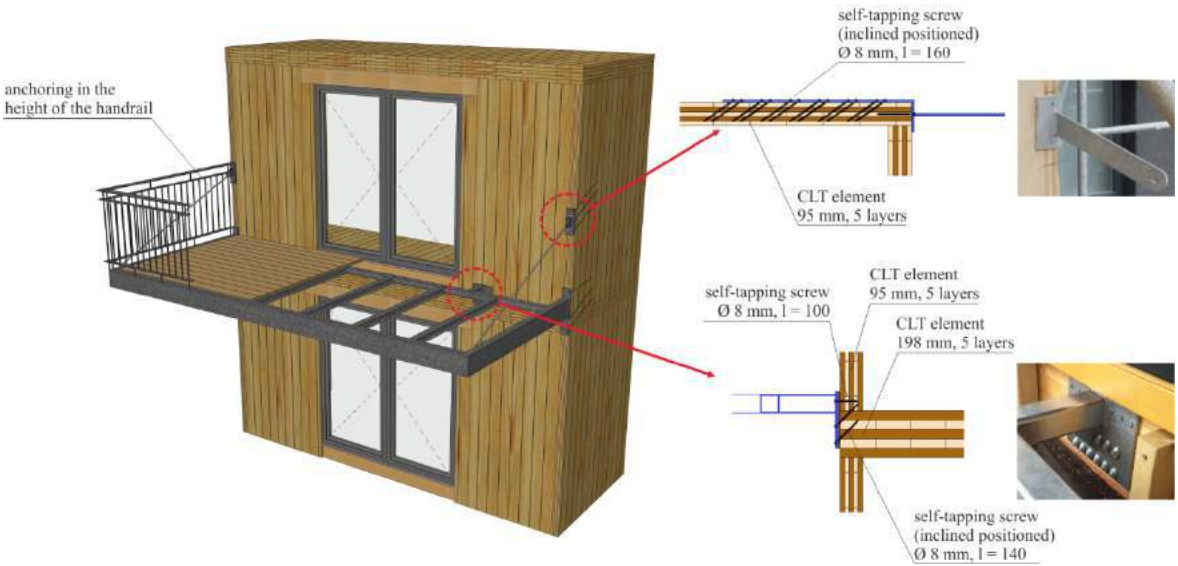

Fig. 9 Schematic illustration of the balcony

The on-site installation of linear timber products is quite cumbersome compared to the assembly of large-sized CLT elements and can be avoided by means of precise planning right from the start. Only the lintels for big wall openings (double window elements) and the supporting members where the floor span direction changes in one of the four unit types, had to be carried out in form of laminated timber beams. But even these lintel beams could have been avoided by taking into consideration the two-dimensional structural behaviour of CLT and by dividing the elements in a suitable way (perpend joint not in the window area) (see [4]). After all the whole timber volume consists of only one percent of linear bearing components.

Because of the relatively low height of the structure, its position in a not earthquake prone area and the already mentioned positive design of elevation, conventional joints have been used for the connection of wall and floor elements:

- Connection wall:underside-of-floor or wall:top-of-floor:
  Angle brackets in general and hold-downs in horizontal highly stressed bearing walls, situated at the ends of the wall
- Connection floor:wall, wall:wall (butt joint) and floor:floor (stepped fold):
  fully threaded self-tapping screws (inclined arrangement)

In view of the different requirements of solid timber construction, the use of more expensive hold-downs instead of angle joints for the transfer of uplift forces at the end of walls, a principle taken from timber frame construction, should be reconsidered. Within the framework of a research project at the Institute of Timber Engineering and Wood Technology, project comparative experiments of horizontally stressed CLT shear walls with different joining techniques for the connection joint have been carried out (see [5]). These experiments form the basis of the following statement: The difference in load bearing of walls with hold-downs at the end of walls compared to those using angle brackets justify in no way the additional costs in joining technique.

As already mentioned earlier in the paper, movement joints have been devised to allow for differential horizontal movements between parts of the structure. They are presented in the next figures.

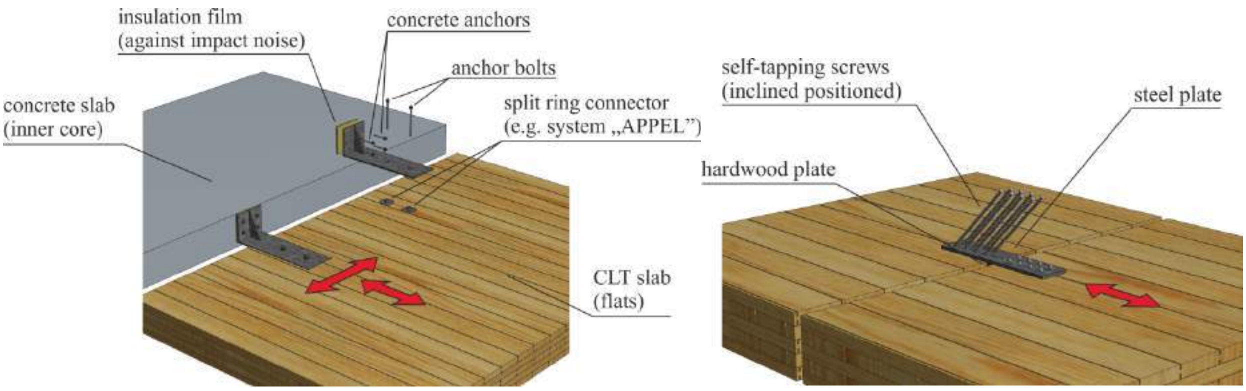

Fig. 10 Left: connection of CLT floors to the inner core (each storey)
Right: connection of CLT to CLT (at roof level)

In conclusion Fig. 11 summarizes the design principle of the building in solid timber construction, applied and explained in this chapter.

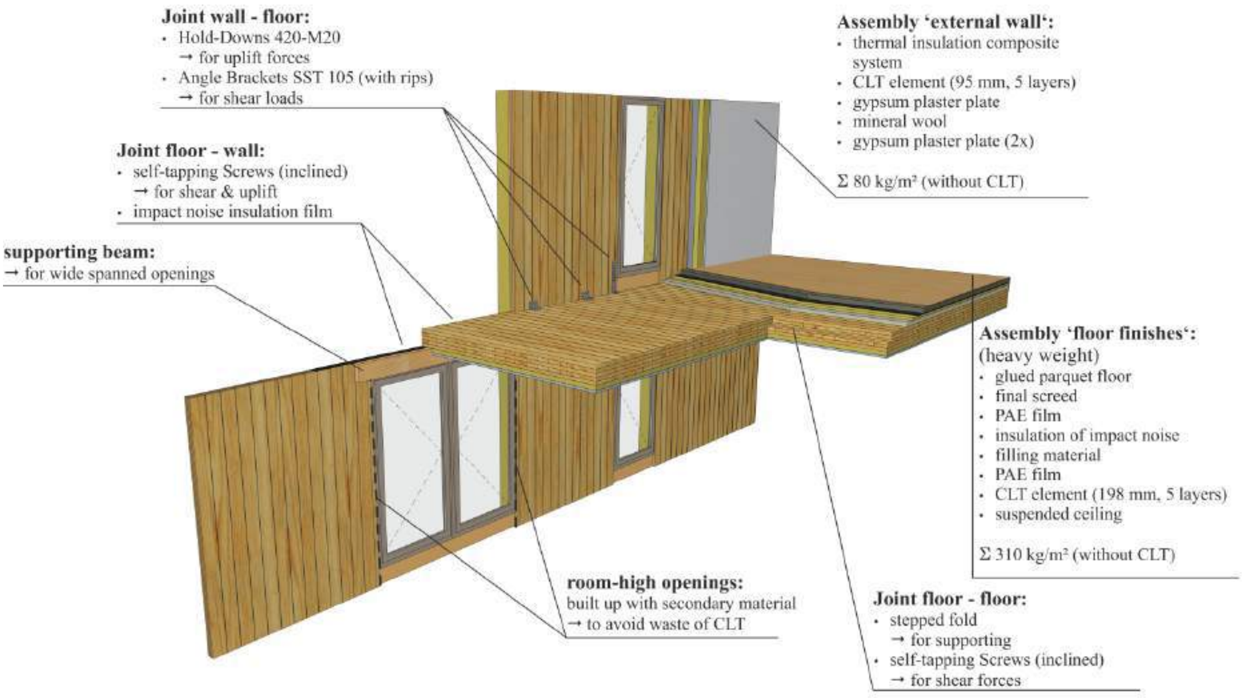

Fig. 11 Illustration of CLT supporting structure for this project

2.1.3 Essential constructive aspects

As already briefly discussed in chapter 1, if multi-storey buildings in solid timber construction technique with CLT to be built it is essential to guarantee the quality of the construction over the whole lifetime cycle of the structure. This corresponds to the basic requirements of durability according to EN 1990:2002.

It is known from experience, that if the drainage of surface water is not carried out properly, due to damage in waterproofing and the uncontrollable increase of moisture content in the load bearing construction, the result can have very negative effects on the life cycle of the supporting structure. Particularly affected are horizontal surfaces, such as floors and of course flat roofs. To avoid this possible structural damage, particular attention should be paid to the construction of such components. At this point it is worth to taking a closer look at the flat roof construction because there are, according the opinion of the authors, some positive problem-solving approaches available.

As Fig. 12 shows, the roofing system is in principle a back-ventilated and green flat-roof construction with a bearing layer of CLT (186 mm, 5-layered). The back-ventilation is the core aspect of the system and fulfils two essential functions. Due to the permanent air change in this zone, it provides, on the one hand, a certain degree of protection against overheating of the top floors during summertime, and ensures, on the other hand, that, in case of unexpected moisture of the wooden under roof, construction can dry out. Surface water is normally collected in the highest layer (layer of vegetation), with external gutters (and downspouts) draining into the soil. A second protection layer, situated behind the back-ventilated level, serves as additional protection layer against moisture for the supporting structure, in case of damage.

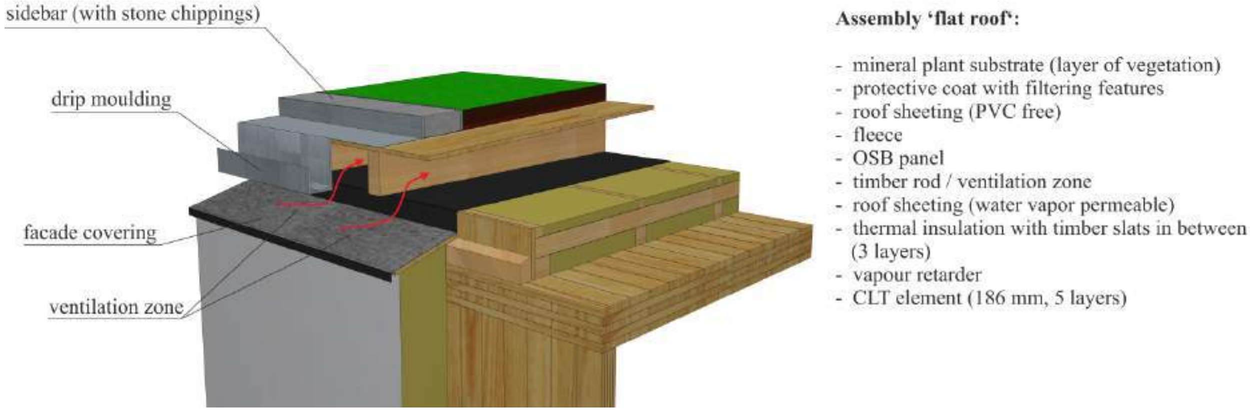

Fig. 12 Assembly of the flat roof construction in CLT

For future construction projects, it would make sense to construct back-ventilation inclined and at accessible height. This method would increase the cross section of ventilation and thus the air renewal rate, and enables a permanent control of the drainage levels in a non-destructive way. According H. Gamerith [3] it should be considered that:

"Constructions should be drafted in a way that they are easy to maintain, to control if they are fully functional and easy to repair in case of necessity (e.g. fastening technology, flat roof construction, installation technology etc.)"

As the major part of the exterior walls is equipped with an external thermal insulation composite system (ETICS) the combination of such a system and CLT elements as load-bearing structure should be enlarged upon at this point. As already included in the designation, these are system solutions that offer an economical alternative to back-ventilated construction. Because of the lack of a normative standard, they are regulated by European Technical Approvals (ETA), which indicates, besides the components "surface coating", "reinforcement", "insulating material" and "fastening" also suitable base coat (if mineral then brick or concrete wall; if organic then wood-based panel material). When studying these approvals it can be seen that many thermal insulation composite systems, especially those with synthetic isolating material such as EPS, are decidedly not approved for structures consisting of plate-shaped wooden composites.

Other systems, which were especially designated for timber base coats (commonly with mineral or organic insulation products), limit them to certain specified products, so that CLT elements are only allowed in a few cases. These cases, found in the frame of investigations concerning this topic (without making claim to be complete), are systems using fibreboards as insulation product. In contrast to that, external wall assemblies in CLT, combined with ETICS, using mineral wool panels are commonly used in present and – according to the opinion of the authors – proven to be suitable. The grey area in law, caused by the missing approval, should be kept clearly in mind however. To summarise the following cite by H. Gamerith [3] is appropriate:

"Reliable detail systems are safer than unreflected in-house developments."

2.2 Project “Wohnen am Fluss (Living on the river)”, Graz

Fig. 13 Image of the project (preliminary draft) [1]

Fig. 14 Image of the project (preliminary draft) [1]

2.2.1 Project description

In contrast to the already finished construction described in section 2.1, this project is being planned in present. The developing process is based on a pre-investment study [1], which was performed by three architects, in cooperation with three industrial firms, under the coordination of the Institute of Timber Engineering and Wood Technology at Graz University of Technology in the year of 2012.

As shown in Fig. 14, seventeen buildings, with five to eight storeys and containing approximately 400 flats, are designated to be erected in solid timber construction with CLT. This would lead to a living space of roughly 30,000 m², with overall costs of €60million (internal assumption). As a consequence of this high value the investor plans to erect the buildings in three phases of construction, which will last the whole decade 2010-2020.

2.2.2 Principles of structural design

Besides extensive investigations concerning the architectural feasibility with a special focus on urban requirements, alternate structural designs were part of the pre-investment study mentioned above. The following sections will demonstrate these results, on the basis of a representative building type.

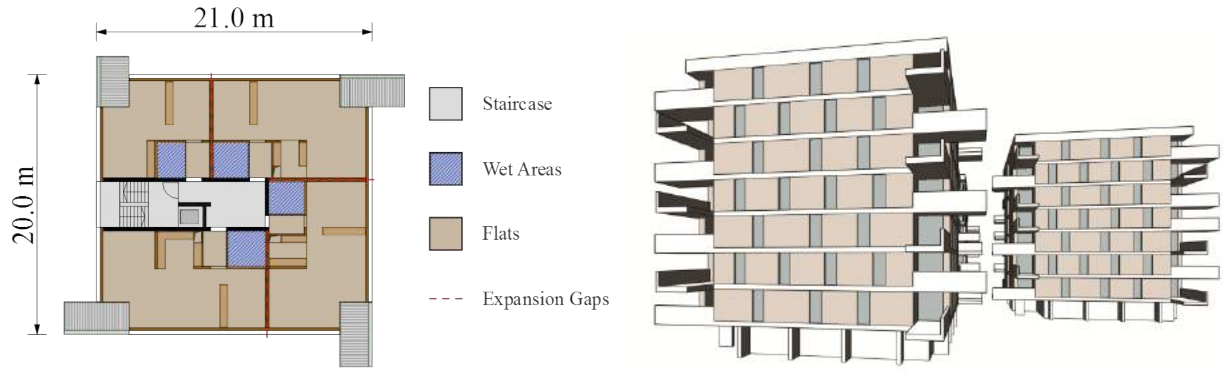

Fig. 15 Floor plan with function sharing in different colours (left)
Impression of the chosen building type (right) [1]

As shown in Fig. 15, many principles to increase the efficiency and building quality, described in section 2.1.2, have already been considered in this preliminary draft version. Thus, two-span systems (160 mm, 5-layered; see Fig. 16), with consistent widths and beams as supporting members are used. Furthermore, there are room-high wall segments, without openings, as well as pre-fabricated balcony systems as secondary structures. In contrast to the project described before, not only external but also internal walls and, especially, separating walls of the flats are designated to be part of the bearing structure. Those internal and separating walls will provide enough horizontal stiffness and will give more freedom for creative design of the external walls. The inner core (again in reinforced concrete because of local fire protection requirements) is in this case also planned to be part of the bearing system against horizontal loads (especially wind loads).

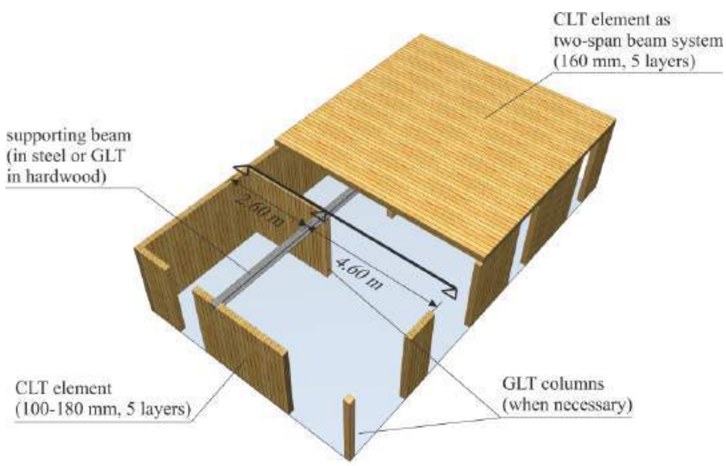

Fig 16 Floor plan of the floor system of one representative flat

Because of the height of the 10-storey building, high horizontal wind forces have to be considered in the design of connections. The hold-downs and angle brackets used for the project in section 2.1.2 are useless if their number exceeds a certain value per running meter wall joint. Dowel-type connections with local steel plates between the CLT wall elements could be used instead, especially for the joints in the first storeys; see Fig. 17.

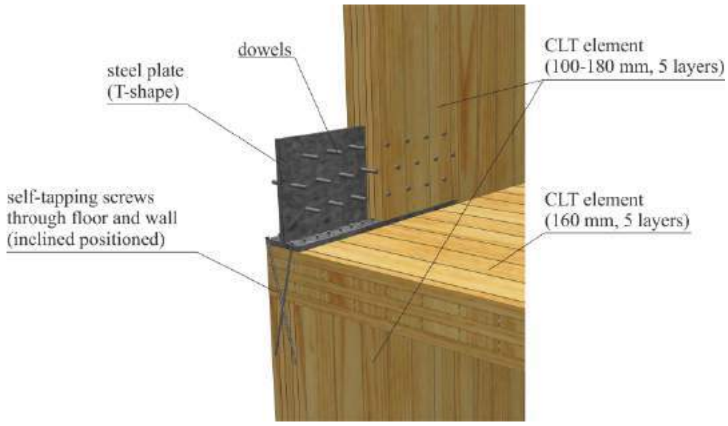

Fig. 17 Dowel-type connection with steel plate in between the wall element for efficient joint design

As shown in Fig. 16 and Fig. 17, the thicknesses of CLT wall elements range from 100 to 180 mm (increasing from the top to the bottom). The reason for these dimensions can be seen not only in the surcharge resulting from floor and roof systems, but also in the criteria for fire protection of R90 (fulfilling a structural capacity during 90 minutes burn-off) given for buildings with building class 5 in Austria, or rather the resulting economical optimisation of the ratio of covering to element thickness.

2.2.3 Essential constructive aspects

Fig. 11 in section 7.1 also gives insight into the arrangement of the wet rooms of the two described buildings. It is obvious that all of them are situated centrally in each flat. Consequently all service pipes containing water run through the timber construction. In case of a defect this situation may lead to unseen and uncontrollable moisture ingress in the bearing structure Fig. 18 represents this scenario to emphasise the problem.

Fig. 18 Damage of the CLT bearing structure caused by moisture ingress in a wet room

Because of the high costs caused by rehabilitation works, such damage needs to be avoided in multi-storey residential buildings erected in solid timber construction with CLT. In the worst case four flats may be affected by a single damage. Therefore, to provide the durability of the timber construction against moisture ingress, it is important to consider this problem in the course of developing the preliminary draft

This aspect has been considered in the context of the pre-investment study and for the present, resulted in the arrangement of wet rooms around the building core of reinforced concrete. This first approach enables the main lines to be run between the transition zone of reinforced concrete:CLT; see Fig. 19.

By adjustment of channels, with possibilities for observation (or with a simple sensor system) beneath the water pipes, damage may be easily detected and repaired by removing the shell construction. Wet rooms, or other areas with a need of water supply (kitchens, etc.), which are not situated close to the core, may be reached by duct located in the suspended ceiling. Possibilities for observation of the system would be given by providing inspection doors in the ceiling. Furthermore, possible damage that could be noticed easily would only affect the non-bearing part of the lay-up of the ceiling. According to H. Gamerith [3] it can be said:

"Because of different service lives, carcass and extension have to be conceived separately from each other. Especially supply and delivery pipes containing water (added by G. Schickhofer) have to be i) creatively integrated into the building, ii) structurally disintegrated and iii) accessibly organised."

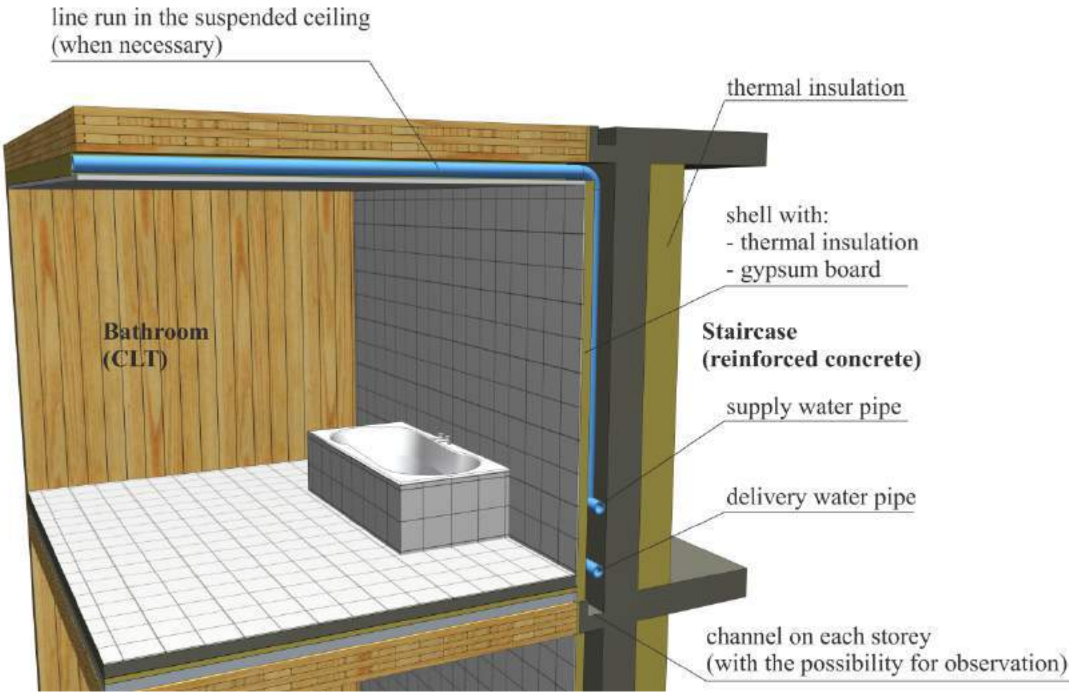

Fig. 19 Possible solutions for line runs in flats of CLT

2.3 Project „bio-impuls centre Styria“, Graz

Fig. 20 Image of the project “bio-impuls centre Styria”, preliminary draft [2]

In contrast to the multi-story buildings described in sections 2.1 and 2.2, a commercial building in solid timber construction with CLT is presented here. The main reason for choosing this project is to demonstrate the application of optimised CLT slab-systems to wide spanned floors, which can rarely be found in residential buildings.

2.3.1 Project description

This project includes the erection of an office, administrative and event building and has been started in the second half of the year 2012 by organising an architectural competition. The image presented in Fig 20 shows the preliminary draft of the winner of this challenge.

According to this design proposal, the building is going to contain two storeys with separate functions. The ground floor will be used for events, including an exhibition and presentation hall, an entrance area and storage rooms. On the first floor, administration offices and meeting rooms have been planned. On the basis of the floor plans and the cross section given in Fig. 21, an open interior design, leading to wide span floor systems of up to 10 m, has been created for both storeys. The systematic solution for this building, which makes use of CLT, is provided in section 2.3.2 for these situations.

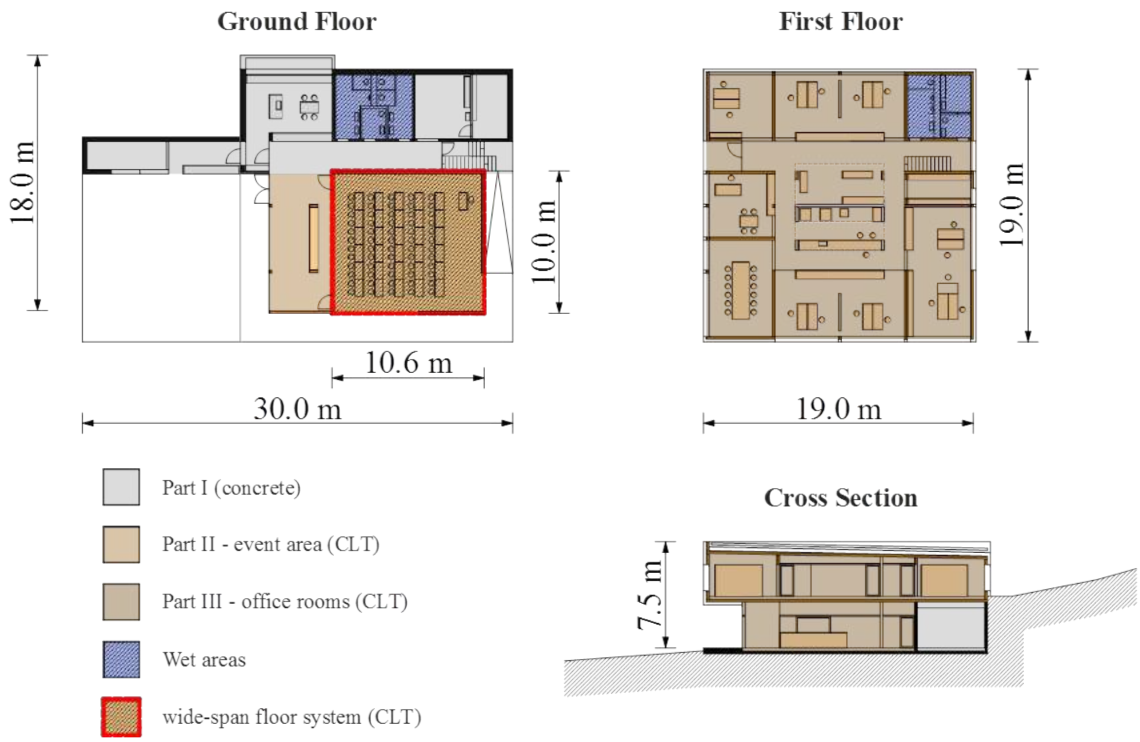

Fig. 21 Floor plans and cross section of the preliminary draft [2]

Based on the results of the architectural competition, the planning team is currently working on the development of the building. Commencement is not earlier than in the beginning of 2014. The overall costs are roughly estimated to be €1.3million.

2.3.2 Structural concept

By considering an estimated weight of 200 kg/m² for the assembly of the floor and traffic loads of 3.00 kN/m², the thickness of this 10 m span, 9-layered CLT element would amount to 360 mm, controlled by SLS-verification. Consequently, this unusual dimension would cause high manufacturing costs and problems with the room height; hence, this system is hard to accomplish. Furthermore, the 1st eigenfrequency of 4.3 Hz, calculated according to the method of Hamm/Richter [7] for this one-dimensional system, is far too low to fulfil the verification of vibrations and, therefore, an optimised bearing system is needed. Fig. 22 and Fig. 23 show two possible solutions for this situation. The spatial trussed structure given in Fig. 22 not only reduces the span length (the point support separates the system into three parts), but also enables two-way spanning structural behaviour of the CLT-element. Thereby an optimised lay-up of the element is assumed. In contrast to that, Fig. 23 demonstrates a GLT-CLT ribbed plate with a strict orientation in one direction. In this way, the CLT-element's dimension is minimised and the rigid bonded GLT members are located in the suspended ceiling.

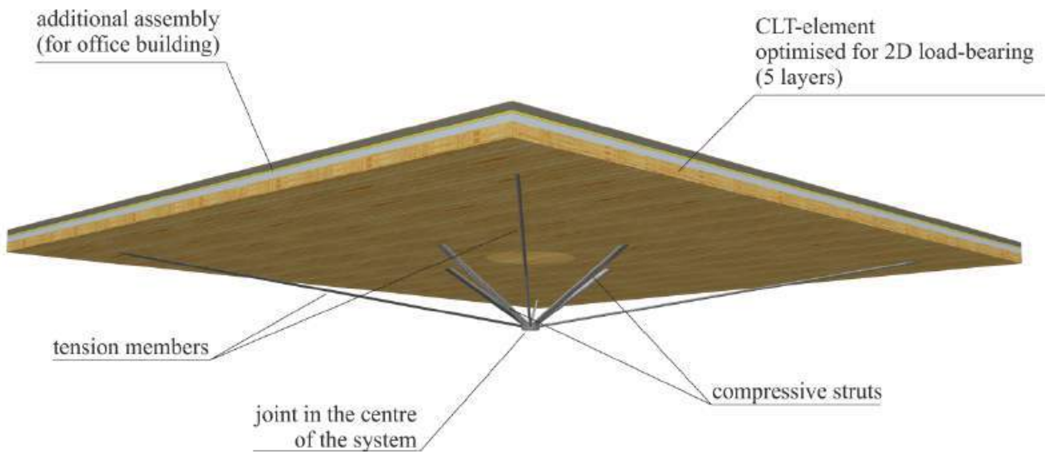

Fig. 22 Spatial trussed CLT floor system

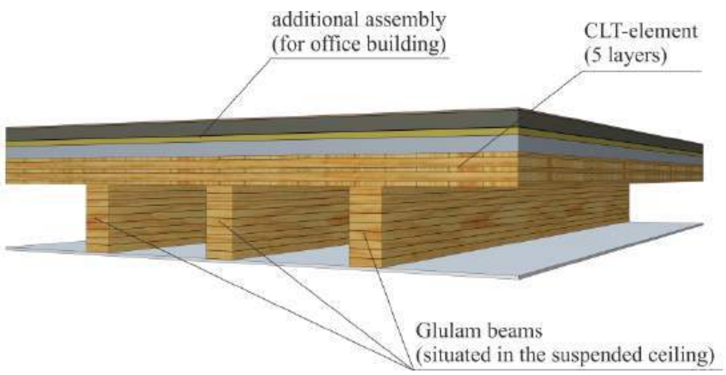

Fig. 23 GLT-CLT ribbed plate

Similar structural solutions are the roof construction of the Centre of Building Technology at Graz University of Technology, which has been erected between 2000 and 2001 [10]; see Fig. 24. If these systems are used for floors (and not for roofs), it is necessary to verify their serviceability, with a special focus on vibrations.

Fig. 24 Special solutions for the centre of Building Technology at Graz University of Technology:
Trussed CLT system as roof construction for the great testing hall (left)
GLT-CLT ribbed plate as roof construction for the offices (right)

2.4 Outlook regarding further projects

In addition to the projects demonstrated in the previous sections, in which the Institute of Timber Engineering and Wood Technology at Graz University of Technology has been involved, the project "Peter Roseggerstraße" will be briefly described in this section. This planned construction contains 12 buildings with three, four and five storeys and is going to be realised to the west of Graz. Three phases of construction are going to include 143 flats overall. Applied concepts of alternative energies are worth mentioning in this context [22].

Fig. 25 Image of a five storey residential building of the project "Peter Roseggerstraße"[22]

3. Conclusion, outlook and acknowledgements

As well as in international overview, in the course of describing selected projects, which have been partly completed in Greater Graz, this report also attempts to represent a snap shot of using Cross Laminated Timber as basic material for constructing multi-storey buildings as well as office- and administration buildings Rather than simply presenting the existing opportunities for top quality, state-of-the-art approaches in timber construction, the focus of attention is on demonstrating principles of (conceptual) design in order to increase efficiency and guarantee high levels of performance throughout life.

To summarise, these principles are presented again without making claim to be complete:

- use of superabundant and/or local wood species to produce Cross Laminated Timber as an opportunity to make effective use of resources;
- conception of uniform structural systems for regular floor plans and elevations (floor spans, continuous stiffening walls) as well as finding special, innovative solutions for specific situations (trussed systems, ribbed plates and box girder cross sections);
- arrangement of almost full-faced floor-to-floor bearing walls in Cross Laminated Timber to avoid cutaways and, hence, material loss;
- concept of adaptability of structure, in terms of secondary load-bearing structures, which are replaceable and weather-proof;
- provision of approved system solutions for the main assemblies "panel" and "floor";

- interdisciplinary thinking and acting across multiple building phases (carcassing – extension – method) in the course of designing and constructing critical building parts (flat roof, wet rooms);

“Timber is the new concrete”, is the slogan used by architect A. de Rijke. Based on his fundamental experience with Cross Laminated Timber, this quotation can be seen as a prophecy of new market segments and field of application. In fact, a nine-storey structure, correctly dimensioned in terms of ULS and SLS and built in timber solid construction with CLT, shares the same characteristics as concrete construction. Panels, floors, roofs and staircases are massive. Wooden floors have no vibration problems, but show similar features compared to floors of reinforced concrete and even have a similar thickness due to their low density. If the wood had the same colour as concrete, one could hardly distinguish between them. However, there are some substantial differences: Wood is a natural product and, consequently, does not share the same strengths and weaknesses with concrete. Wood reacts to high moisture conditions by changing its features. In case of continuously high moisture conditions, wood loses its substance and load-bearing capacity. Therefore, in the context of designing, it is of utmost importance to guarantee a permanently dry wood structure. This also implies the need for building services appropriate to timber construction. To summarise, this means that (a) water-bearing utility- and waste disposal lines need to be separated from the timber construction (b) the details for panels, roofs and floors need to be compatible with building physics. One point cannot be stressed enough: “Timber is **not** the new concrete”.

Added to the necessity of finding permanent, efficient and economic system solutions, the focus now shifts to vibration, mentioned in section 2.1.2; to the development of a connection technique related to this type of construction and to a detailed analysis of new structural systems to cope with wide spans in the context of office- and administration buildings (especially with regard to the functional efficiency).

To conclude, the author of this article would like to express his sincere thanks to the following persons, and their companies, for providing graphical material, planning documents and information:

Mr. Martin Strobl sen. and Mr. Martin Strobl jun. of *Architekturbüro Strobl* for many helpful documents regarding the projects “Kinderkrippe Schönbrunngasse Graz” and “Bio-Impuls Zentrum Steiermark”;

Mr. Michael Schluder and Ms. Nicole Wohlmuth of *schluderarchitektur ZT GmbH* für graphical material regarding the project “Wagramerstraße Wien”;

Mr. Jürgen Posch of *Die Frohnleitner Gemeinnütziges Steirisches Wohnungsunternehmen GmbH* for providing various documents;

Mr. Peter Rossegg of *Stora Enso Building and Living* for graphical material regarding the projects “Via Cenni” and “Peter Roseggerstraße”;

4. References

[1] Hohensinn J., Strobl M., Zinganel P., *Timber in Town – Masterplan Konzepte*, Report, Graz, 2012 (German)

[2] Strobl M., Strobl M., *Bio-Impuls Zentrum Steiermark | Alt-Grottenhof | Graz*, Competition Brochure, Graz, 2013 (German)

[3] Gamerith H., *Grundprinzipien guter Hochbaukonstruktionen*, Report, Graz, 2013 (German)

[4] Bogensperger T., Silly G., *2-achsige Lastabtragung von Brettsperrholz-Platten*, Report, Competence Centre holz.bau forschungs gmbh, 2012 (German)

[5] Flatscher G., *Versuchstechnische Betrachtung zyklisch beanspruchter Wandelemente in der Holz-Massivbauweise*, 18. IHF Garmisch-Partenkirchen, 2012 (German)

[6] Zimmer S. E., *Ein Beitrag zur Aufarbeitung der Schwingungsthematik für die Holz-Massivbauweise in Brettsperrholz*, Master Thesis, Graz University of Technology, 2013 (German)

[7] Hamm P., Richter A., *Personeninduzierte Schwingungen bei Holzdecken – Neue Erkenntnisse führen zu neuen Bemessungsregeln*, Ingenieurholzbau – Karlsruher Tage: Forschung für die Praxis, Universität Karlsruhe, 2009 (German)

[8] White G., *Cross Laminated Timber – What's all the fuss?*, Presentation, 3. Grazer Holzbau-Sonderfachtagung, Graz, 2012

[9] Ringhofer A., Wallner B., Schickhofer G., *SSTC 1.1.4 clt_building_physics – Dauermessungen der Luftfeuchtigkeit und Bauteiltemperatur in Wandaufbauten aus Fichten- und Birken-Brettsperrholz*, Research Report, Competence Centre holz.bau forschungs gmbh, 2012 (German)

[10] Schickhofer G., Hasewend B., *Solid timber construction – A construction system for residential houses, office and industrial buildings*, proceeding, In: "Seismic behaviour of timber buildings – Timber construction in the new millennium", COST Action E5 "Timber frame building systems" workshop, Venice, 2000

[11] EN 391:2001-10, Glued laminated timber – Delamination test of glue lines

[12] EN 1990:2003-03, Eurocode – Basis of structural design

[13] ÖNORM B 1995-1-1:2010-08, Eurocode 5: Bemessung und Konstruktion von Holzbauten – Teil 1-1: Allgemeines – Allgemeine Regeln und Regeln für den Hochbau – Nationale Festlegungen, nationale Erläuterungen und nationale Ergänzungen zur ÖNORM EN 1995-1-1 (German)

[14] Schickhofer G., Jeitler G., Brandner R., *'Immer länger, breiter, höher?' Der Holzbau in der Zukunft – Möglichkeiten und Grenzen*, Presentation, Holzleimbausymposium der JOWAT AG, Buchrain, 2008 (German)

[15] Hübner U., *SSTC 1.1.2-6 birch4GLT|CLT – Birke für Brettschichtholz und Brettsperrholz*, Research Report, Competence Centre holz.bau forschungs gmbh, 2012 (German)

[16] Smith S., *CLT – Cross Laminated Timber or Consumes Lots of Timber*, presentation, Solid Wood Solutions Conference & Exhibition, Birmingham, 2013

[17] Linz M., *Weder Mangel noch Übermaß – über Suffizienz und Suffizienzforschung*, Wuppertal Institut für Klima, Umwelt, Energie GmbH, Wuppertal, 2004 (German)

[18] www.architecture.at, 04.04.2013

[19] www.modernarchitecturecenter.com, 27.04.2012

[20] www.tekne.ws, 27.04.2012

[21] www.pirminjung.ch, 27.04.2012

[22] www.aktivklimahaus.at, 04.04.2013

[23] www.oib.or.at, 05.04.2013

CLT: Some Building Science Aspects for building with CLT

Heinz J. Ferk

Head of Laboratory

Institute of Building Construction

Building Physics Laboratory

Graz University of Technology

Graz, Austria

Summary

The following pages give a comprehensive overview of the building science related aspects of building with CLT. Starting with some material related issues, heat, air- and moisture control strategies are discussed. A special part deals with the acoustic performance of cross-laminated timber component constructions, of connections and building systems. Some hints on CLT panel conceptual design and examples of master details for the building enclosure design of cross-laminated timber constructions will round off the content of this topic.

1. Introduction

When I started my first encouraging experiences in building with CLT in 1996 and 1998, with the first CLT based 3-level multi-family house in Austria, it soon became quite clear, that on the one hand this brand new type of building material would have an enormous potential and on the other hand that there are some specific building science challenges that would have be to solved. Now, about 15 years later, the material is on a successful way around the world as a basis for emerging new building systems, increasing the use of wood also in a non-traditional way. Despite that we need to be very attentive to use the advantages of CLT and to prevent problems caused by misuse, abuse, neglect or erroneous interpretation of that special design and quality material. CLT is not a new type of concrete, as we can hear by several voices - some material properties are diametrically opposed to that of concrete. It is a special material with great advantages in some building construction related issues, but on the other hand – CLT consists of natural wood – and we have to pay attention especially on moisture control: under this condition building with CLT can be sustainable and durable.

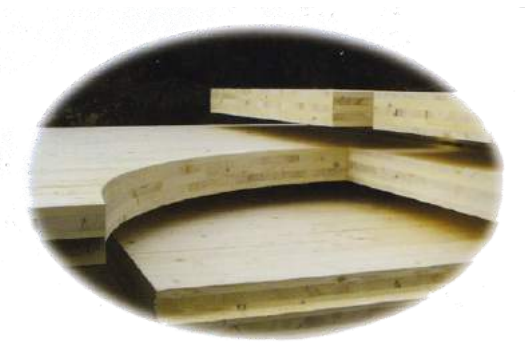

Fig. 1 5-layer panels with different cuts

2. CLT Characteristics from a Building Physics Point of View

CLT is a plane, rigid, lightweight thermally insulating material with water vapour absorption and storage capacity, as well as thermal and moisture storage capacity. Some characteristic values for a 100 mm thick CLT panel are:

- Weight: ~ 45 - 50 kg/m²
- U-Value: ~ 1.0 W/m²K
- U-Value with 10 cm insulation: U ~ 0.30 W/m2K
- Equivalent air layer thickness: sd ~ 2 -5 m
- Fire resistance: REI 30-60 (depending on load and board direction)
- Airborne Sound Insulation: Rw ≈ 33 - 38 dB
- Impact sound Pressure level: Lnw ≈ > 85 dB
- Air permeability: Quality depends on the type of the panel

Fig. 2 5-layer panels with different air permeability

Very important: on account of the fact that CLT consists mainly of wood, it naturally is NOT resistant against permanent moisture load – we have to design the construction in a way, that helps to keep the construction dry, and also supports fast drying after getting wet!

Fig. 3 CLT can be damaged or destroyed by extended action of humidity.

CLT is a very special type of a massive timber panel, and this special layout has consequences for a lot of characteristic properties – and this has to be taken into account for successful use. There are also modified panel types, with different material properties.

Fig. 4 left fig.: Vertical boards timber panel, nailed or glued; right fig.: CLT, 3 layered

Fig. 5 left fig.: Uniaxial; right fig.: Biaxial.

Practically all these types of timber panels are orthotropic but in different ways – therefore, also, differences in the building physics behaviour in the different directions of these materials have to be considered in construction work.

3. CLT - Hygrothermal Aspects

3.1 CLT and fire resistance

The combustion speed of CLT panels is about 0.7 mm/min to 0.8 mm/min, cause of faster combustion at seems and joints. Outer layers with a thickness of more than 31 mm have a fire resistance of 30 min in almost every case.

Fig. 6 left fig.: Fire test; right fig.: Standard fire test of a slab with load

If one layer is completely burnt off, the statically effective board height is reduced to the next layer that can transmit the load in the direction of force. If only the outer layer burns off, the joints only play a small role thanks to the statically effective height/thickness. In such a case the combustion speed of solid wood (0.65 mm/min) can be assumed.

In the case of a 5 –layer panel with a thickness of about 10 cm, a fire resistance of 60 min can be achieved, depending on load. In the case of walls 5-layer boards could achieve a fire resistance REI 60 even with combustion from both sides, when the outer layer is directed in the longitudinal direction of the wall. For multi-storey houses, often further linings (plasterboard, OSB.) will give additional fire protection for the construction. Experience shows, that a detailed fire protection concept can improve the fire performance of rooms and buildings in a very favourable way, which can help to largely exclude any negative combustibility effects of the material.

3.2 Thermal Insulation

3.2.1 Background

The implementation of the EPBD – Energy Performance of Buildings Directive in whole Europe states that all new buildings have to be “nearly zero-energy buildings” from the year 2020. So the energy performance of future buildings will be one of the key challenges of future building. The heating demand is one part of that challenge and construction assemblies with CLT are a possible way to solve the problem of the envelope heat transfer in a simple manner.

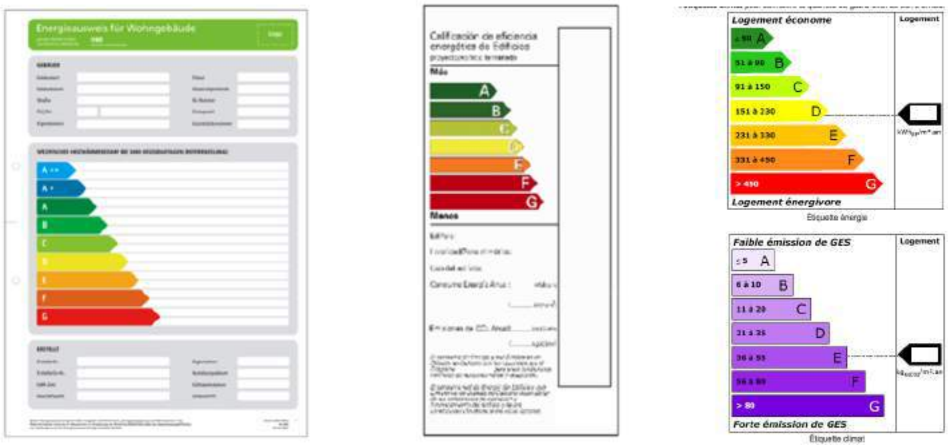

Fig. 7 Examples for the declaration the of energy performance: Austria, Spain, France

In all European countries there exist minimal requirements for the heating demand of the construction assemblies of the building envelope and further the whole energy demand is limited depending on the use and several building aspects (e.g. surface-to-volume ratio). The thermal conduction for a 3-dimensional inhomogeneous material can be derived from

$$\frac{\partial}{\partial t}\vartheta(\vec{r},t) = \lambda \cdot \Delta\vartheta(\vec{r},t) \quad \text{with} \quad \Delta = \frac{\partial^2}{\partial x^2} + \frac{\partial^2}{\partial y^2} + \frac{\partial^2}{\partial z^2} \tag{1}$$

with

λ thermal conductivity

x,y,z Cartesian coordinates

ϑ temperature

Φ heat-flow from heat sources or heat sinks.

When neglecting any period influences, as it is used for energy demand certificate calculations, w e can get the following equation:

$$\frac{\partial}{\partial x}\left(\lambda_x \frac{\partial\vartheta}{\partial x}\right) + \frac{\partial}{\partial y}\left(\lambda_y \frac{\partial\vartheta}{\partial y}\right) + \frac{\partial}{\partial z}\left(\lambda_z \frac{\partial\vartheta}{\partial z}\right) + \Phi = 0 \tag{2}$$

with

Φ heat-flow from heat sources or heat sinks.

Although we have a layered material consisting of different boards in different directions for CLT we use that equation simplified just for the x-coordinate:

$$\Phi = \frac{\Delta Q}{\Delta t} \tag{3}$$

with

Φ heat flow in J/s

Q heat quantity

The Heat flow per area unit than can be written as:

$$q = \frac{\Delta\Phi}{\Delta A} \tag{4}$$

with

q thermal flow density in W/m²

Equation for the thermal flow density in case of thermal conductivity, one-dimensional, steady state:

$$q = -\lambda \cdot \frac{\Delta T}{\Delta x} = -\lambda \cdot \frac{T_2 - T_1}{d} \tag{5}$$

with

λ thermal conductivity

x Cartesian coordinate in x-direction

ϑ temperature

Q heat quantity

The thermal conductivity of CLT without any modifications is practically equal to the thermal conductivity of timber. Thus the factor of thermal conductivity of CLT is 3 times that of thermal insulation material, e.g. mineral wool.

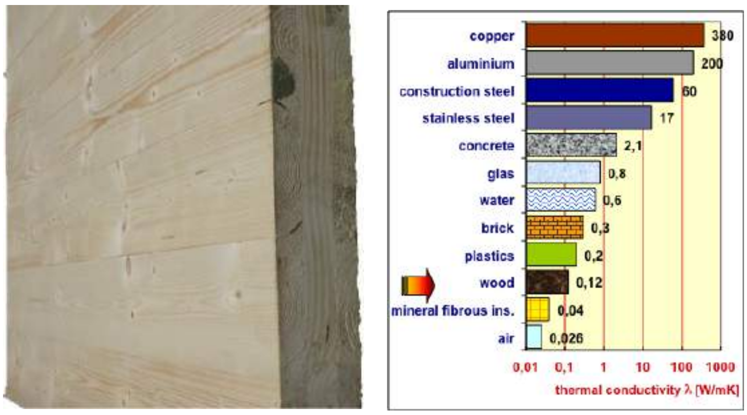

Fig. 8 Comparison of the thermal conductivity of different building materials

The European Standard EN ISO 10456:2010 “Building materials and products - hydrothermal properties - Tabulated design values and procedures for determining declared and design thermal values” [1] specifies the following thermal conductivity values depending on the density.

Table 1 Thermal conductivity values depending on the density; acc. to ISO EN 10456 [1]

Material Group ISO EN 10456	**Density**	**Thermal conductivity**
Material density	ρ	λ
Timber	450 kg/m³	0,12 W/mK
	500 kg/m³	0,13 W/mK
	700 kg/m³	0,18 W/mK

The conductivity values in the European standard EN 13986:2005 "Wood-based panels for use in construction – Characteristics, evaluation of conformity and marking" [2] vary slightly compared to the conductivity values given above.

Table 2 Thermal conductivity values depending on the density; acc. to EN 13986 [2]

Material Group EN 13986	**Density**	**Thermal conductivity**
Material density	ρ	λ
Solid wooden panels	300 kg/m³	0,09 W/mK
	500 kg/m³	0,13 W/mK
	700 kg/m³	0,17 W/mK
	1000 kg/m³	0,24 W/mK

In practice the calculation of the overall U-Value of CLT building components is much more simple and, in some cases, is sometimes closer to reality than that of Timber Frame Constructions. The calculation of the heat transfer through a building assembly depends on the design.

3.2.2 Timber frame structures

Thermal insulation between posts: "parallel heat transfer":

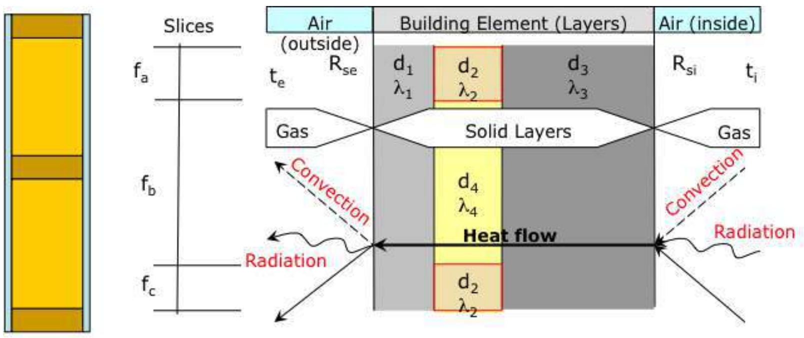

Fig. 9 Calculation Model for the U-Value of construction assemblies with inhomogeneous layers

The heat transfer in this case can be calculated according to EN ISO 6946:2008 "Building components and building elements – Thermal resistance and thermal transmittance – Calculation method Point 6.2" [3]

Upper limit of overall heat transfer resistance

$$\frac{1}{R_T} = \frac{f_a}{R_{Ta}} + \frac{f_b}{R_{Tb}} + \frac{f_c}{R_{Tc}} \quad [W/m^2K] \tag{6}$$

Heat transfer resistance for slice j

$$\frac{1}{R_j} = \frac{f_a}{R_{aj}} + \frac{f_b}{R_{bj}} + \frac{f_c}{R_{cj}} \quad [W/m^2K] \tag{7}$$

Lower limit of overall heat transfer resistance

$$R'_T = R_{si} + R'_1 + R'_2 + R'_3 + R'_j + R_{sa} \quad [W/m^2K] \tag{8}$$

Thermal resistance

$$R_T = R'_T + R''_T \quad [m^2K/W] \tag{9}$$

Heat transfer coefficient

$$U = \frac{1}{R_T} \quad [W/m^2K] \tag{10}$$

Due to the conductivity difference between wood and thermal insulating material the framework works as a thermal bridge in this case.

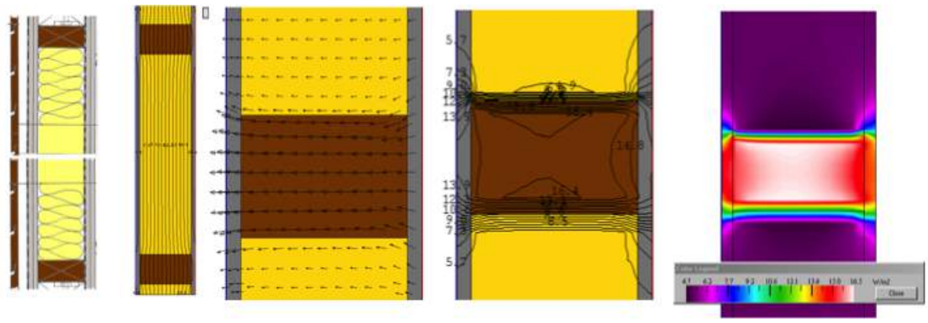

Fig. 10 Timber frame construction and thermal transmittance

If we add the other necessary layers for a timber frame construction, it looks quite complicated:

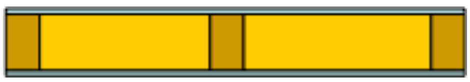

Example – external wall construction:

1,25 cm	plasterboard
5,00 cm	installation cavity / batten
	Moisture barrier
18,00 cm	insulation between frames
	Air barrier
5,00 cm	batten
3,00 cm	timber lagging

Fig. 11 Example of a timber frame construction

In some cases, the loading has to be taken into account for the thermal behaviour. For example, if the direction of stress of the slab is between the exterior walls, but the architectural design calls for large windows, the load-bearing posts may have to be arranged closer to each other. Therefore it may occur, that the assumed values for the thermal calculation are not valid when the wooden part of the wall is adapted according the final structural calculation results.

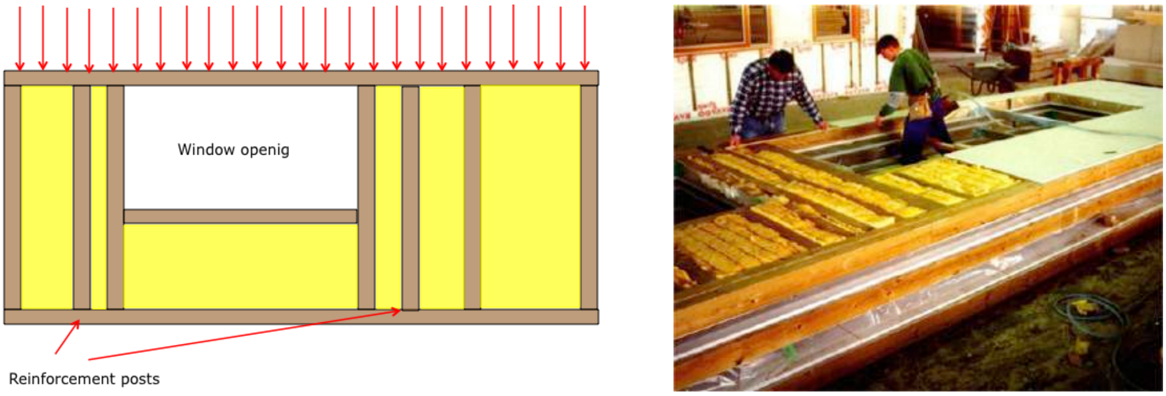

Fig. 12 Timber frame construction: Load bearing exterior wall with window

In this case the calculated thermal transmittance is sometimes "slightly" different from reality.

3.2.3 CLT Construction and thermal transmittance

CLT- Structure: Thermal insulation as part of layer structure: "serial heat transfer"

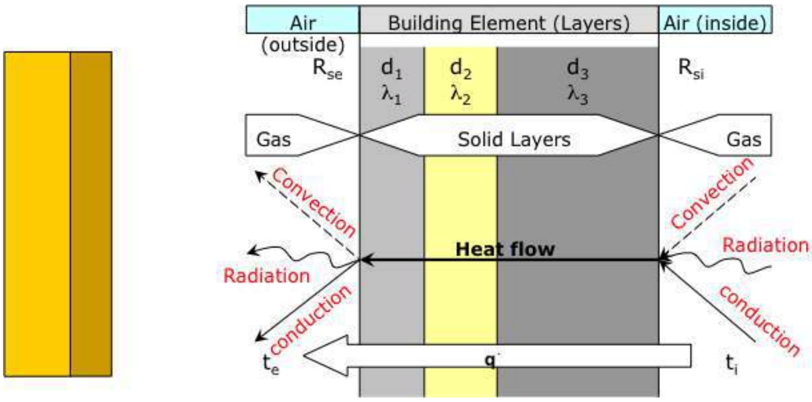

Fig. 13 CLT construction: "serial" heat transmittance for construction assemblies with homogeneous layers

In this case the calculation of the heat transfer coefficient is much simpler.

Calculation of the thermal resistance

$$R_T = R_{se} + \frac{d_1}{\lambda_1} + \frac{d_2}{\lambda_2} + \frac{d_3}{\lambda_3} + R_{si} \quad [m^2K/W] \tag{11}$$

Calculation of the heat transfer coefficient

$$U = \frac{1}{R_T} \quad [W/m^2K] \tag{12}$$

Thus, the layer construction system of CLT panel based building construction assemblies brings less complicated construction details.

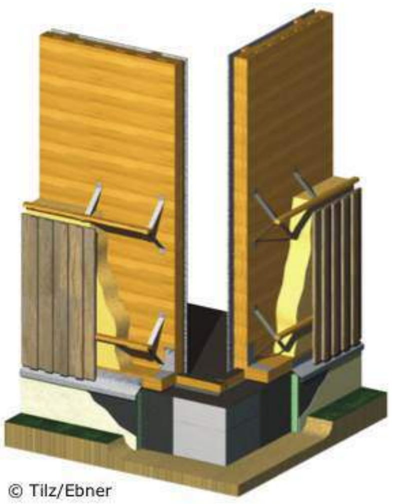

Example – CLT external wall construction:

1,25 cm	plasterboard
5,00 cm	installation cavity / batten
12,50 cm	CLT
	vapour/air barrier (if needed)
16,00 cm	insulation
5,00 cm	batten
3,00 cm	timber lagging

Fig. 14 Example of a CLT based construction

Simplified, the thermal heat transfer coefficient can be estimated by the following chart:

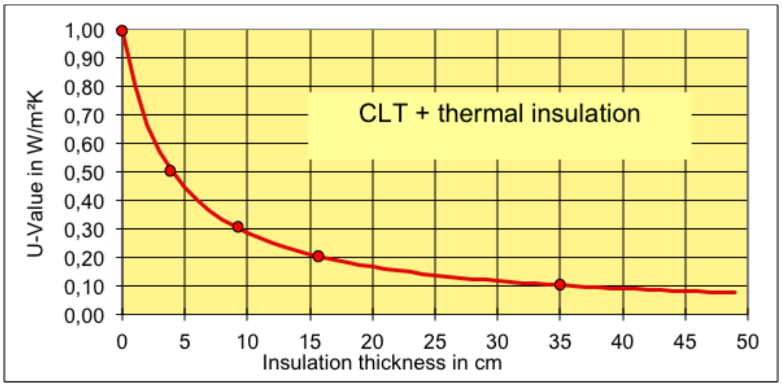

Fig. 15 Chart for estimation of the U-Value of a CLT based construction with exterior thermal insulation

Examples:

CLT 10 cm		U ≤ 1,1W/m²
with	12 cm thermal insulation (0,04)	U-Value ≈ 0,25 W/m²K
	16 cm thermal insulation (0,04)	U-Value ≈ 0,20 W/m²K
	35 cm thermal insulation (0,04)	U-Value ≈ 0,10 W/m²K

Common exterior wall insulation systems:

A common way for thermal insulation is the use of ETICS (external thermal insulation composite systems), which are glued and dowel fastened, cladding fixed in battens, mounted with special screws or mounted with brackets between the thermal insulation layer.

Fig. 16 Examples: thermal insulation of the exterior wall

Fastening causes thermal bridges. In EN ISO 6946 [3] there is a specific rule for the thermal influence of the fastening. If the heat transfer percentage through anchors, fasteners, mounting etc. reaches 3% of whole over U-Value of the exterior wall, this should be taken into account by adding this part ΔU to the U-Value of the construction to get the corrected U_c:

$$U_c = U + \Delta U \tag{13}$$

It is important to give attention to this fact especially for highly insulated constructions!

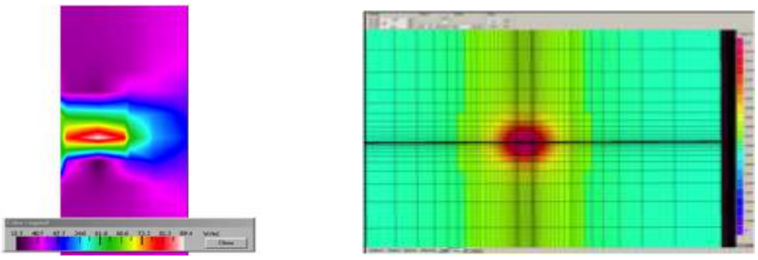

Fig. 17 Examples: thermal bridges: fastening of the ETICS or cladding

In some cases under certain weather conditions, depending on the colour and nature of the surface, the thermal bridges or substructure can become visible through the influence of moisture. This may be caused by thermal radiation exchange with a cold sky and therefore hypothermia of the surface below the dew point of the surrounding air.

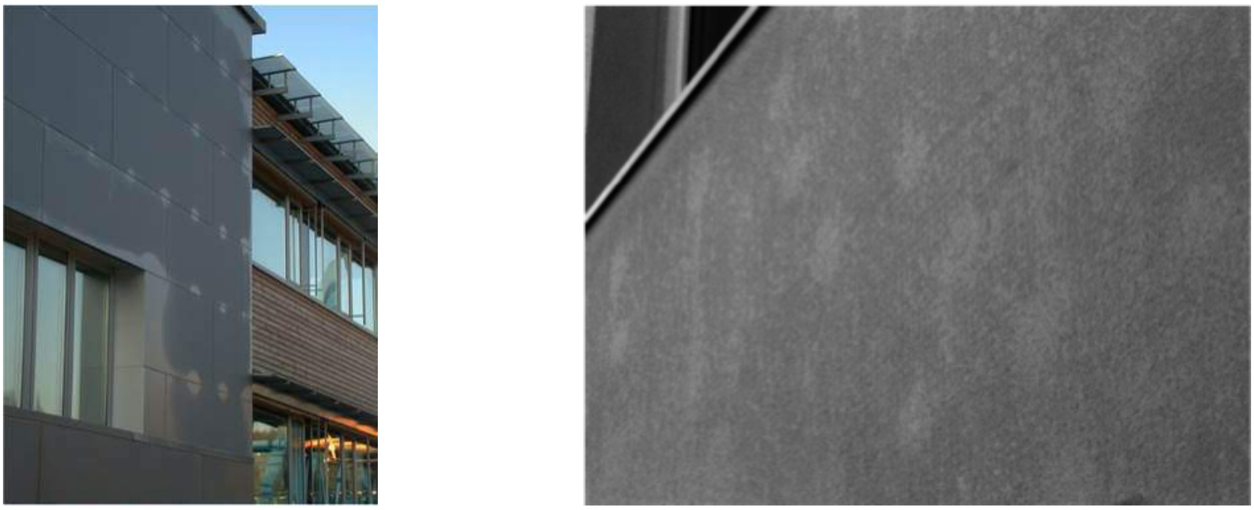

Fig. 18 Left fig.: Cladding with visible fastening; right fig.: ETICS System with fastening, visible by moisture

3.3 Summer Overheating Control

Overheating of rooms during the warmer part of the season has to be avoided. There are different limits for this aim. In Austria e.g. the "operative temperature" has to be lower than a defined limit temperature t*:

Limit Temperature during the day: t* $\leq$ 27°C

Limit Temperature during the night: t* $\leq$ 25°C

The operative temperature is calculated by the equation

$$t_o = 0.5 \cdot \left(t_a + \sum_{K=1}^{n} \phi_K \cdot t_K \right) \approx 0.5 \cdot \left(t_a + t_{oi} \right) \quad [°C] \tag{14}$$

with:

t_o operative temperature

t_a ambient temperature inside

t_{oi} surface temperature inside

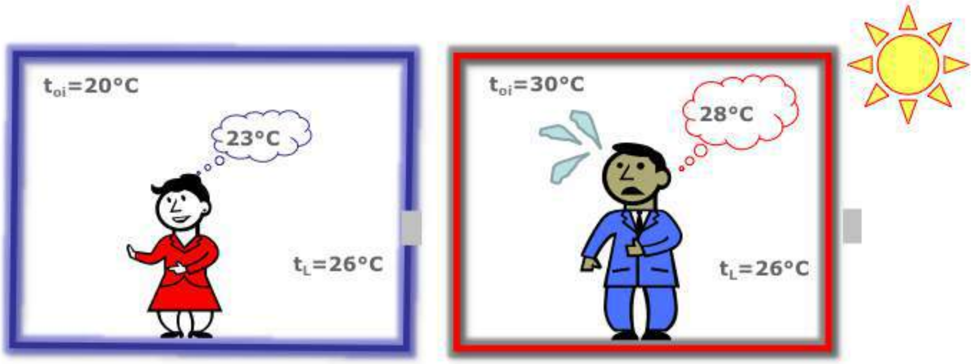

Fig. 19 Left: Acceptable operative temperature, right: Too high operative temperature

Thus, the surface temperature has an important influence on the operative temperature.

There are a lot of different heat sources in our rooms. To get an acceptable room temperature in summer, some of the key elements are:

- Area and shading coefficient (b-value or g-Value) of the glazing, Orientation, shading
- Reducing of internal heat sources
- Cooling effective ventilation exchange rate and air temperature inside and outside
- Heat storage capacity inside the room and especially the room surfaces

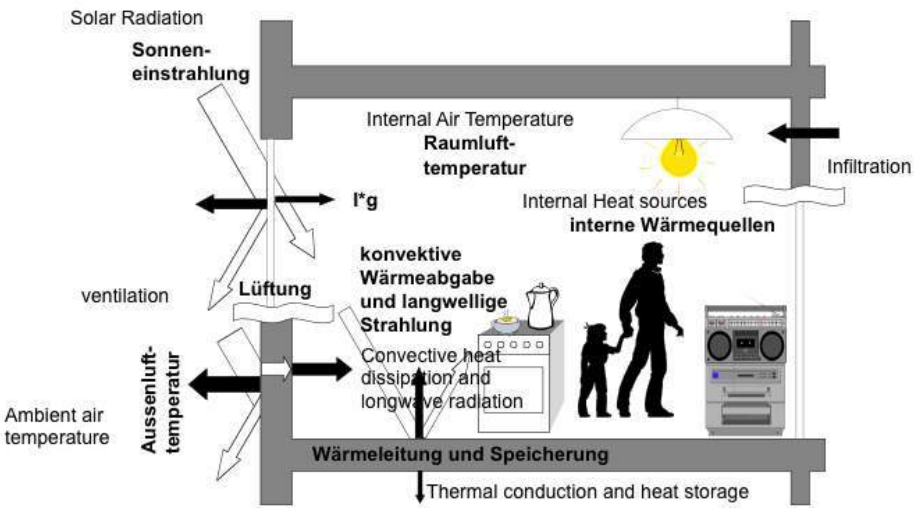

Fig. 20 Influences for the room temperature during the overheating period

Thus measures against overheating are:

- To reduce heat sources, keep out solar radiation (depending on building orientation, construction, glazing area, shading, enhancing ventilation during the cooler part of the day (night ventilation).
- To use the thermal mass of the building to reduce the increase of the temperature.

$$\frac{\partial}{\partial t}\partial(\vec{r},t) = \lambda \cdot \Delta\partial(\vec{r},t) \quad with \quad \Delta = \frac{\partial^2}{\partial x^2} + \frac{\partial^2}{\partial y^2} + \frac{\partial^2}{\partial z^2} \tag{15}$$

The summer overheating calculation is a non-steady state process. For the discussion of a wall this can be reduced to a one-dimensional equation

$$\vartheta(x,t) = \sin(2c^2\lambda \cdot t - xc) \cdot e^{(-cx)} \tag{16}$$

with

λ thermal conductivity in W/mK

x Cartesian coordinate in m

ϑ temperature in K

c spec. heat capacity in J/kgK

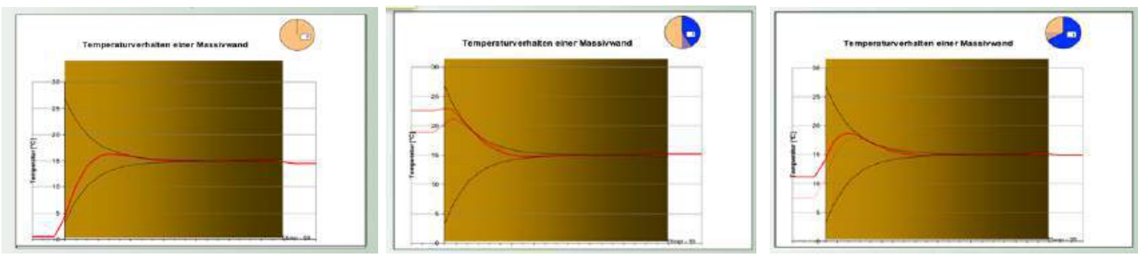

Fig. 21 Transient temperature curve of a solid wall

The penetration depth of the temperature change depends on the period length, the thermal conductivity, the density of the material and the specific heat capacity. Wood has a relatively high specific heat capacity caused by its water content, but a limited penetration depth is limited by a low thermal conductivity.

$$\delta = \sqrt{\frac{\lambda \cdot T}{\rho \cdot c \cdot \pi}} \tag{17}$$

Non-steady state heat penetration depth with

T length of period

λ thermal conductivity

ρ density of the material

C specific heat capacity

Table 3 Heat penetration depth of different materials

Material	ρ [kg/m³]	λ [W/mK]	c [J/kgK]	δ [cm]
Steel	7850	60,0	480	66,2
Concrete	2400	2,30	1130	15,3
Brick	1000	0,45	920	11,6
Timber	600	0,15	1600	6,60
XPS-insulation	35	0,03	1400	13,6
Glass	2500	0,81	840	10,3

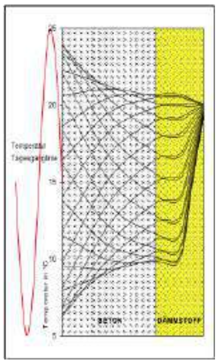

Thus, it is necessary to pay attention to the fact that, for a CLT surface, just about 5 to 6 cm are active as a storage mass for a temperature period of 24 hours. An inside insulation facing shell will reduce the advantage of a relatively high thermal mass of CLT panels for the 24 h period. As the following calculations show the thermal mass is reduced from 38 kg/m^2 to 15 kg/m^2 with a 5 cm mineral wool layer beyond the gypsum board facing inside.

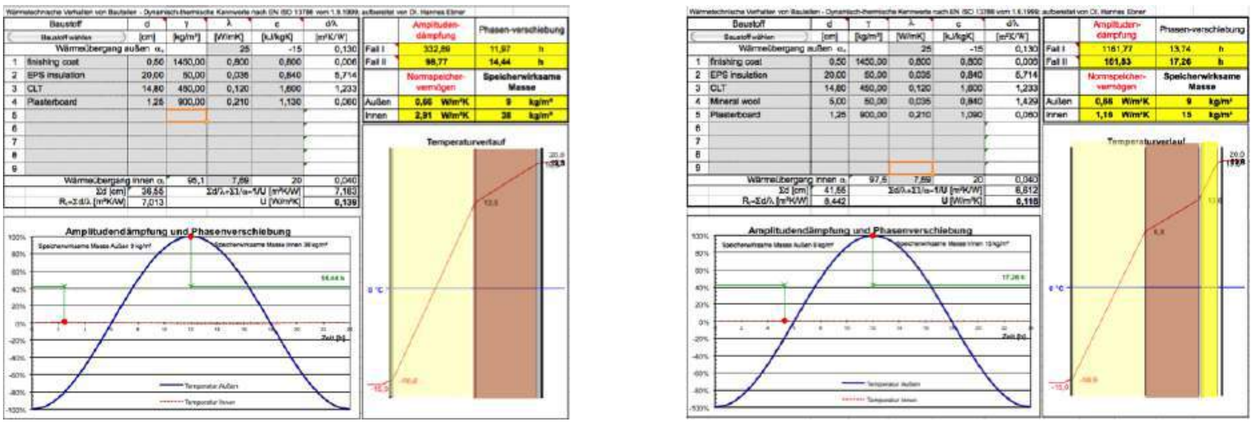

Fig. 22 Results of the calculation of U-Value, amplitude damping, phase shift and heat storage mass of different CLT wall assemblies

By using transient simulation software it is possible to calculate the operative temperature and to analyse the effect of different measures.

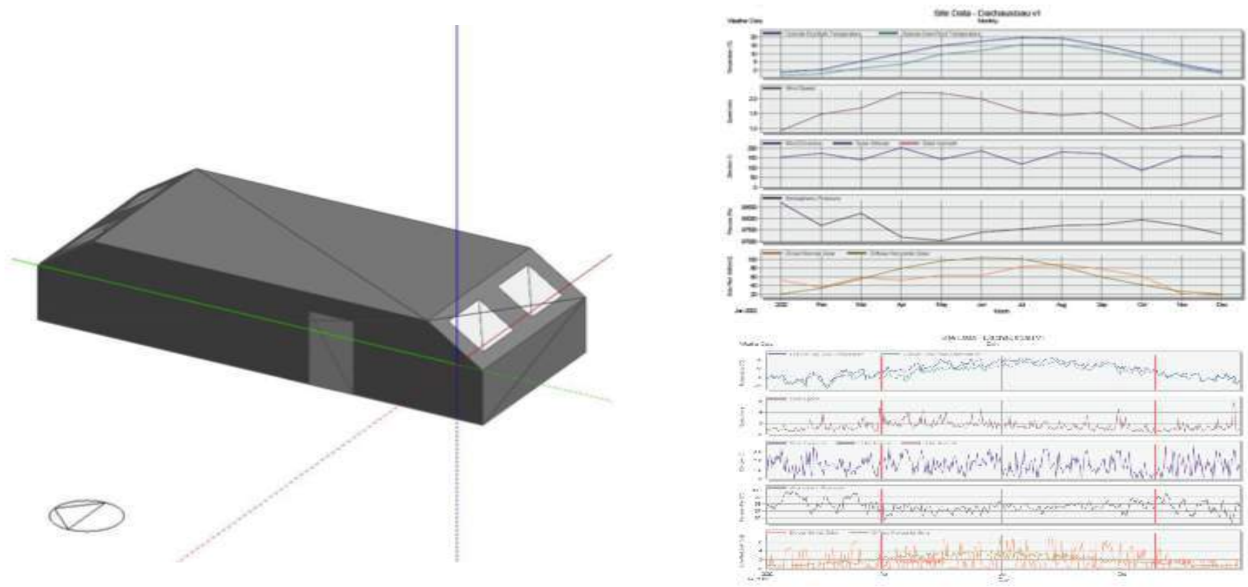

Fig. 23 *Example of a simulation of a loft extension with weather boundary conditions (charts)*

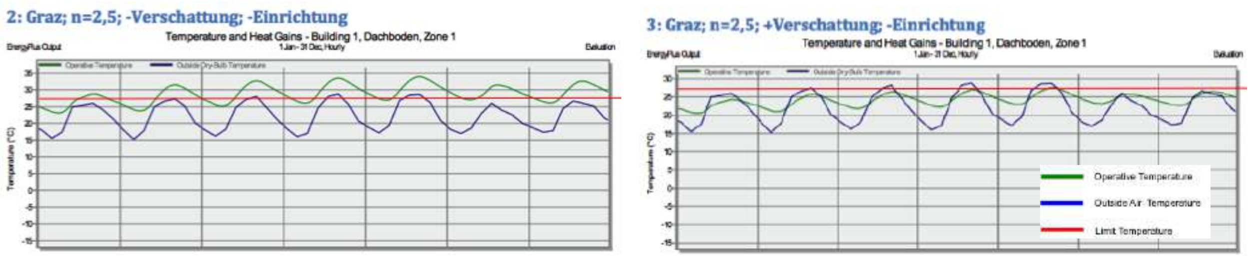

Fig. 24 *Influence of shading*

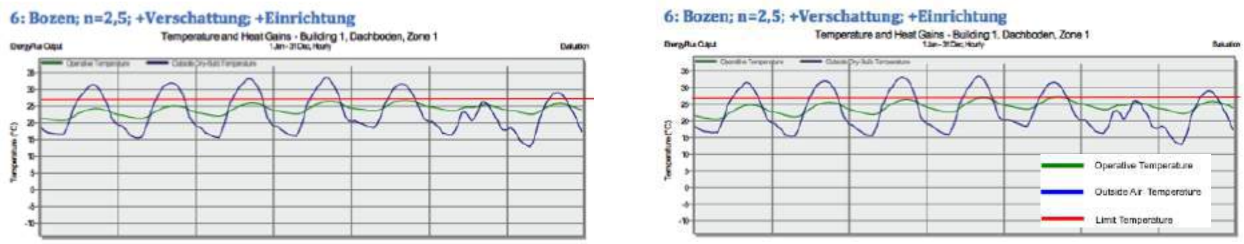

Fig. 25 *Influence of heat storage mass (right: CLT, left: lightweight construction)*

3.4 Rainwater, Exterior and Interior Moisture Control

Moisture control is an essential issue for sustainable and durable buildings with wood based building components – and so also for building with CLT.

For all buildings it is essential to keep the building site dry, both because wet construction may have a negative influence on the heating demand and also because the risk of mould and the damage of materials. Coverings or protection measures can help, but in the future prefabrication should be developed in a way, that the erection time could be minimised.

There are many different moisture sources:

- Driving Rain
- Exterior Humidity
- Indoor Humidity

- Surface Condensation
- Building Humidity
- Convection of moist air
- Prevention against water from building

Fig. 26 Weather protection Limnologen, Växjö. Source: SP Technical Research Institute of Sweden, Per-Eric-Eriksson

It has to be considered, that nowadays the increasing thermal insulation and air tightness of the buildings interferes with the construction and the room climate in different ways.

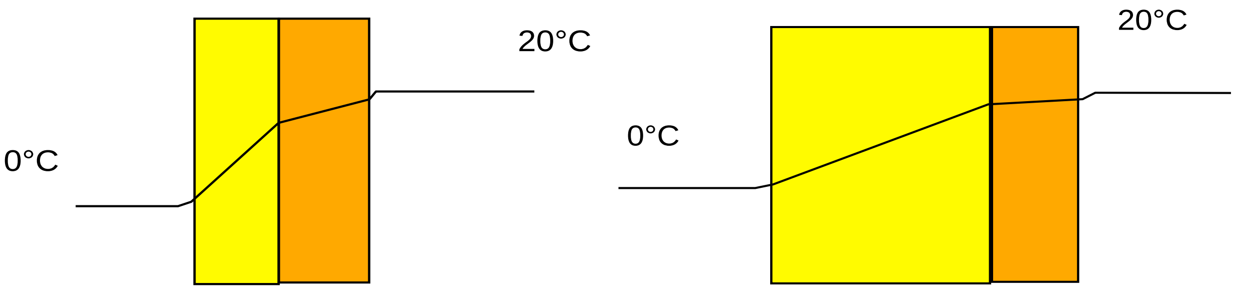

Fig. 27 Temperature curve caused by different thermal insulation thickness

On the one hand, especially the external insulation system has the effect of a higher temperature of the inner surface of the exterior wall. On the other hand, the temperature gradient is flatter, and the temperature and energy input of the air heating will be lower. One of the results is, that the thermal insulation's potential for drying out will be reduced. This means, that, to avoid construction damage caused by influence of longer lasting humidity influence, there is a high priority for moisture control with highly thermally insulated wood based construction.

Therefore, depending on the moisture load, e.g. penetrating rain, we have to pay attention in choosing the right type of the outer wall and, especially, the façade system. All structural components should be developed in a way that the construction is controllable and has a second "moisture prevention system".

It is essential for durability that intruded water can dry out rapidly or can be detected easily. Also the integration of building services should follow this rule. Moisture proofing, in its different aspects, becomes a more and more important factor for sustainable, low maintenance wood based buildings. Therefore the façade construction type should be chosen depending on architecture or vice-versa.

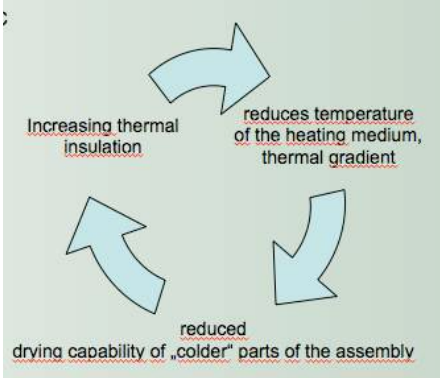

Fig. 28 Schematic influence of thermal insulation

Fig. 29 left: Extremely weather exposed façade; right: Wooden façade with and without cantilever roof

There are two different methods for moisture proofing against driving rain:

- One-level proofing: the exterior surface has to provide tightness against rainwater and wind.
  Examples for this façade type are Assemblies with ETICS (External Thermal Insulation Compound Systems).
- Two-level proofing: the exterior surface is designed in a way, that the water is deposited there and runs down the exterior shell, and the interior structure just has to be tight against wind. This type of façade is called ventilated curtain wall.

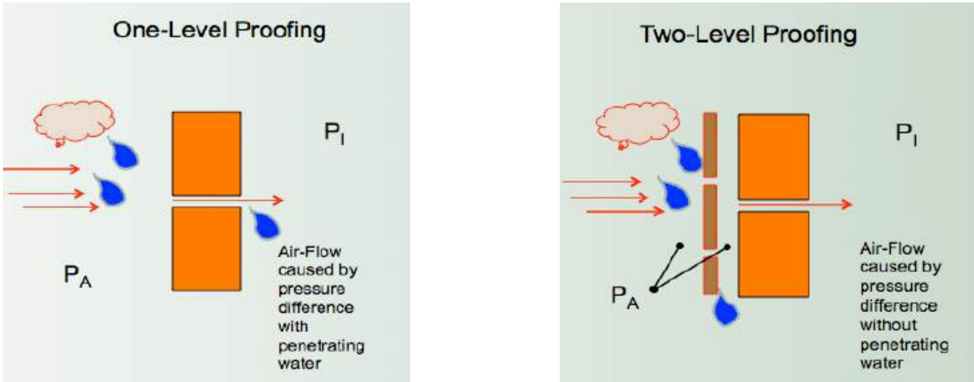

Fig. 30 left: One-level moisture proofing; right: Two-level moisture-proofing

A further valuable rule for sustainable design is to choose good solutions for plinth, windowsills and all things that are fixed to the external walls and exposed to the weather.

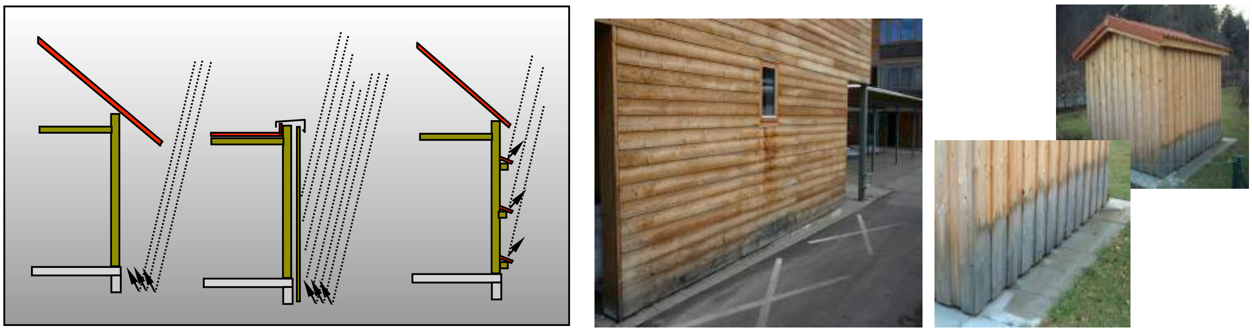

Fig. 31 Splashwater sensitive façade parts; Plinth Zone: horizontal boards can be exchanged more easily

Fig. 32 Left fig.: Splash-proofed window sill; right fig.: Bad example with a hole in the corner

In every case it is recommended to put a waterproof foil below the windowsill, so that penetrating water can get out in every case. As some bad examples have shown, this could be an expensive design mistake within three to five years, if the penetrating rain load is high:

Fig. 33 Example of bad moisture-proofing design: a small leakage at the corner of an exterior windowsill led to expensive moisture damage of the exterior wall and parts of the wooden slab

A lot of moisture related problems are located at the plinth. For this reason, a minimum height of about 30 cm above the surrounding ground is necessary for moisture proof plinths. At doors a drainage channel should be used.

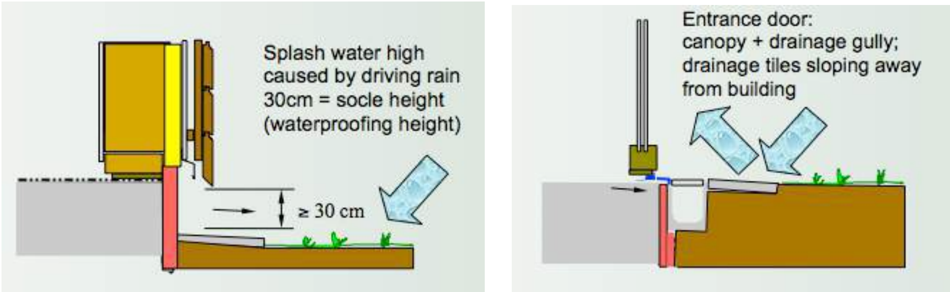

Fig. 34 Left fig.: Splash-proofed plinth; right fig.: Drainage channel - solution for entrance doors

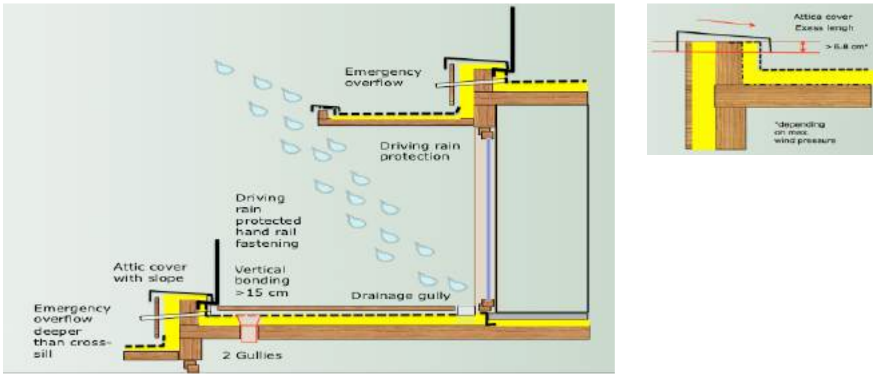

Fig. 35 Example for a vertical section through a terrace roof, cantilever roof and wall edge

Further paths for penetrating moisture are fastenings. Fastenings have to be designed in a way that the water will be diverted away from the façade.

Fig. 36 Badly designed fastenings

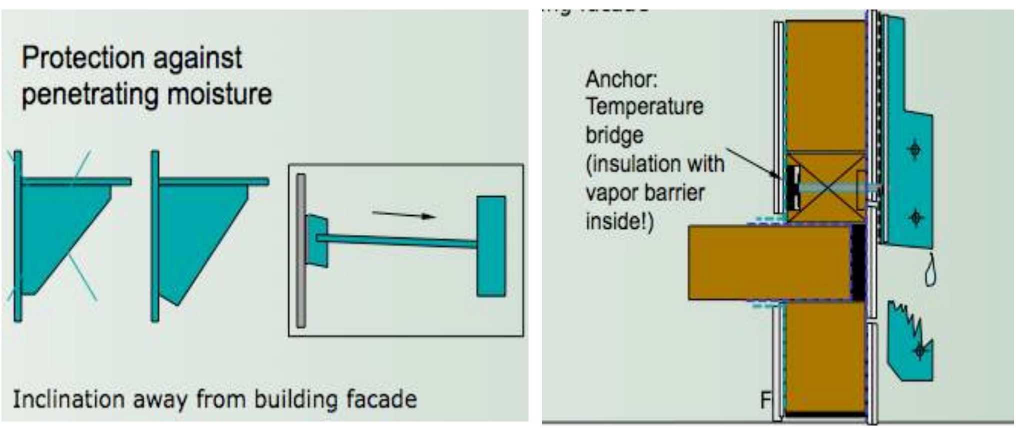

Fig. 37 The inclination of fastenings always should divert rainwater and condensate away from the facade.

Fig. 38 Building damage caused by wrong mounting of a satellite dish and satellite dish cable

3.5 Vapour Diffusion

In contrast to framework constructions, one of the advantages of CLT-based components is the possibility of designing the components in a way that an overall vapour barrier is not necessary in every case. In most cases, CLT has the same vapour permeability as timber. Thus the equivalent air layer thickness s_d of CLT ($s_d = \mu \cdot d$) for timber and CLT is the same, e.g. a 10 cm thick CLT Panel in most cases has an s_d of about 2 m to 7 m.

Table 4 Vapour permeability for different materials, timber values acc. to EN 12524 [4]

Material	**μ** **[-]**
Air	1
Timber, CLT	20/50 (wet); 50/200 (dry)
Concrete	60/120
Bitumen	20.000 – 50.000
Metals, Glass	1.000.000/∞

The European standard EN 12524:2000 “Building materials and products – Hygrothermal properties – Tabulated design values” [4] provides vapour permeability values of 20 (for dry timber) to 50 (for wet timber). The European standard EN 13986:2010 “wood-based panels for use in construction – characteristics evaluation of conformity and marking” [2] provides vapour permeability for wood based panels depending on the average raw density.

Table 5 Vapour permeability for timber products, according to EN 13986 [2]

Material	**Average raw density [kg/m³]**	**Water vapour permeability μ [-]**	
		wet	**dry**
Wood based panels, Plywood, Veneer laminates	300	50	150
	500	70	200
	700	90	220
	1000	110	250

A comparative hygrothermal calculation (based on a Glaser calculation model) for a framework construction based wall and a CLT based panel wall, shows, that it will be necessary in most cases to have a vapour barrier on the warm side of the framework based wall, but there are only a few cases of condensation in the CLT based panel wall construction, depending on the exterior surface material.

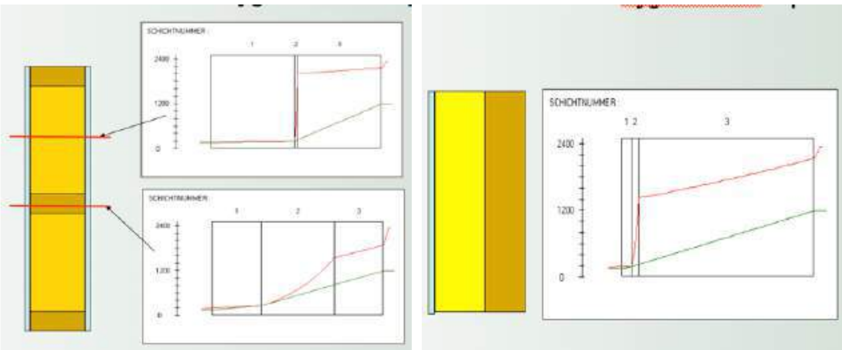

Fig. 39 Examples for hygrothermal calculation acc. Glaser: Left fig.: Framework construction; right fig.: CLT based construction; (yellow:thermal insulating material)

The Glaser model just takes into account the mass flow of water vapour caused by partial water vapour pressure difference, calculated by applying the ideal gas equation and Fick's law:

$$m^{o} = D/(R \cdot T) \cdot \Delta p / \Delta x = \delta\, \Delta p / \Delta x \tag{18}$$

But in reality the CLT panel has a further advantage: it has a thermal and a moisture storage capacity. Therefore the calculation method according Glaser gives us a worst-case scenario, but in reality the hygrothermal behaviour of CLT is much better. To include this advantage into our calculations, we have to use modern transient calculation models with better models for water transport mechanisms, including the storage capacities.

In reality we have a multiphase system and we have to introduce the non-linearity of the heat conductance through moisture and temperature effects. For the humidity transport we can include different transport equations e.g. for the liquid phase, the normal diffusion, the gas phase and also the pressure diffusion. If we consider the storage effects we can get e.g. the following results:

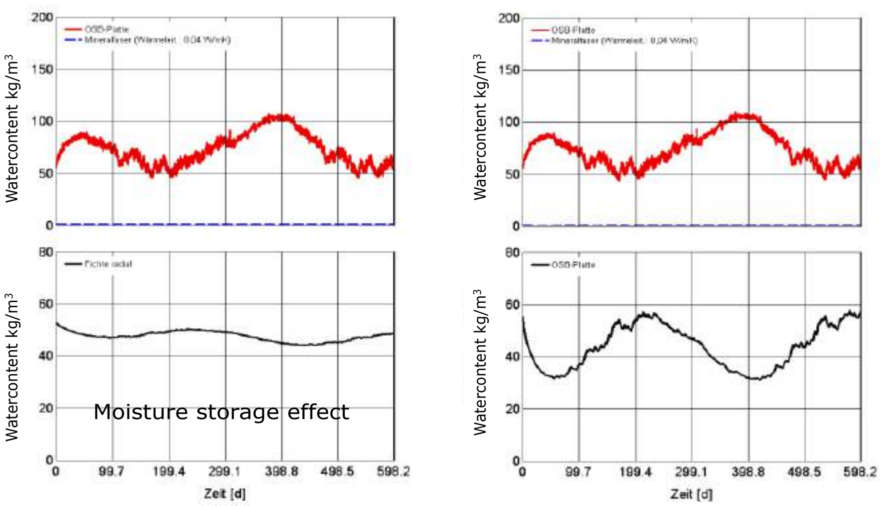

Fig. 40 Left fig.: CLT panel based construction; right fig.: Framework construction

So the CLT panel based construction has the ability for a moisture-adjustment by storage. This can be an advantage for the seasonal hygrothermal loadings, but is a disadvantage for uncontrolled ingress of moisture, because in these cases the wood will stay wet for a long time and, to prevent moisture-loading risks, this should be borne in mind when designing construction details for CLT panel based buildings. One example for that is the construction without basement on a base plate.

If we put the thermal insulation above the base plate, the CLT walls will stay in contact with the cold base plate – with a risk of condensation and moisture intrusion also caused by rain and other water loadings. Therefore it is an advantage either to put the thermal insulation under the base plate or to have a basement. It is also important not to put the end grain in contact with the base plate.

A better design is it to have an indicative threshold made of hard wood as a supporting board or a small base made in concrete, which provides a small difference in height between base plate and CLT panel based wall. This will help to avoid moisture loading on end-grain parts of the load bearing CLT panels cut surface.

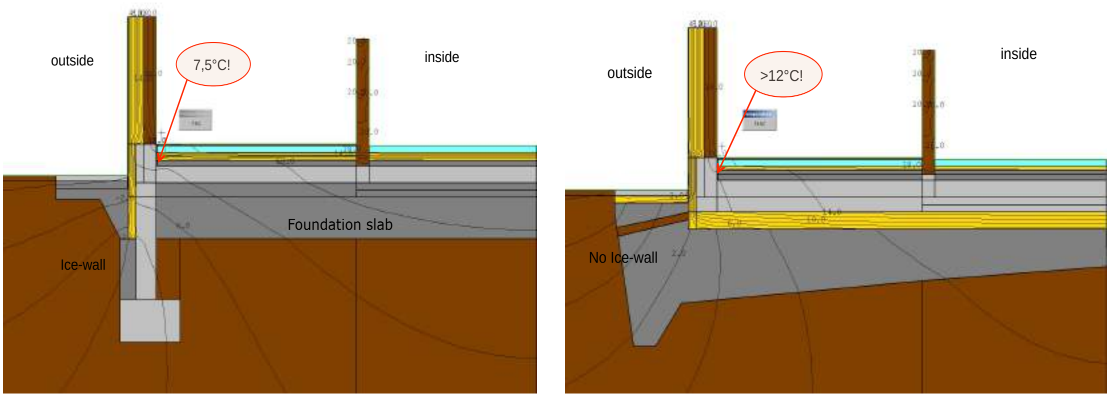

Fig. 41 Left fig.: Thermal insulation above base plate; right fig.: Thermal insulation below base plate

As the example shows, the thermal insulation below the base plate is the better choice for a temperature above the dew point - which helps to avoid condensation risk that exists in the other case. This works not only for the exterior wall but also for internal walls.

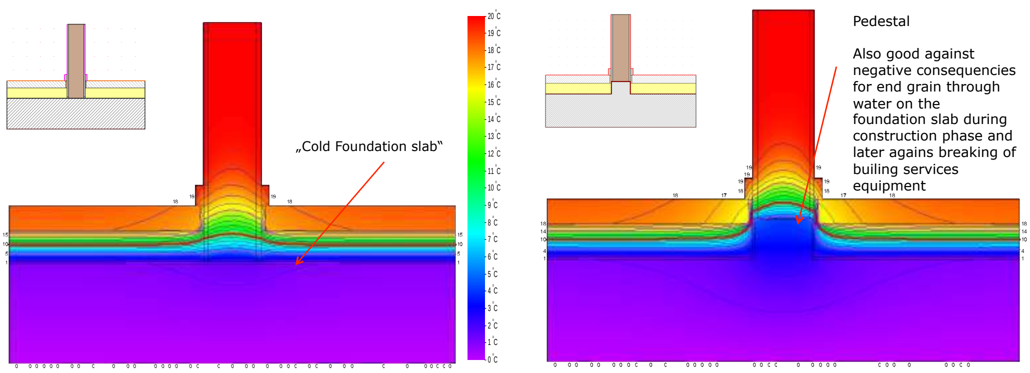

Fig. 42 Left fig.: Thermal insulation above base plate; right fig.: Same situation with pedestal

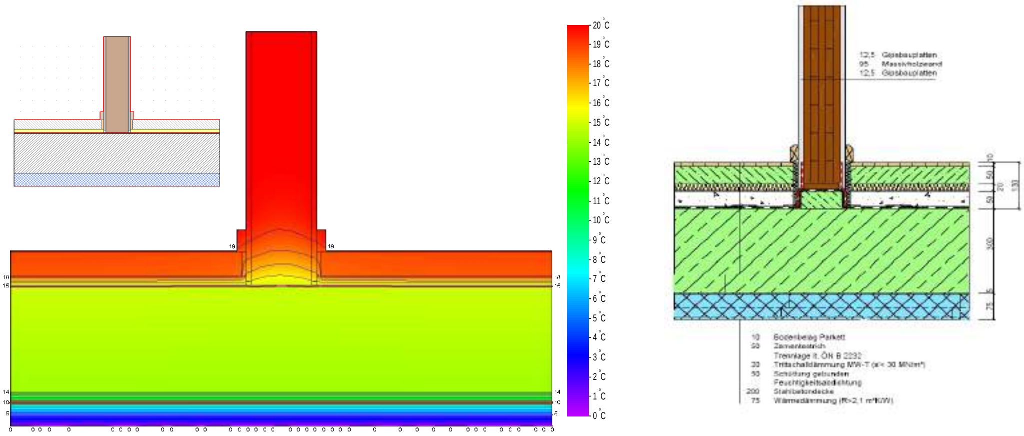

Fig. 43 “warm base plate”: thermal insulation below base plate

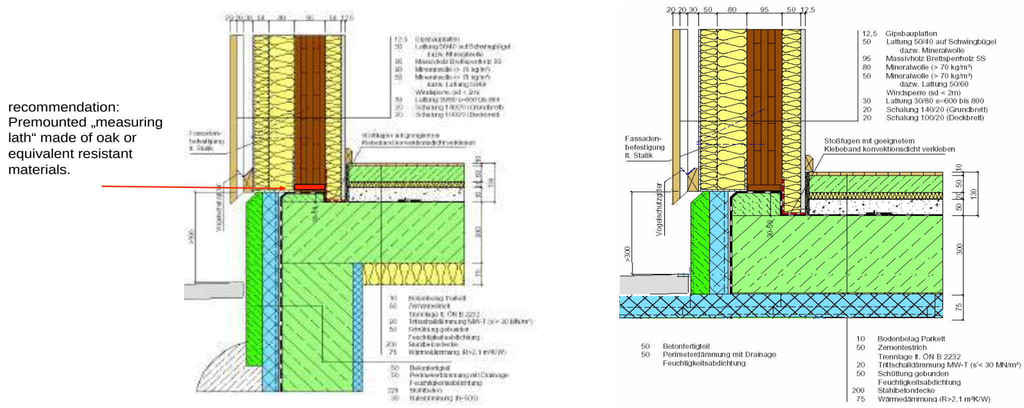

Fig. 44 Left fig.: Basement with small pedestal for the walls ; right fig.: Warm base plate

Some of the most sensitive components of wood-based building constructions are flat roof structures. E.g. in ÖNORM B 7220 “Roofs with sealings – Process standard” [5] there are the following loads are mentioned:

- Weather:
  rain, snow, ice, sun, UV, radiation, hail, heat, cold
- Emissions by industry, cars…
- Traffic by pedestrians etc.
- Leaves, biological
  loads, roots
- Sharp or peaked objects
- Expansion and
  contraction forces
- Flying sparks and radiated heat
- Heating and cooling
- Vapour diffusion, condensate, moisture

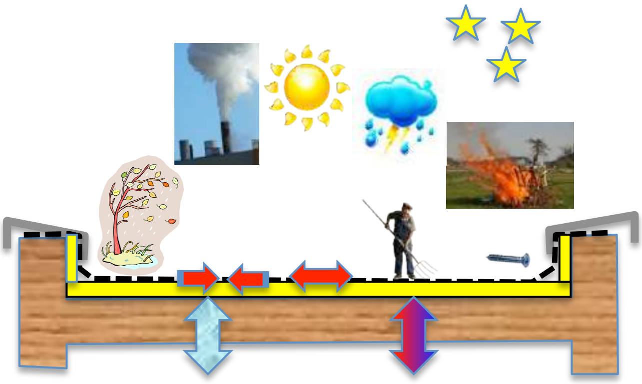

Fig. 45   Different climate, use and mechanical loadings of a flat roof

The hygrothermal behaviour of a flat roof is very complex and not steady state as often is assumed. Moisture is included in the wooden beams or panels. When the structure gets warmer, part of the moisture and water vapour diffuses from the warm side to the cold side of the structure. Therefor the moisture content accumulates at the colder parts of the construction during wintertime. If there is a lot of moisture in the construction, the moisture content will get too high, and will damage the wooden construction. For this reason, the wooden construction should never be included between foils, it should be designed in a way that the wooden parts can dry out, even when they get wet (which naturally should also be avoided).

Fig. 46   Fungal damage caused by moisture in a flat roof

A good solution for a flat roof is the following:

- roof sealing
- thermal insulation (tapered)
- vapour barrier, build as an emergency roof
- the emergency roof should also be equipped with a gully, and the outlet should be located at a place where intruded water would be released
- The CLT panel is located at the warm side of the building component, without any vapour barrier inside.
- If needed, a suspended ceiling can be used (hygrothermal calculation)

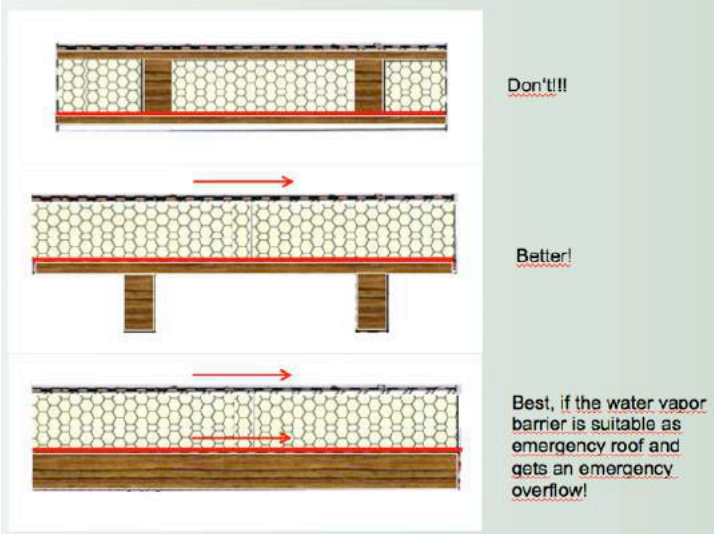

Fig. 47 Bad and good flat roof construction designs

3.6 Air permeability of CLT panels

The air permeability depends on the type of CLT panel. There are panels with a relatively high permeability but there are also panels that are tight.

Fig. 48 Test rig for air tightness at the laboratory for Building Physics Graz University of Technology

Table 6 Air permeability versus pressure difference – different examples

CLT-Element	Length of joints in m – element area	Air Permeability m³/hm²	
	1,61 m²	**at 50 Pa**	**at 100 Pa**
5 layers	12,6	7,90	11,5
	1,40	0,12	0,12
3 layers	12,6	10,9	15,4
	1,40	below measureable limit	0,59

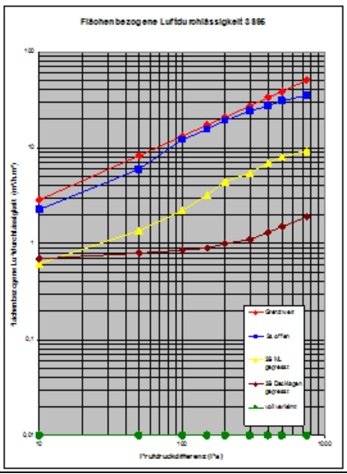

The air permeability depends on the type of gluing, the size and type of boards, moisture content and the production process, but sometimes also the location of installation may have an influence on it.

Fig. 49 Left figure: high air permeability; Right figure: Very tight CLT boards

Air permeability is of great importance for an airtight building envelope for low energy houses, especially with ventilation systems, but in some cases also to avoid the intrusion of wet air into the construction. Furthermore, the sound insulation quality can depend on airtightness. If there are criss-cross leakages the sound insulation may be lower, and in some cases the flanking sound transmission can be badly influenced.

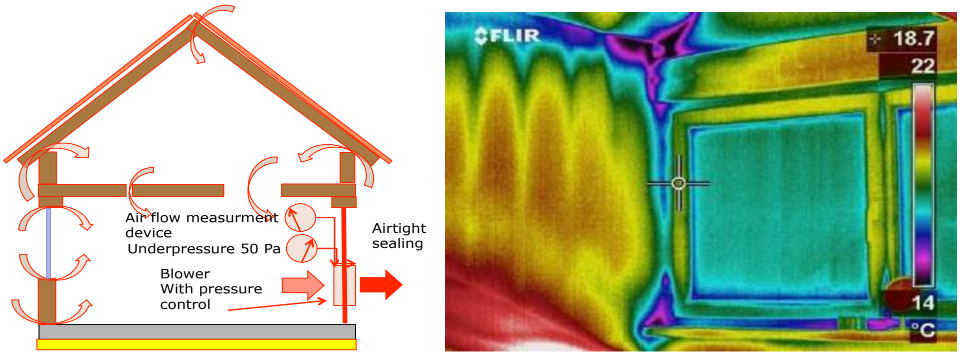

Fig. 50 Left figure: Scheme of fan pressurized method; Right figure: Thermography of air leakages

The European Standard for the determination of the air permeability of buildings is EN 13829 “Thermal performance of buildings – Determination air permeability of buildings – Fan pressurization method” [6] (ISO 0072:1996, modified) and a second one for building components: EN 12114 “Thermal performances of buildings – Air permeability of building components and building elements – Laboratory test method”. [7]

The indoor air pressure depends on the buoyancy the air through temperature and moisture, the wind pressure, and potentially the ventilation pressure by air conditioning. The pressures will extent, when we have a “shaft type building”.

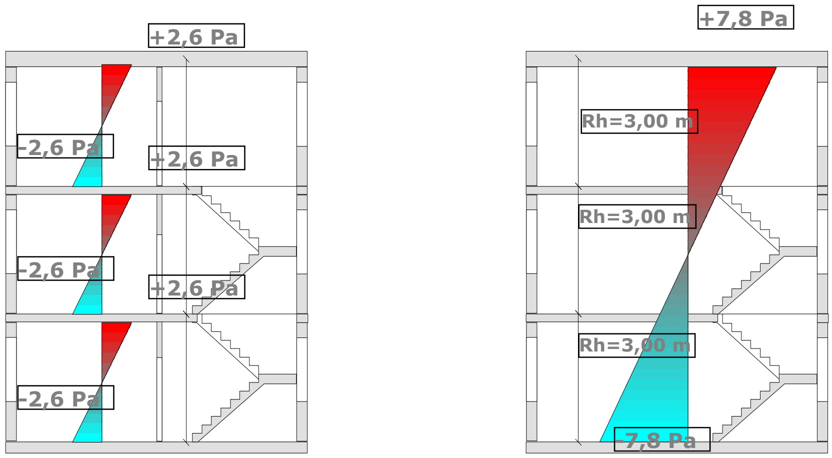

Fig. 51 Pressure distribution: Left figure: tight levels; Right figure: Shaft type building

This pressure caused by buoyancy will be overwhelmed by windward and leeward pressure, so there are zones with more or less constant overpressure. Here the risk for dampness entrance caused by convection of moist air from the room is high.

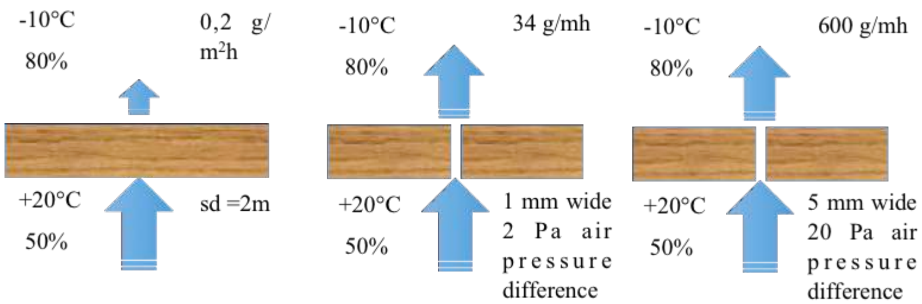

Fig. 52 Comparison of convective dampness transport: diffusion and leakage

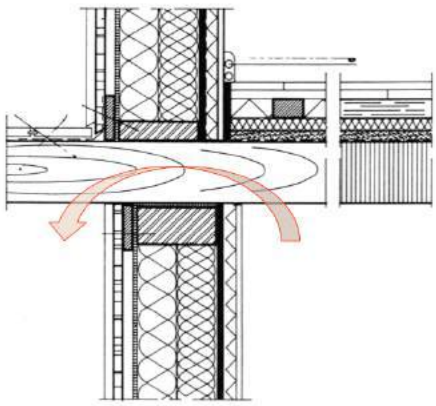

Fig. 53 Slabs with cantilever balconies should be avoided

Cantilever slabs also should be avoided: on the one hand the equilibrium moisture is different inside and outside the building and on the other hand the risk of leakages is high. Therefore it is better to have balconies on a separated construction or fixed with brackets for wall mounting. Gaps or leakage can cause many different moisture problems, depending on the pressure difference, the situation and the weather.

Fig. 54 Two examples for convection of dampness: Left Figure: Base gap; Right figure: Ice around a cantilever beam

Fig. 55 Bad example of a canopy with a gap from inside to outside

If the CLT panel is tight, it is just necessary to tighten up the joints in a durable manner.

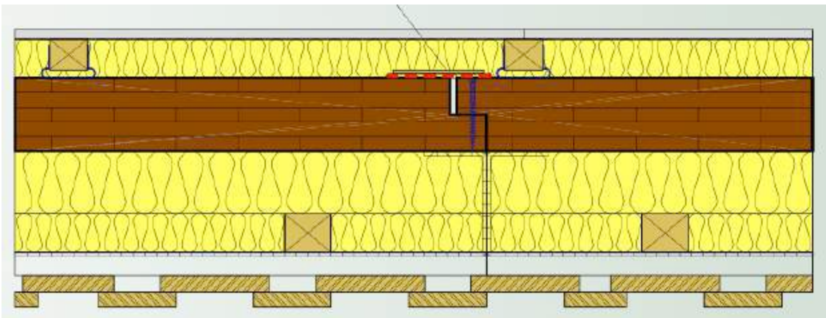

Fig. 56 Wall joint, tightened up with a convection inhibiting tape, mechanically fixed

Fig. 57 Example for an airtightness solution with a convection inhibiting foil beyond the exterior thermal insulation. (not necessary for tight CLT panels)

Good joint design is very helpful. It is important not to change the layer system of the building components, as shown in the following example for a sloping ceiling.

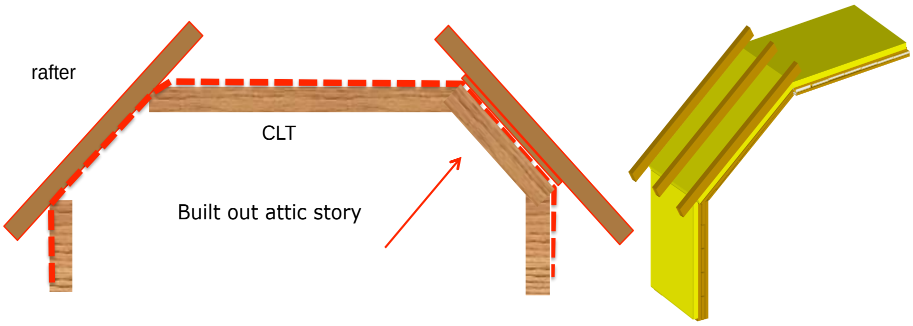

Fig. 58 If framework construction and CLT-panel construction are mixed up e.g. at the sloping ceiling, there will be problems with the exterior convection inhibiting foil of the CLT panel and the vapour barrier, which is necessary for the framework construction inside – both should be connected for airtightness.

Fig. 59 Difficult airtight joint between the airtight layer and the vapour barrier of the sloping ceiling

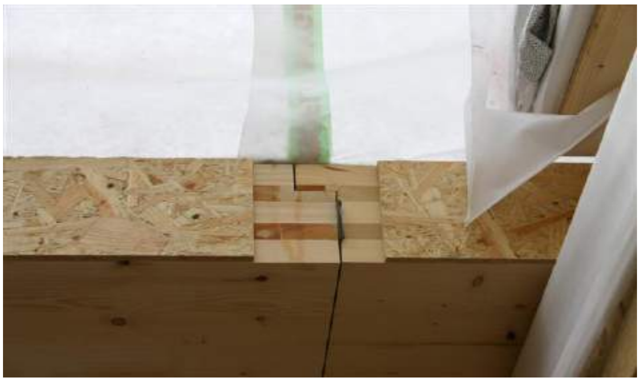

Fig. 60 Left fig.: Examples for good construction design of an exterior slab joint. The joint is covered here with an OSB-strip. Right fig.: Closing of the gap between wall and slab with a compressed sealing strip, an airtight foil and a thin three-layer panel

4. Acoustic Performance of CLT panel based building constructions

Building acoustics performance of construction with CLT is assessed in the laboratory according EN ISO 10140 “Acoustics – Laboratory measurements of sound insulation of building elements” [8] and on site according to EN ISO 140 “Acoustics – Measurement of sound insulation in buildings and of building elements” [9]. The single number rating follows EN ISO 717-1 [10] and EN ISO 717-2 [11]. In Austria we have the following minimum requirements for airborne and impact sound insulation, see Table 7.

Table 7 Austrian minimum requirements for airborne and impact sound insulation

Austria	**Apartment houses / row houses** $D_{nT,w}$ **[dB]**	**Apartment houses / row houses** $L'_{nT,w}$ **[dB]**
Minimum requirements	≥ 55 dB / 60 dB	≤ 48 dB / 43 dB

The comparison of the sound insulation requirements in European and neighbouring countries shows that there are different levels of sound insulation and also different single number quantities used for the description of these different levels. But several investigations into satisfaction with sound insulation in European dwellings show that there are more than 30% of more or less dissatisfied people.

One of the reasons may be that the single number values that are used, calculated in the frequency range from 100 Hz to 3250 Hz, are not able to fulfil all demands of satisfying sound protection, especially in the frequency range below 100 Hz, which is not represented. Thus, in future, it will be necessary to pay more attention to that frequency range. This also will influence lightweight construction, especially for impact sound insulation.

Experience shows that when we pay attention to a sufficiently high sound insulation in the low frequency range (below 200 Hz) there is no trouble with lightweight constructions and inhabitants are satisfied with the Austrian sound insulation requirements.

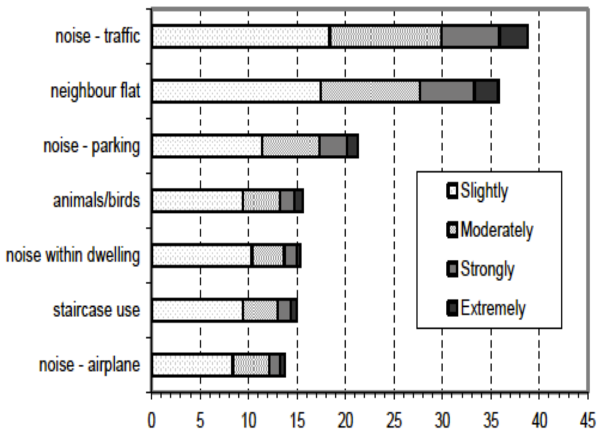

Fig. 61 Dissatisfied people in dwellings in Europe; Niemann H., Maschke C.: "WHO LARES" [12]

Land	Kenngröße	Anforderung in dB	
		MF-Haus	Reihen-Haus
Österreich	$D_{n,T,w}$	55	60
Deutschland	R'_w	53	57
Italien	R'_w	50	50
Dänemark	R'_w	55	55
Norwegen	R'_w	55	55
Schweden	$R'_w + C_{50\text{-}3150}$	53	53
Finnland	R'_w	55	55
Großbritannie	$D_{n,T,w} + C_{tr}$	45	45
Frankreich	$D_{n,T,w} + C$	53	53
Schweiz	$D_{n,T,w} + C$	52	55
Niederlande	$I_{lu;k}$	0	0
Belgien	$D_{n,T,w}$	54	58
Spanien	$D_{nT,w} + C_{100\text{-}500}$	50	50
Portugal	$D_{n,w}$	50	50
Polen	$R'_w + C$	50	52
Tschechien	R'_w	52	57
Slovakai	R'_w	52	52
Ungarn	$R'_w + C$	51	56
Slovenien	R'_w	52	52
Estland	R'_w	55	55
Lettland	$D_{n,T,w}$ oder R'_w	54	54
Lithauen	R'_w	55	55
Island	R'_w	52	55
Irland	$D_{n,T,w}$	53	53

Land	Kenngröße	Anforderung in dB	
		MF-Haus	Reihen-Haus
Österreich	$L'_{nT,w}$	48	43
Deutschland	$L'_{n,w}$	53	48
Italien	$L'_{n,w}$	63	63
Dänemark	$L'_{n,w}$	53	58
Norwegen	$L'_{n,w}$	53	53
Schweden	$L'_{n,w} + C_{I,50\text{-}2500}$	56	56
Finnland	$L'_{n,w}$	53	53
Großbritannie	$L'_{nT,w}$	52	0
Frankreich	$L'_{nT,w}$	58	58
Schweiz	$L'_{nT,w} + C_I$	53	50
Niederlande	I_{co}	5	5
Belgien	$L'_{nT,w}$	58	50
Spanien	$L'_{nT,w}$	65	65
Portugal	$L'_{n,w}$	60	60
Polen	$L'_{n,w}$	58	53
Tschechien	$L'_{n,w}$	58	53
Slovakai	$L'_{n,w}$	58	58
Ungarn	$L'_{n,w}$	55	45
Slovenien	$L'_{n,w}$	58	58
Estland	$L'_{n,w}$	53	53
Lettland	$L'_{n,w}$	54	54
Lithauen	$L'_{n,w}$	53	53
Island	$L'_{n,w}$	58	53
Irland	$L'_{nT,w}$	62	0

Fig. 62 Sound insulation requirements in Europe: Left fig.: Airborne Sound insulation; Right fig.: Impact sound. (Source: Rasmussen, 2010 [13])

Experiences with lightweight constructions show that we should be careful with the sound insulation design for lightweight construction especially in the lower frequency range and especially for impact noise. The existing single number values do not correspond with the perception in those cases where the frequency dependent sound insulation is decreasing too much at the lower frequency range. To get a high quality building it is better to take this frequency range into account when choosing the building components and design the joints. We could show in many examples where excellent sound insulation can be realized with lightweight buildings and intelligent concepts.

4.1 Airborne sound insulation: Acoustic performance of CLT wall panels

Cross-laminated timber boards are a rigid, lightweight material. This brings advantages in statics, but as you know, it is necessary to use further layers if you need a higher sound reduction. The material has two bearing directions, is not isotropic, it works orthotropic with a different bending stiffness in the main bearing direction and transverse to that. The typical sound reduction index of a raw CLT panel (thickness 95 mm, about 48 kg/m^2):

$R_w(C;C_{tr})$ = 33 (-1;-4) dB; R_A = 32 dB

Fig. 63 Left fig.: Sound insulation test facility - Laboratory for Building Physics, Graz University of Technology;
Right fig.: Sound reduction index chart of a typical 95 mm 3-layer CLT panel

For some types of CLT Panels small air leakages may decrease the sound insulation, a second drop is visible in the sound insulation chart at the critical frequency range. CLT panels are lightweight and stiff. So the critical frequency can be found in the frequency range between 200 Hz – 500 Hz.

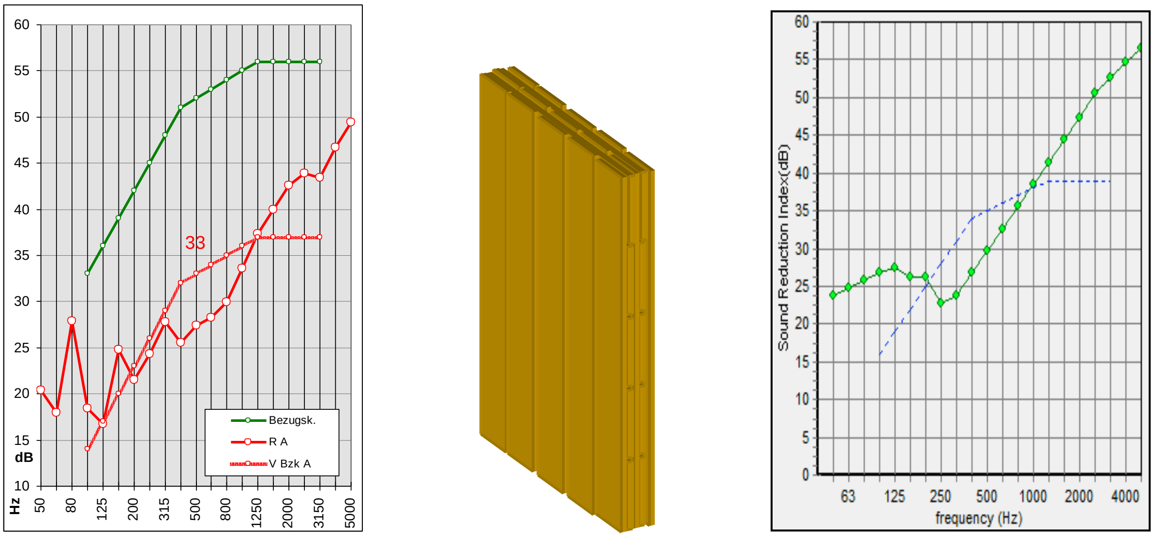

Fig. 64 Left fig.: Sound reduction index chart of a typical 95 mm 3-layer CLT panel - measurement result;
Right fig.: Calculation result

The critical frequency can be found in the above chart in the range of around 250 Hz, for the measured example maybe in combination with effect of some very small leakages, which often may cause a decrease of the sound insulation around 800 Hz. There are a lot of improvement possibilities of CLT panel constructions.

Basis:

Solid, rigid panels:
e.g. CLT Panels

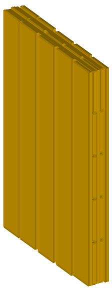

Structural Faktors:

- distance
- Elastic and/or sound aborbing layers
- Mounting Technology
- Independent panels/ frames
- Elastic and sound aborbing layers
- Matching of the material characteristics (critical frequency, stiffness/flexibility, mass)
- Air tightness
- damping

Solid CLT Panel
or lightweight, flexible boards:
e.g. thin OSB-boards
plasterboard and fiber-plasterboards...

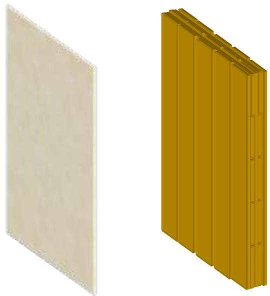

Fig. 65 Examples for sound insulation improvement possibilities

- CLT Panel with a plasterboard lining:

The plasterboard lining has a lower radiation factor, increases the mass and reduces the transmission through leakages. A further improvement factor is the fixing method. Point fixing gives better values than linear (e.g. gluing stripes) or all over gluing.

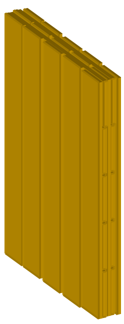

Rw (C; Ctr) = 33 (-1;-4) dB

R_A = 32 dB

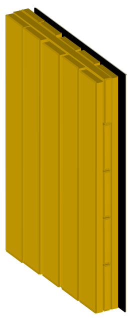

R_w (C; C_{tr}) = 38 (-1;-5) dB

R_A = 37 dB

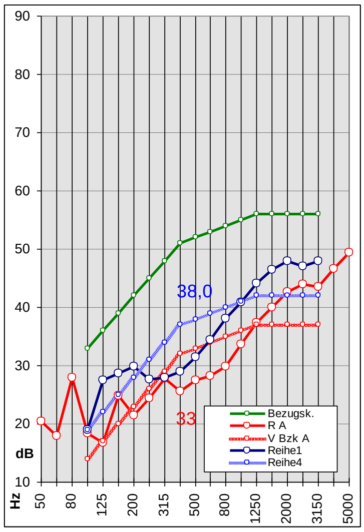

Fig. 66 Left fig: Raw CLT panel; mid: CLT panel with gypsum board (point fixing); Right fig.: Sound reduction index chart

For exterior wall constructions a thermal insulation as an ETICS or an external cladding or a ventilated rain screen is most common.

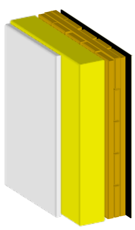

R_w = 37 - 47 dB

R_A = 36 - 46 dB

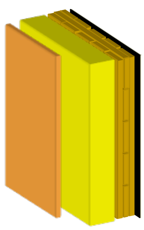

R_w = 42 - 58 dB

R_A = 41 - 57 dB

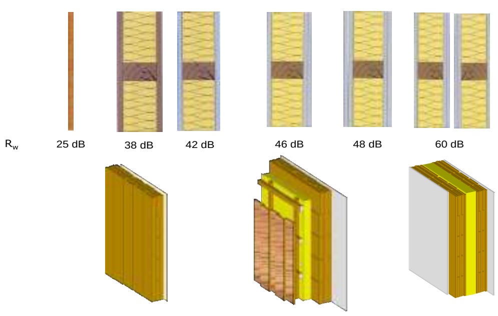

Fig. 67 Left fig.: Exterior walls; Right fig.: Comparison of different wall constructions

For separating walls one possible design is a double CLT wall with different layers. If possible, for a high sound insulation the construction should be designed asymmetric. For a better behaviour in the low frequency range the distance between the two panels should be chosen not less than 6 or 7 cm, better would be more. There may not be any connections between the two panels, otherwise the sound insulation would be reduced. Therefor the insulation material should have a dynamic stiffness of not more than 10 MNs^3.

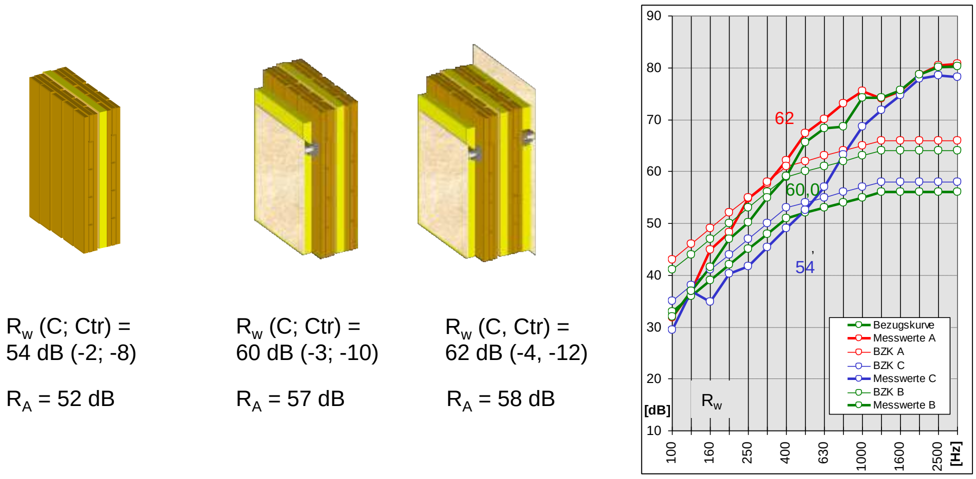

Fig. 68 Examples for separating cavity walls

If possible, an asymmetrical design should be chosen for the panels, the gaps and the coverings. To get better values for the low frequency range, the distance between panels should be selected as large as possible. Additional lining with a low resonance frequency can be used to get better results also for airborne sound insulation as well as for impact noise reduction. The resonance frequency is best chosen if it is situated below 35 Hz. The following equation may be used for calculation:

$$f_0 = 160 \cdot \sqrt{\frac{0{,}12}{d} \cdot \left(\frac{1}{m_1'} + \frac{1}{m_2'} \right)} \qquad (19)$$

with

f_0 resonance frequency

d distance in m

m'1 area related mass 1

m'2 area related mass 2

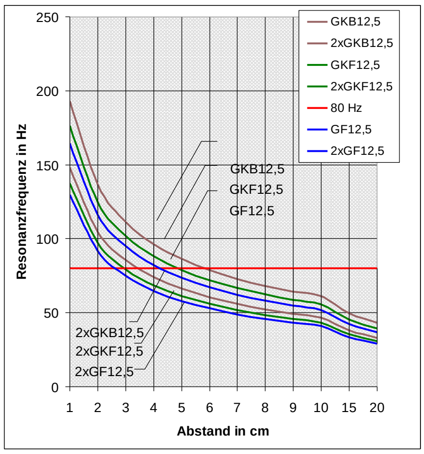

Fig. 69 Resonance frequency of a CLT panel and different independent gypsum (GKB) and gypsum fibre (GKF) boards with mineral wool between, depending on the distance.

4.2 Slabs: Acoustic performance of CLT panel-based slabs

Raw CLT Slabs have a sound reduction Index R_w of about ≈ 33 – 38 dB (R$_A$ ≈ 32 – 37 dB) and a normalized impact sound pressure level $L_{n,w}$ of > 85 – 90 dB.

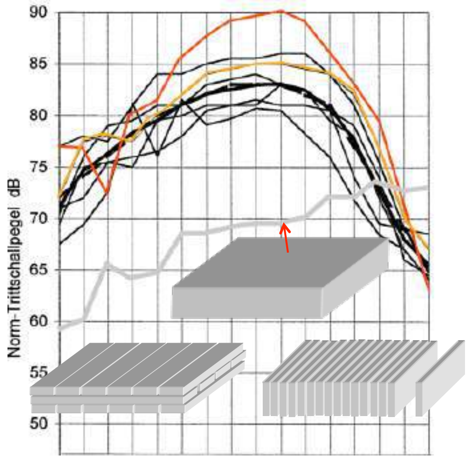

Fig. 70 Left fig.: CLT Panel slab; Right fig.: Comparison of different slabs; concrete, CLT, BSP

As it can be seen, the CLT Slab has the maximum level in the mid frequency range, whereas the concrete slab has its maximum in the high frequency range. Therefore the impact sound of a CLT panel naturally cannot really be reduced by a carpet.

The following measures can be successful to reduce impact sound:

- Floating floor
- Resilient Layer
- Ballasting without stiffness (e.g. grit)
- Absorbent material
- Suspended ceiling

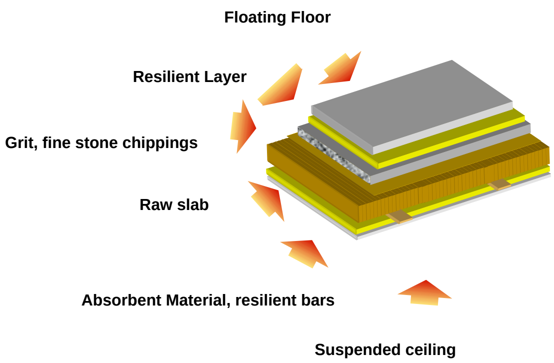

Fig. 71 Exemplary measures for impact sound reduction

In is necessary to design the mass – spring – mass systems to a low resonance frequency, otherwise the impact sound insulation performance will be rated bad, although so the single number rating shows an acceptable number. The mass - spring - mass effect reduces the entry of impact sound into the slab –the effect starts at about 1.4 above resonant frequency.

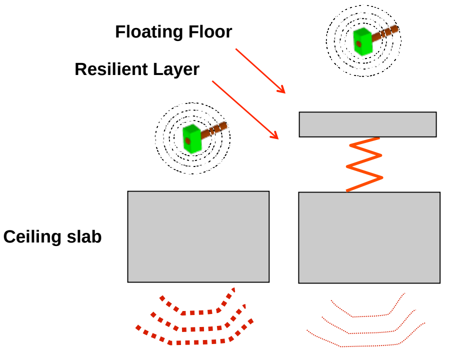

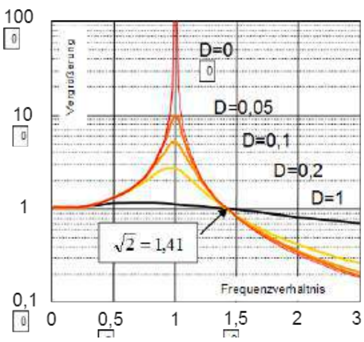

Fig. 72   mass – spring – mass effect and transfer function depending on frequency ratio

Rigid Bridges between the floating floor and the wall or ceiling can destroy the function of this construction type through a “short circuit” – in this case the mass – spring – mass effect can become ineffective.

Fig. 73   Effect of an acoustic bridge

Ballasting:

- The ballasting of the ceiling should not enhance the ceiling stiffness
- The ballasting should not be stiff
- Grit/stone chippings without any binder is best solution
- If a binding is necessary, cut the ballasting in pieces or use elastic binding
- Otherwise take concrete paving units (e.g. 50x50 cm)
- Stay dry (with your ballasting
- Sand in unfavourable – because of it moisture storage capability
- Better: grit/stone chippings (dry fine crushed stone 4-8 mm)

Table 8   Examples for CLT panel based slab constructions; Part 1

Material layer	**Thickness [mm]**
fibreboard floating floor	10
fibreboard floating floor	10
mineral wool resilient layer	30
fine chippings	70
CLP	102
gap	20
mineral wool	50
plasterboard (ceiling treatment)	15

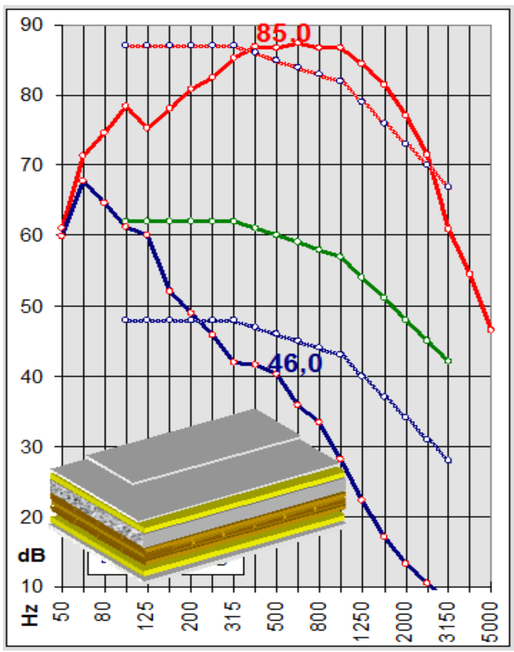

Table 9 Examples for CLT panel based slab constructions; Part 2

Material layer	Thickness [mm]
cementitious screed (without a bridge to the floor base!)	60
PAE membrane	0.2
mineral wool TDP 45/42 resilient layer	42
fine chippings	60
fleece	0.2
CLT ceiling panel	152
air gap	20
mineral wool (sound absorption)	50
plasterboard	12.5

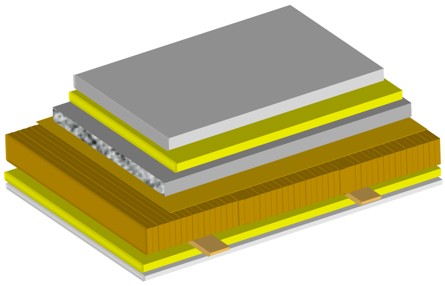

Impact Sound Level:

L_{nw} = 44 dB

Table 10 Examples for CLT panel based slab constructions; Part 2

Material layer	Thickness [mm]
cementitious screed	60
PAE membrane	0.2
mineral wool TDPS 30/25 resilient layer	42
fine chippings	95
fleece	0.2
CLT ceiling panel	146

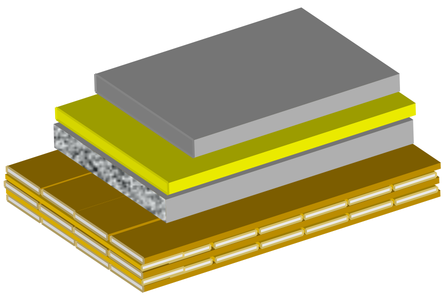

Impact Sound Level:

L_{nw} = 42 dB grit/chippings

L_{nw} = 48 dB grit/chippings, cement bonded

4.2 Acoustic performance of CLT panel based buildings: flanking transmission

Beneath the sound transmission through the building components the flanking transmission of sound energy has a high relevance for CLT based buildings. Therefore it is necessary to optimize the acoustical concept already at the beginning of the design phase of the building development. The flanking transmission in some cases can be enhanced through gaps within the CLT panel.

There may be various solutions for this problem. One is, to close the gaps at the end face of the panels. Another one may be to separate the flanking panels or to put a stripe of plywood, OSB or a board at the end face. If the flanking panel can be separated, it also could be favourable in this case to close up the end face in the joint in the same manner. A further possibility is to have a break of the flanking panel by the separating panel or to have (independent) panelling covering the leaking panel.

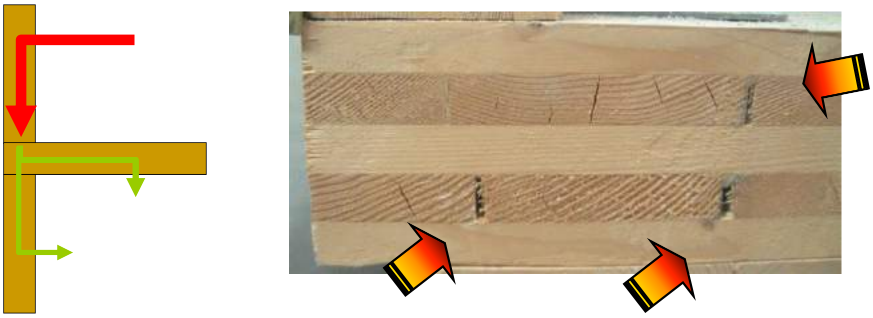

Fig. 74 Example for flanking transmission through gaps and reducing solutions

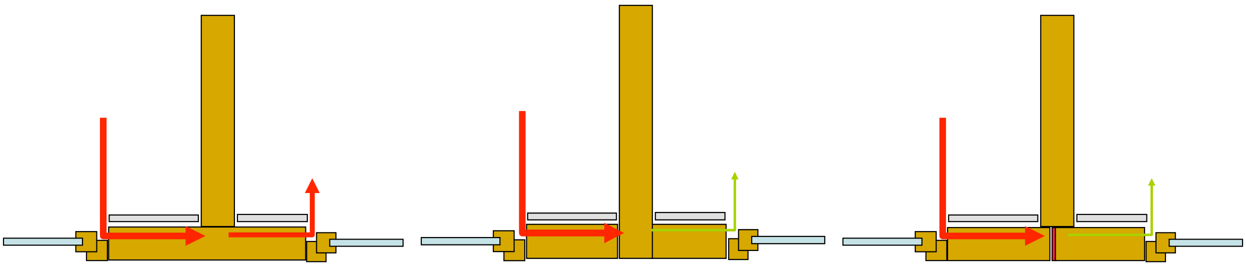

Fig. 75 Examples for reducing solutions

Fig. 76 Additional lining, OSB Strip at the end face or the use of tight panels

4.3 Joints and Construction Systems

CLT is a lightweight and stiff material with a low sound insulation. Therefor also the flanking transmission may be unacceptable high in some cases, where a higher sound insulation is necessary. To improve this behaviour, it is recommended to take this into consideration when designing the structural system. The flanking transmission can be influenced by e.g.

- the wall/ceiling components
- the construction system
- type of joints
- floor coverings
- additional lining or independent lining
- special bearing systems.

The Estimation of the acoustic performance of buildings there exist the European Standard

- EN 12354-1 “Building Acoustics – Estimation of acoustic performance of buildings from the performance of elements – Part 1: Airborne sound insulation between rooms” [14]
- EN 12354-2 “Building Acoustics – Estimation of acoustic performance of buildings from the performance of elements – Part 2: Impact sound insulation between rooms” [15]
- EN 12354-3 “Building Acoustics - Estimation of acoustic performance of buildings from the performance of elements – Part 3: Airborne Sound insulation against outdoor sound” [16]

For lightweight and also CLT based buildings there are some limitations in using this standard, for example it is difficult to estimate the damping of the joints, which is very connected to the fixing measures, the often unknown correction of the radiation factors, the effect of the coincidence frequency and so on.

Therefore in some cases it is the best to have a mock-up and get the basic values by systematic measurements and supplementary calculations . Furthermore, there are some calculation models in development, which could be very useful for the future design process.

4.3.1 Vertical flanking transmission

There are a lot of possibilities to reduce flanking transmission:

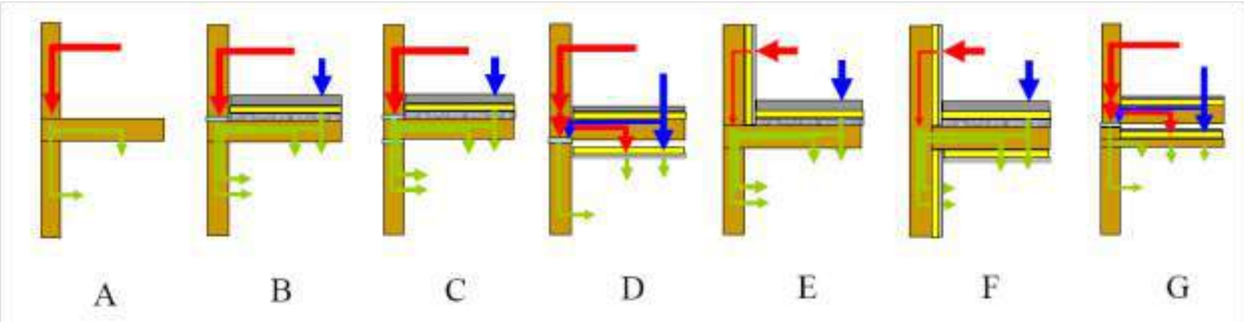

Fig. 77 Different possibilities to reduce flanking transmission

Case B

Control of the vertical flanking transmission by an elastic bearing membrane beyond the wall-supporting surface

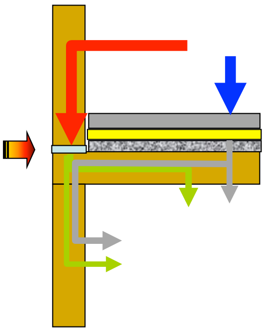

Fig. 78 elastic membrane beyond the wall combined with a floor assembly with high impact sound reduction

Case C

Control vertical flanking transmission by double elastic membrane bearings.

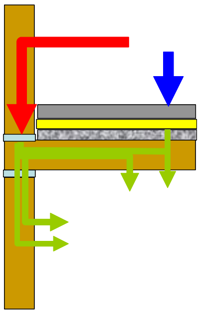

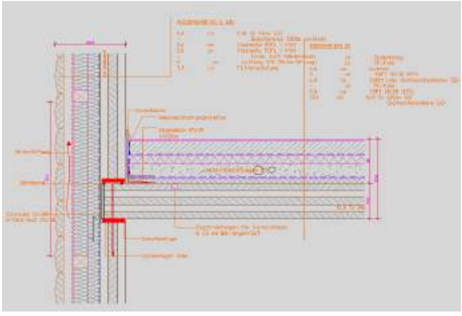

Fig. 79 Floor with high impact sound reduction: elastic membrane beyond the wall

Case D

Control vertical flanking transmission by an elastic membrane bearing below slab supporting surface.

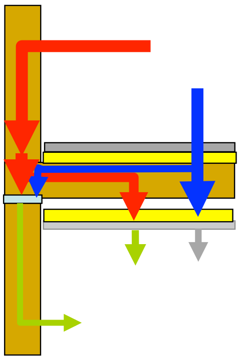

Fig. 80 Elastic membrane bearing below slab supporting surface- suspended ceiling with resilient bars

Case E

Exterior wall separated by slab with high impact sound reduction floor construction: additional independent panels at the wall (independent gypsum board or similar)

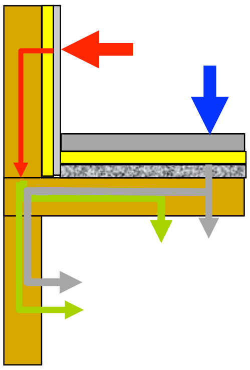

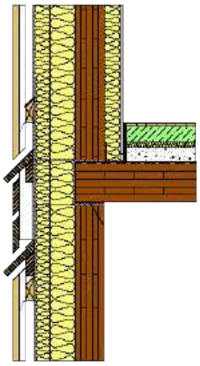

Fig. 81 Elastic membrane bearing below slab supporting surface- suspended ceiling with resilient bars

Case F

Continuous façade and high impact sound reduction floor construction with additional lining on the wall (“room-in-room” system). A lot of different materials for the facing shell are possible.

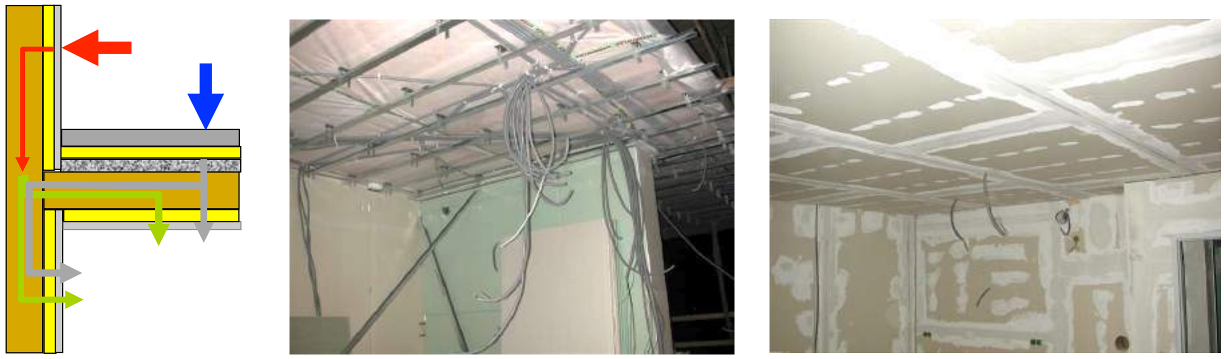

Fig. 82 “Room-in-room” construction system

Case G

Cavity floor slab systems: elastic layer beyond the floor. Additional linings can be used to optimize the frequency related sound insulation. “Cell structure” based construction”

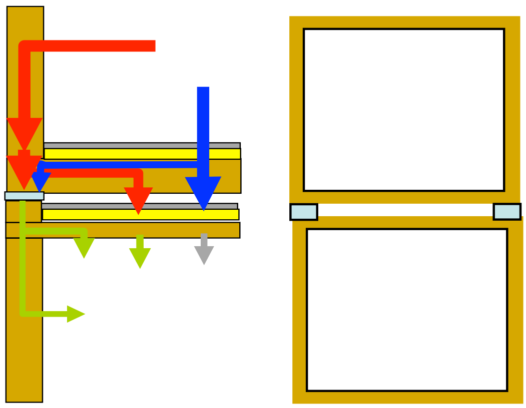

Fig. 83 “Cell Structure” construction system

The vertical flanking transmission is highly influenced by the type of alignment of the wall components. If the wall is continuous, we have a really high flanking transmission.

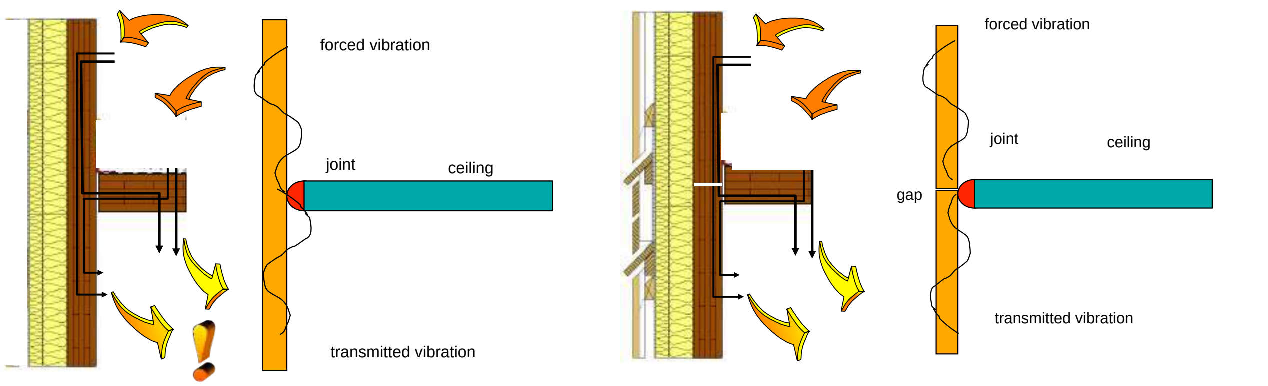

Fig. 84 Left fig. continuous wall and flanking transmission Right fig.: gap to reduce flanking transmission

The Effect of an elastic bearing membrane under the supporting area of a slab with a high insulating floor construction and a suspended ceiling on resilient bars strongly depends on the way of fixing the construction. “Whatever the structural engineer wants to fix, the acoustician wants to separate.“

Table 11 Example results for case D for airborne sound insulation and impact sound level

Sound insulation [dB]	**Without elastic membrane**	**With elastic membrane**		
		without fixing	**fixing as usual**	**strong fixing**
$L_{n,w}$	≈ 47	≈ 47	40-45	45-47
$D_{n,w}$	≈ 53-57	≈ 67	60-62	57-60

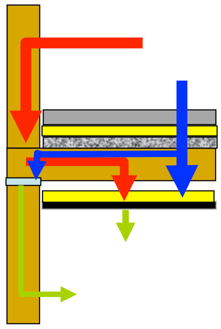

4.3.2 Typical vertical sections

In Austria common types of floor constructions are such with a cement floating floor or similar floating floor systems (e.g. plasterboard based).

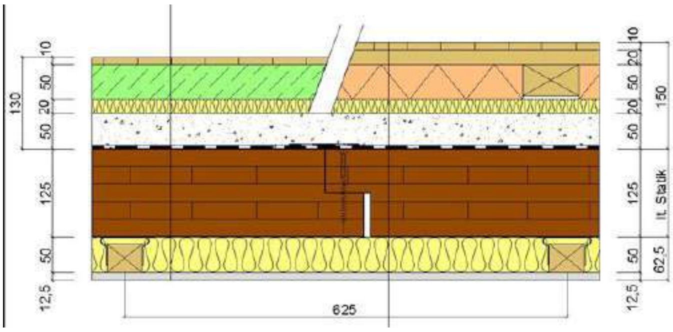

Fig. 85 Slab with floating floor (left section) and timber raft floating floor (right section)

To have a low horizontal flanking transmission a simply method is to have a cavity wall with two bearing CLT panels, and – for a high sound insulation with independent coverings.

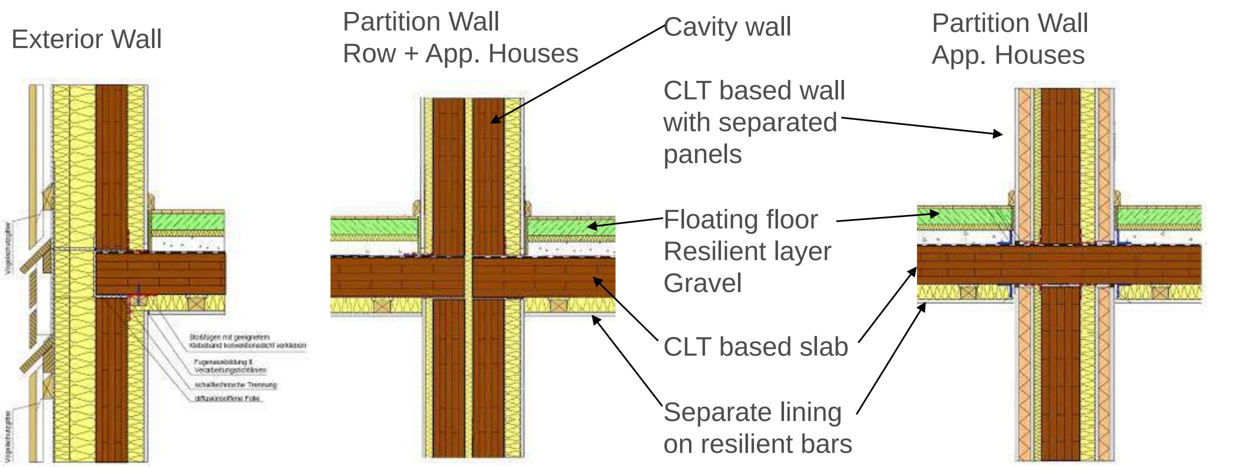

Fig. 86 Vertical section: Exterior wall, separating cavity wall, separating wall with independent layers

Mainly we can distinguish between three building construction systems from a building acoustics point of view:

- Cavity wall system with measures to reduce vertical flanking transmission
- Continuous slab with “room in room” system
- Cell Structure with cavity wall and cavity slab constructions

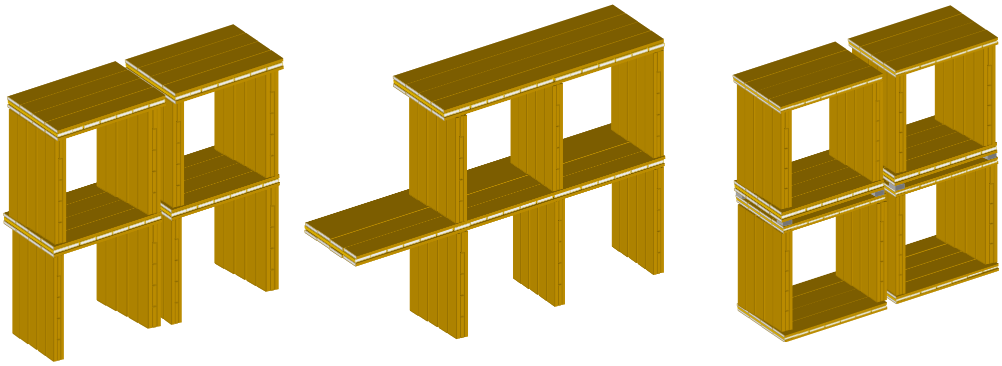

Fig. 87 Examples for CLT panel based basic building construction systems



Fig. 88 from left to right: Leoben-Leitendorf, Spöttelgasse Vienna, Office Park Reininghaus Graz

All this example building systems are able to fulfil the high Austrian requirements of $D_{n,T,w} \geq 55$ dB and $L_{n,T,w} \leq 48$ dB. The results of a survey e.g. in the apartments of the Vienna Spöttelgasse buildings showed, that the inhabitants are very satisfied with the hygrothermal comfort and also the sound insulation of the building.

CLT panels offer comprehensive opportunities for future sustainable buildings.

To take advantage of these opportunities we have to take into account building science aspects and moisture control for comfort and durability and for a sustainable development of building with CLT!

5. Component Catalogue

Based on a lot of experiences we developed an example component catalogue for building with CLT and other timber based lightweight constructions. This catalogue can be downloaded under http://portal.tugraz.at/portal/page/portal/Files/i2190/files/Forschung/Projekte/Leitdetails_fuer_den_Holzwohnbau.pdf and also under www.dataholz.com.

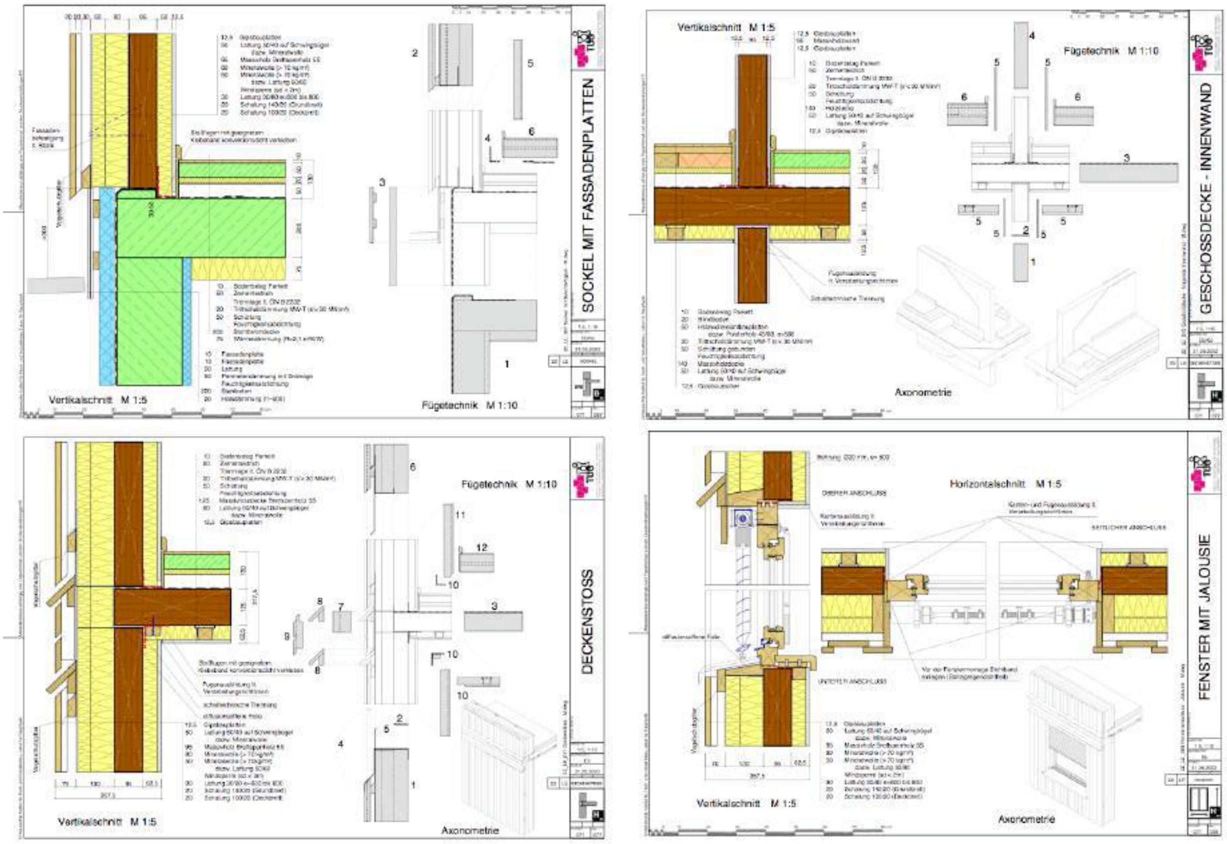

Fig. 89 Wood based building component and system construction details: catalogue examples

contact:

DI Heinz J. Ferk
Head of Laboratory

Building Physics Laboratory
Institute for Building Construction
Graz University of Technology

Inffeldgasse 24
8010 GRAZ
AUSTRIA

ferk@tugraz.at
Tel. +43 (0)316 873 1300

6. References

[1] EN ISO 10456:2010, Building materials and products - hydrothermal properties - Tabulated design values and procedures for determining declared and design thermal values.

[2] EN 13986:2005, Wood-based panels for use in construction – Characteristics, evaluation of conformity and marking.

[3] EN ISO 6946:2008, Building components and building elements – Thermal resistance and thermal transmittance – Calculation method Point 6.2.

[4] EN 12524:2000, Building materials and products – Hygrothermal properties – Tabulated design values.

[5] ÖNORM B 7220, Dächer mit Abdichtungen – Verfahrensnorm.

[6] EN 13829:2001, Thermal performance of buildings – Determination air permeability of buildings – Fan pressurization method.

[7] EN 12114:2000, Thermal performances of buildings – Air permeability of building components and building elements – Laboratory test method.

[8] EN ISO 10140:2012, Acoustics – Laboratory measurements of sound insulation of building elements.

[9] EN ISO 140, Acoustics – Measurement of sound insulation in buildings and of building elements.

[10] EN ISO 717-1:2013, Acoustics -- Rating of sound insulation in buildings and of building elements -- Part 1: Airborne sound insulation.

[11] EN ISO 717-2:2013, Acoustics -- Rating of sound insulation in buildings and of building elements -- Part 1: Impact sound insulation.

[12] Niemann H., Maschke C., *WHO LARES*, Research Report, Berlin Center of Public Health, 2004

[13] Rasmussen B., “Sound insulation between dwellings – Requirements in building regulations in Europe”, *Applied Acoustics*, Vol. 71, 2010, pp. 373-385.

[14] EN 12354-1:2000, Building Acoustics – Estimation of acoustic performance of buildings from the performance of elements – Part 1: Airborne sound insulation between rooms.

[15] EN 12354-2:2000, Building Acoustics – Estimation of acoustic performance of buildings from the performance of elements – Part 2: Impact sound insulation between rooms.

[16] EN 12354-3:2000, Building Acoustics – Estimation of acoustic performance of buildings from the performance of elements – Part 3: Airborne Sound insulation against outdoor sound.

ISBN Number: 1 85790 181 9